UNIVERSITÀ DEGLI STUDI DELLA TUSCIA DI VITERBO

Dipartimento per l'agricoltura, le foreste, la natura e l'energia

DAFNE

Corso di Dottorato di Ricerca in

Biotecnologie Vegetali - XXVII Ciclo.

Transcriptional regulation and dynamics of Arabidopsis nuclear proteome in response to auxin and oligogalacturonides.

settore scientifico-disciplinare
BIO/04

Tesi di dottorato di:

Dott. Jacopo Ciarcianelli

Coordinatore del corso

Prof. Stefania Masci

Firma ……..

Tutore

Prof. Benedetta M. Mattei

Firma ……

12 giugno 2015

Index

1. Introduction

1.1. Plant immunity

In an environment that is rich in harmful microbes, the survival of higher eukaryotic organisms depends on efficient pathogen sensing and rapidly mounted defence responses. Such protective mechanisms are found in all multicellular organisms and are collectively referred to as innate immunity (Medzhitov and Janeway, Jr., 1997; Akira et al., 2006). Because of their sessile lifestyle, plants cannot run away from invaders and need to defend themselves from threatening organisms by mounting a wide array of defense responses in a timely manner. Due to the absence of an adaptive immune system, plants rely on a so-called "innate immune system", analogous to that found in animals (Nurnberger et al., 2004; Gomez-Gomez, 2004). The ability to detect and mount a defense response to potential pathogenic microorganisms has been paramount to the evolution and developmental success of modern-day plants. They are constantly exposed to microbes. To be pathogenic, most microbes must access the plant interior, either by penetrating the leaf or root surface directly or by entering through wounds or natural openings such as stomata, pores in the underside of the leaf used for gas exchange. Once the plant interior has been breached, microbes are faced with another obstacle: the plant cell wall, a rigid, cellulose-based support surrounding every cell. Penetration of the cell wall exposes the host plasma membrane to the microbe, where they encounter extracellular surface receptors that recognize pathogen- or microbe-associated molecular patterns (PAMPs or MAMPs) (Nurnberger and Kemmerling, 2006). Perception of a microorganism at the cell surface initiates PAMP-triggered immunity (PTI) (Dodds and Rathjen, 2010), which usually halts infection before the microbe gains a hold in the plant. Signals similar to PAMPs may arise from the plant itself because of the damage caused by microbes, which are now described as damage-associated molecular patterns (DAMPs) (Lotze et al., 2007) and can trigger PTI as well. Pathogenic microbes have evolved the means to suppress PTI by interfering with recognition at the plasma membrane or by secreting effector proteins into the plant cell cytosol that presumably alter resistance signalling or manifestation of resistance responses (Figure 1.1). Interestingly, the ability to deliver pathogen proteins directly into plant host cells to alter plant defence has become a unifying theme among plant pathogens (phytopathogens).

Once pathogens acquired the capacity to suppress primary defences, plants developed a more specialized mechanism to detect microbes, referred to as effector-triggered immunity (ETI) (Dodds and Rathjen, 2010). Effector-triggered immunity involves the direct or indirect recognition of the very microbial proteins used to subvert PTI by plant resistance (R) proteins. Activation of R protein-mediated resistance also suppresses microbial growth, but not before the invader has had an opportunity for limited proliferation. Not surprisingly, pathogens seem to have adapted effectors to interfere with ETI.

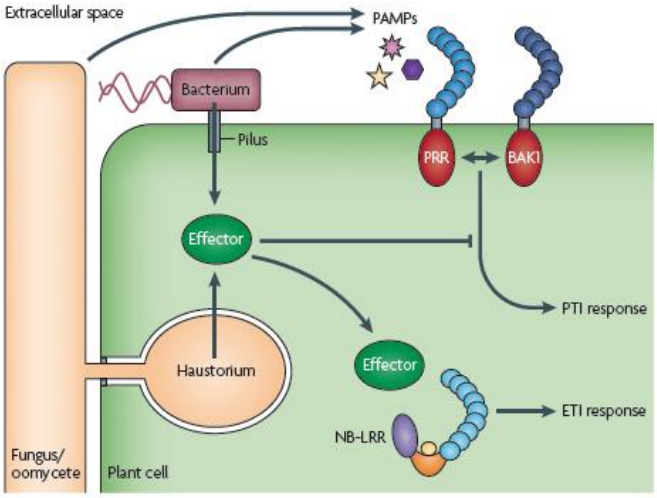

Figure 1.1: The plant immunity. Recognition of pathogen-associated molecular patterns (such as bacterial flagellin) by cell surface pattern recognition receptors (PRRs) promptly triggers PTI leading to basal immunity. Many PRRs interact with the related protein BRASSINOSTEROID INSENSITIVE 1-ASSOCIATED KINASE 1 (BAK1) to initiate the PTI signalling pathway. Pathogenic bacteria use the type III secretion system to deliver effector proteins that target multiple host proteins to suppress basal immune responses. Plant resistance proteins (such as NB-LRR) recognize effector activity and restore resistance through effector-triggered immune responses (ETI). Adapted from (Dodds and Rathjen, 2010).

Disease is actually a relatively rare phenomenon in plants; the majority of plant species are resistant to infection by all isolates of any given microbial species (Dangl and Jones, 2001). The ability of an entire plant species to resist infection by all isolates of a pathogen species is termed non-host (or species) resistance. This is the commonest form of disease resistance in plants, and the infrequent change in the range of host species colonized by plant pathogens is indicative of its stability (Nurnberger and Lipka, 2005). Non-host resistance is thought to rely on both pre-formed barriers, such as the waxy cuticle and cell wall, which physically impede the growth and spread of the potential pathogen, and on the

induction of the basal defence system mounted in response to the recognition of non-self by the plant (Nurnberger and Lipka, 2005). An array of microbial-derived molecules termed pathogen-associated molecular patterns are recognized by pattern recognition receptors (PRRs) in the plant leading to signal transduction and the activation of a range of basal defence mechanisms including ethylene production, an oxidative burst, callose deposition, induction of defence related gene expression and, in some cases, hypersensitive response (HR)-like cell death (Nurnberger et al., 1994). The PAMP detection system present in plants corresponds conceptually to that of the innate immune system in animals; both recognize highly conserved microbial molecules and act as an early warning system for the presence of a potential pathogen (Ausubel, 2005). Plants also have a second system, cultivar-specific resistance, involving pairs of gene products—effector molecules from the pathogen and corresponding resistance (R) proteins in the plant. Recognition of an effector, or of its activity, by the appropriate R protein in the host leads to the HR and curtailment of pathogen growth, while loss of either of these proteins results in disease (Dangl and Jones, 2001). Since effectors are specific to particular pathogen strains, it has been proposed that cultivar-specific resistance fulfills an analogous role in plants to that of the adaptive immune system in vertebrates (Gomez-Gomez and Boller, 2002; Ausubel, 2005).

For many years view of the plant immune system was represented as a four phased 'zigzag' model (figure 1.2). In phase 1, PAMPs are recognized by PRRs, resulting in PTI that can halt further colonization. In phase 2, successful pathogens deploy effectors that contribute to pathogen virulence. Effectors can interfere with PTI. This results in effector-triggered susceptibility (ETS). In phase 3, a given effector is 'specifically recognized' by one of the NB-LRR proteins, resulting in effector-triggered immunity (ETI). Recognition is either indirect, or through direct NB-LRR recognition of an effector. ETI is an accelerated and amplified PTI response, resulting in disease resistance and, usually, a hypersensitive cell death response (HR) at the infection site. In phase 4, natural selection drives pathogens to avoid ETI either by shedding or diversifying the recognized effector gene, or by acquiring additional effectors that suppress ETI. Natural selection results in new R specificities so that ETI can be triggered again.

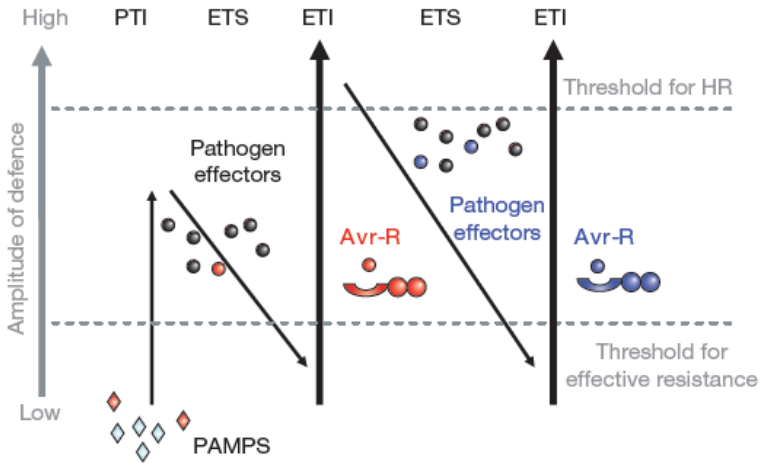

Figure 1.2: A zigzag model illustrates the quantitative output of the plant immune system. In this scheme, the ultimate amplitude of disease resistance or susceptibility is proportional to [PTI – ETS1ETI]. In phase 1, plants detect microbial/pathogen-associated molecular patterns (MAMPs/ PAMPs, red diamonds) via PRRs to trigger PAMP-triggered immunity (PTI). In phase 2, successful pathogens deliver effectors that interfere with PTI, or otherwise enable pathogen nutrition and dispersal, resulting in effector-triggered susceptibility (ETS). In phase 3, one effector (indicated in red) is recognized by an NB-LRR protein, activating effector-triggered immunity (ETI), an amplified version of PTI that often passes a threshold for induction of hypersensitive cell death (HR). In phase 4, pathogen isolates are selected that have lost the red effector, and perhaps gained new effectors through horizontal gene flow (in blue)—these can help pathogens to suppress ETI. Selection favours new plant NB-LRR alleles that can recognize one of the newly acquired effectors, resulting again in ETI. Adapted from (Jones and Dangl, 2006).

In a recent work (Boller and Felix, 2009) it was proposed a new way to explain plant immunity in which effective innate immunity in plants, as in the case of innate immunity in vertebrates, is mediated through a single overarching principle, the perception of signals of danger. What may be categorized as PAMPs (or MAMPs), DAMPs, and effectors, might appear to the plant as one and the same type of signal that indicates a situation of danger (Figure 1.3).

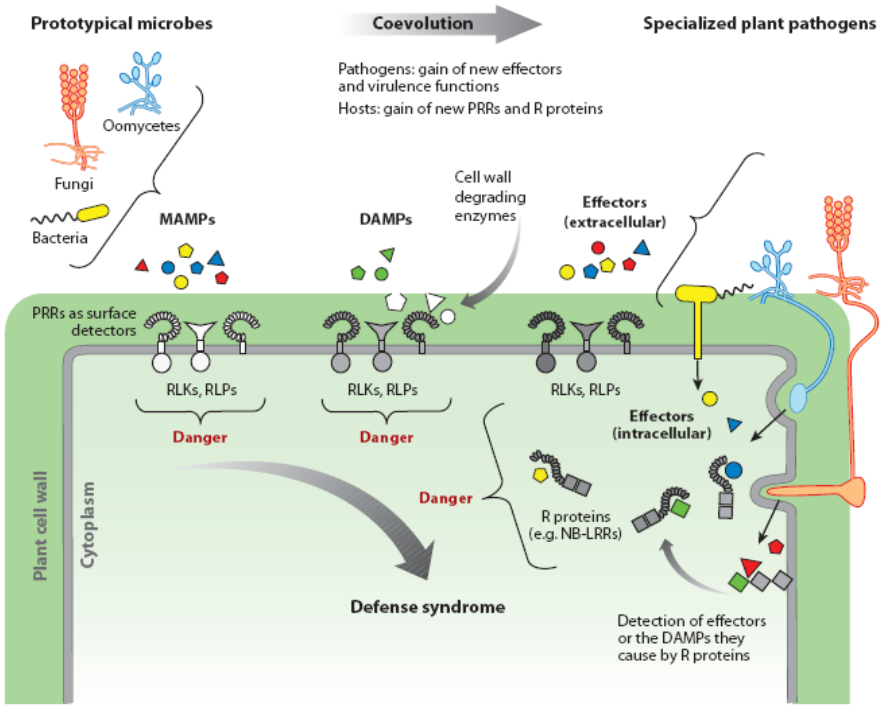

Figure 1.3: Microbe-associated molecular patterns (MAMPs), damage-associated molecular patterns (DAMPs), and effectors are perceived as signals of danger. Extracellular MAMPs of prototypical microbes and DAMPs released by their enzymes are recognized through pattern recognition receptors (PRRs). In the course of coevolution, pathogens gain effectors as virulence factors, and plants evolve new PRRs and resistance (R) proteins to perceive the effectors. When MAMPs, DAMPs, and effectors are recognized by PRRs and R proteins, a stereotypical defense syndrome is induced. RLK, receptor-like kinase; RLP, receptor-like protein; NB-LRR, nucleotide binding-site–leucine-rich repeat. Adapted from (Boller and Felix, 2009).

Indeed, gene expression data indicate that considerable overlap exists between the defense response induced by MAMPs, effectors, and endogenous elicitors. It remains to be seen, as an important challenge for future research, how signaling through MAMPs, endogenous DAMPs, and effectors converges into a stereotypical defense response.

1.2. Basal defence

Induction of PTI in response to PAMPs or DAMPs occurs in both host and non-host plant species and is based on basal defense mechanisms. Studies of the effects of PAMPs and DAMPs point to a

stereotypical response, indicating that signaling converges to a common defense response. This is exerted trough a time course of events following PRR activation:

Very Early Responses (1–5 Minutes):

Ion fluxes. Among the earliest and most easily recordable physiological responses to MAMPs and DAMPs in plant cell cultures, starting after a lag phase of ~0.5–2 min, is an alkalinization of the growth medium due to changes of ion fluxes across the plasma membrane (Boller, 1995; Nurnberger et al., 2004). These changes include increased influx of H^+ and Ca^{2+} and a concomitant efflux of K^+; an efflux of anions, in particular of nitrate, has also been observed (Wendehenne et al., 2002). The ion fluxes lead to membrane depolarization. PAMPs and DAMPs are known to stimulate an influx of Ca^{2+} from the apoplast and cause a rapid increase in cytoplasmic Ca^{2+} concentrations, which might serve as second messenger to promote the opening of other membrane channels (Blume et al., 2000; Lecourieux et al., 2002), or to activate calcium-dependent protein kinases (Boudsocq et al., 2010).

Oxidative burst. Another very early response to PAMPs and DAMPs, with a lag phase of ~2 min, is the oxidative burst (Chinchilla et al., 2007). Reactive oxygen species can act as antibiotic agents directly or they may contribute indirectly to defense by causing cell wall crosslinking; in addition, reactive oxygen species may act as secondary stress signals to induce various defense responses (Apel and Hirt, 2004). The oxidative burst is an immediate and localized reaction that is believed to have several roles in plant defense (Low and Merida, 1996; Bolwell et al., 1999). The quantities of reactive oxygen species produced can be cytotoxic and thus are expected to be antimicrobial. Reactive oxygen species are thought to have direct (through cytotoxicity) and indirect (through signaling) roles in the plant cell death required for the HR. Reactive oxygen species induce the expression of defense related genes (Lamb and Dixon, 1997), and are implicated as second messengers that elicit other defense responses, including systemic acquired resistance (SAR) and the HR (Bolwell et al., 1999). SAR is the induction of defense mechanisms at locations remote from the original wound or infection site that serve to prepare the plant to defend itself against new attacks by pathogens (Sticher et al., 1997). In addition, reactive oxygen species drive the rapid peroxidase-mediated oxidative cross-linking of cell wall lignins, proteins, and carbohydrates, thereby reinforcing the wall against enzymatic maceration by the pathogen (Cote and Hahn, 1994).

O_2- generating nicotinamide adenine dinucleotide phosphate (NADPH) oxidases are generally considered to be a major enzymatic source of ROS in the oxidative burst of plant cells challenged with pathogens or elicitors (Torres and Dangl, 2005; Torres et al., 2006). Two different NADPH oxidase genes in potato (*Solanum tuberosum*) are responsible for the elicitor induced biphasic oxidative burst(Yoshioka et al., 2001). In Arabidopsis, several genes encoding proteins with high similarity to the mammalian NADPH oxidase gp91phox subunit have been characterized. Among them, AtrbohD is required for the production of ROS during infection with different bacterial and fungal pathogens, including *B. cinerea* (Torres and Dangl, 2005) (Torres et al., 2006). Besides NADPH oxidases, other enzymes appear to be important in the elicitor-mediated oxidative burst, including apoplastic oxidases, such as oxalate oxidase (Dumas et al., 1993), amine oxidase (Allan and Fluhr, 1997), and pH-dependent apoplastic peroxidases (Frahry and Schopfer, 1998; Bolwell et al., 1995), which generate either O_2- or H_2O_2.

Several studies report a PAMP-induced production of the reactive oxygen species nitric oxide (NO), a well-known second messenger in animals. However, contrary to animals, plants have no obvious NO synthase; furthermore, the indirect method used to measure NO may not be specific enough to discriminate it from other ROS products (Neill et al., 2008).

Activation of MAPKs. An early response to PAMP and DAMP signals is an activation of Mitogen-Activated Protein Kinase (MAPK) cascades (Pedley and Martin, 2005). The MAPK phosphorylation cascade is a highly conserved signal transduction mechanism that plays a key role in regulating many aspects of growth and development in eukaryotes. In plants, MAPK cascades have been associated with hormonal, abiotic stress, and disease defense responses and with the regulation of the cell cycle (Tena et al., 2001). A MAPK cascade consists of a core module of three kinases that act in sequence: a MAPK kinase kinase (MAPKKK) that activates, via phosphorylation, a MAPK kinase (MAPKK), which activates a MAPK (Figure 1.4). Activated MAPKs phosphorylate a number of different target proteins; the majority of targets appear to be transcription factors, but other targets include various protein kinases, phospholipases, and cytoskeletal proteins, all of which effect changes in gene expression and/or physiological responses appropriate to the stimulus in question (Widmann et al., 1999).

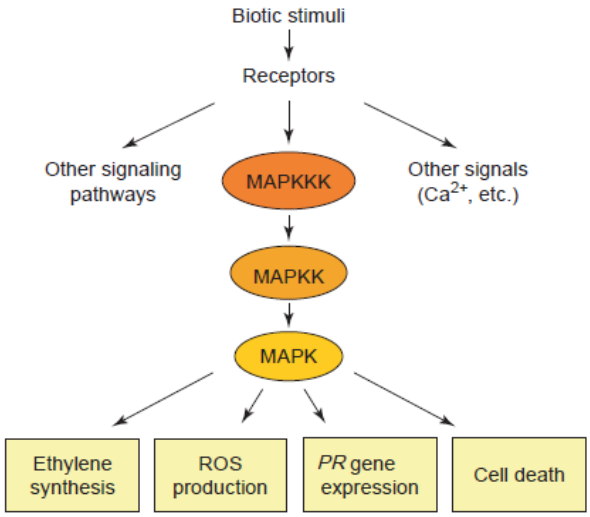

Figure 1.4. MAPK cascades and the cellular responses they influence following the recognition of microbial pathogens. Adapted from (Pedley and Martin, 2005).

Within the Arabidopsis genome sequence, 60 genes are predicted to encode MAPKKKs, 10 genes to encode MAPKKs, and 20 genes to encode MAPKs {2002 25518 /id}. Although there is likely to be some degree of functional redundancy, the high number of genes for MAPK cascade components indicates that plants rely heavily upon MAPK cascades for signal transduction. In particular, in Arabidopsis, a MAPK cascade, leading to AtMPK3 and AtMPK6 activation, is required for flg22-mediated responses (Asai et al., 2002). In *Arabidopsis* stimulated with flg22, a transient increase in AtMPK6 activity was observed, starting with a lag phase of ~1–2 min and peaking after 5–10 min (Nuhse et al., 2000). A subsequent study made use of *Arabidopsis* leaf protoplasts transfected with various MAPK-related constructs to demonstrate the activation of two complete MAPK cascades by flg22, leading to the activation of AtMPK3 and AtMPK6 and culminating in the activation of WRKY-type transcription factors (Asai et al., 2002). DAMPs such as AtPep1 similarly induce a MAPK cascade (Huffaker et al., 2006).

Changes in protein phosphorylation. Activation of MAPK is accompanied by changes in protein phosphorylation. Pulse-labeling of Arabidopsis cells with radioactive phosphate, followed by two-dimensional gel electrophoresis, revealed dozens of proteins that showed increased phosphorylation within minutes of flg22 stimulation (Peck et al., 2001). With the advent of technologies that allow large-scale analysis of phosphopeptides, a number of proteins showing elicitor-responsive phosphorylation could be directly identified and their phosphorylation sites determined (Widmann et al., 1999). Using different technologies, two groups found a number of membrane proteins that display flg22-responsive phosphorylation in Arabidopsis cells;

intriguingly, both reported that RESPIRATORY BURST OXIDASE HOMOLOGUE D (RbohD), the NADPH oxidase that mediates the oxidative burst, is among these proteins (Nuhse et al., 2007; Benschop et al., 2007).

Early Responses (5–30 Minutes).

Ethylene biosynthesis. Among the earliest responses to MAMPs is an increased production of the stress hormone ethylene. Typically, an increased activity of l-aminocyclopropane-1-carboxylate (ACC) synthase activity can be detected within 10 min of treatment with MAMPs (Spanu et al., 1994).

Receptor endocytosis. Interestingly, FLS2, the PAMP flg22 receptor, undergoes ligand-induced endocytosis. A biologically functional FLS2-GFP fusion construct, stably expressed in *Arabidopsis* plants, disappears from its plasma membrane localization and appears in vesicles within ~10–20 min of flg22 stimulation (Robatzek et al., 2006). FLS2 possibly has specific signaling functions after endocytosis, as described for certain receptors in animals, but endocytosis may also simply serve to remove and degrade the activated receptor (Robatzek et al., 2006).

Gene activation. Treatment of *Arabidopsis* plants with flg22 caused the induction of almost 1000 genes within 30 min and the downregulation of approximately 200 genes (Zipfel et al., 2004). The pattern of gene regulation in response to different PAMPs is almost identical, indicating that signaling through various PRR converges at an early step (Zipfel et al., 2006). In fact, fungal chitin and endogenous elicitors such as OGA seem to induce a similar set of genes (Ramonell et al., 2002; Ferrari et al., 2007), which suggests a stereotypical gene activation response to all PAMPs and DAMPs. Interestingly, among the induced genes, Receptor-like kinases (RLKs) are overrepresented. *FLS2* and *EFR* are included in the induced genes, indicating that one role of early gene induction is a positive feedback to increase PRR perception capabilities (Zipfel et al., 2004).

Late Responses (Hours–Days).

Callose deposition. Arabidopsis leaves treated with flg22 and fixed and stained with aniline blue ~16 h later display strong accumulation of fluorescent spots thought to represent callose deposits

(Gomez-Gomez et al., 1999). Although the biological foundation of this response is not clear, it has been used frequently, particularly to characterize pathogen effectors that interfere with MAMP signaling (Chisholm et al., 2006; Jones and Dangl, 2006).

Seedling growth inhibition. In *Arabidopsis*, a robust bioassay for PAMPs such as flg22 and elf18 is seedling growth inhibition. This response may reflect a physiological switch from a growth to a defense program, and it may be connected to the induction of amiRNA that negatively regulates the F-box auxin receptors TIR1 (transport inhibitor response 1), AFB2, and AFB3 (auxin signalling F-box proteins 2 and 3) and the consequent down regulation of auxin-responsive genes (Navarro et al., 2006).

1.3. Growth-Defense trade off

In their natural environments , plants are under continuous biotic stress caused by different attackers (e.g., bacteria, fungi, viruses, oomycetes, and insects) that compromise plant survival. Plants have thus evolved a variety of resistance mechanisms that can be induced after pathogen or pest attack (Glazebrook, 2005) but defense activation comes at the expense of plant growth. A fine regulation of the immune responses is necessary because the use of metabolites in plant resistance may be detrimental to other physiological processes impacting negatively in other economically interesting plant traits, such as biomass and seed production. This negative impact on growth could result from a diversion of resources away from growth and towards defense. Diversion of plant resources has been shown to occur at all levels, including machinery involved in transcription, translation, and protein secretion from cells as well as prioritization of carbon and nitrogen towards production of defense compounds. Transcriptomic and proteomic studies have demonstrated transcriptional reprogramming and altered protein profiles upon pathogen/herbivore detection to promote defense at the expense of growth (Jung et al., 2007; Denoux et al., 2008; Bilgin et al., 2010). The defense responses are regulated by phytohormones , that are small molecules which synergistically and/or antagonistically work in a complex network to regulate many aspects of plant growth , development , reproduction, and response to environmental stimuli. Then in adaptation to natural conditions, plants have evolved sophisticated mechanisms to regulate growth and defense responses, understanding the molecular mechanisms used by plants to balance growth and defense can enrich plant breeding and engineering strategies for

selection of elite genetic traits that will maximize plant fitness. Plant hormones play important roles in diverse growth and developmental processes as well as various biotic and abiotic stress responses in plants; for example, infection by diverse pathogens results in changes in the level of several of them (Robert-Seilaniantz et al., 2007; Adie et al., 2007). Plants hormones include auxins, gibberellins (GA), abscisic acid (ABA), cytokinins (CK), salicylic acid (SA), ethylene (ET), jasmonates (JA), brassinosteroids (BR) and peptide hormones. The identification and characterization of several mutants affected in the biosynthesis, perception and signal transduction of these hormones has been instrumental in understanding the role of individual components of each hormone signaling pathway in plant defense. Substantial progress has been made in the elucidation of individual aspects of phytohormone perception, signal transduction, homeostasis or influence on gene expression. However, the molecular mechanisms by which plants integrate stress induced changes in hormone levels and initiate adaptive responses are still poorly understood. Microbial pathogens have also developed the ability to manipulate the defence-related regulatory network of plants by producing phytohormones or their functional mimics; this results in hormonal imbalance and activation of inappropriate defence responses (Robert-Seilaniantz et al., 2007). For example, production of coronatine — a JA-Ile mimic by *Pseudomonas syringae pv. tomato* (Pst) bacteria, triggers the activation of JA-dependent defence responses leading to the suppression of SA-dependent defence responses and promotion of disease symptoms (Cui et al., 2005; Laurie-Berry et al., 2006). In addition, coronatine has been shown to prevent PAMP-induced stomatal closure which facilitates bacterial entry into the leaf (Melotto et al., 2006).

1.3.1. Salicylic acid, jasmonates and ethylene are involved in defense signaling

Three phytohormones—SA, JA and ET, are known to play major roles in regulating plant defence responses against various pathogens, pests and abiotic stresses such as wounding and exposure to ozone (Glazebrook, 2005; Lorenzo and Solano, 2005; Broekaert et al., 2006; Balbi and Devoto, 2008). SA plays a crucial role in plant defence and is generally involved in the activation of defence responses against biotrophic and hemi-biotrophic pathogens as well as the establishment of systemic acquired

resistance (SAR) (Grant and Lamb, 2006)). Mutants that are affected in the accumulation of SA or are insensitive to SA show enhanced susceptibility to biotrophic and hemi-biotrophic pathogens. Recently, it has been shown that methyl salicylate, which is induced upon pathogen infection, acts as a mobile inducer of SAR in tobacco (Park et al., 2007). SA levels increase in pathogen challenged tissues of plants and exogenous applications result in the induction of pathogenesis related (PR) genes and enhanced resistance to a broad range of pathogens. By contrast, JA and ET are usually associated with defence against necrotrophic pathogens and herbivorous insects. Although, SA and JA/ET defence pathways are mutually antagonistic, evidences of synergistic interactions have also been reported (Schenk et al., 2000; Beckers and Spoel, 2006; Mur et al., 2006). This suggests that the defence signaling network activated and utilized by the plant is dependent on the nature of the pathogen and its mode of pathogenicity. In addition, the lifestyles of different pathogens are not often readily classifiable as purely biotrophic or necrotrophic. Therefore, the positive or negative cross talk between SA and JA/ET pathways may be regulated depending on the specific pathogen (Adie et al., 2007).One of the important regulatory components of SA signaling is non-expressor of PR genes 1 (NPR1), which interacts with TGA transcription factors that are involved in the activation of SA-responsive PR genes. Arabidopsis *npr1* plants are compromised in the SA-mediated suppression of JA responsive gene expression indicating that NPR1 plays an important role in SA-JA interaction (Spoel et al., 2007). Downstream of NPR1, several WRKY transcription factors play important roles in the regulation of SA-dependent defence responses in plants (Eulgem and Somssich, 2007). Several studies indicate that JA- and ET-signaling often operate synergistically to activate the expression of some defence related genes after pathogen inoculation (Penninckx et al., 1998; Thomma et al., 2001; Glazebrook, 2005). Microarray analysis of defence related genes revealed significant overlap in the number of genes induced by both JA and ET (Schenk et al., 2000). It has been shown that an Arabidopsis transcription factor, ethylene response factor 1 (ERF1) acts as a positive regulator of JA and ET signaling (Lorenzo et al., 2003). Recently, several members of ERF family have been shown to play important role in mediating defense responses in Arabidopsis (McGrath et al., 2005). However, how plants coordinate these complex interactions and what are the molecular mechanisms involved is not clear.

1.3.2. The growth-promoting hormone Auxin is also involved in defense responses

Auxins regulate many fundamental aspects of plant growth and development including stem and petiole elongation and root architecture in response to light, temperature, and gravity (Kazan, 2013). Auxin promotes the degradation of a family of transcriptional repressors called Auxin/Indole-3-acetic acid (Aux/IAA). Aux/IAA proteins bind to auxin response factors (ARFs) and inhibit the transcription of specific auxin response genes (Leyser, 2006). It has been shown that transport inhibitor response 1 (TIR1) is an auxin receptor that interacts with Aux/IAA proteins (Dharmasiri et al., 2005). TIR1 encodes an F-box protein that forms an Aux/IAA-SCFTIR1 (SKP1, Cullin and F-box proteins) complex and leads to the degradation of Aux/IAA proteins via ubiquitin/26S proteasome pathway (Parry and Estelle, 2006). To regulate plant growth and development, auxin can induce the expression of three groups of genes: Aux/IAA family, GH3 family and small auxin-up RNA (SAUR) family (Woodward and Bartel, 2005). GH3 genes encode IAA-amido synthetases that are involved in the regulation of auxin homeostasis by conjugating excess IAA to amino acids (Staswick et al., 2005). Most of the total auxin in plants is found in the conjugated form and the formation of auxin conjugates is one of the important regulatory mechanisms for the activation or inactivation of IAA. Auxin responsive GH3 genes have been shown to play roles in plant defence responses in Arabidopsis and rice. Recently, GH3.5 has been shown to acts as a bifunctional modulator in both SA and auxin signaling during pathogen infection (Zhang et al., 2007). Exogenous application of auxin has been shown to promote disease caused by *Agrobacterium tumefaciens* (Yamada, 1993), *Pseudomonas savastanoi* (Yamada, 1993) and *Pst DC3000* (Navarro et al., 2006). Similarly, co-inoculation of *P. syringae pv. maculicola* (*Psm*) *4326* and auxin has been found to promote both disease symptom and pathogen growth in Arabidopsis (Wang et al., 2007). These results indicate that auxin is involved in the attenuation of defence responses in plants. In contrast, blocking auxin responses has been shown to increase resistance in plants. Auxin resistant *axr2-1* mutants of Arabidopsis showed reduction in *Psm* 4326 growth compared to wild type plants (Wang et al., 2007). Several studies have shown that pathogen infection results in imbalances in auxin levels as well as changes in the expression of genes involved in auxin signaling. For example, infection with *Pst* DC3000 resulted in increased IAA levels in Arabidopsis (O'Donnell et al., 2003). Interestingly, the bacterial type III effector *avrRpt2*, which encodes a cysteine protease, has been shown to modulate host auxin physiology to promote pathogen

virulence and disease development in Arabidopsis (Chen et al., 2007). Global gene expression analysis using microarrays revealed that *Pst* DC3000 induces auxin biosynthetic genes and represses genes belonging to Aux/IAA family and auxin transporters. Thus, *Pst* DC3000 activates auxin production, alters auxin movement and derepresses auxin signaling thereby modulating auxin physiology in Arabidopsis (Thilmony et al., 2006). This suggests that auxin promotes disease susceptibility and repression of auxin signaling could potentially result in enhanced resistance in plants. Indeed, down regulation of auxin signaling has been shown to contribute to plant induced immune responses in Arabidopsis. Navarro et al. (2006) showed that down regulation of auxin receptor genes by over expression of a micro RNA (miR393), which targets auxin receptors, increased resistance against *Pst* DC3000 in Arabidopsis. In contrast, activation of auxin signaling through over expression of an auxin receptor that is partially refractory to miR393-mediated transcript cleavage, enhanced susceptibility to *Pst* DC3000 (Navarro et al., 2006). These results suggest that auxin promotes susceptibility to bacterial disease, and that down-regulation of auxin signaling is part of the plant induced immune response. Treatment of Arabidopsis plants with an SA analog, benzothiadiazole S-methyl ester (BTH) results in the repression of a number of auxin responsive genes, including an auxin importer AUX1, an auxin exporter PIN7, auxin receptors TIR1 and AFB1, and genes belonging to auxin inducible SAUR and Aux/IAA family (Wang et al., 2007). Similarly, it was found that majority of the above auxin-inducible genes were also repressed in systemic tissues after induction of SAR, indicating that SAR response involves down-regulation of auxin responsive genes. However, the level of free auxin did not change after SA treatment. In addition, SA has been shown to inhibit the expression of the auxin-inducible reporter DR5::GUS (Zhang et al., 2007), leading to the hypothesis that SA stabilizes Aux/IAA auxin repressors by limiting auxin receptors needed for the down-regulation of Aux/IAA proteins.

1.3.3. Non-self recognition - Pathogen-Associated Molecular Patterns (PAMPs) and Pattern Recognition Receptors (PRRs)

The ability to determine self from non-self is critical for plants to mount an effective immune response against potential pathogens. PAMPs, also known as general elicitors, offer one such opportunity. PAMPs are highly conserved and ubiquitous molecules widely distributed amongst microbial species

(pathogenic or not) where they carry out an essential function, but absent in the potential host species (Nurnberger and Lipka, 2005). A number of PAMPs that fulfill these criteria and elicit a defense response in plants have been identified from plant pathogens and reviewed in Nurnberger et al. (2004) (Table 1.1).

Table 1: Selected pathogen-associated molecular patterns (PAMPs) and their plant defence-inducing activities. Adapted from (Nurnberger et al., 2004).

PAMP	Pathogen(s)	Minimal structural motif required for defence activation	Biological response	References
LPS	Gram-negative bacteria (Xanthomonads, Pseudomonads)	lipid A?	oxidative burst, production of antimicrobial enzymes in pepper, tobacco, potentiation of plant defences in response to bacterial infection	(Meyer *et al.*, 2001; Newman *et al.*, 2002; Zeidler *et al.*, 2004)
flagellin	Gram-negative bacteria	flg 22 (amino-terminal fragment of flagellin)	induction of defence responses in tomato, Arabidopsis	(Felix *et al.*, 1999)
elongation factor (EF-Tu)	Gram-negative bacteria	Elf18 (N-acetylated amino-terminal fragment of EF-Tu)	induction of defence responses in Arabidopsis and other Brassicaceae	(Kunze *et al.*, 2004)
harpin (HrpZ)	Gram-negative bacteria (Pseudomonads, *Erwinia*)	undefined	HR-like cell death, induction of defence responses in various plants, systemic acquired resistance to microbial infection	(Wei *et al.*, 1992; He *et al.*, 1993; Lee *et al.*, 2001)
cold shock protein	Gram-negative bacteria, Gram-positive bacteria	RNP-1 motif (amino-terminal fragment of the cold shock protein)	oxidative burst, production of the plant stress hormone ethylene in Solanaceae	(Felix and Boller, 2003)
necrosis-inducing proteins	bacteria (*Bacillus* spp.), fungi (*Fusarium* spp.), oomycetes (*Phytophthora* spp., *Pythium* spp.)	undefined	HR-like cell death, induction of defence responses in many dicot plants	(Bailey, 1995; Fellbrich *et al.*, 2002; Mattinen *et al.*, 2004; Pemberton and Salmond, 2004; Qutob *et al.*, 2002; Veit *et al.*,
transglutaminase	oomycetes (*Phytophthora* spp.)	Pep-13 motif (surface-exposed epitope of the transglutaminase)	induction of defence responses in parsley, potato	(Nürnberger *et al.*, 1994; Brunner *et al.*, 2002)
lipid-transfer proteins (elicitins)	oomycetes (*Phytophthora* spp., *Pythium* spp.)	undefined	HR-like cell death, induction of defence responses in tobacco, systemic acquired resistance to microbial infection	(Osman *et al.*, 2001)
xylanase	fungi (*Trichoderma* spp.)	TKLGE pentapeptide (surface-exposed epitope of the xylanase)	HR-like cell death, ethylene production in tobacco, tomato	(Enkerli *et al.*, 1999; Ron and Avni, 2004)
invertase	yeast	N-mannosylated peptide (fragment of the invertase)	activation of the phenylpropanoid pathway, ethylene production in tomato	(Basse *et al.*, 1993)
β-glucans	fungi (*Pyricularia oryzae*), oomycetes (*Phytophthora* spp.), brown algae	tetraglucosyl glucitol, branched hepta-β-glucoside, linear oligo-β-glucosides	induction of defence responses in legumes, tobacco, rice	(Klarzynski *et al.*, 2000; Fliegmann *et al.*, 2004; Yamaguchi *et al.*, 2000)
sulphated fucans	brown algae	fucan oligosaccharide	induction of defence responses in tobacco, systemic resistance to viral infection	(Klarzynski *et al.*, 2003)
chitin	all fungi	chitin oligosaccharides (degree of polymerization > 3)	induction of defence responses in tomato, Arabidopsis, rice, wheat, barley	(Baureithel *et al.*, 1994; Ito *et al.*, 1997)
ergosterol	all fungi		induction of ion fluxes in tomato	(Granado *et al.*, 1995)
cerebrosides A, C	fungi (*Magnaporthe* spp.)	sphingoid base	phytoalexin production in rice	(Koga *et al.*, 1998)

Different plant species respond to different PAMPs. For example tobacco responds to cold-shock protein while Arabidopsis does not, and only members of the Brassicaceae have so far been shown to respond to EF-Tu (Felix and Boller, 2003; Kunze et al., 2004). While this represents a diverse set of molecules, within the proteinaceous PAMPs two themes have emerged. These molecules typically contain a short (10–25) amino acid epitope that elicits a stronger defence response than the complete protein. For example, from Gram-negative bacteria flg22, a highly conserved stretch of 22 amino acids from the N terminus of flagellin, is a more potent elicitor than flagellin (Felix et al., 1999), and the same is true of a highly conserved 15 amino acid stretch including the RNA-binding motif RNP-1 from the cold shock protein (Felix and Boller, 2003) and an 18 amino acid stretch from the N terminus of the

elongation factor EF-Tu (Kunze et al., 2004). However, there are exceptions; the elicitor effect of NPP1 (necrosis-inducing Phytophthora protein 1) requires an intact protein and overlapping peptide fragments were inactive (Fellbrich et al., 2002), perhaps indicating that it is the activity of this protein that is detected by the plant rather than a specific amino acid sequence. Presumably, there would be a huge selective advantage for mutations within these epitopes that rendered them inactive as elicitors of plant defense systems. However, it would seem that, in many cases, such mutations also have a deleterious effect on the function of these proteins in the pathogen. For example, in Pep-13, a 13 amino acid internal peptide of a 42 kDa transglutaminase enzyme from the cell wall of *Phytophthora sojae*, substitution of Trp231 to Ala abolished elicitor activity in parsley but with a concurrent 98% reduction in transglutaminase activity (Brunner and et al., 2002). Thus, it appears that plants have evolved receptors that recognize short highly conserved amino acid stretches of certain microbial proteins that cannot easily be altered without loss of the protein function. That said, certain microbes may have evolved the capacity to avoid detection by specific PRRs. For example, *Agrobacterium tumefaciens* and *Ralstonia solanacearum* (pathogens) as well as *Rhizobium meliloti* (symbiont) possess functional flagellins that do not elicit a defence response in Arabidopsis and the N-terminal peptide from *Pseudomonas syringae* pv. *tomato* DC3000 (Pst) EF-Tu is not as potent an elicitor in Arabidopsis as those from other bacteria (Kunze et al., 2004; Sun et al., 2006). The evolution of non-eliciting PAMPs is one way in which pathogens can overcome non-host resistance in plants; however, the lack of a single eliciting PAMP has not yet been directly shown to affect the virulence of the pathogen. Some experiments have shown that deletion of a specific PRR in the host affects susceptibility; however, in other studies wild-type plants and plants lacking a PRR were equally susceptible (Sun et al., 2006) (Zipfel et al., 2004). This could be explained by the evolution in plants of recognition systems for multiple PAMPs from the same micro-organism. For example, Arabidopsis recognizes both flagellin and EF-Tu and these PAMPs activate the same signalling and defence responses in a nonsynergistic manner (Zipfel et al., 2006). A recent gene expression profiling study has also demonstrated that the lack of flagellin perception does not dramatically alter PAMP-induced gene expression during infection of Arabidopsis by Pst (Thilmony et al., 2006).

1.3.4. Damage-Associated Molecular Patterns (DAMPs)

In addition to sensing invading microbes by means of PAMPs (infectious non-self), plants and animals can also sense infectious-self or modified-self via damage-associated molecular patterns (DAMPs). Many plant pathogens produce lytic enzymes to breach the structural barriers of plant tissues. The products generated by these enzymes may function as endogenous elicitors. Such DAMPs typically appear in the apoplast and, as in the case of PAMPs, can serve as danger signals to induce innate immunity (Matzinger, 2002).

1.3.4.1. Oligogalacturonides

Oligogalacturonides (OGs) are linear molecules of two to about twenty α-1,4-d-galactopyranoslyuronic acid (GalA) residues. OGs were the first plant oligosaccharins, biologically active carbohydrates that act as signal molecules, to be discovered (Bishop et al., 1981; Hahn, 1981). OGs are released upon fragmentation of homogalacturonan (HG) from the plant primary cell wall (Cote et al., 1998) by wounding or by pathogen-secreted cell wall-degrading enzymes (for example polygalacturonases, PGs). Indeed, PGs are not elicitors *per se*, but are rather able to release elicitor-active molecules from the host cell wall. When the activity of a fungal PG is modulated by apoplastic PG-inhibiting proteins (PGIPs), long-chain oligogalacturonides are produced (De Lorenzo et al., 2001; De Lorenzo and Ferrari, 2002) (Figure 1.5). OGs cannot be considered true PAMPs, since they are not derived from the pathogen. However, they are considered the classic examples of DAMPs that are generated by the host cell during the infection process.

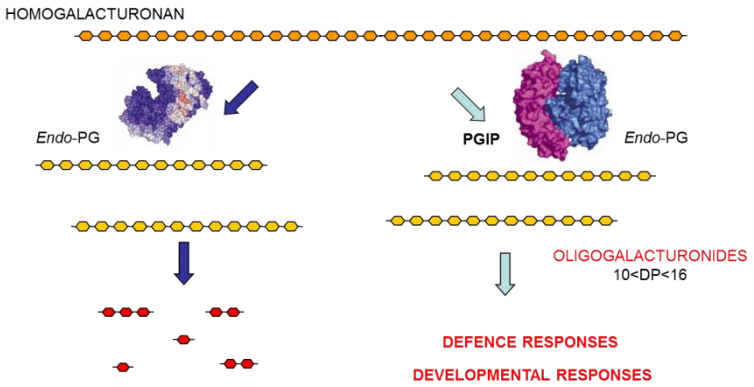

Figure 1.5 : Model for the OG accumulation during pathogen infection.

Chemically pure OGs can act as endogenous elicitors (Galletti et al., 2009). Biological responses to OGs occur in at least five of the six subclasses of dicotyledonous plants *Magnoliidae*, *Hamamelidae*, *Asteridae*, *Rosidae*, *Dilleniidae* (Reymond et al., 1996; Cote and Hahn, 1994) in a monocot (Moerschbacher et al., 1999) and a gymnosperm (Asiegbu et al., 1994). A number of different biological responses to OGs have been reported, and the particular response observed depends on the plant species, the bioassay, and the chemical structure of the OG used (Cote et al., 1998). A spectrum of modified and unmodified OGs of various lengths are active in different systems (reviewed by (Cote and Hahn, 1994).

The biological responses of plants to OGs can be divided into two broad categories: plant defense and plant growth and development (Cote and Hahn, 1994).

1.3.4.2. Oligogalacturonide-induced responses involved in plant defense

Pathogens enter plant tissues in at least three ways: digesting cell walls, entering through wounds, and invading through natural openings such as stomata. Pectins are one of the first targets of digestion by invading pathogens (Pagel and Heitifuss, 1990). OGs are released when PGs and endopectate lyases (PLs) secreted from the pathogen degrade the homogalacturonan in the cell (Cote et al., 1998). The OGs released are a carbon source for the pathogens, but can also be detected by plants as signals to initiate defense responses. Exogenously added OGs inhibit the light-induced opening of stomata in tomato and *Commelina communis L*. leaves (Lee et al., 1999) and elicit a variety of defense responses, including accumulation of phytoalexins (Davis et al., 1986), glucanase and chitinase (Davis and Hahlbrock, 1987; Broekaert and Pneumas, 1988). Stomatal openings provide access to inner leaf tissues required by many plant pathogens (Agrios, 1997), suggesting that the constriction of stomatal apertures is beneficial for plant defense. One of the first responses observed after the addition of OGs that is clearly involved in plant defense is the production of active oxygen species, including H_2O_2, and O_2- (Low and Merida, 1996). This oxidative burst occurs within a few minutes after the addition of OGs to suspension-cultured soybean (Legendre et al., 1993), tobacco (Rout-Mayer et al., 1997; Binet et

al., 1998) and tomato (Stennis et al., 1998) cells. Recently it was shown that, in Arabidopsis, production of H_2O_2 in response to OGs is mediated by AtrbohD (Figure1.6) (Galletti et al., 2008).

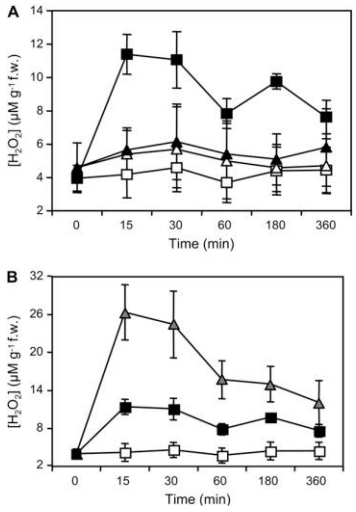

Figure 1.6 : Accumulation of extracellular H_2O_2 in response to OGs or G/GO in Arabidopsis seedlings. *(*a) Arabidopsis wild-type and *atrbohD* seedlings were treated with water (H_2O) or OGs for the indicated time (min). Arabidopsis wild-type (squares) and *atrbohD* (triangles) seedlings were treated with water (white symbols) or OGs (black symbols). (b) Arabidopsis seedlings were treated with water (H_2O, white squares), OGs (black squares), or G/GO (gray triangles). H_2O_2 accumulation in the culture medium, expressed as mM g21 fresh weight, was measured at the indicated times (min). Adapted from (Galletti et al., 2008).

OGs initiate signaling cascades that activate a plant defense. OGs rapidly activate AtMPK3 and AtMPK6 (Denoux et al., 2008), suggesting that, even though OGs and flg22 are perceived by distinct receptors, the signaling pathways mediated by these elicitors converge very early. Arabidopsis full-genome expression analysis reveals that OGs influence the expression of ~4000 genes (Ferrari et al., 2007). Some of these, such as *AtWRKY40* (At1g80840), encoding a transcription factor that acts as a negative regulator of basal defense (Xu et al., 2006), *CYP81F2* (At5g57220), encoding a cytochrome P450 and *RetOx* (At1g26380), encoding a protein with homology to reticuline oxidases, a class of enzymes involved in secondary metabolism and in defense against pathogens (Dittrich and Kutchan, 1991), are rapidly and strongly up-regulated upon exposure to elicitor. Early activation of genes in response to OGs is independent of SA, ET, and JA signaling pathways and of AtRbohD (Galletti et al., 2008). Exogenous treatment with OGs protects grapevine (*Vitis vinifera*) and Arabidopsis leaves against infection with the necrotrophic fungus *Botrytis cinerea* (Aziz et al., 2004; Ferrari et al., 2007), suggesting that production of this elicitor at the site of infection, where large amounts of PGs are

secreted by the fungus, may contribute to activate defenses responses. A variety of plant defense responses against microbial pathogens are regulated by the signaling molecules SA, JA and ET. Resistance to *Botrytis cinerea* induced in Arabidopsis by OGs is independent of SA, ET or JA signaling, but requires *PHYTOALEXIN DEFICIENT3* (PAD3) (Ferrari et al., 2007), a gene involved in the metabolism of Trp-derived secondary compounds (Zhou et al., 1999).

1.3.5 PAMP-Triggered Immunity Crosstalk with Auxin

Auxin has long been implicated in suppressing plant defense due to the fact that many pathogens, including *Pseudomonas syringae* and *Agrobacterium tumefaciens*, can directly synthesize auxin or manipulate auxin synthesis and signaling in plants to promote disease (Chen et al., 2007). Analysis of plant transcriptional reprogramming following some pathogen infections has shown a general de-repression of the auxin pathway including promotion of auxin biosynthetic genes and repression of AUX/IAA genes resulting in enhanced plant susceptibility (Thilmony et al., 2006). To combat the effects of pathogen produced or induced auxin to promote disease, plants actively suppress auxin signaling during defense (Navarro et al., 2004). Following flg22-treatment, wild-type Arabidopsis plants show a reduction in both transcript and protein levels of the auxin F-box receptors, resulting in stabilization of AUX/IAA proteins and repression of auxin-responsive genes (Navarro et al., 2006). This suppression is partially due to the activity of the microRNA miR393 , which is induced by flg22 and directly targets and cleaves TIR1, AFB2, and AFB3 transcripts (Navarro et al., 2006). Suppression of auxin signaling has been shown to be biologically relevant to PTI, as overexpression of miR393 enhances resistance to virulent pathogens and overexpression of AFB1 increases susceptibility relative to that observed in wild-type plants, as measured by bacterial growth (Navarro et al., 2006).

1.3.6 Salicylic Acid Crosstalk with Auxin

One of the primary ways SA has been shown to inhibit growth is by suppression of auxin signaling. A microarray study revealed that a number of auxin responsive genes were affected by BTH treatment; 21 genes encoding proteins involved in auxin reception, import and export and signaling were down-regulated and two genes encoding GH3 enzymes were up-regulated (Wang et al., 2007). As GH3 enzymes are responsible for regulating auxin homeostasis by conjugating IAA with different amino acids (Staswick et al., 2005), the transcriptional profile indicates a general BTH-dependent repression of auxin homeostasis and signaling. A follow-up study confirmed this by investigating the effect of SA on auxin levels, uptake, sensitivity, and signaling (Wang et al., 2007). It was shown that SA does not affect auxin synthesis, but instead represses the expression of the TIR1/ABF F-box genes , resulting in stabilization of AUX/ IAA repressor proteins to decrease auxin signaling (Wang et al., 2007). One of the two GH3 genes identified in the microarray study encodes GH3.5 (Wang et al., 2007), which conjugates IAA with Asp (Staswick et al., 2005). The GH3.5 knockout mutants were shown to be compromised in SAR while overexpression lines exhibited a dwarf phenotype, accumulated higher levels of SA, had elevated expression of PR1, and increased resistance to Pto DC3000 (Park et al., 2007; Zhang et al., 2007).

1.3.7 Oligogalacturonides Crosstalk with Auxin

The biological responses triggered by OGs are well documented and similar in many aspects to those of MAMPs (Galletti et al., 2009). For example, OGs and flg22 activate defense responses effective against the microbial pathogens Botrytis cinerea and Pseudomonas syringae, respectively, independently of SA, ET, and JA (Zipfel et al., 2004; Ferrari et al., 2007). Both elicitors trigger a fast and transient response characterized by activation of early stages of multiple defense signaling pathways. However, the response to flg22 is stronger in both the number of genes differentially expressed and the amplitude of change. Even at very high concentrations, OGs do not induce a response that is as comprehensive as that seen with flg22. For example, SA-dependent secretory pathway genes and PR1 expression are substantially induced only by flg22 (Denoux et al., 2008). Exogenously added OGs influence the growth and development of plant tissues (Cote and Hahn, 1994). OGs inhibit auxin-induced pea stem elongation (Branca et al., 1988) and are also active in the tobacco thin-cell layer (TCL) (Tran Thanh Van et al., 1985) (Mohnen et al., 1990), and the tobacco leaf explant

bioassays (Bellincampi et al., 1993). When biologically active OGs are added to media containing specific auxin concentrations, TCLs that would normally form few or no organs form flowers, while TCLs that normally form roots form significantly fewer roots (Eberhard et al., 1989). Biologically active OGs inhibit root formation on tobacco (Bellincampi et al., 1993) and Arabidopsis (Savatin et al., 2011) leafs respectively and increase stomata formation (Altamura et al., 1998) on tobacco leaf explants incubated in media with specific auxin concentrations. OGs also inhibited the expression, induced by exogenous auxin, of GUS driven by the synthetic promoter DR5; and inhibited the accumulation of auxin early up-regulated transcripts (IAA5 [At1g15580], IAA19 [At3g15540], IAA20 [At2g46990], IAA22 [At1g19220], SAUR16 [At4g38860], SAUR-AC1 [At4g38850], and GH3.3 [At2g23170]). In every case reported to date where OGs regulate the growth and development of plant tissues, with the exception of fruit ripening, their effect is the opposite of the effect of added auxin (Branca et al., 1988; Eberhard et al., 1989) (Altamura et al., 1998; Savatin et al., 2011). The mechanism by which OGs act in opposition to the action of auxin is presently unknown; in Savatin D. V. et al. 2011 it was shown that OG - auxin antagonism does not involve any of the following mechanisms: (1) stabilization of auxin-response repressors; (2) decreased levels of auxin receptor transcripts through the action of microRNAs. These data suggest that OGs antagonize auxin responses independently of Aux/Indole-3-Acetic Acid repressor stabilization and of posttranscriptional gene silencing; It was therefore speculated that OG – auxin antagonism can be played at the level of transcriptional regulation on the promoter of auxin-inducible genes antagonized by OGs.

2 Materials and Methods

2.1 Cloning of the promoter of *IAA5*

The promoter of the auxin-responsive gene *IAA5* (INDOLE-3-ACETIC ACID INDUCIBLE 5; TAIR accession: At1G15580) was cloned into the binary vector pCAMBIA 1391z (CambiaLab) using the "Cut & Paste" method . This involves preparing both a DNA fragment to be cloned (insert) and a self-

replicating DNA plasmid (vector) by cutting with two unique restriction enzymes that flank the DNA sequence and are present at the preferred site of insertion of the vector, often called the multiple cloning site (MCS). By using two different restriction enzymes, two non-compatible ends are generated, thus forcing the insert to be cloned directionally, and lowering the transformation background of re-ligated vector alone. The pCAMBIA 1391z vector contains the GUS reporter gene downstream of the MCS and two antibiotic resistance genes; the kanamycin resistance gene for selection of *Escherichia coli* and *Agrobacterium tumefaciens* transformants and the hygromycin resistance gene for the selection of plant transformants Figure 2.1. The promoter of *IAA5* (*PIAA5*), the –1279 bp sequence upstream of the coding region of *IAA5* gene, was amplified by PCR from genomic DNA of *Arabidopsis thaliana*. The primers used for the amplification contain at the 5' extremity a restriction site for restriction enzymes; the forward (fw) primer contains the restriction site of pSTI restriction enzyme, while the reverse (rev) primer contains the restriction site of ECORI restriction enzyme. The PCR product was separated and visualized on 1% agarose gel stained with ethidium bromide (EtBr) and the fragment purified using QIAquick PCR Purification Kit (QIAGEN). Two hundred and fifty ng of the fragment containing the promoter of *IAA5* and 100 ng of pCAMBIA 1391z were digested in parallel with pSTI and ECORI restriction enzymes (FastDigest—Thermo Scientific) according to the manufacturer instructions and purified using QIAquick PCR Purification Kit for the fragment and QIAprep Spin Miniprep Kit (QIAGEN) for the vector.

The digested fragment (18 ng) and vector (60 ng) were ligated with T4 ligase (Promega) according to the manufacturer instructions. The ligation between the fragment and the vector was confirmed by mixed primers PCR using the forward primer of *PIAA5* that anneal on the fragment and the reverse primer that anneal on GUS reporter gene. The ligation product was subsequently used to transform *E. coli* DH5α electro-competent cells. *E. coli* DH5α electro-competent cells were transformed with 3 ng of ligation product between *PIAA5* and pCAMBIA1391z by electroporation. Cell suspension was thawed on ice and 3 ng of ligation product were added. The cells were kept 2 min on ice, transferred in the electroporation cuvette and electroporated with BIO-RAD MicroPulser, electrical condition of 1.5 kV. After the electric pulse 1 mL of Luria Bertani (LB; tryptone 10 g ; yeast extract 5 g and NaCl 10 g in 1 L of deionized water) medium was quickly added to electroporated cells. Cells were recovered at 37 °C for 1 h with shaking, plated on LB containing 20 µg/ml of kanamycin and grown 16 hours at 37 °C to select the transformants. Transformants were screened by colony-PCR and positive colonies containing pCAMBIA1391z ligated with *PIAA5* were inoculated in 5 ml of LB with 20 µg/ml of kanamycin and grown 16 hours at 37 °C to increase the copy number of the *PIAA5* containing construct. The *PIAA5*

containing construct was purified with QIAprep Spin Miniprep Kit (QIAGEN), sequenced to verify the sequence of *PIAA5* and digested with pSTI and ECORI restriction enzymes (FastDigest—Thermo Scientific) to confirm the presence of *PIAA5*. *A. tumefaciens* strain GV3101, containing rifampicin resistance on the genome and gentamycin resistance in the helper plasmid, was transformed by electroporation with the *PIAA5* containing construct. Cell suspension was thawed on ice and 50 ng of *PIAA5* containing construct were added. The cells were kept 2 min on ice, transferred in the electroporation cuvette and electroporated with BIO-RAD MicroPulser, electrical condition of 1.5 kV. After the electric pulse, 1 mL of Luria Bertani medium was quickly added to electroporated cells. Cells were recovered at 28 °C for 2 h with shaking, plated on LB containing 20 µg/ml of kanamycin, 20 µg/ml of rifampicin, 20 µg/ml gentamycin and grown 16 hours at 28 °C to select the transformants. The presence of *PIAA5* containing construct was confirmed by colony-PCR on the trasformants. Positive colonies were inoculated in 5 ml of LB containing 20 µg/ml of kanamycin, 20 µg/ml of rifampicin, 20 µg/ml gentamycin and grown 16 hours at 28 °C, pelleted, re-suspended with LB containing 20% (v/v) glycerol and stored at -80 °C.

Primers used:

PIAA5 pSTI fw-5'AGCTCTGCAGAATTCGGTTGTATTTGCGGA-3'

PIAA5 ECORI rev-5'AAGCTGAATTCCTTTGATGTTTTTGATTGAAAAGTATT3'

GUSrev-5' AGTTGCAACCACCTGTTGAT

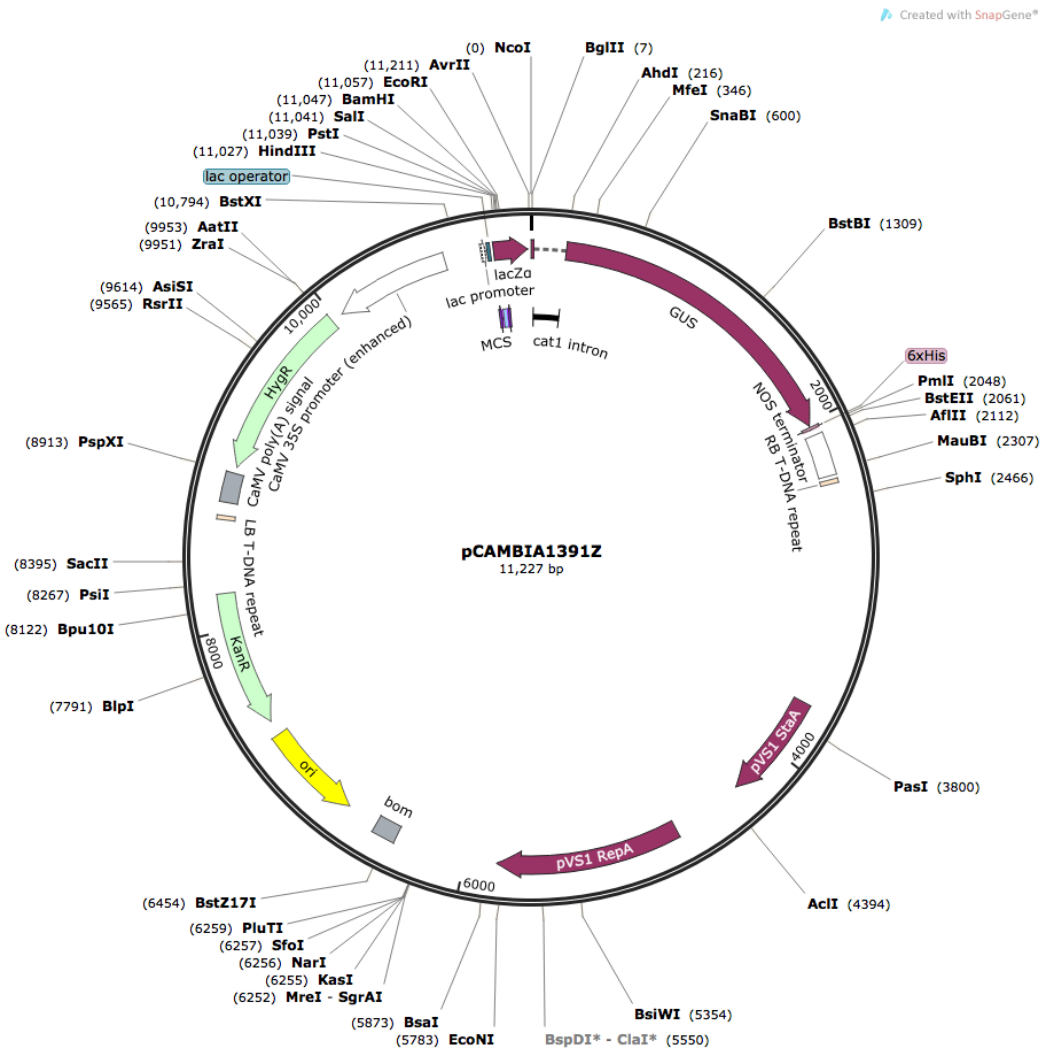

Figure 2.1: the pCAMBIA 1391z vector is an *Agrobacterium* binary vector for plant transformation; it contains the GUS reporter gene downstream of the MCS and two antibiotic resistance genes; the kanamycin resistance gene for selection of *E. coli* and *A. tumefaciens* transformants and the hygromycin resistance gene for the selection of plant transformants.

2.2 Plant growth and transformation with *PIAA5*-GUS

The promoter (–1279 bp sequence upstream of the coding region) of the auxin-responsive gene *IAA5*, was cloned into the binary vector pCAMBIA 1391z (CambiaLabs), upstream of the GUS reporter gene (Jefferson et al., 1987). *Arabidopsis thaliana* plants (Columbia-0 ecotype) were grown on soil in a growth chamber for 30 days at 22°C, 70% relative humidity, with a photoperiod of 16 h light and light intensity of 100 µE m^{-2} s^{-1}. Flowering plants were transformed by *Agrobacterium tumefaciens* mediated transformation using the floral dip method (Clough and Bent, 1998). The seeds collected after the floral-dip transformation were washed for 1 min in 1 mL of isopropanol and for 1 min in sterile ultrapure H_2O (for two times). Seeds were surface sterilized for 10 min in 1 mL sterilization solution (1.6 % NaClO, 0.01% SDS) with shaking. To remove the sterilization solution, the seeds were washed under sterile flow hood with sterile ultrapure H_2O (for five times). The sterilized seeds were wrapped in aluminum foil and placed at 4 ° C for 3 days to synchronize the germination (vernalization). In order to select the PIAA5:GUS transformant plants, seeds were plated on Petri dishes containing the selective solid medium, prepared by dissolving 2.2 g of Murashige and Skoog medium with vitamins (MS/2); 0.5% sucrose, 1% plant agar, and the antibiotic hygromycin (20 µg/ml) in 1 L of distilled water at pH 5.5.

2.3 Induction of GUS expression driven by the promoter of *IAA5*

To induce the expression of GUS reporter gene in response to auxin (IAA), seeds from T2 generation of PIAA5:GUS transgenic lines and T3 generation of DR5:GUS transgenic lines (Ulmasov et al., 1997) were surface sterilized and vernalized as described above and grown 5 or 15 days in 6 well plates containing 5 mL of sterile MS/2 medium including vitamins and 1% sucrose in a growth chamber at 22°C, 70% relative humidity, with a photoperiod of 16 h light and light intensity of 100 µE m^{-2} s^{-1} ., The seedlings were treated for 6h with 2.5 µM IAA or 5µM IAA, to induce GUS expression under the control of *PIAA5*, or mock treated with H_2O. DR5:GUS seedlings were treated for 6h with 2.5 µM IAA and used as positive control. To observe the effect of OG on the IAA-induced GUS expression the seedlings were treated for 6h with 5 µM IAA + 50 µg/mL OG or mock treated with H_2O.

2.4 Histochemical Localization of GUS Activity

To reveal the auxin-induced GUS activity driven by *PIAA5* or DR5; IAA-treated, IAA + OG co-treated and mock-treated seedlings, were placed in 6 well plates with 5 mL of GUS staining solution (50 mM Phospate Buffer pH 7 , 0.2% Triton-X 100 , 2 mM $K_3Fe(CN)_6$, 2 mM $K_4Fe(CN)_6$, 2 mM 5-bromo-4-chloro-3-indolyl-D-glucuronide); vacuum infiltrated for 5 min and placed at 37°C overnight (Jefferson et al., 1987). To reveal the GUS staining, seedlings were discolored with 5 washes of boiling ethanol. Seedlings were observed with a light microscopy (Nikon).

2.5 Analyses of GUS transcript level in response to IAA and IAA + OG co-treatment

T2 generation of PIAA5:GUS transgenic lines were grown in 6 well plates containing 5 mL of sterile MS/2 medium including vitamins and 1% sucrose in a growth chamber at 22°C, 70% relative humidity, with a photoperiod of 16 h of light and light intensity of 100 µE m-2 s-1 . Seedlings were treated for 1 h with 1.5 µM IAA ; 1.5µM IAA + 100 µg/mL of OGs or mock treated with sterile ultrapure H_2O. Treated seedlings were frozen in liquid nitrogen, homogenized with a MM301 ball mill (Retsch), and total RNA was extracted with Isol-RNA lysis reagent (5 prime) according to the manufacturer's protocol. RNA was treated with RQ1 DNase (Promega) and first-strand cDNA was synthesized using ImProm-II reverse transcriptase (Promega) according to the manufacturer's instructions. Real-time qPCR analysis was performed as previously described (Galletti et al., 2011) using a CFX96 real-time system (Bio-Rad). One microliter of cDNA (corresponding to 50 ng of total RNA) was amplified in a 30 mL reaction mix containing 1X GoTaq real-time PCR system (Promega) and 0.4 mM of each primer. Expression levels of GUS, relative to UBQ5, were determined using a modification of the Pfaffl method (Pfaffl, 2001) as previously described (Ferrari et al., 2006).

Primer sequences are:
-UBQ5fw-5'-GGAAGAAGAAGACTTACACC,
-UBQ5rev-5'-AGTCCACACTTACCACAGTA;
-GUSfw-5'- AATGGTGATTACCGACGAAA
-GUSrev-5'- AGTTGCAACCACCTGTTGAT

2.6 Plant material and growth conditions

Arabidopsis thaliana Columbia-0 seeds (10 mg; approximatively 500 seeds) were surface sterilized and vernalized as described above. One liter of liquid medium was prepared by dissolving 2.2 g of Murashige and Skoog medium with vitamins (MS/2) and 1% sucrose, in distilled water at pH 5.5. The liquid medium was sterilized with filtration apparatus under a sterile flow hood. The seeds were placed in 500 mL Erlenmeyer flasks containing 100 mL of medium previously autoclaved at 120°C for 20 min, and grown for 15 days at 22°C, 70% relative humidity, with a photoperiod of 16 h light and light intensity of 100 μE m^{-2} s^{-1} .

2.7 Plant treatments

For the DNA Affinity Purification experiments 15-days-old *Arabidopsis thaliana* seedlings were treated in the Erlenmeyer flasks for 1 h with IAA and IAA+ OG co-treatment.

For the nuclear proteomic analyses 15-days-old *Arabidopsis thaliana* seedlings were treated in the Erlenmeyer flasks for 1 h with IAA, OG , IAA+ OG co-treatment and mock treated.

Auxin treatments were performed by adding 100 μL of 1.5mM IAA dissolved in sterile ultrapure H_2O to the Erlenmeyer flasks to a final concentration of 1.5 μM IAA. Ten mg of oligogalacturonides (degree of polymerization 10-15) were dissolved in 1 mL of sterile ultrapure H_2O (10 mg/mL) and added to the Erlenmeyer flasks to a final concentration of 100 μg/mL of OGs. Co-treatments were performed by adding 100 μL of 1.5mM IAA dissolved in sterile ultrapure H_2O and 1 mL of 10mg/mL OG solution into the Erlenmeyer flasks to a final concentration of 1.5 μM IAA + 100 μg/mL of OGs. Mock treatments were performed by adding 1 mL of sterile ultrapure H_2O to the Erlenmeyer flasks.

2.8 Analyses of the transcript levels of *IAA5* and *RetOX* in response to the treatments

To evaluate the effectiveness of the treatments, the transcript levels of *IAA5* and *RetOx* were analysed by semi-q PCR. Seedlings were frozen in liquid nitrogen, homogenized with a MM301 ball mill

(Retsch), and total RNA was extracted with Isol-RNA lysis reagent (5 prime) according to the manufacturer's protocol. RNA was treated with RQ1 DNase (Promega) and first-strand cDNA was synthesized using ImProm-II reverse transcriptase (Promega) according to the manufacturer's instructions. *IAA5* transcript levels were measured to verify the response to IAA treatment and IAA + OG co-treatment, while *RetOX* transcript levels were measured to verify the response to OG treatment. *UBQ5* is not involved in the response to IAA or OG and was used as reference gene. The mixture of the reagents for the PCR were prepared in sterile tubes on ice, according to the manufacturer instruction (RBC Bioscencies):

1X Reaction Buffer

0.1 μM dNTP mix

0.2 μM Primer mix

1 μL cDNA

1.25U RBC Taq DNA polymerase (5U/μl)

sterile ultrapure H_2O.

Semi-qPCR were performed on Mycycler personal thermal cycler (Bio Rad) and the program used was:

- 94°C for 2 min
- 35 cycles at 94°C for 20 sec; 58°C for 20 sec; 72°C for 20 sec

UBQ5 and *RetOx* amplicons were taken at the step of primers annealing of the 29^{th} cycle while *IAA5* amplicons were taken at the step of primers annealing of the 35^{th} cycle.

PCR products were separated and visualized onto 1% agarose gel stained with EtBr .

Primer sequences:

-UBQ5fw-5'-GGAAGAAGAAGACTTACACC-3'

-UBQ5rev-5'-AGTCCACACTTACCACAGTA-3'

-IAA5fw-5'- ACCGAACTACGGCTAGGTCT-3'

-IAA5rev-5'- CTGTTCTTTCTCCGGTACGA-3'

-RetOxfw-5'- AGGTTCTCGAACCCTAACAACA-3'

-RetOxrev-5'- GCACAGACGACACGTAAGAAAG

2.9 Purification of Nuclei

Purified nuclei extracted from treated seedlings are the starting material for extraction of nuclear proteins for both the DNA affinity purification experiments and nuclear proteome analysis. Purification of nuclei from *Arabidopsis thaliana* seedlings was based on precedent work (Folta and Kaufman, 2007) with some modifications: *Arabidopsis* seedlings were harvested and excess liquid medium was removed with filter paper. All the following steps were performed on ice or in a cold chamber. Plant material was homogenized in a pre-cooled Waring blender in 4 mL of Extraction Buffer (2.0 M hexylene glycol, 20 mM PIPES-KOH pH 7.0, 10 mM $MgCl_2$ and 5 mM 2-mercaptoethanol, 1 mM phenyl-methyl-sulphonyl-fluoride and protease inhibitor cocktail) per g of fresh tissue, using 6 pulses of 5 sec at the lowest speed. The crude homogenate was filtered twice through 3 layers of cheesecloth and 25% Triton-X 100 was carefully added to the homogenate to a final concentration of 1%. The crude homogenization filtrate was centrifuged at 1000 xg in a swinging-bucket rotor at 4°C and the pellet consisting of the crude nuclear fraction was re-suspended in 10 mL of 80% Percoll solution (80% Percoll, 0.5 M hexylene glycol, 5 mM PIPES-KOH pH 7.0 , 10 mM $MgCl_2$, 5 mM 2-mercaptoethanol , 1% Triton X-100 , 1 mM phenyl-methyl-sulphonyl-fluoride and protease inhibitor cocktail). Nuclear fraction was enriched using a discontinuous density gradient: the homogenate in the 80% Percoll solution was layered under 10 mL of 60% and 10 mL of 30% Percoll solutions (60% or 30% Percoll, 0.5 M hexylene glycol, 5 mM PIPES-KOH pH 7.0 , 10 mM $MgCl_2$, 5 mM 2-mercaptoethanol, 1% Triton X-100, 1 mM phenyl-methyl-sulphonyl-fluoride and protease inhibitor cocktail) in a 50 mL centrifuge tube Figure 2.2. After centrifuging at 1000 xg for 2 h at 4°C the enriched nuclear fraction was stratified at the interface between Percoll 30% and 60% while the interface between Percoll 60% and 80% contained broken nuclei Figure 2.2. The enriched nuclear fraction was collected with a Pasteur pipette and washed with 1 mL of Gradient Buffer (0.5 M hexylene glycol, 5 mM PIPES-KOH pH 7.0 , 10 mM $MgCl_2$, 5 mM 2-mercaptoethanol , 1% Triton X-100 , 1 mM phenyl-methyl-sulphonyl-fluoride and protease inhibitor cocktail) per g of fresh tissue. Washed nuclei were pelleted at 1000 xg for 10 min at 4°C and re-suspended in 1 mL of Gradient Buffer per g of fresh tissue. Purified nuclei were pelleted at 1000 xg for 10 min at 4°C, re-suspended in 120 μL of Nuclei Storage Buffer (50 mM Tris–HCl (pH 7.8), 10 mM 2-mercaptoethanol, 20% glycerol, 5 mM $MgCl_2$ and 0.44 M sucrose) per g of fresh tissue and stored at -20 °C.

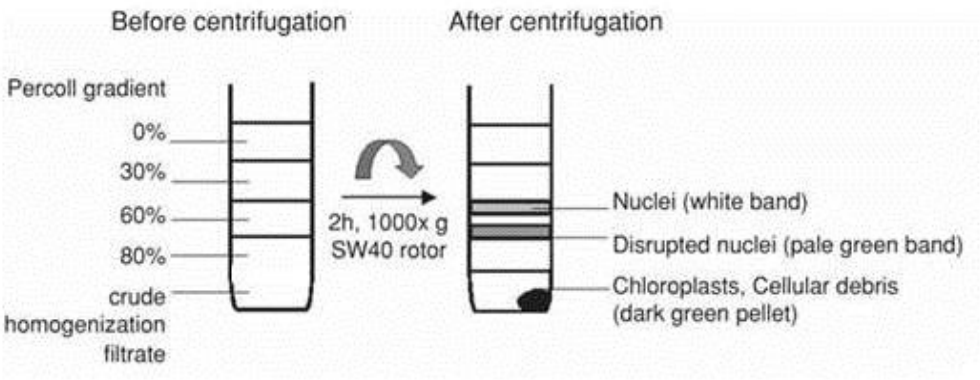

Figure 2.2: Discontinuous Percoll density gradient used for the enrichment of the nuclear fraction. The crude nuclear fraction was resuspended in 80% Percoll solution; discontinuous density gradient was obtained by overlaying with 60% and 30% Percoll solutions. After centrifugation for 2 h at 1000 xg in a swinging bucket rotor, the nuclear fraction stratifies in the interface between 30% and 60% Percoll solution separating from disrupted nuclei, chloroplast and cellular debris. Adapted from (Calikowski and Meier, 2007).

2.10 SDS-PAGE denaturing electrophoresis and western blot analysis

The nuclei purification was monitored by detecting the amount of the H3 histone in different fractions during the purification process.

Before the immunoblotting proteins in the total homogenate, enriched nuclear fraction (30%-60% Percoll interface), broken nuclei (60%-80% Percoll interface) and purified nuclei were quantified with Bradford Assay (Bradford, 1976). 1.5 µg of proteins from each sample were separated on acrylamide gels as described in (Desiderio et al., 1997). Subsequently, the proteins were blotted onto nitrocellulose membranes (Hybond C-EXTRA Amersham ECL) in transfer buffer composed of 100 mL of buffer 10X stock (96.8 tris gr / L, glycine 9.74 g / L, pH 9.2), 200 mL of methanol and 700 ml of ultrapure H_2O, using a trans-blot apparatus (BIORAD) at a constant voltage of 100 V for 1 h at 4 ° C. After transfer, the nitrocellulose membrane was immersed for 2 h under gentle shaking at room temperature in 100 mL of blocking buffer, consisting of 10 X 10 mL of TBS (Tris-HCl 50 mM, NaCl 150 mM), 0.1% Tween 20 , 5 g of BSA. The filter was washed with washing buffer consisting of 50 mL of buffer stock 10 X TBS, 0.2% Tween 20 (1x 10 min and 2x 5 min). Next, the membrane was incubated for 12 h at room temperature under shaking in a solution of primary antibody αH3 diluted 1: 1000 in wash buffer with 5% BSA. The membrane was washed in wash buffer as described above and incubated for

1.5 h at room temperature with the secondary antibody (anti-rabbit IgG conjugated to a peroxidase - Amersham RPN 2108) diluted 1: 5000 in wash buffer with 5% BSA . After the washes (as described above), the filter was immersed in 3 mL of solution 2 ECL + 3 mL of solution 1 ECL (Amersham ECL Western blotting analysis system) for 1 min and then dried between two sheets 3 MM paper. Image acquisition was performed using a ChemiDoc system (Biorad) with exposure times between 120 and 1800 sec.

2.11 Fluorescent microscopy

DAPI (4',6-diamidino-2-phenylindole) binds strongly to A-T rich regions in DNA. It is used extensively in fluorescence microscopy and can be used to stain nuclei. When bound to double-stranded DNA, DAPI has an absorption maximum at a wavelength of 358 nm (ultraviolet) and an emission maximum at 461 nm (blue). Therefore for fluorescence microscopy DAPI is excited with ultraviolet light and is detected through a blue/cyan filter. To verify the presence of intact nuclei after the purification procedure, one drop of the purified nuclear fraction was fixed on microscope slide, stained with DAPI for 1 min in the dark and observed by fluorescence microscopy.

2.12 Protein extraction for the DNA Affinity Purification Experiments

For the DNA affinity purification experiments the proteins were extracted from purified nuclei according to Calikowski and Meier, 2007. The nuclear suspension in Nuclei Storage Buffer was thawed on ice, and the exact volume was determined before addition of 190µL of buffer per mL of suspension Nuclear Lysis Buffer (50 mM HEPES, pH 7.6, 2.5 M KCl, 5 mM $MgCl_2$, 20% glycerol, 1 mM DTT, protease inhibitor cocktail) to give a final concentration of KCl of 0.47 M . The suspension was kept 30 min at 4°C with gentle shaking. Nuclear suspension was diluted with 3 mL of Dialysis Buffer (20 mM HEPES, pH 7.9, 100 mM KCl, 0.1 mM EDTA, 10% (v/v) Glycerol) for mL of suspension. The lysed nuclei were centrifuged at 48200 xg for 30 min at 4°C to sediment the chromatin. The supernatant containing the solubilized nuclear proteins was collected without disturbing the viscous, whitish pellet, which contains genomic DNA, transferred into dialysis tubing (5000 MWCO) and dialyzed 4 h at 4°C against 5 changes of 250 mL of dialysis buffer. Nuclear proteins were quantified according to

(Bradford, 1976), against BSA standards prepared in Dialysis Buffer and aliquoted based on protein amount (50 μg) .

2.13 Probes for the DNA Affinity Purification Experiments

The promoter regions of *IAA5* and *UBQ5* genes (-1279 bp and -1000 bp from the ATG respectively) were amplified from genomic DNA using biotinylated primers and purified using QIAquick PCR Purification Kit (QIAGEN) ; biotinylated DR5 and a control fragment (CTR) (Hsieh et al., 2012) were purchased as synthetic sequences from Eurofin Genomics.

Primer sequences:
PIAA5 fw-5'-biotin-AATTCGGTTGTATTTGCGGA-3'
PIAA5 rev -5'-CTTTGATGTTTTTGATTGAAAGTATT-3'
PUBQ5 fw-5'-biotin-CTCTAGGTTTATCTTCCGTCTTATC-3'
PUBQ5 rev-5'-CTTTTGAGGCAACGGCTGCTGAAGA -3'

Synthetic sequences
DR5: 5'-biotin-CCTTTTGTCTCCCTTTTGTCTCCCTTTTGTCTCCCTTTTGTCTCC
CTTTTGTCTCCCTTTTGTCTCCCTTTTGTCTC-3'

CTR 5'-biotin-GAGGTCGACGGTATCGATAAGCTTGATATCGAATTCCTGCAG
CCC-3'

2.14 DNA Affinity Purification of *PIAA5* and DR5 binding proteins

To identify and quantify *PIAA5* and DR5 binding proteins, nuclear proteins (150 μg) extracted after IAA treatment or IAA + OG co-treatment were pre-incubated with 0.1 μg of Poly dI/dC (Sigma) on ice for 10 min before being added to 50 mg of Dynabeads M-280 (Invitrogen) conjugated (according to

the manufacturer instruction) with 500 ng of 5'-end biotin labeled *PUBQ5* for 10 min at 4°C. This is intended to pre-clear the nuclear proteins from experimental contaminants. To identify *PIAA5* specific interactors, pre-cleared proteins were collected and added to Dynabeads (Invitrogen) conjugated with 500 ng of 5'-end biotin labeled *PIAA5* or *PUBQ5* as control fragment. To identify DR5 specific interactors, pre-cleared proteins were collected and added to Dynabeads (Invitrogen) conjugated with 500 ng of 3'-end biotin labeled DR5 or CTR as control fragment. After incubation at room temperature for 30 min with gentle rotation, nonspecific proteins were removed by washing five times with 100 µL of wash buffer (20 mM HEPES/KOH, pH 7.9, 50 mM KCl, 1 mM $MgCl_2$, 0.5 mM DTT, 10% glycerol, protease inhibitor cocktail and 0.1 µg poly dI-dC). DNA-protein complexes were fractionated by a first eluition with high salt wash buffer (20 mM HEPES/KOH, pH 7.9, 100 mM KCl, 1 mM $MgCl_2$, 0.5 mM DTT, 10% glycerol, protease inhibitor cocktail and 0.1 µg poly dI-dC); eluted proteins were vacuum dried and re-suspended in 20 µL of 8M urea, 10 mM tris-HCl pH 8. The proteins bounded to the probes were solubilized with 20 µL of 8M urea, 10 mM tris-HCl pH 8. Proteins were reduced, alkylated and digested with trypsin and protein content quantified with label-free LC-MS/MS as descripted below.

2.15 Reduction, alkylation and in-solution digestion of proteins

The reduction of the disulfide bridges between cysteine residues were performed at 56°C for 30 min by adding 1 µL of 50 mM DTT for 50 µg of proteins. Next, free thiol groups were alkylated with 1 µL of 50 mM iodoacetamide in 50 mM NH_4HCO_3 for 50 µg of proteins, in the dark at room temperature for 20 min. Before trypsin addition, protein samples were diluted with four volumes of 50 mM NH_4HCO_3. Proteolytic digestion was performed by adding 1 µg of trypsin (Promega) for 50 µg of proteins at 37°C over-night. Trypsin cleaves at the carboxy-terminal of lysin and arginine residues. Digestions were blocked by acidifying with 5 µL of 100% formic acid (Sigma).

2.16 Sample preparation for LC-MS/MS analysis

Reverse-phase chromatography in custom made micro-columns (Gobom et al., 1999) was used to clean the samples from salts and detergents, and to concentrate the peptides. In details, a C18

chromatographic resin disk (3M empore C18) was used to block a 200 µL tip that was filled with a suspension of R3 resin (Applied Biosystems, POROS, Reversed-Phase Media) in 70 % CH_3CN. The column was packed applying a moderate pressure with a syringe. After washing with 20 µL of 70% CH_3CN, the column was equilibrated with 100 µL of 0.1 % TFA and the sample was loaded carefully into the column to allow peptide binding to the resin. The column was washed with 100 µL of 0.1 % TFA and peptides were eluted with 100 µL 80% CH_3CN, 0.1% TFA.

2.17 Identification and quantification of proteins with mass spectrometry

Mass spectrometry is one of the most currently used methods for the identification of proteins. A mass spectrometer consists of three main components: an ion source in which the analyte is volatilized and ionized; a mass analyzer which separates ions according to mass / charge ratio (m / z); a detector that detects the ions and produces a mass spectrum with m / z ratio in the abscissa and the signal intensity on the ordinate. There are two types of sources of "soft" ionization used in the analysis of peptides: the MALDI (Matrix Assisted Laser Desorption Ionization) source and ESI (Electro Spray Ionization) source. In the case of ESI ionization the sample is introduced in the liquid phase within a capillary which is applied a voltage rather high which causes, once leaked from the capillary nebulization in the form of droplets containing the ionized sample and the solvent . After evaporation of the solvent, the ions (of the same charge) of the sample tend to repel causing the explosion of the drop and the release of the ions in the gas phase which are then accelerated towards the analyzer. The ESI-MS can be coupled to a separation system in the liquid phase as the capillary electrophoresis or liquid chromatography (LC), with the advantage of being able to separate the peptides and thus reduce the complexity of the sample. In tandem mass spectrometry, the ions formed in the source are selected according to their m / z ratio in a first analyzer which acts as a mass filter, and then directed into a collision cell, inside which there is a flow of inert gas (nitrogen or argon): the collision of peptide ions with the gas causes fragmentation, a phenomenon known as collision induced dissociation (CID). Finally, a second analyzer scans the fragment ions that are directed to the detector, producing a spectrum of mass-mass (MS / MS). When a peptide is fragmented on a peptide bond, only one of the two fragments acquires the charge: the fragments that are ionized at the carboxy-terminal ions are called "y", while those that are ionized amino-terminal end are called "b" ions. In the mass-mass spectrum, each peak corresponds to a fragment "b" or "y"; from the difference in mass between

adjacent fragments of the same series ("y" or "b") is obtained the mass corresponds to a specific amino acid residue. So the analysis of the spectrum of fragmentation is possible to obtain a partial amino acid sequence of the peptide. The quantification of differences between two or more physiological states of a biological system can be achieved with mass-spectrometry-based quantification methods. Differential stable isotope labeling of the peptides create a specific mass tag that can be recognized by a mass spectrometer and at the same time provide the basis for quantification. These mass tags were chemically introduced on the peptides as different isotopes of formaldehyde (Boersema et al., 2009). In contrast, label-free quantification approaches aim to correlate the mass spectrometric signal of intact proteolytic peptides or the number of peptide sequencing events with the relative or absolute protein quantity directly. Currently, two widely used but fundamentally different label-free quantification strategies can be distinguished: (a) measuring and comparing the mass spectrometric signal intensity of peptide precursor ions belonging to a particular protein and (b) counting and comparing the number of fragment spectra identifying peptides of a given protein. In the former approach, the ion chromatograms for every peptide are extracted from an LC-MS/MS run and their mass spectrometric peak areas are integrated over the chromatographic time scale. For low-resolution mass spectra this is typically done by creating extracted ion chromatograms (XICs) for the mass to charge ratios determined for each peptide (Bondarenko et al., 2002). The latter approach, called spectral counting approach is based on the empirical observation that the more of a particular protein is present in a sample, the more tandem MS spectra are collected for peptides of that protein. Hence, relative quantification can be achieved by comparing the number of such spectra between a set of experiments.(Gilchrist et al., 2006). In this work the relative quantification of protein abundance in both control and test probe in the DNA affinity purification experiments was achieved by label free approach, while the quantification of differences between nuclear proteome of differentially treated (IAA, OG, IAA + OG) *Arabidopsis* seedlings was achieved by stable isotope labeling of the peptides and by label-free quantification. The label-free quantification of proteins was achieved by the use of MaxLFQ algorithms, part of the MaxQuant software suite, that rely on XIC-based approaches (Cox et al., 2014).

2.18 LC-MS/MS analyses

The analysis of tandem mass spectrometry coupled with liquid chromatography (LC-MS / MS) were performed using a configuration nano HPLC (Dionex Ultimate 3000 nano LC) coupled to a mass

spectrometer analyzer with hybrid linear ion trap - Orbitrap, equipped with a source nanoESI (LTQ Orbitrap XL Discovery, ThermoFinnigan San Jose, Ca). Through the autosampler, 5 µL of each sample were loaded on a nano-column of 75 µm (ID) x 17 cm, packed manually with reverse phase C18 resin (Magic C18AQ; particle size: 5 m; measurement of pore : 200 Å; Michrom Bioresources, Auburn, CA). The chromatografic separation of the peptides took place at a flow of 300 nL / min using a "multi-step" 180 min gradient from 5% to 80% of solvent B (0.1% formic acid, 90% CH_3CN) Figure 2.3. The instrument operated in data-dependent mode, alternating a full-scan MS event in five events MS / MS on the 5 most abundant ions. Full-scan MS spectra (from m / z 300-2000) were acquired in the Orbitrap analyzer with resolution R = 30,000 at m / z 400. The five most intense peptide ions with charge status ≥2 were sequentially isolated and fragmented by collision induced dissociation (CID) in the LTQ linear ion trap using a collision energy of 35% and an activation time of 30 ms. The spectrometer operated in positive ion mode with a capillary voltage of 37 V and the spray voltage of 1.9 kV.

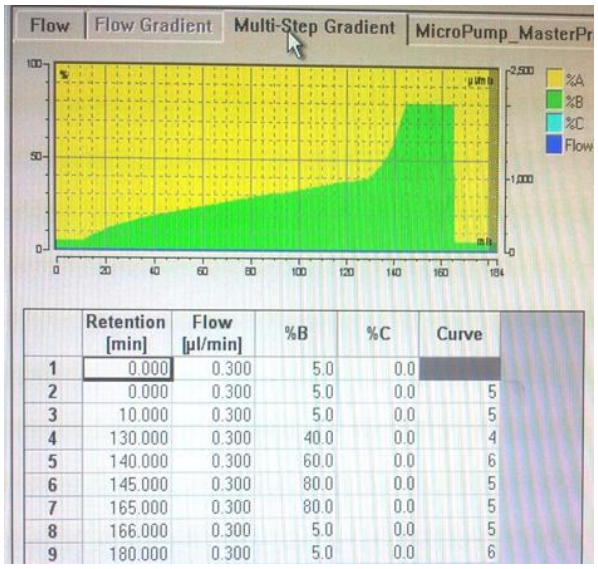

	Retention [min]	Flow [µl/min]	%B	%C	Curve
1	0.000	0.300	5.0	0.0	
2	0.000	0.300	5.0	0.0	5
3	10.000	0.300	5.0	0.0	5
4	130.000	0.300	40.0	0.0	4
5	140.000	0.300	60.0	0.0	6
6	145.000	0.300	80.0	0.0	5
7	165.000	0.300	80.0	0.0	5
8	166.000	0.300	5.0	0.0	5
9	180.000	0.300	5.0	0.0	6

Figure 2.3: Multi-step gradient used for chromatographic separation of peptides. Peptide samples were loaded onto the column for the first 10 min while eluition was achieved by increasing hydrophobicity using B solvent containing 0.1% formic acid, 90% CH_3CN from minutes 10 to 165; afterwards the column was re-equilibrated with 5% solvent B from minutes 166 to 180.

2.19 Protein identification and quantification

Mass spectra were analyzed using the MaxQuant platform version 1.3.0.5 (www.maxquant.org), supported by Andromeda as a search engine. The Andromeda algorithm was used to identify proteins in the genomic database ARATH13 of Arabidopsis thaliana (UNIPROT, (ftp://ftp.uniprot.org/pub/databases/uniprot/current_release/knowledgebase/proteomes/). MaxQuant is characterized by a pattern of work that can be divided into 5 parts or screens:

“Raw files”

“Group-specific parametres”

“MS/MS and sequences”

“Identification and quantification”

“Misc”

The first screen allows you to enter the "raw file" obtained from LC-MS / MS, and enter the Experimental Design. The screen 2, "Group-specific parameters", allows you to define the possible chemical modifications, both fixed and variable, on of peptide sequences. The database search was carried out by setting variable modifications as oxidation of methionine, acetylation to 'N-terminal’ while between fixed modifications (which are set in the third screen) has been set carbamidomethylation of cysteine, generated by the reduction and alkylation of the sample with iodoacetamide; given that the protein quantification is done through a label-free approach, the multiplicity is set to 1. It is also necessary to define the enzyme (trypsin) with which the peptides were generated; the efficiency of the trypsin digestion is never 100%, then 2 missed cleavage were allowed. The database searches were carried out by setting the accuracy of the mass of the precursor ion monoisotopic to 6 ppm (accuracy of the instrument) and that of the peptide fragments to 20 ppm. In the third screen, "MS / MS and sequences" are defined the fixed modifications of the peptide and the genomic database that will be used for the searches. In the research, potential contaminants, such as keratins and peptide fragments of the enzymes used for digestion of proteins are also considered. The fourth screen, "Identification and quantification" allows you to define the parameters regarding the stringency with which will used for the research. Peptides formed of a minimum of seven amino acids are considered. The statistical parameters FDR ("false discovery rate") and PEP ("posterior error probability") are set respectively at 0.01 and 1. In the last screen, “Misc” was set the label-free quantification (Cox et al., 2014) and the time window of alignment of different LC-MS runs that was set to 2 min.

Statistical analysis of data was performed using the Perseus platform version 1.4.1.3.

2.20 Analysis of *PIAA5* and DR5 binding proteins

Proteins isolated with the DNA affinity purification using *PIAA5* and *PUBQ5* or DR5 and CTR were analyzed and quantified with LC-MS/MS analysis using the label free approach. Relative quantification of protein abundance in both control and test probe was used to distinguish true interactions from experimental contaminants. Proteins that bound the promoter (*PUBQ5* or DR5) and that were absent in the affinity with control fragments (*PUBQ5* and CTR for *PIAA5* and DR5 respectively) were considered specific interactors. Among specific interactors, those with a significant quantification (ANOVA p-value < 0.05 and Welch t-test $p<0.05$) where further analyzed for a role in the OG – auxin antagonism.

2.21 Nuclear proteome analysis

For the analysis of the nuclear proteome, proteins were extracted from purified nuclei of *Arabidopsis* seedlings treated differentially with IAA, OG, IAA + OG and mock treated as described below. To get the best coverage of the nuclear proteome, the proteins were extracted with two complementary methods; five independent biological replicates were used for method 1 and three independent biological replicates were used for each method 2. In the first method (method 1), purified nuclei were re-suspended in 8 M urea, nuclear proteins were solubilized and digested with trypsin. The derived peptides were dimethyl labeled, mixed in 1:1:1 molar ratio and fractionated by Strong Anionic eXchange chromatography (SAX) obtaining a fractionation at the peptide level. Each fraction was analyzed with LC-MS/MS. Having four treatments for three isotopic labels, two samples (mock and IAA + OG) were labeled with the same label; the LC-MS/MS analysis was splitted into two terns with a common sample; one tern is composed by peptides deriving from IAA, OG, and to IAA + OG treated seedlings, while the other tern is composed by the peptides derived from IAA, OG and mock treated seedlings. In the second method (method 2) the nuclear proteome is fractionated at the protein level based on the principle of protein solubility at increasing ionic strength. This fractionation yield 4 fractions with functional significance (Gonzalez-Camacho and Medina, 2007). Proteins from each

fraction were digested with trypsin and analyzed with LC-MS/MS and quantified with a label free approach.

2.22 Protein extraction for the nuclear proteome analysis

In the method 1, the purified nuclei were washed with Nuclei Storage buffer, containing 120mM NaCl. After centrifugation at 1000g for 10 min at 4 °C, washed nuclei were recovered in the pellet and suspended in 8 M urea to solubilize the proteins. In the method 2, nuclear proteins were sequentially extracted in four fractions from nuclei as described in (Gonzalez-Camacho and Medina, 2007) with some modifications. The first fraction consists in proteins from nuclear envelope and remnants of the cytoskeleton; the second fraction consists in the soluble fraction; the third fraction (F3) consists in the chromatin fraction and the fourth (F4) consists in the insoluble residue. The fraction 1 was extracted by re-suspending the purified nuclei in 1 mL for g of fresh tissue of Nuclei Storage Buffer with 1% (v/v) Nonidet NP-40 (Sigma) and 0.1% (m/v) of sodium deoxycholate (Sigma) and protease inhibitor cocktail and kept 10 min at 4 °C with shaking. After centrifugation at 2000 xg for 10 min at 4 °C the supernatant consisting in the fraction 1 (F1) was collected; the pellet was re-suspended in 1 mL for g of fresh tissue of 10 mM TRIS-HCl pH 8, 1 mM EDTA and protease inhibitor cocktail and kept 1 h at 4 °C with shaking. After centrifugation at 2000 xg for 10 min at 4 °C the supernatant consisting in the fraction 2 (F2) was collected; the pellet was re-suspended in 400 µL for g of fresh tissue of Nuclei Storage Buffer with 4 µL of RQ1 DNase , 0.5% Triton-X 100 , 2.5 mM $MgCl_2$ and protease inhibitor cocktail and incubated for 30 min at room temperature. After incubation, ammonium sulphate is incorporated until concentration of 0.25M and the sample left at room temperature for 5 min. After centrifugation at 2000 xg for 10 min at 4 °C the supernatant consisting in the fraction 3 (F3) was collected; the pellet was re-suspended in 5 µL for gram of fresh tissue of 8 M urea, 200 mM TRIS-HCl pH 8 , 1% β-mercaptoethanol and consist in the fraction 4 (F4). The nuclear proteins (80 µg for each sample) extracted with the method 1 were digested in solution with trypsin as described above and the derived peptides were dimethyl labeled. The nuclear proteins (20 µg for each fraction,) extracted with the method 2 (except for the F1 that was excluded from the analysis) were digested with trypsin, the peptide mixture were purified from salts with R3 micro-columns and analyzed with LC-MS/MS.

2.23 Isotopic labeling (dimethyl labeling) of peptide mixtures

Peptides deriving from the trypsin digestion of proteins extracted with the method 1 were labeled with different formaldehyde isotopes. In the labeling reactions, primary amines of peptides react with formaldehyde (CH_2O), at a pH between 5 and 8.5 to generate a Schiff's base, that is rapidly reduced by the addition of sodium cyanoborohydride ($NaBH_3CN$) to the reaction mixture (Boersema et al., 2009). The reaction generate a 28 Da mass increment on primary amines of peptides. Using a deuterated formaldehyde (CD_2O) and cyanoborohydride ($NaBH_3CN$) mixture lead to a 32 Da mass increment on primary amines of peptides , while the combination of deuterated formaldehyde containing ^{13}C ($^{13}CD_2O$) and deuterated sodium cyanoborohydride ($NaBD_3CN$) allow to get a 36 Da mass increment on primary amines of peptides (Figure 2.4) . In this work I have studied the dynamics of the nuclear proteome in response to treatments with IAA, OG, and to IAA + OG co-treatment compared to the mock, treated with H_2O. Mock treated and IAA + OG co-treated samples were labeled with the "light" label (+28 Da), the IAA treated samples were labeled with the "medium" label (+32 Da) and the OG treated samples were labeled with the "heavy" label (+36 Da). Samples were vacuum dried and re-suspended in 100 µL of 100 mM TEAB. For 80 µg of peptide mixture, were added 12.8 µL of 4% (v/v) CH_2O and 12.8 µL of 0.6 M $NaBH_3CN$ for the "light" labeled samples (mock; IAA + OG); 12.8 µL of 4% (v/v) CD_2O and 12.8 µL of 0.6 M $NaBH_3CN$ for the "medium" labeled samples (IAA), 12.8 µL of 4% (v/v) $^{13}CD_2O$ and 12.8 µL of 0.6 M $NaBD_3CN$ for the "heavy" labeled samples (OG). The samples were incubated for 1 h at room temperature. The reaction was stopped by adding 32 µL of 1% ammonia (v / v) and 16 µL of formic acid (100%). Labeled peptide mixtures were mixed in 1:1:1 ratio. Each sample was purified from salts with R3 micro-columns as described before. Having four treatments for three isotopic labels, two samples (mock and IAA + OG) were labeled with "light" label; the LC-MS/MS analysis was splitted into two terns with a common sample; one tern is composed by peptides deriving from IAA, OG, and to IAA + OG treated seedlings ("medium", "heavy" and "light" labeled respectively), while the other tern is composed by the peptides derived from IAA, OG and mock treated seedlings ("medium", "heavy" and "light" labeled respectively).

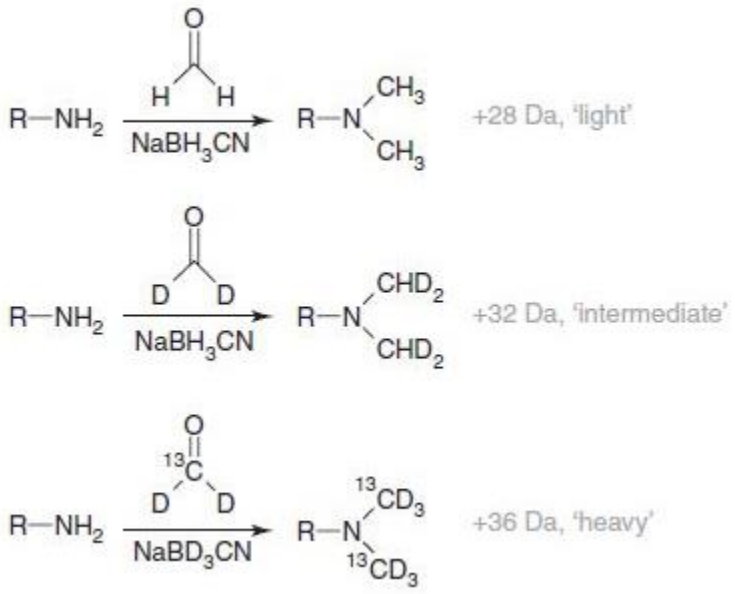

Figure 2.4: Reaction scheme of the isotopic labeling of the peptides. Adapted from Boersema, P. J. et al. 2009.

2.24 Strong Anionic exchange chromatography (SAX)

Peptide samples were fractionated using anion exchange chromatography on custom made micro-columns prepared packing 6 disks of anion exchange resin on a 200 µL tip (Empore/disk Anion Exchange). Micro-columns were washed with 100 µL of Methanol (Sigma) and 100 µL of NaOH, and then equilibrated with 100 µL of pH 11 Buffer (0.02 M CH_3COOH, 0.02 M H_3PO_4 , 0.02 M H_3BO_3 , pH 11). Peptide samples were vacuum dried, re-suspended in the pH 11 Buffer and sonicated on ice for 5 min. Peptides were loaded on the columns and the flow-through (FT) was collected; bound peptides were fractionated by sequential elution using buffers (0.02 M CH_3COOH , 0.02 M H_3PO_4 and 0.02 M H_3BO_3) at decreasing pH, starting at pH 11, 9.5, 8, 6, 5, 4 e 3 as illustrated in Figure 2.5. The fraction were collected after each elution (spin at 7000 xg for 3 min for each step) and purified from salts with R3 micro-columns as described before.

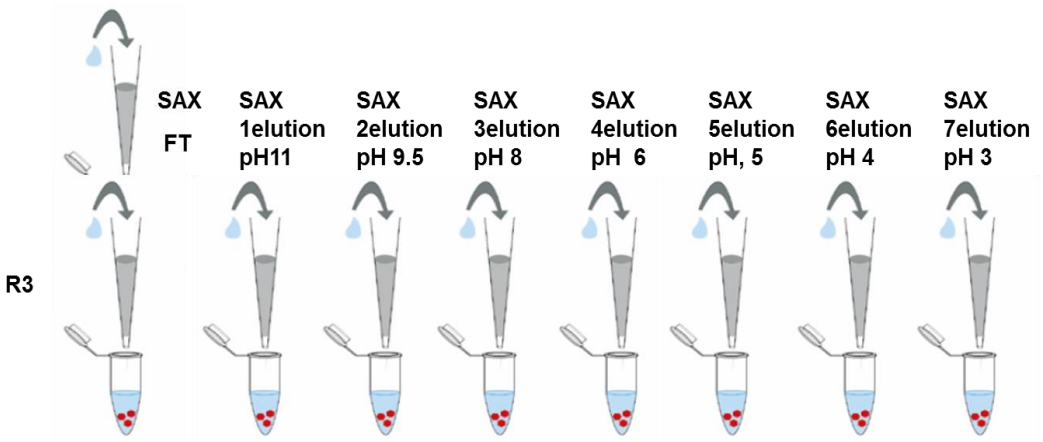

Figure 2.5: schematic representation of peptide fractionation by anion exchange chromatography.

2.25 Protein identification and quantification

Mass spectra acquired during the mass spectrometry analysis were analyzed using the MaxQuant platform version 1.3.0.5 (www.maxquant.org), as described before.

For identification and quantification of proteins from method 1, in the screen "Group-specific parameters", it was also necessary to set the increment of mass due to the labeling of peptides, since 3 isotopic labels have been used (light, medium and heavy isotopes of formaldehyde) and the multiplicity was set to 3. For identification and quantification of proteins from the method 2, since label-free quantification is used, in the screen "Group- specific parameters" the multiplicity was set to 1 and in the "Misc" screen, was set the label-free quantification , and "match between runs" was set to 2 min.

2.26 Statistical analysis

Statistical analysis of data was performed using the Perseus platform version 1.4.1.3.

Only proteins with 3 valid values out of 5 biological replicates per treatment for the method 1 and proteins with 2 valid values out of 3 biological replicates per treatment for the method 2 were used for

statistical analysis. Proteins with a statistically significative quantification (ANOVA p-vaue < 0.05) were used for the quantitative study of the nuclear proteome in response to IAA, OG and IAA + OG co-treatment.

2.27 Subcellular localization of identified proteins and functional annotation enrichment of regulated proteins

The subcellular localisation database for Arabidopsis proteins, SUBA3 (Tanz et al., 2012) was used for *in silico* localization of all proteins identified in the proteomic experiments. SUBA3 was queried for all published experimental evidence (e.g. GFP fusion protein microscopy, MS/MS, protein-protein interaction) and prediction of the subcellular location of a protein. DAVID Bioinformatics Resources version 6.7 (Huang et al., 2009) was used to detect Gene Ontology (GO) Biological Process over-representation in the up- and down-regulated protein groups. The DAVID Functional Annotation Clustering Tool was used to cluster enriched terms using a similarity threshold of 0.45. The most significant representative term from each cluster with $p < 0.05$ was reported.

3 Results

3.1 Construction of a *IAA5* promoter-*GUS* gene fusion

In a previous work it was shown that OGs inhibit the expression, induced by exogenous IAA, of the *β-glucuronidase* (*GUS*) reporter gene under the control of the *DR5* promoter, an artificial auxin-responsive promoter (Ulmasov et al., 1997), indicating that the DR5 promoter is a target of the antagonism.

INDOLE-3-ACETIC ACID INDUCIBLE 5 (*IAA5*) is a gene up-regulated early (within 1 h) by IAA, and its auxin-induced expression is also inhibited by OGs (Savatin et al., 2011). For this reason, it was chosen as a marker gene to study the auxin-OGs antagonism. *IAA5* encodes a protein of 163 amino acids that belongs to the family of Aux/IAA proteins and acts as a short-lived transcriptional repressor of early auxin response genes. It is expressed in seedlings, flowers and guard cells during petal differentiation and expansion stage (TAIR: The Arabidopsis Information Resource). Whether the *IAA5* promoter is, like DR5, a direct target of the auxin-OG antagonism, not known yet. With the aim of assessing whether the antagonism between OG and auxin takes place on the promoter of the IAA5 gene (*PIAA5*), I constructed a plasmid containing *PIAA5* fused upstream of the gene encoding the GUS reporter.

The 1279 bp region upstream of the translation initiation site of *IAA5* was amplified by PCR from genomic DNA of *Arabidopsis thaliana* and the PCR product was separated and visualized on 1% agarose gel (Figure 3.1) stained with EtBr, showing the presence of a fragment of approximately 1200 bp. The primers used for amplification of *PIAA5* were designed to include, at the 5' and 3'-end, the cleavage site of pSTI and EcoRI restriction enzymes, respectively. These cleavage sites are present in the MCS (multiple cloning site) of the cloning vector pCAMBIA 1391z, used to clone the gene fusion. The *PIAA5* amplicon was purified from the reaction mix, and subjected to restriction enzyme digestion with the two enzymes pSTI and EcoRI; a parallel digestion was performed with pCAMBIA 1391z. To verify the successful cleavage by restriction enzymes, two individual digestions of the plasmid in the presence of each enzyme were done simultaneously with the double digestion and the digestion product was visualized on 1% agarose gel stained with EtBr (Figure 3.2) . *PIAA5* was cloned in pCAMBIA 1391z through ligation reaction mediated by the T4 DNA ligase; the amount of insert and vector to be used for the ligation was determined by the formula "ng insert = 3 x (ng vector x bp insert) / (bp

vector)". *PIAA5* (18 ng) and vector (60 ng) were ligated with T4 ligase and 4.5 ng of the ligation product were used to transform *E.coli* DH5α strain by electroporation in order to increase the copy number of the PIAA5 containing vector (*PIAA5*:GUS). Bacteria were plated on selective medium containing kanamycin. The identification of the transformants containing *PIAA5*:GUS was achieved by colony-PCR with two primers: the fw primer pairs on the sequence of the insert and the rev primer pairs on a sequence of the vector, in this case *PIAA5* and GUS respectively. PCR products were separated and visualized on 1% agarose gel stained with EtBr. The presence of an amplified fragment of approximatively 1900 bp (comprising 1279 bp from *PIAA5* and 600 bp of *GUS*) indicated the presence of *PIAA5*:GUS in the colonies 1 and 6 (Figure 3.3). These two colonies, containing *PIAA5*:GUS were inoculated in 5 mL of selective medium to increase the copy number of the *PIAA5*:GUS construct. After 16 h of growth the construct was extracted and purified from the *PIAA5*:GUS containing bacteria. The purified *PIAA5*:GUS was digested with pSTI and EcoRI and sequenced to further confirm the presence in the construct by excision (Figure 3.4) and to verify the sequence of *PIAA5* respectively. *Agrobacterium tumefaciens* GV3101, which contains the resistance to gentamycin and rifampicin in the helper plasmid and in the genome respectively, was transformed by electroporation with 50 ng of *PIAA5*:GUS and the transformants selected on plates containing LB and 3 antibiotics; gentamycin and rifampicin kanamycin. The presence of *PIAA5*:GUS in the transformant colonies was confirmed by colony-PCR with primers designed to amplify the fragment encompassing the fusion point (Figure 3.5) . As expected all the colonies showed the presence of a band of about 1900 bp. Two transformed colonies were inoculated in selective media, and after growth the cells were collected and stored at -80°C.

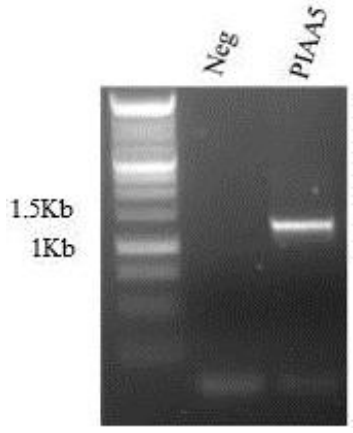

Figure 3.1 : Amplification of *PIAA5* (1279 bp) from gDNA. *PIAA5* amplification was confirmed by the presence of a fragment of approximately 1200 bp in the 1% agarose gel stained with EtBr. "Neg" indicates the negative control.

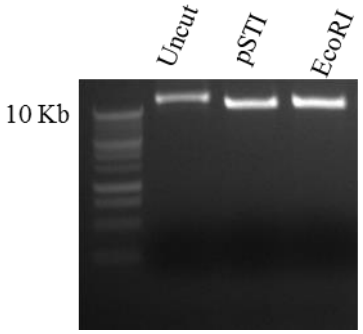

Figure 3.2 : Individual control digestions of pCAMBIA1391z with pSTI and EcoRI. The apparent differences of MW between uncut and pSTI and EcoRI digested pCAMBIA1391z indicates the successful digestion

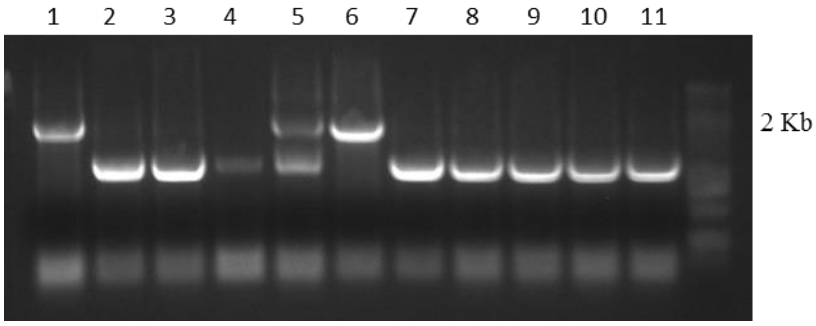

Figure 3.3 : Colony PCR with mixed primers on *E.coli* transformants confirmed the presence of *PIAA5*:GUS (1879 bp) in the colonies 1 and 6 (lanes 1 and 6).

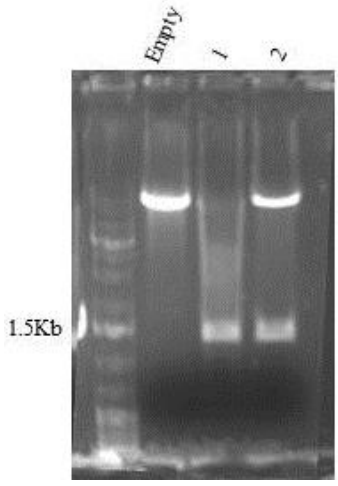

Figure 3.4 : Control excision of *PIAA5* with pSTI and EcoRI on pCAMBIA1391z purified from *E.coli* transformant colonies 1 and 6 (Empty = empty pCAMBIA1391z ; 1; 6 = vector purified from *E.coli* transformant colonies 1 and 6).

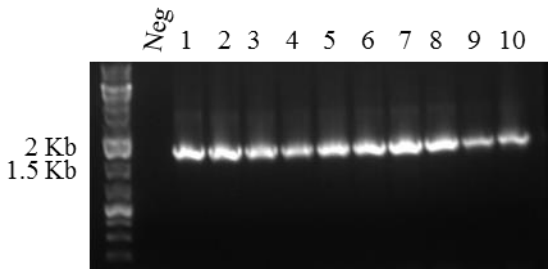

Figure 3.5 : Control excision of *PIAA5* with pSTI and EcoRI on pCAMBIA1391z purified from *E.coli* transformant colonies 1 and 6 (Empty = empty pCAMBIA1391z ; 1; 6 = vector purified from *E.coli* transformant colonies 1 and 6). The presence of a band of approximately 1300 bp after excision with pSTI and EcoRI indicates that *PIAA5* was cloned into pCAMBIA1391z.

3.2 IAA-regulated activation of the *PIAA5* promoter is inhibited by OGs

A. thaliana PIAA5:GUS transgenic lines were generated by *A. tumefaciens*-mediated transformation using the floral dip method as previously described (Clough and Bent, 1998). *A. thaliana* plants were grown until flowering; to obtain more floral buds per plant, primary bolts were clipped, to prevent apical dominance and stimulate emergence of multiple secondary bolts. When the inflorescences developed and floral buds were evident, already developed siliques were removed leaving only the mature bolts. *A. tumefaciens PIAA5*:GUS transformants were pre-inoculated in 5 mL of selective media for 10 h, then the pre-inoculum was used to inoculate 200 mL of selective media until OD of 0.8; cells were pelleted and resuspended in 400 mL of transformation solution containing 200 μM acetosyringone to induce expression of the *vir* genes of *A. tumefaciens.* Transformation solution also contained 0.01% of Silwet detergent, which reduces surface tension and enhances the entry of *A. tumefaciens*. Transformation of *A. thaliana* was achieved by dipping four plants in the transformation solution containing *PIAA5*:GUS transformant *A. tumefaciens*. Plants were grown for 3 weeks until siliques were brown and dry, and seeds were collected. Transformed plants were selected by plating on selective medium containing hygromycin. Two *PIAA5*:GUS T1 transformed plants were grown on soil for seed production and T2 progeny plants were used to study of the regulation of *PIAA5* in response to the treatments with IAA and IAA + OG.

PIAA5:GUS T2 transformed plants were grown for 5 or 15 days and treated with 2.5 μM or 5 μM IAA or mock (water)-treated for 6 h. Five-day-old and 15-day-old DR5:GUS seedlings were treated with 2.5 μM IAA as a positive control. IAA-treated seedlings were stained with the GUS staining solution for the histochemical localization of GUS activity. GUS activity can be observed after GUS staining due to the formation of a blue coloration in the plant tissues where GUS is expressed. After 5 and 15 days of growth no basal activity of *PIAA5* was observed in the mock (Figure 3.6); also seedlings treated with 2.5 μM IAA didn't show any GUS activity (Figure 3.6) while both 5-days-old and 15-days-old seedlings treated with 5 μM IAA showed GUS activity in the root, indicating the induction of GUS expression driven by *PIAA5* in response to IAA treatment. The intensity of the blue coloration in *PIAA5*:GUS seedlings treated with 5μM IAA was weak compared to the positive control. Previous data (Savatin et al., 2011) indicate that IAA – OG antagonism can be better observed at auxin concentration lower than 2.5 μM. Indeed, no reduction of GUS activity was observed when 5- and 15- day-old seedlings were co-treated with 5 μM IAA + 100 μg/mL OG as shown in Figure 3.7. The fact that GUS activity cannot be detected with 2.5μM IAA treatment may indicate a low sensitivity of the GUS histochemical staining. Because it was previously shown that *IAA5* expression is strongly induced in response to 1.5 μM IAA (Savatin et al., 2011), I decided to use a more sensitive method, the quantitative RT-PCR, to detect the induction of GUS expression in response to a lower auxin concentration and the possible reduction of GUS induction in response to the co-treatment. Transcript levels of *GUS* were determined in response to 1 h of 1.5 μM IAA treatment and 1.5 μM IAA + 50 μg/mL OG co-treatment relative to those of UBQ5 (Figure 3.8). The expression of GUS transcript was induced by 1.5 μM IAA compared to the mock and the induction of the GUS transcript was reduced in response to 1.5 μM IAA + 50μg/mL OG co-treatment. These data indicate that OG –auxin antagonism takes place on the promoter of *IAA5*.

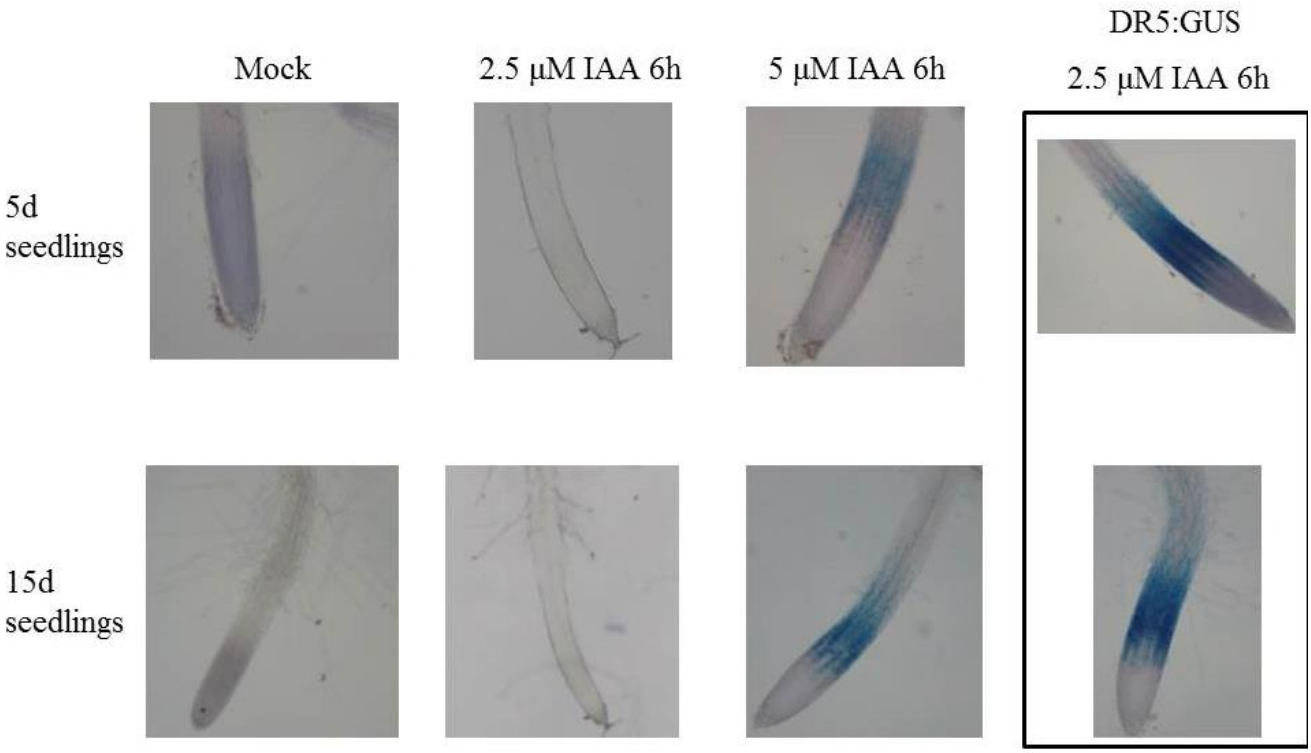

Figure 3.6 : Histochemical localization of GUS activity. Five and 15 days-old *PIAA5*:GUS *Arabidopsis* T2 transformant seedlings treated with 2.5µM or 5µM IAA for 6 h. Induction of GUS activity was observed with 6 h of 5µM IAA treatment in both 5 and 15 days-old seedlings.

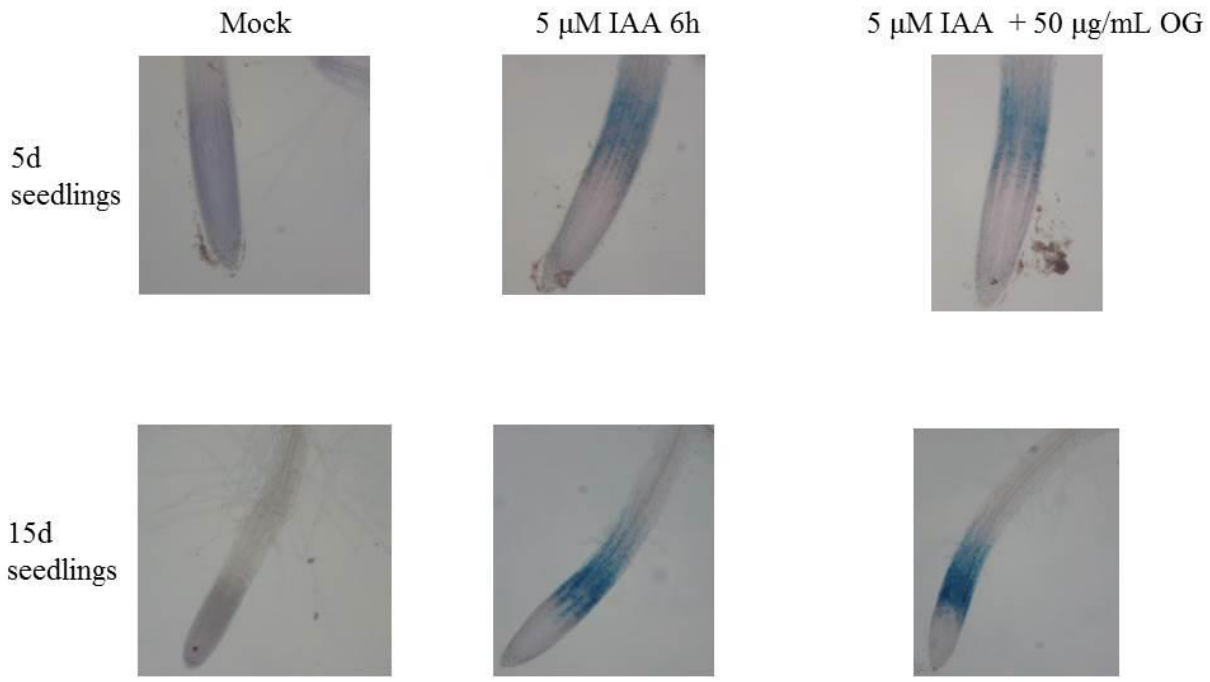

Figure 3.7 : Histochemical localization of GUS activity. Five and 15 days-old *PIAA5*:GUS *Arabidopsis* T2 seedlings treated with 5µM IAA or 5µM IAA + 100µg/mL OG for 6 h. No reduction of GUS activity was observed when 5 and 15 days old seedlings were co-treated with 5µM IAA + 100µg/mL OG.

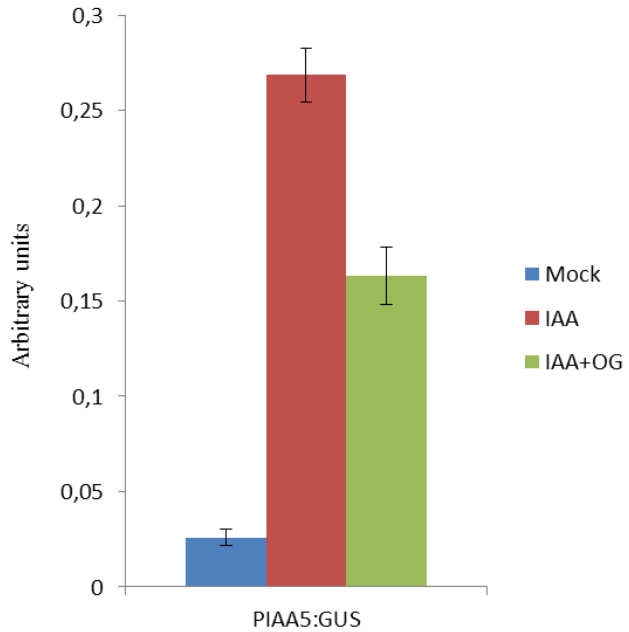

Figure 3.8 : GUS transcript levels were measured by qPCR after 1 h of 1.5 µM IAA treatment or 1.5 µM IAA + 50µg/mL OG co-treatment. The expression of GUS transcript was induced by 1.5 µM IAA compared to the mock and the induction of the GUS transcript was reduced in response to 1.5 µM IAA + 50µg/mL OG co-treatment.

3.3 Isolation and identification of proteins binding *PIAA5* and DR5

Since the OG–auxin antagonism takes place on the promoter of *IAA5* and on DR5, it is likely that the transcriptional regulation may be mediated by transcriptional complexes forming on *PIAA5* and DR5. To understand the molecular basis of the antagonism, the identification of proteins binding *PIAA5* and DR5 in response to IAA and IAA + OG treatments was undertaken, using an *in vitro* approach based on DNA affinity purification. In this technique, a biotinylated *PIAA5* or DR5 probe is bound to streptavidin-coated magnetic beads and placed in contact with nuclear proteins. Non-specific interactors are removed by performing several stringent wash steps, while specific interactors are eluted from the beads and identified by LC-MS/MS.

3.4 Preparations of nuclear extracts for the DNA affinity purification

Thirty-nine flasks of Col-0 *Arabidopsis* seedlings were grown for 15 days on MS/2 liquid medium and treated with 1.5 μM IAA, co-treated with 1.5 μM IAA + 100 μg/mL of OG (six flasks per treatment in three replicates) or mock treated (three flasks) for 1 h. Treated seedlings were frozen in liquid nitrogen and stored at -80°C.

IAA5 transcript levels were measured by semi-qPCR to verify the effectiveness of the IAA or IAA + OG treatments. After treatment, total RNA was extracted from 100 mg of seedling for each treated flask. Two μg of total RNA were treated with RQ1 DNase to degrade genomic DNA and first-strand cDNA was synthesized using ImProm-II reverse transcriptase. *IAA5* transcript level relative to *UBQ5* transcript level used as reference was measured for each treated flask.

The effectiveness of the treatments was confirmed by the induction of *IAA5* transcript in response to IAA and the reduction of the induction *IAA5* transcript in response to the IAA + OG co-treatment (Figure 3.9).

Nuclei were purified from treated seedlings and nuclear proteins extracts were used for the DNA affinity purification experiments. Nuclear proteins were used instead of total extracts because I was searching for proteins that mediate the OG–auxin antagonism at the transcriptional level and therefore

must be present in the nucleus. Moreover the use of only nuclear proteins can decrease the amount of non-specific interactors during the DNA affinity purification experiments. Purification of nuclei from *Arabidopsis thaliana* seedlings was based on previous work (Folta and Kaufman, 2007; Calikowski and Meier, 2007) with some modifications. Seedlings were homogenized in a pre-cooled blender in the presence of hexylene glycole, which acts as a membrane stabilizing agent; the homogenate was filtered through a layer of cheesecloth to remove tissue fragments; differential lysis of organelles was achieved by addition of Triton X-100 to the homogenate until a final concentration of 1 %; plastids and mitochondria were lysed while nuclei remained intact, because in the presence of Mg^{2+} only the outer layer of the nuclear envelope is stripped away. Total homogenate was then centrifuged at 1000 xg for 10 min at 4°C and crude nuclei were recovered in the pellet with other debris. The isolation of nuclei was achieved by isopicnic density gradient in which nuclei were separated from other cellular components on the basis of their density; this was obtained with a discontinuous density gradient formed by 3 layers of Percoll solution with different densities. Crude nuclei were suspended in 80 % Percoll; 60% and 30% Percoll solution were stratified above. After centrifugation, nuclei were recovered at the 30/ 60 % Percoll interface and separated from broken nuclei, that stratify at the of 60/ 80% Percoll interface, and from the cellular debris. A pure nuclear fraction was then obtained by two washings with Triton X-100 containing buffer. The increasing purity of the nuclei after each purification step was monitored by detecting in the different fractions the amount of the H3 histone, a nuclear marker, by western blot (Figure 3.10). In the total homogenate (TH) no signal for the H3 histone could be detected. The amount of histone H3 increased in the enriched nuclear fraction (P30%) recovered at the 30/ 60% Percoll interface. The detection of histone H3 in the fraction stratified at 60/ 80 % Percoll (P60%) indicated that some nuclei were broken during the purification process. The amount of histone H3 increased considerably when enriched nuclear fraction was washed to obtain pure nuclei. The presence of intact nuclei was also observed with fluorescent microscopy using the DAPI stain that binds strongly to A-T rich regions in DNA. The presence of fluorescent round corpuscles indicate the presence of intact nuclei in the pure nuclear preparations (Figure 3.11). Proteins were extracted from purified nuclei from IAA and IAA + OG treated plants according to Calikowski and Meier, 2007. Nuclei were lysed with 470 mM KCl; nuclear extracts were diluted with 3 volumes to a final concentration of 117 mM KCl, a condition in which chromatin is insoluble and can be pelleted by centrifugation. The supernatant containing the nuclear proteins was dialyzed to decrease the salt concentration and nuclear proteins were quantified.

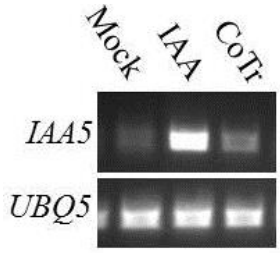

Figure 3.9 : Control of IAA treatment and IAA + OG co-treatment (CoTr) effectiveness by semi-q PCR . The transcript of *IAA5* is induced after 1h of 1.5 µM IAA treatment while is reduced after 1h 1.5 µM IAA + 100 µg/mL of OG co-treatment.

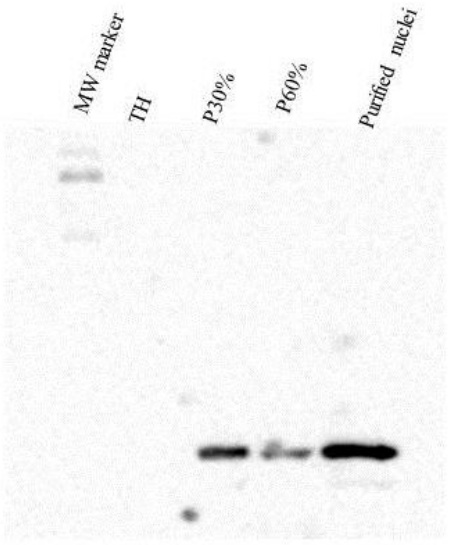

Figure 3.10 : Western blot with αH3 histone. Each lane was loaded with 1.5 µg of proteins. In the total homogenate (TH) no signal for the H3 histone could be detected. The amount of histone H3 increased in the enriched nuclear fraction (P30%) recovered at the 30/60% Percoll interface. The detection of histone H3 in the fraction stratified at 60/ 80 % Percoll (P60%) indicated that some nuclei were broken during the purification process. The amount of histone H3 increased considerably when enriched nuclear fraction was washed to obtain pure nuclei.

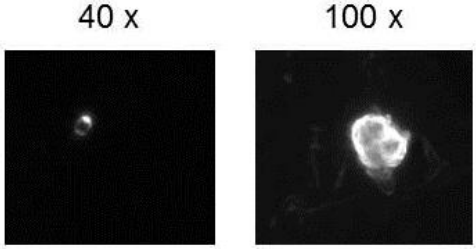

Figure 3.11 : Fluorescence microscopy analysis after DAPI staining of purified nuclei. The presence of fluorescent round corpuscles indicate the presence of intact nuclei in the pure nuclear preparations.

3.5 Probes for the DNA Affinity Purification Experiments

To identify the proteins that may be involved in the OG-auxin antagonism I chose to use two different probes: the promoter of the auxin responsive gene *IAA5* and the synthetic auxin inducible promoter DR5 (Ulmasov et al., 1997). DR5, is constituted by 7 repeats of 11nt composed by the activation sequence 5'-CCTT-3' and the Auxin Responsive Elements (AREs) 5'-TGTCTC-3'(Figure 3.12) . It is known that auxin responsive factors (ARFs) bind to the AREs and that ARF1 (auxin responsive factor 1) can bind to DR5 *in vitro* (Ulmasov et al., 1997).

An unrelated DNA as a negative control was also necessary in order to identify the proteins that bind non-specifically to nucleotide sequences. I chose the promoter of *UBQ5* as negative control for *PIAA5* because it has similar length and because *UBQ5* is not involved in the response to auxin nor involved in the OG – auxin antagonism. A DR5-unrelated control sequence (CTR) (Hsieh et al., 2012) was chosen as a negative control for DR5 because its nucleotide sequence is unrelated to that of DR5 and it has similar length. In the DNA affinity purification experiments, biotinylated nucleotidic probes bind to the streptavidin-coated magnetic beads. The promoter regions of IAA5 and UBQ5 genes (-1279 bp and -1000 bp from the ATG respectively) were amplified from genomic DNA using biotinylated primers and sequenced. DR5 (77 bp) and CTR (47 bp) were purchased as biotinylated synthetic sequences.

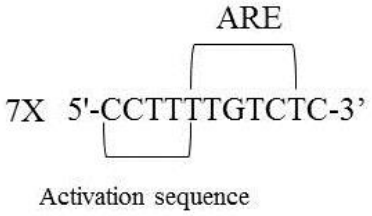

Figure 3.12 : Sequence of the auxin synthetic promoter DR5. DR5 is constituted by 7 repeats of 11nt composed by the activation sequence 5'-CCTT-3' and the Auxin Responsive Elements (ARE) 5'-TGTCTC-3'.

3.6 DNA Affinity Purification of *PIAA5* and DR5 binding proteins

Specific interactors of *PIAA5* and DR5 were isolated from nuclear extracts of IAA and IAA + OG treated seedlings by DNA affinity purification; three biological replicates of the experiments were

performed. Figure 3.13 shows the experimental procedure used. In order to reduce the binding of non-specific interactors, nuclear proteins (150 μg) from IAA and IAA + OG treated seedlings (IAA NPs and IAA + OG NPs respectively) were pre-incubated with poly dI/dC, short synthetic nucleotidic sequences that were also used during the DNA affinity purification steps. Moreover, to further reduce the binding of potential contaminants, nuclear protein extracts were pre-cleared by addition to 50 mg of Dynabeads M-280 conjugated with 500 ng of 5'-end biotin labeled *PUBQ5*. After incubation, pre-cleared proteins were recovered and added to the specific probe-conjugated Dynabeads. For the isolation of *PIAA5* specific interactors, pre-cleared IAA NPs and IAA + OG NPs were added to *PIAA5*-conjugated beads. IAA NPs were also added to *PUBQ5*-conjugated beads as negative control. For the isolation of DR5 specific interactors, pre-cleared IAA NPs and IAA + OG NPs were added to DR5-conjugated beads. IAA NPs were also added to CTR-conjugated beads as negative control. After incubation, to decrease non-specific interaction between NPs and probes, beads were washed and recovered;, this step was repeated for five times. Washings were performed in the presence of 50 mM KCl and poly dI/dC in washing buffer. DNA-protein complexes were recovered in two sequential elution steps. A first elution was performed with high salt wash buffer containing 100 mM KCl, to elute weak interactors and to decrease the complexity of the sample, increasing the possibility to find low abundant proteins in the LC-MS/MS analysis. Eluted proteins (WF, weak interactors fraction) were vacuum dried, re-suspended in 8 M urea, 10 mM tris-HCl pH 8, reduced/alkylated and digested with trypsin. Strong interactors, still bound to the probes (SF, strong interactors fraction), were recovered with 8 M urea, 10 mM tris-HCl pH 8, reduced/alkylated and digested with trypsin directly in the presence of the beads, to minimize protein loss.

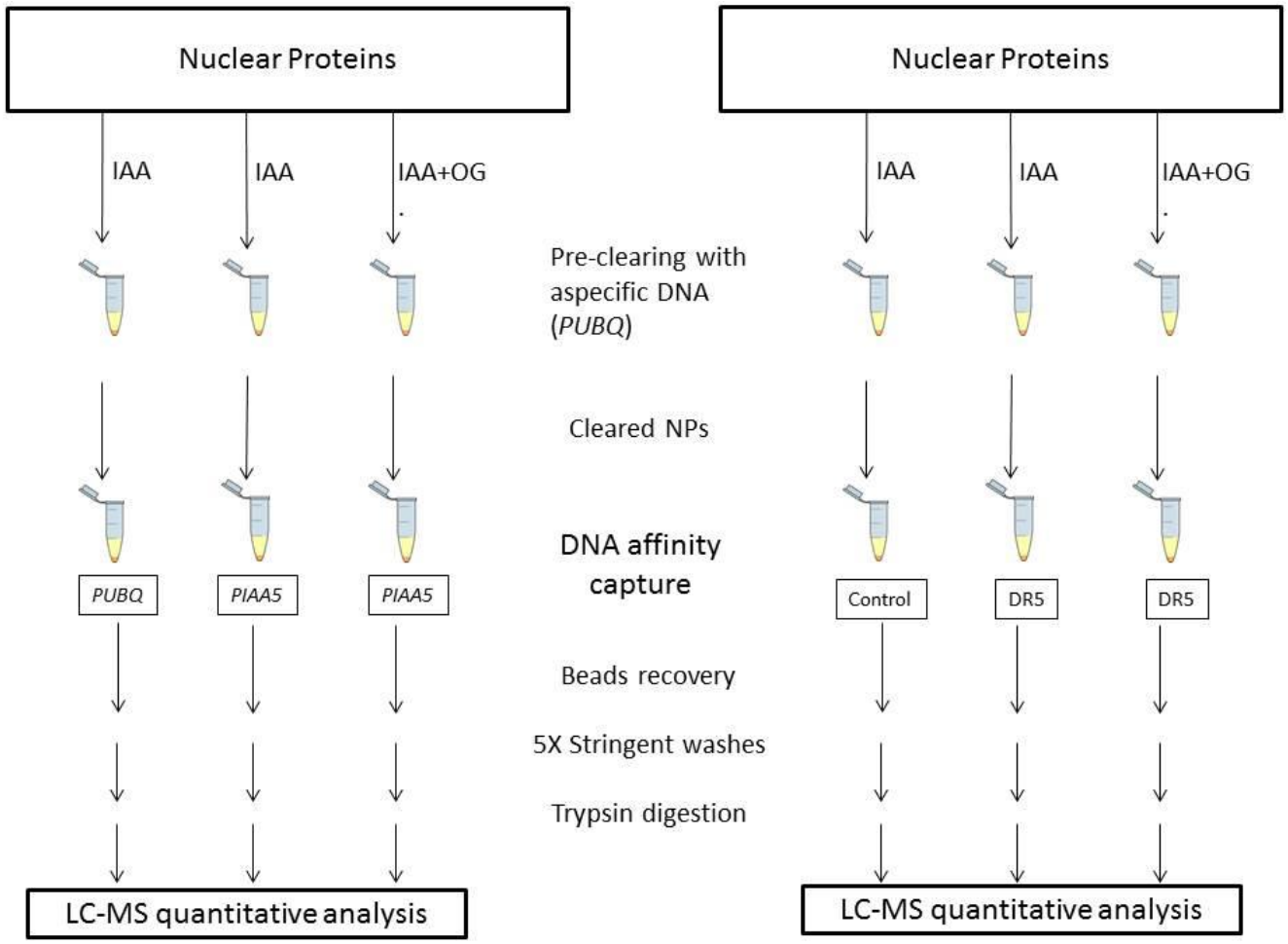

Figure 3.13 : Experimental procedure used for the DNA affinity purification. NPs were pre-cleared by addition to 50 mg of Dynabeads M-280 conjugated with 500 ng of 5'-end biotin labeled *PUBQ5*. After incubation, pre-cleared proteins were recovered and added to probe-conjugated Dynabeads. For the isolation of *PIAA5* or DR5 specific interactors, pre-cleared IAA NPs and IAA + OG NPs were added to *PIAA5*- or DR5-conjugated beads. IAA NPs were also added to *PUBQ5*-and CTR-conjugated beads as negative controls for *PIAA5* and DR5 respectively. After incubation, to decrease aspecific interaction between NPs and probes, beads were washed and recovered with magnetic field, this was repeated for five times. DNA-protein complexes were digested with trypsin and identified with LC-MS/MS.

3.7 LC-MS/MS analysis of proteins isolated with DNA affinity purification

Peptides derived from trypsin digestion were separated and analyzed by reverse phase liquid chromatography coupled to tandem mass spectrometry (LC-MS/MS). Mass spectra were analyzed

using the MaxQuant platform version 1.3.0.5 (www.maxquant.org), supported by Andromeda as a search engine. The Andromeda algorithm was used to identify proteins in the genomic database ARATH13 (UniProtKB version released on July 2013, containing 33339 sequences) of *Arabidopsis thaliana*. In the LC-MS/MS analysis 1226 proteins where identified across all the samples.

3.8 Identification of DR5 and *PIAA5* binding proteins

Proteins that bound the promoter (*PIAA5* or DR5) and that were absent in the control fragments (PUBQ5 and CTR for *PIAA5* and DR5, respectively) were considered specific interactors. Only proteins identified in at least two replicates were considered. The number of proteins identified in the affinity with DR5 are reported in the numeric Venn diagram (Table 3.1). In total 190 proteins were identified in the affinity purification with DR5 and not with CTR and were considered as specific interactors of DR5. Among the specific interactors, the transcription factor GT2 (Riechmann et al., 2000) was found in both IAA and IAA + OG treatments; ARF5 (Hardtke et al., 2004) was found only with IAA + OG NPs and TGA7 (Jakoby et al., 2002) was found with both IAA and IAA + OG NPs. GT2 belongs to the family of Trihelix transcription factors and its transcriptional regulation activity was inferred from sequence similarity. ARF5 (Auxin responsive factor 5) is a transcriptional factor that belongs to the ARF family and is known for the role in the auxin-dependent gene regulation. TGA7 is a transcriptional factor belonging to the family of basic region/leucine zipper motif (bZIP) transcription factors which regulate processes including pathogen defence, light and stress signalling, seed maturation and flower development.

The proteins identified in the *PIAA5* affinity purification are summarized in the numeric Venn diagram Table 3.2. A total of 544 proteins were identified in the affinity purification with *PIAA5* that were not recovered with *PUBQ5* and were considered as specific interactors. Among the specific interactors we found again GT2, ARF5 and TGA7, all isolated from both IAA and IAA + OG NPs. The isolation of ARF5, predicted to bind to the AREs that are present both on DR5 and *PIAA5*, supports the validity of the DNA affinity purification approach.

DR5 affinity purification			
CTR	DR5 IAA + OG	DR5 IAA	N° of Proteins
+	+	+	370
+		+	170
	+	+	83
		+	104
	+		3
+			4

Table 3.1 : Numeric Venn diagram of proteins identified with DR5 affinity purification. + indicates the samples in which the specified number of proteins were identified

PIAA5 affinity purification			
PUBQ5	PIAA5 IAA + OG	PIAA5 IAA	N° of Proteins
+	+	+	398
		+	321
	+	+	211
+		+	77
	+		12
+			4
+	+		3

Table 3.2 : Numeric Venn diagram of proteins identified with *PIAA5* affinity purification. + indicates the samples in which the specified number of proteins were identified

3.9 Label-free quantitative proteomics to find proteins involved in the OG – auxin antagonism

Because OGs reduce but not "turn off" the transcription of auxin induced genes (Savatin et al., 2011), the mere identification of the proteins isolated by DNA affinity purifications does not give complete information about possible candidates for a role in the OG – auxin antagonism, as the same bound protein may be only reduced in its levels upon a treatment . Quantification was therefore performed, by the label-free method, to obtain information about a relative protein abundance for DR5 and *PIAA5* specific interactors in response to IAA and OG + IAA treatments.

In label-free quantitative proteomics each sample is analyzed in single LC-MS/MS runs measuring the mass spectrometric signal intensity of peptide precursor ions belonging to a particular protein; the intensity value for each peptide in one experiment was compared to the respective signals of other experiments to yield relative quantitative information.

Candidate proteins for a role in the OG-auxin antagonism are expected to bind to *PIAA5* or DR5 in response to IAA treatments and to show a decreased abundance in response to the OG + IAA co-treatments. Protein intensities were Log2 transformed and normalized by median subtraction (Ting et al., 2009) in order to center the distribution of protein intensities on zero. Non-specific interactors were filtered away and specific interactors of *PIAA5* and DR5 were subjected to statistical analysis. As protein groups in the control and treated samples contain a different number of proteins, I chose to use the Welch t-test, which is more reliable when the two samples have unequal variances and unequal sizes (Ruxton, 2006). Proteins with statistically significant quantification (Welch t-test $p<0.05$) were further analyzed for a role in the OG - auxin antagonism.

Among the 190 specific interactors of DR5, seven proteins showed a significant differential abundance and are reported in Table 3.3 and Figure 3.14. In the case of *PIAA5*, thirty-four showed a significant differential abundance (Table 3.4 and figure 3.15).

		DR5 specific interactors involved in OG – auxin antagonism
Gene identifier	**Protein**	
At4g40030	H3.3	Histone superfamily protein
At4g09000	GRF1	Encodes a 14-3-3 gene, designated GRF1 chi (for general regulatory factor1-G-box factor 14-3-3 homolog isoform chi). The major native forms of 14-3-3s are homo- and hetero-dimers, the biological functions of which are to interact physically with specific client proteins and thereby effect a change in the client. As a result, 14-3-3s are involved in a vast array of processes such as the response to stress, cell-cycle control, and apoptosis, serving as adapters, activators, and repressors. There are currently 133 full-length sequences available.
AT4g17520	AT4g17520	Hyaluronan / mRNA binding family
At3g62170	VGDH2	Acts in the modification of cell walls via demethylesterification of cell wall pectin.

At1g71260	ATWHY2	Single-stranded DNA-binding protein that associates with mitochondrial DNA and may play a role in the regulation of the gene expression machinery. Seems also to be required to prevent break-induced DNA rearrangements in the mitochondrial genome. Can bind to melt double-stranded DNA in vivo.
At1g12310	CML13	Probable calcium-binding protein
At2g09990	RPS16A	40S ribosomal protein S16-1

Table 3.3 : Specific interactors of DR5 involved in OG – auxin antagonism.

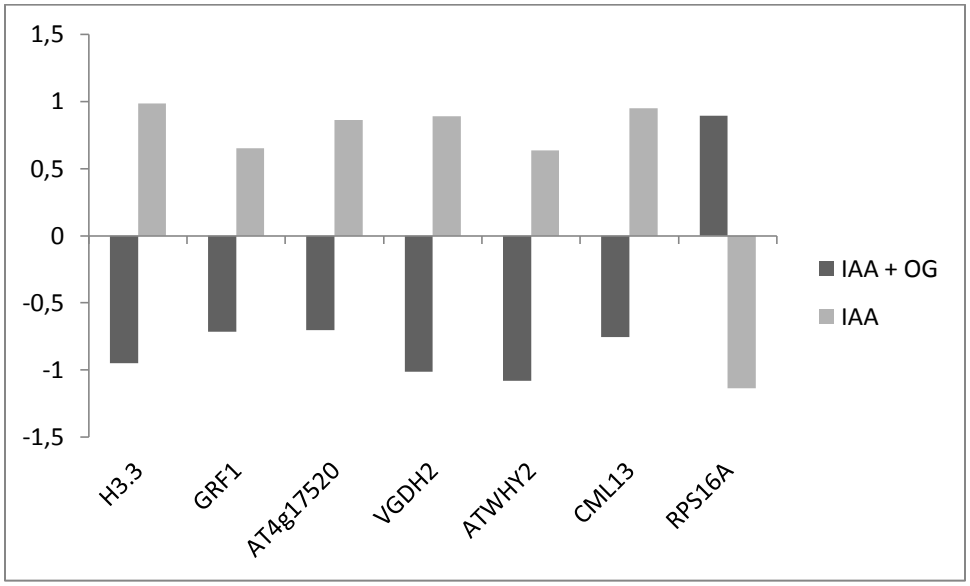

Figure 3.14 : Log2 normalized quantification of DR5 specific interactors involved in OG – auxin antagonism.

***PIAA5* specific interactors involved in OG – auxin antagonism**		
Transcriptional and translational regulation		
Gene identifier	**Protein**	
At1g77920	TGA7	Transcriptional activator that binds specifically to the DNA sequence 5'-TGACG-3'. Recognizes ocs elements like the as-1 motif of the cauliflower mosaic virus 35S promoter. Binding to the as-1-like cis elements mediate auxin- and salicylic acid-inducible transcription. May be involved in the induction of the systemic acquired resistance (SAR) via its interaction with NPR1
At1g22910	At1g22910	RNA-binding (RRM/RBD/RNP motifs) family protein

AtCg00650	rps18	30S ribosomal protein S18, chloroplastic
At1g64090	RTNLB3	Reticulon-like protein B3 ; endoplasmic reticulum tubular network organization.
At5g46430	RPL32B	60S ribosomal protein L32-2
AtCg00760	rpl36	50S ribosomal protein L36, chloroplastic
At3g50670	RNU1	U1 small nuclear ribonucleoprotein 70 kDa. Mediates the splicing of pre-mRNA by binding to the loop I region of U1-snRNA.
Signalling		
Gene identifier	**Protein**	
At3g02880	At3g02880	Leucine-rich repeat protein kinase family protein
At2g32730	RPN2A	Acts as a regulatory subunit of the 26 proteasome which is involved in the ATP-dependent degradation of ubiquitinated proteins.
At1g08520	CHLD	Involved in chlorophyll biosynthesis. Catalyzes the insertion of magnesium ion into protoporphyrin IX to yield Mg-protoporphyrin IX. The magnesium-chelatase is a complex of three subunits, CHLI, CHLD and CHLH. The reaction takes place in two steps, with an ATP-dependent activation followed by an ATP-dependent chelation step. Does not bind abscisic acid.
At4g29130	HXK1	Fructose and glucose phosphorylating enzyme. May be involved in the phosphorylation of glucose during the export from mitochondrion to cytosol. Acts as sugar sensor which may regulate sugar-dependent gene repression or activation. Mediates the effects of sugar on plant growth and development independently of its catalytic activity or the sugar metabolism. May regulate the execution of program cell death in plant cells.
At1g20200	RPN3A	Acts as a regulatory subunit of the 26 proteasome which is involved in the ATP-dependent degradation of ubiquitinated proteins.
At1g51370	FDL6	F-box/RNI-like/FBD-like domains-containing protein
Trafficking		
Gene identifier	**Protein**	
At2g34250	AT2G34250	SecY protein transport family protein
At3g59020	SAD2H	Functions probably in nuclear protein import, either by acting as autonomous nuclear transport receptor or as an adapter-like protein in association with other importin subunits.
At1g60780	AP1M2	Subunit of clathrin-associated adaptor protein complex 1 that plays a role in protein sorting at the trans-Golgi network and early endosomes (TGN/EE). The AP complexes mediate the recruitment of clathrin to membranes and the recognition of sorting signals within the cytosolic tails of transmembrane cargo molecules. Required for KNOLLE localization at the cell plate to mediate cytokinesis. Functions redundantly with AP1M1 in multiple post-Golgi trafficking pathways leading from the TGN to the vacuole, the plasma membrane, and the cell-division plane.
At4g04910	NSF	Involved in vesicle-mediated transport. The ATPase activity of NSF serves to disassemble the SNARE complex, freeing the components for subsequent pairing and fusion events.
At1g03780	TPX2	Targeting protein for Xklp2-like protein

At3g01780	TPLATE	Functions in vesicle-trafficking events required for site-specific cell wall modifications during pollen germination and for anchoring of the cell plate to the mother wall at the correct cortical position.
At3g22845,	P24B3	Involved in vesicular protein trafficking. Mainly functions in the early secretory pathway but also in post-Golgi membranes. Thought to act as cargo receptor at the lumenal side for incorporation of secretory cargo molecules into transport vesicles and to be involved in vesicle coat formation at the cytoplasmic side (By similarity)
At1g47550	SEC3A	Component of the exocyst complex involved in the docking of exocytic vesicles with fusion sites on the plasma membrane during regulated or polarized secretion. Involved in polarized cell growth and organ morphogenesis. During cytokinesis, involved in cell plate initiation, cell plate maturation and formation of new primary cell wall. During cytokinesis, involved in cell plate initiation, cell plate maturation and formation of new primary cell wall.
At1g15690	AVP1	Encodes a H(+)-translocating (pyrophosphate-energized) inorganic pyrophosphatase (H(+)-PPase; EC 3.6.1.1) located in the vacuolar membrane. Expression is found in all tissues examined, including meristems and floral organ primordium. Expression is particularly enhanced in pollen, and is repressed by light. Over expression and loss of function phenotypes suggest AVP1 is involved in regulation of apoplastic pH and auxin transport. The effect on auxin transport likely involves effects of extracellular pH on subcellular localization of auxin efflux carriers such as PIN1.
Response to stress		
Gene identifier	**Protein**	
At2g02130	PDF2.3	Confers broad-spectrum resistance to pathogens
At3g58750	CSY2	Peroxisomal citrate synthase required for the fatty acid respiration in seedlings, citrate being exported from peroxisomes into mitochondria during respiration of triacylglycerol (TAG). Indeed, complete respiration requires the transfer of carbon in the form of citrate from the peroxisome to the mitochondria.
At5g54430	PHOS32	Contains a universal stress protein domain. Protein is phosphorylated in response to Phytophthora infestans zoospores and xylanase
At5g25980	TGG2	May degrade glucosinolates (glucose residue linked by a thioglucoside bound to an amino acid derivative) to glucose, sulfate and any of the products: thiocyanates, isothiocyanates, nitriles, epithionitriles or oxazolidine-2-thiones. These toxic degradation products can deter insect herbivores. Seems to function in abscisic acid (ABA) and methyl jasmonate (MeJA) signaling in guard cells.
Cell wall metabolism		
Gene identifier	**Protein**	
At1g19360	RRA3	Reduced residual arabinose 3. Encodes an arabinosyltransferase that modifies extensin proteins in root hair cells.
At3g61130	GAUT1	Involved in pectin biosynthesis. Catalyzes the transfer of galacturonic acid from uridine 5'-diphosphogalacturonic acid onto the pectic polysaccharide homogalacturonan.
At3g18080	BGLU44	Hydrolyzes p-nitrophenyl beta-D-glucoside, p-nitrophenyl beta-D-mannoside, cellobiose, 4-

		methylumbelliferyl-beta-D-glucoside, laminarin, amygdalin, esculin and gentiobiose.
At1g04430	PMT8	S-adenosyl-L-methionine-dependent methyltransferases superfamily protein
At5g59090	SBT4.12	Serine-type endopeptidase activity
Miscellanoeus		
Gene identifier	**Protein**	
At5g24700	AT5G24690	Unknown protein
At3g06650	ACLB-1	ATP citrate-lyase is the primary enzyme responsible for the synthesis of cytosolic acetyl-CoA, used for the elongation of fatty acids and biosynthesis of isoprenoids, flavonoids and malonated derivatives. May supply substrate to the cytosolic acetyl-CoA carboxylase, which generates the malonyl-CoA used for the synthesis of a multitude of compounds, including very long chain fatty acids and flavonoids. Required for normal growth and development and elongation of C18 fatty acids to C20 to C24 fatty acids in seeds. In contrast to all known animal ACL enzymes having a homomeric structure, plant ACLs are composed of alpha and beta chains
At3g26620	LBD23	LOB domain-containing protein 23

Table 3.4 : Specific interactors of *PIAA5* involved in OG – auxin antagonism.

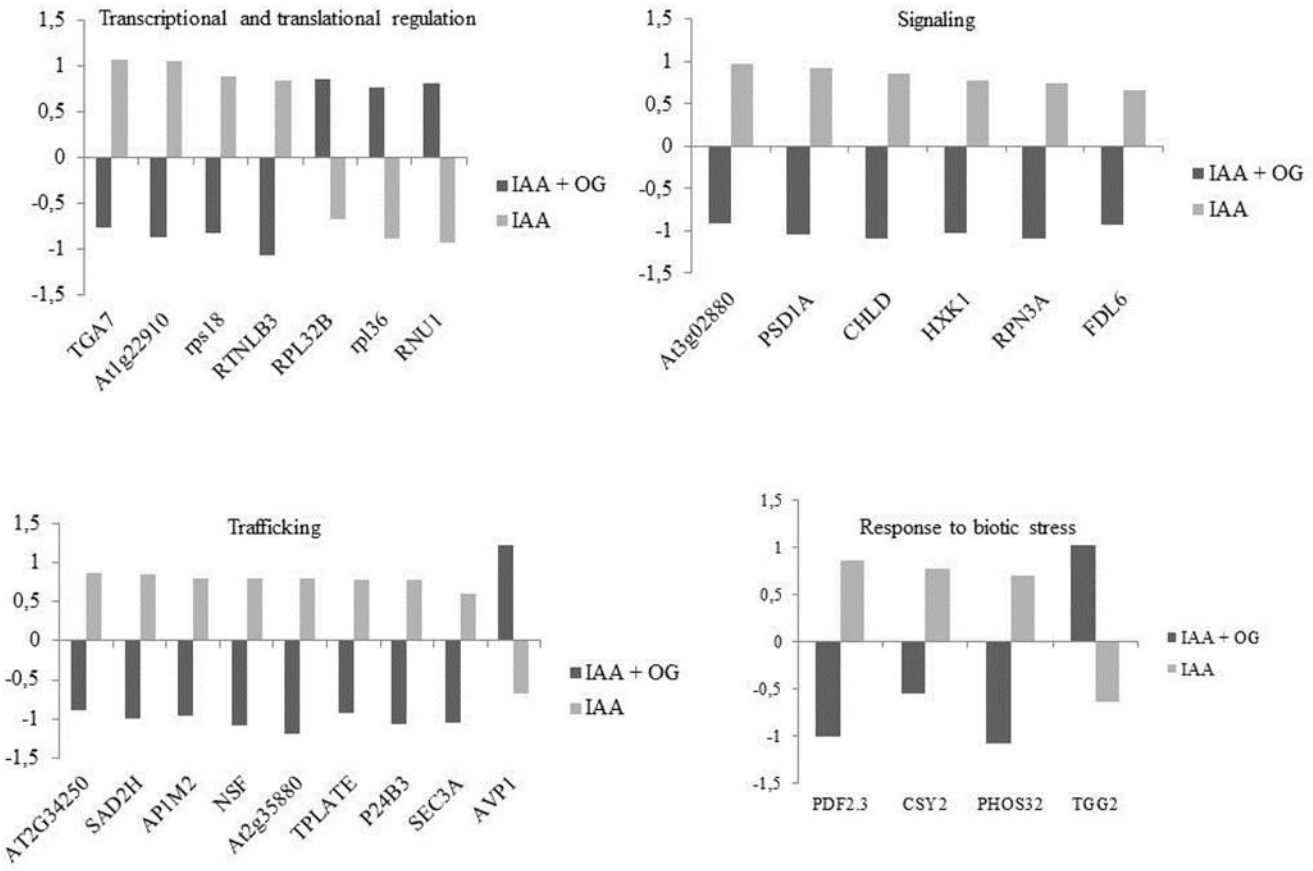

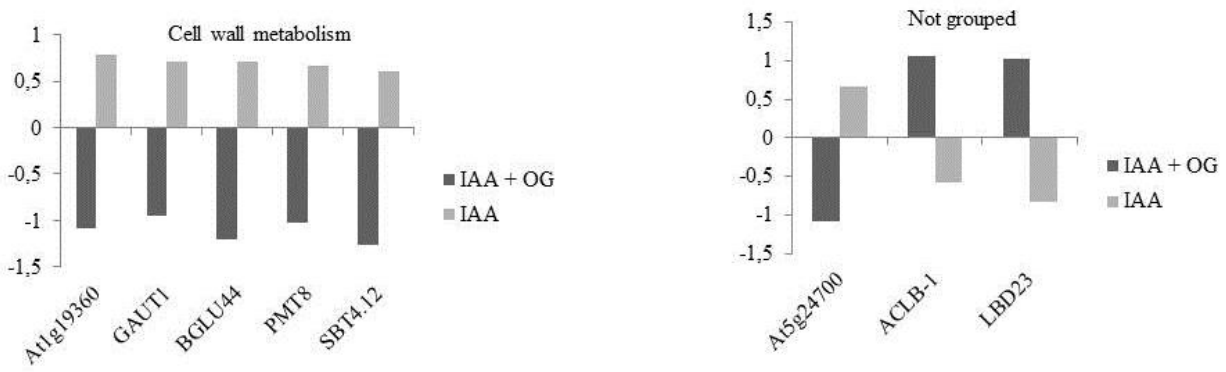

Figure 3.15 : Log2 normalized quantification of *PIAA5* specific interactors involved in OG – auxin antagonism.

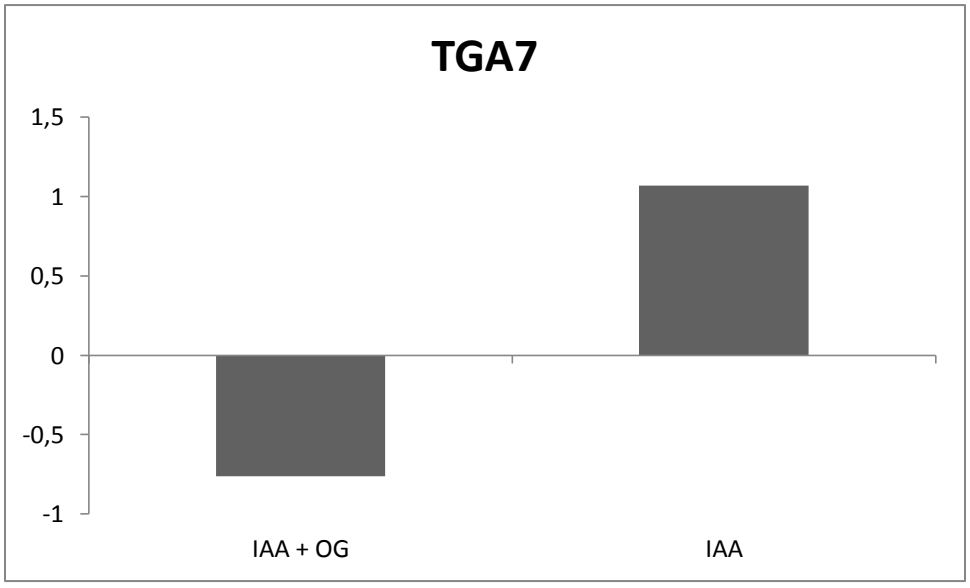

Figure 3.16 : Log2 of the normalized intensity of TGA7 bound on *PIAA5* in response to IAA treatments and to IAA + OG co-treatment.

3.10 TGA7 is a good candidate for a role in the OG – auxin antagonism

The transcription factors GT2, ARF5, which specifically interact with both *PIAA5* and DR5, did not appear among the differential proteins identified in my analyses. In the quantification, ARF5 and GT2 were below the significance threshold; TGA7, instead, showed differential abundance in the IAA and

IAA + OG treatments. Relative protein quantification reported as Log2 of the normalized intensity (Figure 3.16) shows that the amount of TGA7 bound on *PIAA5* in response to IAA treatments was higher (1.83 fold) respect to the amount of TGA7 bound on *PIAA5* in response to IAA + OG co-treatment. This indicate that TGA7 is positively regulated by IAA while OGs negatively affect on the protein abundance, indicating a possible role in the OG - auxin antagonism.

TGA7 (bZIP 50) is a transcriptional activator that binds specifically to the DNA sequence 5'-TGACG-3‘ (as-1 like elements); promoter analysis confirmed that *PIAA5* contains one as-1 like elements (Figure 3.17), that may act as TGA7 binding site. It was shown that binding to the as-1 like elements mediate auxin- and salicylic acid- inducible transcription (Xiang et al., 1996). TGA7 may be a mediator of the auxin-OGs antagonism.

Figure 3.17 : Nucleotide sequence of *IAA5* (AT1G15580.1) and its promoter (*PIAA5*). Black characters indicates non-coding regions while coding sequence is indicated in yellow and purple (exons and introns respectively). The promoter of *IAA5* shows the presence of TGA7 binding site (TGACG, circled in red). *PIAA5* also shows the presence of the ARE (TGTCTC, circled in black) .

3.11 Dynamics of the nuclear proteome in response to IAA, OG, IAA + OG

In my thesis work, I also studied the changes of the total nuclear proteome in response to IAA, OG, IAA + OG treatments through quantitative shotgun proteomics, as an alternative approach to investigate the processes that are affected by the OG – auxin antagonism. For the analysis of the nuclear proteome, proteins were extracted from purified nuclei of *Arabidopsis* seedlings treated differentially with IAA, OG, IAA + OG and mock- (water-) treated. To obtain the best coverage of the nuclear proteome, proteins were extracted and analyzed with two complementary methods (Figure 3.18). In the first method I used a label-based quantitative proteomics approach: purified nuclei were re-suspended in 8 M urea, nuclear proteins were solubilized and digested with trypsin. The tryptic peptides were dimethyl labeled, mixed in 1:1:1 molar ratio and fractionated by Strong Anion eXchange chromatography (SAX). Each fraction was analyzed by LC-MS/MS. In the second method I used a label-free quantitative proteomics approach: the nuclear proteome was fractionated at the protein level by extracting the purified nuclei with buffers of increasing ionic strength (Gonzalez-Camacho and Medina, 2007). The sequential extraction yielded 4 fractions containing different classes of proteins, as described in more detail below. Proteins from each fraction were digested with trypsin, analyzed by LC-MS/MS and quantified with a label-free approach.

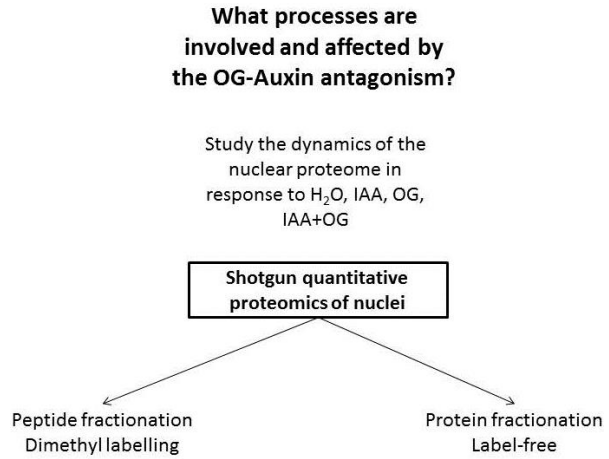

Figure 3.18 : schematic representation of the approach used to study the dynamics of the nuclear proteome in response to IAA, OG, IAA + OG through Shotgun quantitative proteomics. To get the best coverage of the nuclear proteome, the proteins were extracted and analyzed with two complementary methods, in the former a fractionation is performed at

peptide level and peptides were dimethyl-labeled for a label-based approach; while in the latter the fractionation is performed at the protein level and samples analyzed with label-free approach.

For these analyses, Col-0 *Arabidopsis* seedlings were grown 15 days on MS/2 liquid medium and treated with 1.5 µM IAA, 100 µg/mL of OG; co-treated with 1.5 µM IAA + 100 µg/mL of OG or mock treated for 1 h. Five independent biological replicates were used for the label-based quantitative proteomics and 3 independent biological replicates were used for the label-free quantitative proteomics. Treated seedlings were frozen in liquid nitrogen and stored at -80°C.

To verify the effectiveness of the treatments, the transcript levels of *IAA5* for IAA and IAA + OG treatments and *RetOx* for the OG were measured by semi-qPCR. After the treatments, total RNA was extracted from 100 mg of seedling for each treated flask. Two µg of total RNA were treated with RQ1 DNase to degrade genomic DNA and first-strand cDNA was synthesized using ImProm-II reverse transcriptase. *IAA5* and *RetOx* transcript levels relative to *UBQ5* transcript levels were measured for each differentially treated flask. The effectiveness of the treatments was evaluated as the induction of *IAA5* transcript in response to IAA treatments and as reduction of the induction *IAA5* transcript in response to the IAA + OG co-treatment (Figure 3.19a); while the induction of *RetOx* transcript was used to evaluate the OG treatment (Figure 3.19b). Samples in which the effectiveness of the treatments was confirmed were subsequently used for nuclei purification.

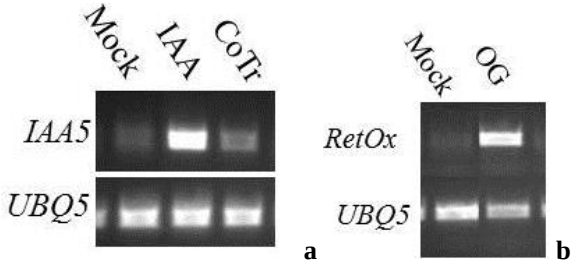

Figure 3.19 : (a) Control of IAA treatment and IAA + OG co-treatment (CoTr) effectiveness by semi-q PCR . The transcript of *IAA5* is induced after 1h of 1.5 µM IAA treatment while is reduced after 1h 1.5 µM IAA + 100 µg/mL of OG co-treatment. **(b)** Control of OG treatment effectiveness by semi-q PCR. The transcript of RetOx is induced after 1h of 100 µg/mL of OG treatment

3.12 Label-based quantitative proteomics of nuclei

For quantitative analysis ot the total nuclear proteome, nuclei were purified and the quality of nuclei preparations was assessed by Western blot and fluorescence microscopy, as previously described. In order to minimize the presence of protein contaminants that may co-purify with nuclei, purified nuclei were washed with Nuclei Storage buffer containing 120 mM NaCl. Washed nuclei were recovered after centrifugation at 1000g for 10 min at 4 °C, and suspended in 8 M urea to solubilize the proteins; chaotropic compounds such as urea disrupt hydrogen bonds and hydrophobic interactions both between and within proteins and are used to completely solubilize the nuclear proteins. Eighty μg of proteins from each differentially treated sample were digested with trypsin and the resulting peptides were desalted as described in Materials and Methods. The protein samples solubilized with 8 M urea will be called hereafter UNP (Unfractionated Nuclear Proteome).

Label-based mass spectrometry relies on the fact that a stable isotope-labeled peptide is chemically identical to its native counterpart and therefore the two peptides also behave identically during chromatographic and/or mass spectrometric analysis. Given that a mass spectrometer can recognize the mass difference between the differentially labeled forms of a peptide, quantification is achieved by comparing their respective signal intensities. In order to obtain quantitative information about the changes of the nuclear proteome in response to the treatments, peptides generated after trypsin digestion of the UNP samples were labeled with different isotopic forms of formaldehyde. Differentially labeled peptides were mixed in equimolar ratio and analyzed with LC-MS/MS. The labeling reaction is easy to perform, has a stoichiometric yield, and has the advantage of using inexpensive reagents. The analysis of the relative intensities of the peptides in the light, medium and heavy form allows to compare their relative abundance. Mock treated and IAA + OG co-treated US were labeled with the “light” label (+28 Da), the IAA treated samples were labeled with the “medium” label (+32 Da) and the OG treated samples were labeled with the “heavy” label (+36 Da). Labeled peptide mixtures were mixed in 1:1:1 ratio; each sample was purified from salts with R3 micro-columns. Having four treatments and three isotopic labels, the LC-MS/MS analysis was splitted into two terns with two shared sample; one tern was composed by peptides deriving from IAA, OG, and to IAA + OG treated seedlings (“medium”, “heavy” and “light” labeled respectively), while the other tern was composed by the peptides derived from IAA, OG and mock-treated seedlings (“medium”, “heavy”

and “light” labeled respectively). Two samples (mock and IAA + OG) were therefore labeled with “light” label.

Mixing the peptides increases the complexity of the sample, decreasing the possibility to identify and quantify low-abundant species. To overcome the complexity of UNP labeled peptide mixtures, I fractionated them by strong anionic exchange chromatography yielding 8 fractions as described in materials and methods. Each fraction was analyzed with LC-MS/MS.

3.13 Label-free quantitative proteomics of nuclei

In order to increase the coverage of the nuclear proteome analysis, a fractionation of the proteins in the preparation of purified nuclei extracted from IAA, IAA + OG , OG and mock-treated seedlings was performed. Fractionation was obtained by exploiting the solubility of proteins in buffers of increasing ionic strength, yielding four fractions: the first fraction contained proteins associated with the nuclear envelope and remnants of the cytoskeleton and was extracted by the use of Nonidet P-40 and sodium deoxycholate. This fraction was not further analyzed and this step was intended as a further wash of the purified nuclei. The second fraction was extracted with 10 mM TRIS-HCl pH 8.0, 1 mM EDTA and contained ribonucleoproteins active in nuclear RNA metabolism. Subsequently the chromatin in the pellet of the second extraction was digested with DNase and precipitated by increasing the ionic strength using ammonium sulphate and the third fraction was recovered as a supernatant after centrifugation. Finally the fourth fraction corresponding to the nuclear matrix was extracted with harsh conditions with 8 M urea, 200 mM TRIS-HCl pH 8.0 , 1% β-mercaptoethanol. Twenty μg of proteins from each fraction (2, 3 and 4) were digested with trypsin and the derived peptides were desalted as described in Materials and Methods prior to the LC-MS/MS analysis hereafter called NSP (Nuclear Sub-Proteomes).

3.14 Differentially regulated proteins

Mass spectra were analyzed using the MaxQuant platform version 1.3.0.5 (www.maxquant.org), supported by Andromeda as a search engine to identify protein sequences. The database search was conducted using the ARATH13 database, released in July 2013 with 33339 protein sequences of Arabidopsis thaliana. The proteins considered are those identified with at least two peptides. LC-MS/MS analysis of the UNP and NSP led to the identification of 2972 and 1808 proteins respectively. The subcellular location database for Arabidopsis proteins, SUBA 3 (Tanz et al., 2012), was used for *in silico* localization of all proteins identified in our experiments. SUBA was queried for all published experimental (GFP fusion protein microscopy, MS/MS, protein-protein interactions) and predicted evidence of the subcellular location of a protein. Considering the proteins identified by LC-MS/MS analysis in the UNP, 870 proteins (31%) out of 2972 had been previously experimentally observed in the nucleus, while 2242 proteins (79%) out of 2972 are predicted to be nuclear or to spend some time in the nucleus. Considering the proteins identified by LC-MS/MS analysis of the NSP, 724 proteins (40%) out of 1808 had been previously experimentally observed in the nucleus, while 1301 72%) out of 1808 proteins are predicted to be nuclear or to spend some time in the nucleus. The discrepancy between the percentage of nuclear proteins experimentally observed and those predicted is explained by the fact that the predicted nuclear localization is based on the prediction of the interaction between non-nuclear and nuclear proteins; in fact many non-nuclear proteins that do not contain the nuclear localization sequence (eg. hexokinase-1 of *A. thaliana*) are translocated into the nucleus in response to certain stimuli.

For the quantitative analysis, proteins that had been quantified in at least 3 biological replicates out of 5 in the UNP samples and in at least 2 biological replicates out of 3 in the NSP samples were taken into consideration for statistical analysis. The significance of the quantification of each protein in response to IAA, OG, IAA + OG compared to the mock was assessed by ANOVA; proteins with ANOVA p-value < 0.05 were considered as statistically significant.

A total of 247 proteins out of 2972 and 860 proteins out of 1808 were statistically significant in the analysis of UNP and NSP samples respectively. Among statistically significant proteins, those with a fold change greater or equal to $\pm$ 1.5 were considered as differential proteins. Out of 247 proteins, a total of 183 were found as differentially regulated in the UNP samples (Figure 3.20 a) and 760 out of 860 were found as differentially regulated in the NSP samples (Figure 3.20 b).

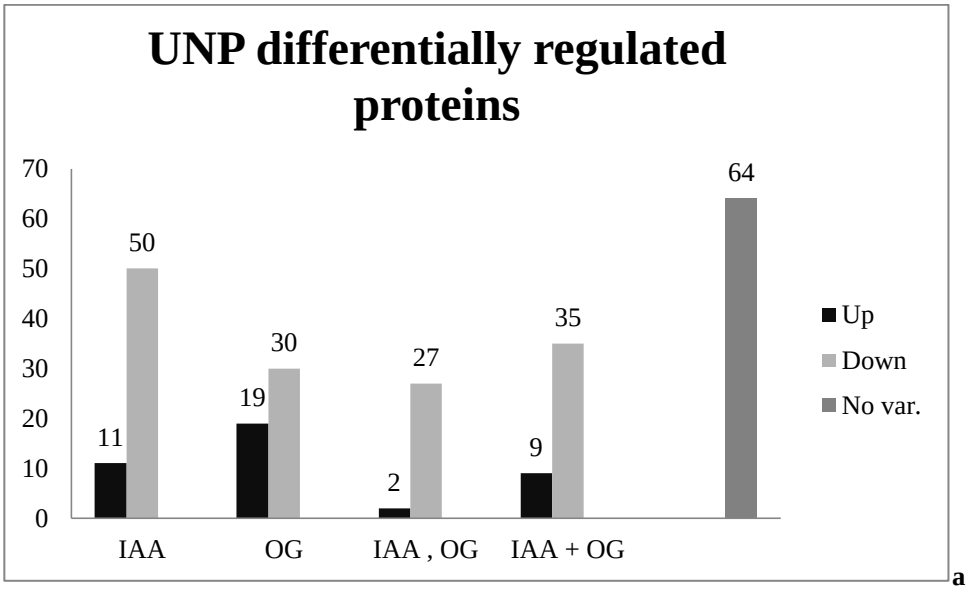

a

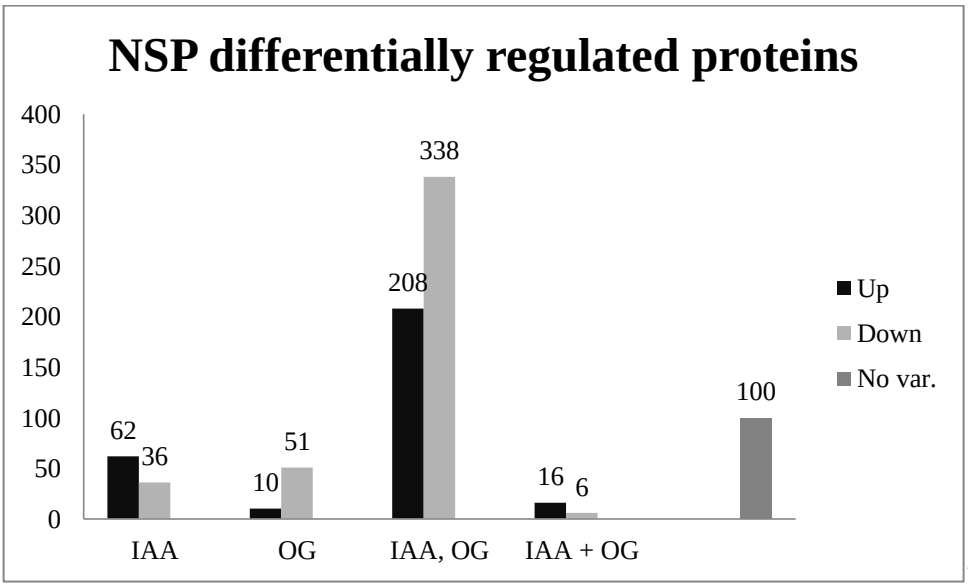

b

Figure 3.20 : (a) Proteins with statistically significant quantification (ANOVA p-value <0.05) quantified within the UNP samples; a total of 247 proteins are differentially regulated in response to IAA, OG, IAA + OG treatments. **(b)** Proteins with statistically significant quantification (ANOVA p-value <0.05) quantified within the NSP samples; a total of 760 proteins are differentially regulated in response to IAA, OG, IAA + OG treatments.

Differentially regulated proteins from UNP and NSP proteomic dataset were combined to study the dynamics of the nuclear proteome. In total, 911 proteins were differentially regulated while 168

proteins did not show no significant variation. The majority of differential proteins showed decreased abundance in response to IAA, OG, IAA + OG treatments. Figure 3.21 shows the number of proteins that are regulated only in response to IAA (157 proteins: 70 up-regulated, 87 down-regulated), only in response to OG (110 proteins: 31 up-regulated , 79 down-regulated), and in the same direction by both IAA and OG (581 proteins: 210 up-regulated, 371 down-regulated); this last result indicates a partial overlap in the response of the nuclear proteome to IAA and OG. Finally 59 proteins change abundance only in response to IAA + OG co-treatment (21 up-regulated, 38 down-regulated).

Among the 70 IAA up-regulated proteins, 20 are also down-regulated in response to the IAA + OG co-treatment, suggesting that these proteins are subjected to the antagonism by the OG, while 23 OG up-regulated proteins are down-regulated in response to IAA + OG co-treatment.

All the regulated proteins are listed in appendix A.

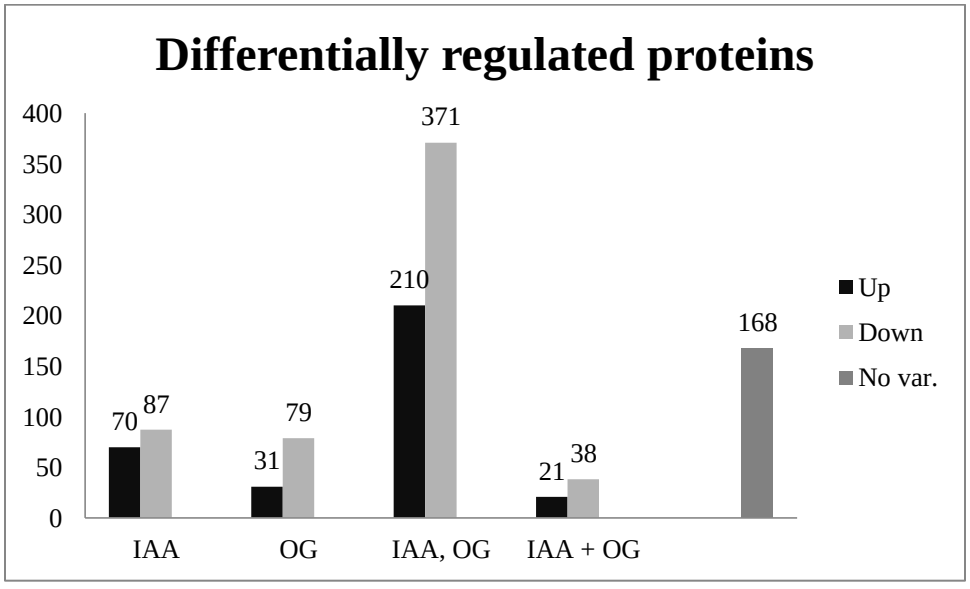

Figure 3.21 : 157 proteins are regulated only in response to IAA (70 up-regulated , 87 down-regulated) ; 110 proteins are regulated only in response to OG (31 up-regulated , 79 down-regulated); 581 proteins are regulated in the same way by both IAA and OG (210 up-regulated , 371 down-regulated); finally 59 proteins are regulated only in response to IAA + OG co-

treatment (21 up-regulated , 38 down-regulated). *Among the 70 IAA up-regulated proteins, 20 are also down-regulated in response to IAA + OG co-treatment.

3.15 Biological Process over-representation of differentially regulated proteins

To better understand the biological significance underlying differentially regulated proteins, biological process enrichment was performed using the DAVID Bioinformatics Resources annotation tool (http://david.abcc.ncifcrf.gov). Process over-representation was determined relative to the background set of all *A.thaliana* proteins. The complete list of the over-represented Biological Process in response to IAA, OG, IAA + OG treatments is reported in appendix B. Not all the proteins were grouped as part of Biological Processes, and Biological Process over-representation was used as indication to create a frame in which develop a putative model to describe the dynamics of the nuclear proteome with a focus on the antagonism of OG versus IAA induced processes.

3.16 IAA up-regulated processes

IAA treatment affects different processes in the nucleus (Figure 3.22). There is an increase of proteins involved in the oxidative stress response (TKL1,ANXD1,APX1,FUM1, FBA2,G3PC1,T15N1,PLDA1;VDAC1) and Ribosome biogenesis (CDC48A, L61, L13a3, RRS1, RL313, R35A3, RSSA1, RS91, RL303, NOP5B, CBF5). It was also observed the increase of proteins involved in transcriptional activation (FIB2; HTR4; ENO2; CYP18-2;MD36B; SPT51) and repression (HDT1,4 ; H2B.3; H2A7; SPT51) as well as proteins involved in splicing (SCL30;RSZ22;RH51; T5J8.16; T5J8.16;SR45; U2AFA) and in export of mRNA (NUP98A; LINC-1; SUN1); some proteins that were not grouped in Biological process were also reported as Miscellaneous (CPFTSY;ASP2; Waxy; At3g62530). On the other hand I observed the reduction of many regulatory subunits of the 26S proteasome (PSD8A;PS12A;PSD11;PSD3A;PSDE;PSMD6;PRS7A;PS6AA;PRS6B).

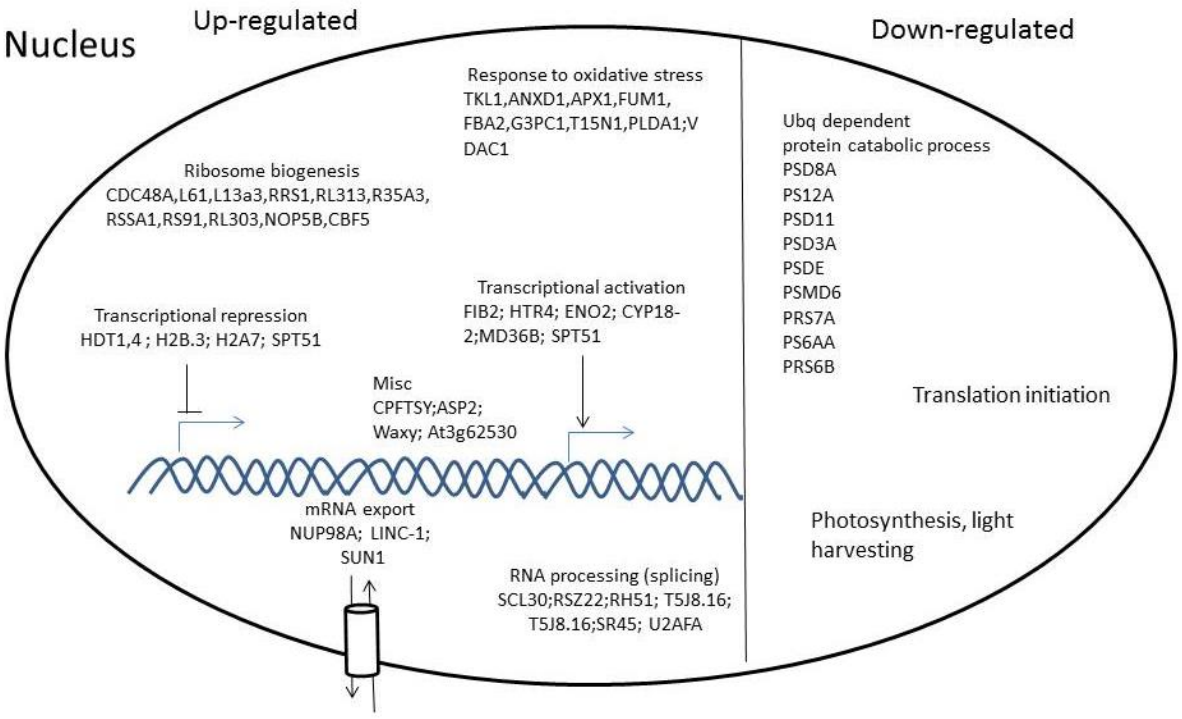

Figure 3.22 : IAA treatment involves the regulation of diverse processes in the nucleus. There is an increase of proteins involved in the oxidative stress response and Ribosome biogenesis. It was also observed the increase of proteins involved in transcriptional activation and repression as well as proteins involved in splicing and in export of mRNA; not grouped proteins were reported as Miscellaneous. On the other hand it observed the reduction of many regulatory subunits of the 26S proteasome.

3.17 OGs and IAA shows antagonistic effect on the regulation of proteins

Among the IAA up-regulated proteins, 20 are also down-regulated in response to IAA + OG co-treatment, indicating that these proteins are subjected to the antagonism by the OG (Figure 3.23 and Table 3.5). The antagonized proteins are part of Response to oxidative stress (FBA2,PLDA1) ; Ribosome biogenesis (RL303,CBF5); Transcriptional repression (H2B.3; H2A7;SPT51); Transcriptional activation (HTR4;CYP18-2;MD36B; SPT51); Splicing (RH51; T5J8.16;SR45; U2AFA); mRNA export (LINC-1;SUN1) and Miscellaneous (CPFTSY;ASP2; Waxy; At3g62530).

On the other hand among the OG up-regulated proteins, 17 are also down-regulated in response to IAA + OG co-treatment, indicating that these proteins are subjected to the antagonism by the IAA (Table 3.6). The antagonized proteins are part of Signaling (AT2G34040;CAND1;

CSN3;CSN6A;CSN7;DCAF1;RPN8A;AT2G26780); Transcription (La1;NPRB3;VIP3); Carbohydrate metabolism (BGLU22 and BGLU21) and Miscellaneous (AT2G40430 ; HSBP; PGDH1; Per32).

OG antagonism versus IAA	
Response to oxidative stress	
FBA2	Probable fructose-bisphosphate aldolase 2, chloroplastic
PLDA1	Phospholipase D alpha 1
Transcriptional repression	
H2B.3	Histone H2B.3
H2A7	Probable histone H2A.7
SPT51	Putative transcription elongation factor SPT5 homolog 1
Transcriptional activation	
MED36B	Probable mediator of RNA polymerase II transcription subunit 36b
CYP18-2	Peptidyl-prolyl cis-trans isomerase
HTR4	Histone superfamily protein
SPT51	Putative transcription elongation factor SPT5 homolog 1
Ribosome biogenesis	
CBF5	H/ACA ribonucleoprotein complex subunit 4
RL313	60S ribosomal protein L31-3 GN
Splicing	
SR45	Ribonucleoprotein
U2AFA	Isoform 3 of Arginine/serine-rich protein 45
RH51	Splicing factor U2af small subunit A
T5J8.16	DEAD-box ATP-dependent RNA helicase 51
mRNA export	
LINC1	Protein little nuclei1
SUN1	ARABIDOPSIS SAD1/UNC-84 DOMAIN PROTEIN 1
Misc	
CPFTSY	chloroplast SRP receptor homolog, alpha subunit
ASP2	ASPARTATE AMINOTRANSFERASE 2
Waxy	GBSS1, GRANULE BOUND STARCH SYNTHASE 1

Table 3.5 : IAA up-regulated proteins also down-regulated by OGs

IAA antagonism versus OG	
Signaling	
AT2G34040	Apoptosis inhibitory protein 5 (API5)
CAND1	Cullin-associated NEDD8-dissociated protein 1
CSN3	COP9 signalosome complex subunit 3
CSN6A	COP9 signalosome complex subunit 6a
CSN7	COP9 signalosome complex subunit 7
DCAF1	DDB1- and CUL4-associated factor homolog 1
RPN8A	Probable 26S proteasome non-ATPase regulatory subunit 7
AT2G26780	ARM repeat superfamily protein
Transciption	
La1	La protein 1
NRPB3	DNA-directed RNA polymerases II, IV and V subunit 3
VIP3	At4g29830
Carbohydrate metabolism	
BGLU22	Beta-glucosidase 22
BGLU21	Beta-glucosidase 21
Miscellaneous	
AT2G40430	Uncharacterized protein
HSBP	At4g15810
PGDH1	EDA9 (embryo sac development arrest 9)
PER32	Peroxidase 32

Table 3.6 : OG up-regulated proteins also down-regulated by IAA

3.18 Promoter analysis of IAA-induced proteins subjected to antagonism by OG

Considering that the transcription factor TGA7 was demonstrated to be a potential candidate for a role in the OG – auxin antagonism, I wondered if also the expression of the proteins subjected to antagonism can be regulated through the involvement of TGA7. Therefore the promoter regions of the IAA-induced proteins subjected to antagonism by OG were analyzed for the presence of the As1-like motif (TGACG) with the "Statistical Motif Analysis in Promoter" tool provided by TAIR (The Arabidopsis Information Resource ; https://www.arabidopsis.org/). Promoter analysis shows that 14 proteins out of 20 reported in Figure 3.23 and in Table 3.7 contains the As-1 like motif in their promoters.

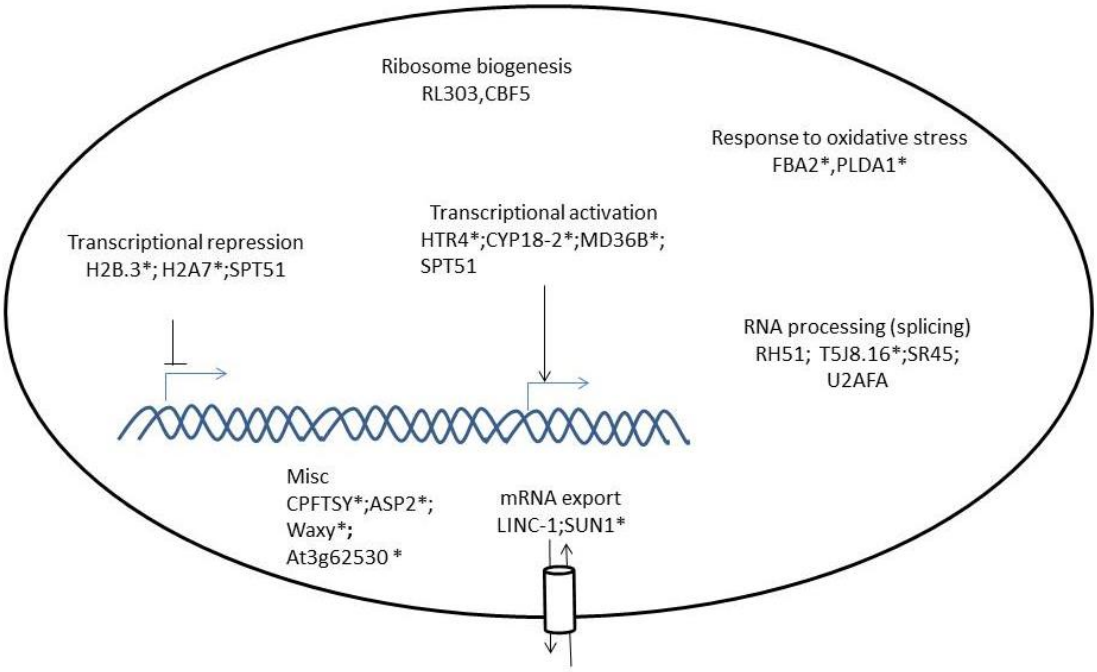

Figure 3.23 : proteins up-regulated by IAA and down-regulated in response to IAA + OG co-treatment. The antagonized proteins are part of Response to oxidative stress; Ribosome biogenesis; Transcriptional repression; Transcriptional activation ; Splicing ; mRNA export and Miscellaneous. Proteins that contains the As1-like motif in their promoter are signed with an asterisk (*).

Response to oxidative stress	
FBA2	Probable fructose-bisphosphate aldolase 2, chloroplastic
PLDA1	Phospholipase D alpha 1
Transcriptional repression	
H2B.3	Histone H2B.3
H2A7	Probable histone H2A.7
Transcriptional activation	
MED36B	Probable mediator of RNA polymerase II transcription subunit 36b
CYP18-2	Peptidyl-prolyl cis-trans isomerase
HTR4	Histone superfamily protein
Splicing	
T5J8.16	Ribonucleoprotein
mRNA export	
SUN1	ARABIDOPSIS SAD1/UNC-84 DOMAIN PROTEIN 1
Misc	
CPFTSY	chloroplast SRP receptor homolog, alpha subunit
ASP2	ASPARTATE AMINOTRANSFERASE 2
Waxy	GBSS1, GRANULE BOUND STARCH SYNTHASE 1

Table 3.7 : IAA up-regulated proteins, also down-regulated in response to IAA + OG co-treatment that contains the As1-like motif in their promoter.

4 Discussion

Plants respond to pathogens through a complex set of defense mechanisms, including both preformed and induced physicochemical barriers. Induced defences start with the perception of the pathogen: pathogen conserved motifs known as microbe-associated molecular patterns (MAMPs) and plant derived molecules modified upon infection, known as damage-associated molecular patterns (DAMPs), are recognized by pattern recognition receptors (PRR). Exogenous activation of plant resistance may be achieved by the application of plant non-self determinants such as chitin oligomers or plant cell wall derived oligosaccharides to simulate the presence of pathogens.

α-1-4-Linked oligogalacturonides (OGs) derived from plant cell walls are a class of damage-associated molecular patterns and well-known elicitors of the plant immune response. OGs are released when PGs degrade the homogalacturonan in the cell (Cote et al., 1998). Pectins are one of the first targets of cell wall degrading enzymes produced by invading pathogens, therefore the early detection of OGs can be a good strategy for plants to initiate defense responses and elicit a variety of defense responses.

OG treatment has been reported to induce a range of defense responses, like accumulation of phytoalexins, β-1,3-glucanase and chitinase, or generation of ROS by triggering nitric oxide (NO) production (Rasul et al., 2012). During an infection process, OGs may prepare the plant defense system in a so-called primed state (priming process), sensitizing the plant immune system and leading to a stronger induction of defence responses upon pathogen recognition.

Exogenous treatments with OGs protect grapevine leaves against necrotrophic pathogen *Botrytis cinerea* infection in a dose-dependent manner (Aziz et al., 2004). In *Arabidopsis*, OGs increase resistance to *Botrytis cinerea* independently of JA-, SA-, and ethylene (ET)-mediated signaling. A microarray analysis has shown that about 50% of the genes regulated by OGs display a similar change of expression during *Botrytis cinerea* infection (Ferrari et al., 2013).

It was recently shown that expression of a PGIP–PG chimera results in the in vivo production of OGs and that transgenic plants expressing the chimera under control of a pathogen-inducible promoter are more resistant to the phytopathogens *Botrytis cinerea*, *Pectobacterium carotovorum,* and *Pseudomonas syringae* (Benedetti et al., 2015). On the other hand, elevated levels of expression of the chimera cause the accumulation of salicylic acid, reduced growth, and eventually lead to plant death, indicating that

high concentrations of endogenous OGs interfere with normal developmental programs. This finding is consistent with the current notion that trade-off occurs between growth and defense. Maintenance of immunity is costly and immune responses are typically counterbalanced by decreasing the allocation of resources to biomass production.

Growth regulators that are involved in development are also key elements of immune response cascades and immune elicitors often inhibit auxin responses (Ferrari et al., 2013). The growth-promoting hormones BR and auxin inhibit PAMP-triggered immunity (PTI), and PAMPs (e.g., flagellin and elongation factor peptides flg22 and elf18, respectively) inhibit plant growth. Plants that constitutively express defense responses are often dwarf (Vos et al., 2013).

OGs also regulate growth and development of plant cells and organs, due to an auxin-antagonistic activity. The mechanism by which OGs act in opposition to the action of auxin is presently unknown; Savatin and colleagues (Savatin et al., 2011) have recently shown that OG - auxin antagonism does not involve any of the following mechanisms: (1) stabilization of auxin-response repressors; (2) decreased levels of auxin receptor transcripts through the action of microRNAs. These data suggest that OGs antagonize auxin responses independently of Aux/Indole-3-Acetic Acid (Aux/IAA) repressor stabilization and of posttranscriptional gene silencing; It was therefore speculated that OG – auxin antagonism can be played at the level of transcriptional regulation on the promoter of auxin-inducible genes antagonized by OGs.

INDOLE-3-ACETIC ACID INDUCIBLE 5 (*IAA5*) is a gene up-regulated early (within 1 h) by IAA, and its auxin-induced expression is also inhibited by OGs (Savatin et al., 2011). For this reason, it was chosen as a marker gene to study the auxin-OGs antagonism.

In my work I constructed *PIAA5*:GUS transformed plants to study the regulation of *PIAA5* in response to the treatments with IAA and IAA + OG. The expression of GUS transcript was induced by 1.5 μM IAA compared to the mock and the induction of the GUS transcript was reduced in response to 1.5 μM IAA + 50μg/mL OG co-treatment. These data indicate that OG –auxin antagonism takes place on the promoter of *IAA5*.

The transcription processes requires the interaction of proteins with the promoter of target genes. Since the OG – auxin antagonism is played at the promoter level of *PIAA5* and DR5, I thought that sequence-

specific transcriptional factors (TFs) may be involved as target and that the OG – auxin antagonism may be putatively exerted through the regulation of such TFs.

I have developed a pull-down assay to selectively extract protein-DNA complexes formed at the promoter of IAA5 and DR5. I have used *PIAA5* and DR5 labeled with biotin, which allows the probe to be immobilized on streptavidin-coated magnetic beads and used these as baits to isolate DNA-protein complexes from nuclear extracts of plants treated with IAA or IAA+OGs. The proteins were then recovered from the DNA and identified by mass spectrometry.

Methods combining DNA-affinity protein capture with MS-based protein identification should ideally provide the identity of all the proteins bound to a DNA sequence of interest. However, a major challenge comes from the fact that DNA can interact with an intricate protein network displaying a high dynamic range between some very low abundant transcriptional regulators and high abundant unspecific DNA-binding proteins. Moreover identification of proteins interacting with a relatively long DNA sequence (1279 bp in the case of PIAA5) certainly represents a technical challenge, as it requires the analysis of a complex mixture of peptides generated by the digestion of many proteins whose abundance may be distributed on a large dynamic range. Current progress in nano-LC-tandem mass spectrometry (LC-MS/MS) encouraged me to choose a gel-free approach rather than a one- or two-dimensional electrophoresis protein separation that might suffer from poor detection of low abundant proteins. Proteins purified by DNA affinity were digested with trypsin. The complex peptide mixture obtained was separated by reverse-phase chromatography before being sequenced by MS.

To reinforce protein identification resulting from the DNA-affinity, sets of data were accumulated from three independent biological replicates. All the identified proteins captured by the promoters were pooled in a global list and proteins identified only in one replicate were not considered.

In total 190 proteins were identified in the affinity purification with DR5 and not with CTR and were considered as specific interactors of DR5. Among the 190 specific interactors of DR5, seven proteins showed a significant differential abundance between IAA and IAA+OG treatment and are reported in Table 3.3 and Figure 3.14. Among these proteins we did not identify transcription factors or other potential candidates directly related to the hypothesized mechanism of OG–auxin antagonism.

A total of 544 proteins were identified in the affinity purification with *PIAA5* that were not recovered with *PUBQ5* and were considered as specific interactors. In the case of *PIAA5*, thirty-four proteins

showed a significant differential abundance between IAA and IAA+OG treatment (Table 3.4 and figure 3.15). According to Uniprot general protein annotations and to information from the literature, proteins involved in the OG-auxin antagonism isolated with *PIAA5* affinity were further classified into six categories based on their functions, specifically: Transcriptional and translational regulation, Signaling, Trafficking, Response to stress, Cell wall metabolism, and Miscellaneous that includes proteins with diverse functions.

The method allowed enrichment of low abundant targets such as transcription factors:

- GT2 belongs to the family of Trihelix transcription factors and its transcriptional regulation activity was inferred from sequence similarity (Riechmann et al., 2000); current information suggests that trihelix transcription factors regulate light-responsive genes and also play important roles in the regulation of developmental processes involving flowers, trichomes, stomata, embryos and seeds and in responses to biotic and abiotic stresses, (Wang et al., 2014). Presently there aren't known interactors of GT2 and there are no evidences for the involvement of GT2 in auxin-regulated processes.
- ARF5 (Auxin responsive factor 5) is a transcriptional factor that belongs to the ARF family and is known for the role in the auxin-dependent gene regulation ; it mediates organ and vascular tissue formation throughout the *Arabidopsis* life cycle (Hardtke et al., 2004).
- TGA7 is a transcriptional factor belonging to the family of basic region/leucine zipper motif (bZIP) transcription factors which regulate processes including pathogen defence, light and stress signalling, seed maturation and flower development (Jakoby et al., 2002); has a role in the auxin inducible gene transcription (Xiang et al., 1996).

The isolation of ARF5, predicted to bind to the AREs that were present both on DR5 and *PIAA5* and TGA7, both involved in auxin-mediated gene regulation, gives consistency to the experimental results and indicated that the DNA affinity purification procedure could isolate *PIAA5* and DR5 specific interactors.

TGA transcription factors belong to the group of bZIP transcription factors which are found in all eukaryotes. TGA factors bind specifically to variants of the palindrome TGACGTCA. Two of these sequences separated by 4 bps are called an activation sequence-1 (as-1).
The bZIP proteins are transcription factors which contain a basic region for specific DNA contact and a leucine zipper domain for dimerization. All bZIP factors bind to specific DNA sequences as homo- or

heterodimers (Landschulz et al., 1988). These transcription factors are believed to contribute to the efficiency with which RNA polymerase II binds and initiates transcription at the promoter of a gene. They are generally activators of transcription in response to external stimuli either constitutively or in a regulated manner usually through post-translational modification such as phosphorylation. However, bZIP proteins can also be repressors in some cases.

The family of TGA factors has 10 members in the model plant Arabidopsis thaliana. Seven of these TGAs were further characterized and were divided into three clades based on sequence homology: TGA1 and TGA4 comprise clade I; TGA2, TGA5, and TGA6 belong to clade II; TGA3 and TGA7 make up clade III. TGA2, TGA3, TGA5, TGA6, and TGA7 constitutively interact with NPR1 in yeast and in planta when transiently expressed. Interestingly, the two TGA factors (i.e. TGA1 and TGA4) that showed no interaction with NPR1 in yeast were found to bind NPR1 only in SA-induced leaves. Reduction of two Cys residues that are uniquely present in TGA1 and TGA4 are responsible for this SA-dependent interaction (Després et al., 2003).

Pathogen-induced transcriptional reprogramming of the plant genome is mediated predominantly by the cofactor NPR1 (NON-EXPRESSOR OF PATHOGENESIS-RELATED GENES1). NPR1 lacks any known DNA-binding domain and is proposed to regulate transcription through interactions with TGA transcription factors that bind to as-1-like promoter elements. Previous studies have focused on the interaction of NPR1 with subgroup I (TGA1, TGA4) or subgroup II (TGA2, TGA5, TGA6) factors. TGA7 interacts with wild-type NPR1, and NPR1 substantially increased the binding of TGA7 to cognate promoter elements in vitro, including a salicylic-acid-inducible element of the PR-1 promoter. NPR1-mediated DNA binding of TGA7 could regulate the activation of defense genes. It has been shown that SA inhibits growth by suppression of the auxin signaling; it represses the expression of the TIR1/ABF F-box genes , resulting in stabilization of AUX/ IAA repressor proteins to decrease auxin signaling (Wang et al., 2007).

No target genes regulated by TGA7 and involved in auxin responses have been identified so far. To investigate a possible role of TGA7 in regulating trade-off between development and immunity it will be necessary to identify the target genes of TGA7 in the *Arabidopsis thaliana* genome by performing chromatin immunoprecipitation followed by sequencing (ChIP-Seq) and RNA sequencing (RNA-Seq).

The 34 specific interactors of *PIAA5* potentially involved in the OG – auxin antagonism were grouped in 5 functional categories on the basis of their known function (Figure 3.15).

-Trafficking: 9 proteins out of 34 were involved in trafficking. Polar transport of auxin regulates various processes in plant growth and development, such as apical dominance, growth related tropisms, vascular patterning and axis formation. Polar auxin flux is achieved by the asymmetric distribution of efflux carriers localized at the plasma membrane (PIN1) then vesicle trafficking plays an important role on the regulation of responses to auxin. In fact the vesicle-trafficking inhibitor brefeldin A mimics physiological effects of those caused by auxin transport inhibitors (Geldner et al., 2001). A possible mechanism by which OGs may regulate auxin responses could involve the modulation of vesicle trafficking processes, as suggested by the fact that many proteins involved in cell polarity formation (SEC3A, TPX2 ,TPLATE,AP1M2) were down-regulated in response to IAA+OG co-treatment. Interestingly AVP1, a H(+)-translocating (pyrophosphate-energized) inorganic pyrophosphatase (H(+)-PPase), which is involved in regulation of apoplastic pH and auxin transport, was up-regulated in response to IAA+OG co-treatment.

-Signaling: 6 proteins out of 34 were involved in signaling. Signaling processes control the responses of the plant cells to environmental and phytochemical stimuli. For example auxin signaling is based on the perception of free auxin by the TRANSPORT INHIBITOR RESPONSE1/AUXIN SIGNALING F-BOX PROTEIN1-3 (TIR1/AFB1-3) receptors, triggering the degradation of AUXIN/INDOLE-3-ACETIC ACID (AUX/IAA) proteins by the 26 S proteasome. The 26 S proteasome is a multisubunit protease complex responsible for degrading a wide range of intracellular proteins in eukaryotes, especially those polyubiquitinylated; RPN2A and RPN3A regulatory subunit of the 26 S proteasome which are involved in the ATP-dependent degradation of ubiquitinated proteins were down-regulated by OG + IAA co-treatment. At3g02880, a leucine-rich repeat protein kinase family protein with a role in protein tyrosine kinase signaling pathway acting respiratory burst involved in defense responses and root hair elongation, was also down-regulated by OG + IAA co-treatment. Furthermore HXK1, a sugar sensor that mediates the effects of sugar on plant growth and development, was also down-regulated by OG + IAA co-treatment. These data indicate that OG may modulate auxin responses by regulating the levels of proteins involved in various signaling processes.

-Transcriptional and translational regulation: 7 proteins out of 34 were involved in transcription and translation. Transcriptional regulation through the regulation of specific transcription factors is a well-known mechanism for the responses to environmental and phytochemical stimuli. OGs could modulate the responses to auxin through the regulation of the transcription factor TGA7.

OGs also modulated the levels of other proteins involved in translation. Among these, ribosomal proteins may also play a role in the translation process and in development; it was shown that mutants, in which the ribosomal RPL24B protein had been deleted, showed specific defects in the apical-basal patterning of the gynoecium (Nishimura et al., 2005).

-Cell wall metabolism: 5 proteins out of 34 were involved in the cell wall metabolism. It is known that auxin regulates cell expansion through modification of the cell wall, activating the expansin proteins; those, lead to a loosening of the cell wall and expansion driven from the turgor pressure. In this frame, cell wall-modifying enzyme could be necessary to exert the correct process of cell expansion. In this work we found RRA3, an arabinosyltransferase that modifies extensin proteins in root hair cells, that could be involved in the auxin-mediated expansin activation. PTM8 a S-adenosyl-L-methionine-dependent pectin-methyltransferase could be involved in pectin methylation, that leads to a decrease in sthe cell wall stiffness by reducing the amount of the so called "Egg Box" of the pectin matrix. The homogalacturonan of the pectic fraction seems to have a role in the auxin-mediated cell wall modification regulated by OG, due to the fact that the level of two proteins GAUT1 and PTM8 is decreased in response to OG + IAA co-treatment. GAUT1 is a pectin biosynthetic enzyme that catalyzes the transfer of galacturonic acid from uridine 5'-diphosphogalacturonic acid onto the pectic polysaccharide homogalacturonan; PTM8 is a S-adenosyl-L-methionine-dependent pectin-methyltransferase that can be involved in pectin methylation.

-Response to stress: 4 proteins out of 34 are grouped in the class "response to stress".

Nuclear proteome dynamics in response to IAA, OG, IAA+ OG treatments was studied by two complementary proteomics strategies: label-based quantitative proteomics of the Unfractionated Nuclear Proteome (UNP) and label-free quantitative proteomics of a fractionated Nuclear Sub Proteome (NSP).

The proteomic study is described through a simplified flowchart showing the different steps from experimental material to protein identification, as illustrated in **Figure** 4.1 . Density gradient methods was used to prepare a nuclear fraction.

The first method led to the identification and quantification of the most abundant proteins such as Ribosomal proteins and proteins involved in translation. This was due to the fact that the nuclear proteins extraction yielded a complex mixture of proteins with a high dynamic range of abundances. Even though a fractionation was performed at the peptide level using SAX chromatography, the

peptides originating from abundant proteins were spread in the fractions obtained by SAX and the ratio between abundant and low-abundant peptides was nearly unaltered respect to the unfractionated sample. Furthermore the Label-based analysis implied mixing of the differentially-labeled peptides prior of the analysis, that inevitably led to an increase of the complexity of the peptidic sample, and thus in a reduction of the coverage of the nuclear proteome. Moreover the quantification of a given protein requires that all the differentially-labeled peptides must be detected by the mass spectrometer, and in our LC-MS/MS runs less than 10% (247 out of 2972 proteins) of the total identified proteins could be significantly quantified.

The most efficient method to separate NPs is based on sequential extraction of protein fractions with increasing ionic strength (Gonzalez-Camacho and Medina, 2007). In brief, the procedure yielded four fractions: the first fraction contained proteins associated with the nuclear envelope and remnants of the cytoskeleton; this fraction was not further analyzed and its extraction was intended as a further wash of the purified nuclei. The second fraction contains ribonucleoproteins active in nuclear RNA metabolism; the third fraction contains the chromatin fraction while the fourth contains the insoluble proteins such as proteins of the nuclear matrix. After separation the fractions are digested to allow identification of proteins by mass spectrometry. Identification of proteins was done by peptide sequencing using liquid chromatography coupled to MS (LC-MS/MS). The fractionation at the protein level coupled with the label-free analysis lead to a better coverage of the nuclear proteome and above all an increased number of significantly quantified proteins (247 out of 2972 proteins in the UNP and 860 out of 1808 proteins in the NSP analysis). Considering that the number of fractions in the NSP were less compared to UNP (4 and 8 respectively) but the number of significantly quantified proteins was about 4 fold in NSP respect to UNP led us to consider that the label-free approach allows a more accurate quantification of the protein samples. Analysis of NSP led to the identification of a higher number of proteins with certain nuclear localization, probably due to the fact that the extraction of the first fraction led to a "cleaning" of the nuclei from proteins that can co-purify with nuclei.

Considering the dynamics of the nuclear proteome the first phenomenon that can be observed is the high of down-regulated proteins; this can be due to the necessity of the cell to turn-off the processes acting in the stationary state in order to get the right response to the new perceived stimuli. Protein down-regulation can be achieved by degradation, while the up-regulation is likely to be achieved by protein translocation, considering that protein synthesis requires more than 1 hour. The other interesting phenomenon is the fact that some proteins are regulated exclusively by the co-treatment,

indicating that may indicate that the regulation of this particular group of proteins may occur when auxin and OG are present simultaneously.

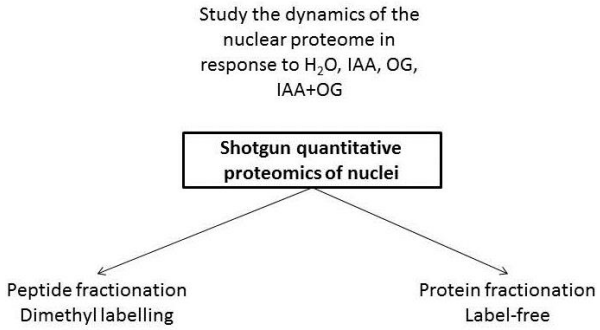

Figure 4.1 : schematic representation of the approach used to study the dynamics of the nuclear proteome in response to IAA, OG, IAA + OG through Shotgun quantitative proteomics. To get the best coverage of the nuclear proteome, the proteins were extracted and analyzed with two complementary methods, in the former a fractionation is performed at peptide level and peptides were dimethyl-labeled for a label-based approach; while in the latter the fractionation is performed at the protein level and samples analyzed with label-free approach.

To better understand the biological significance underlying differentially regulated proteins, biological process enrichment was performed using the DAVID Bioinformatics Resources annotation tool (http://david.abcc.ncifcrf.gov). Process over-representation was determined relative to the background set of all *A.thaliana* proteins. The complete list of the over-represented Biological Process in response to IAA, OG, IAA + OG treatments is reported in appendix B while the most enriched Biological processes (p-value < 0.01) were reported in Figure 4.2 a,b,c. Not all the proteins were grouped as part of Biological Processes, and Biological Process over-representation was used as indication to create a frame in which develop a putative model to describe the dynamics of the nuclear proteome with a focus on the antagonism of OG versus IAA induced processes.

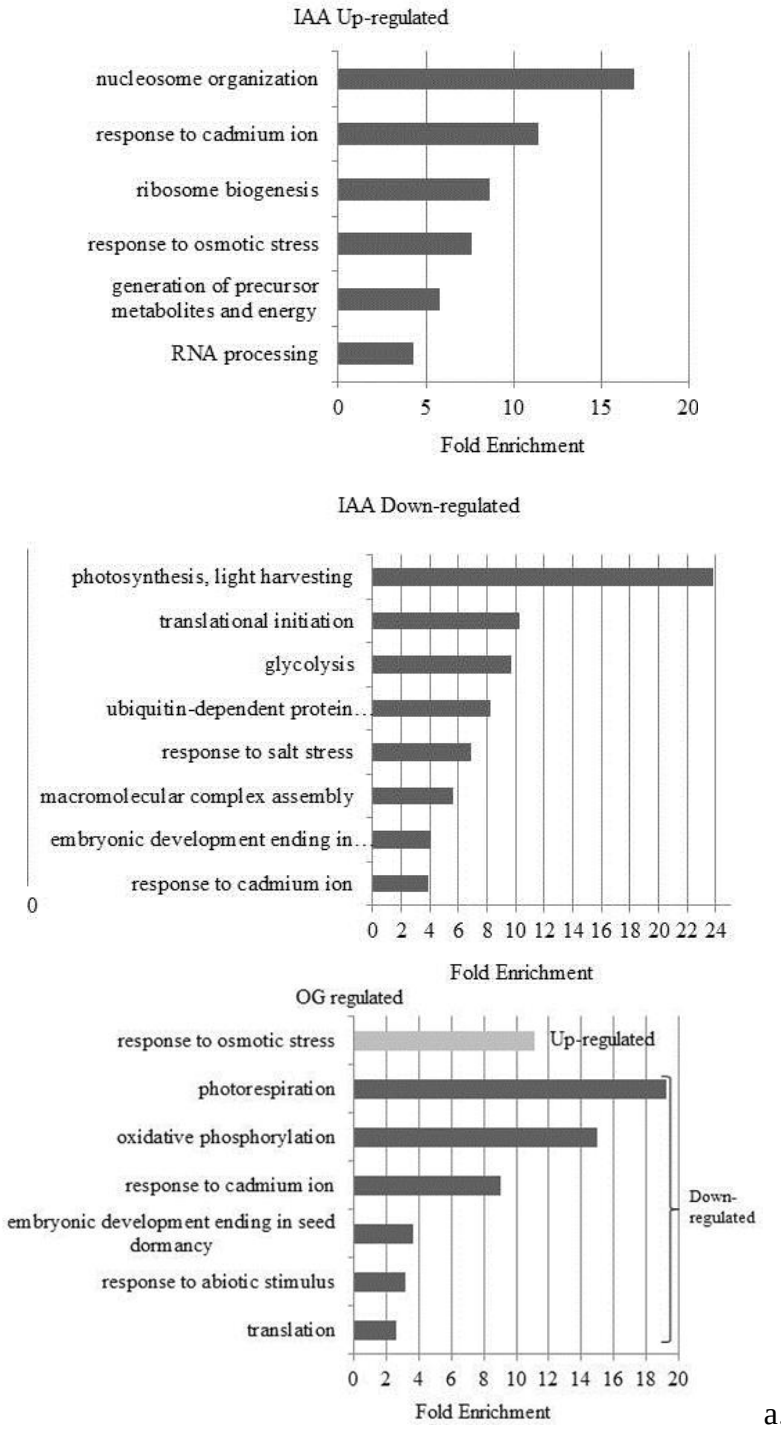

a.

Figure 4.2 a : Bar chart of the Gene ontology (GO) bar chart for the over-represented Biological Processes in response to IAA, OG, IAA + OG treatments. GO categories with at least 2 genes and $p < 0.01$ are identified as enriched.

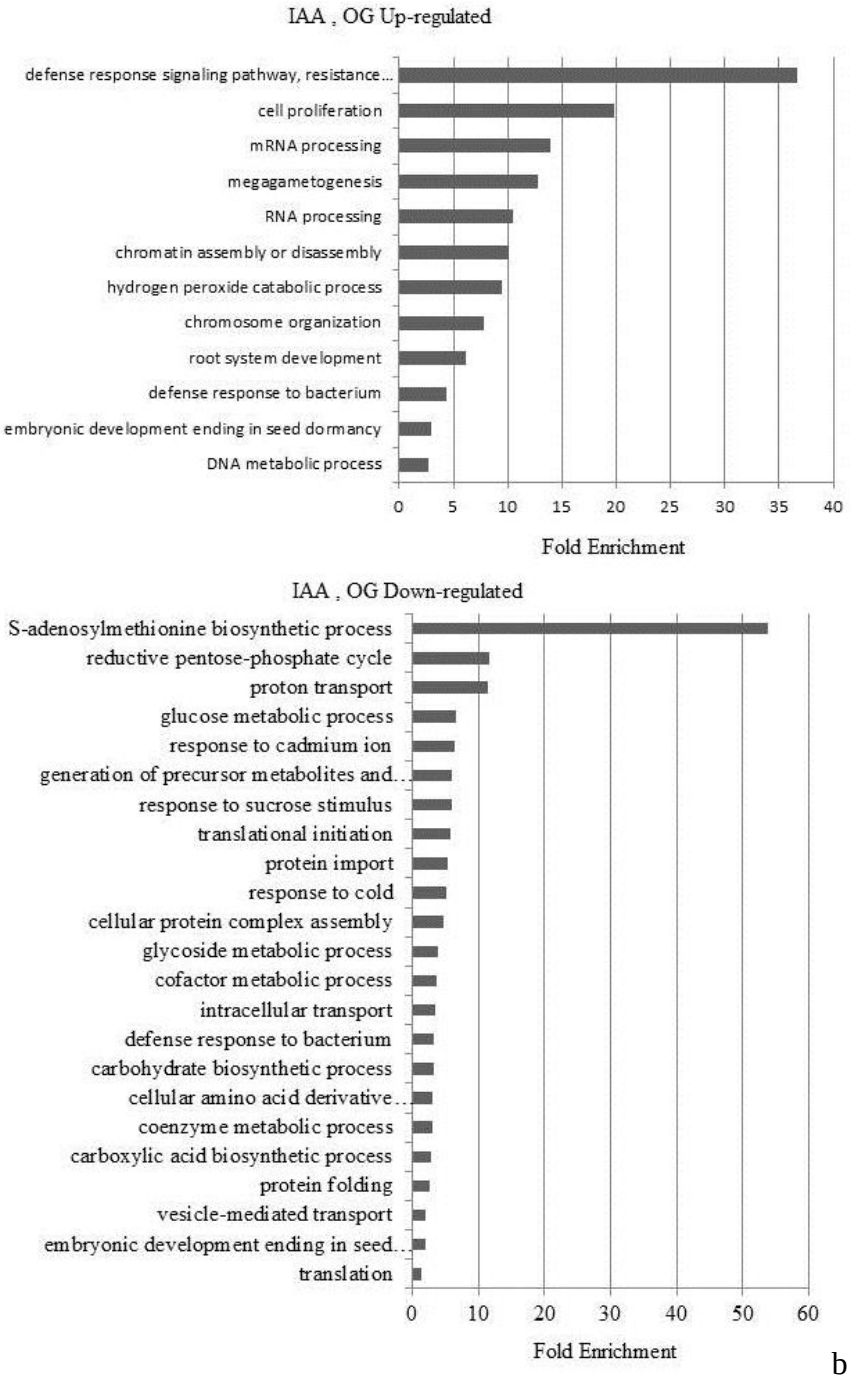

Figure 4.2 b : Bar chart of the Gene ontology (GO) bar chart for the over-represented Biological Processes in response to IAA, OG, IAA + OG treatments. GO categories with at least 2 genes and $p < 0.01$ are identified as enriched.

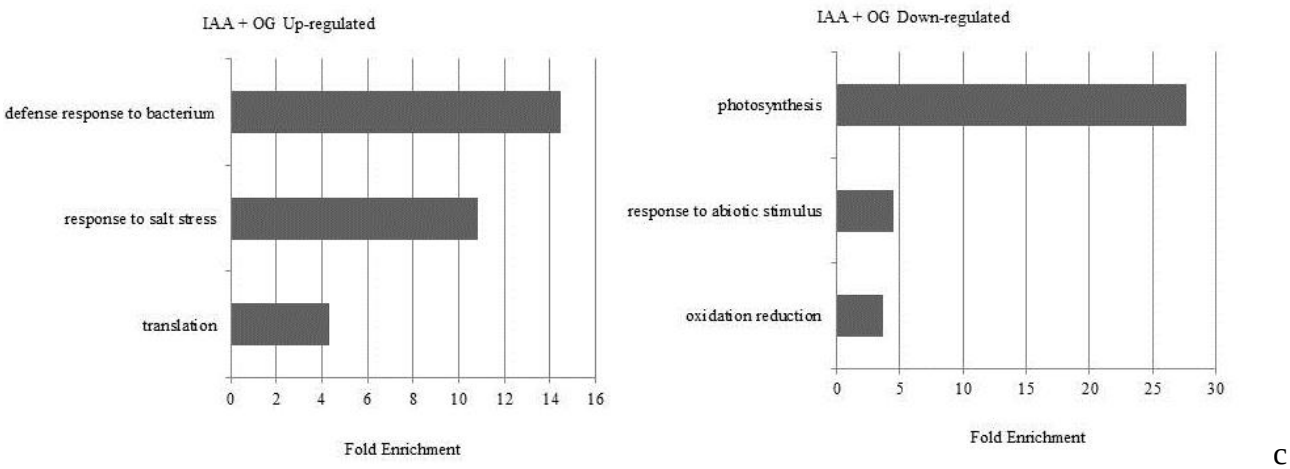

c

Figure 4.2 c : Bar chart of the Gene ontology (GO) bar chart for the over-represented Biological Processes in response to IAA, OG, IAA + OG treatments. GO categories with at least 2 genes and $p < 0.01$ are identified as enriched.

Among the IAA up-regulated proteins, 20 are also down-regulated in response to IAA + OG co-treatment, indicating that these proteins are subjected to the antagonism by the OG (Table 4.1). The antagonized proteins are involved in different processes: Response to oxidative stress (FBA2,PLDA1) ; Ribosome biogenesis (RL303,CBF5); Transcriptional repression (H2B.3; H2A7;SPT51); Transcriptional activation (HTR4;CYP18-2;MD36B; SPT51); Splicing (RH51; T5J8.16;SR45; U2AFA); mRNA export (LINC-1;SUN1) and Miscellaneous (CPFTSY;ASP2; Waxy; At3g62530).

Promoter analysis of their corresponding genes shows that 14 out 20 genes (Table 4.1) contain the As-1 like motif in their promoters, suggesting that the transcription of these genes may be regulated by TGA7. On the other hand among the OG up-regulated proteins, 17 were also down-regulated in response to IAA + OG co-treatment, indicating that these proteins are subjected to the antagonism by IAA (Table 3.6). The antagonized proteins are part of Signaling (AT2G34040;CAND1; CSN3;CSN6A;CSN7;DCAF1;RPN8A;AT2G26780); Transcription (La1;NPRB3;VIP3); Carbohydrate metabolism (BGLU22 and BGLU21) and Miscellaneous (AT2G40430 ; HSBP; PGDH1; Per32).

OG antagonism versus IAA	
Response to oxidative stress	
FBA2	Probable fructose-bisphosphate aldolase 2, chloroplastic
PLDA1	Phospholipase D alpha 1
Transcriptional repression	
H2B.3	Histone H2B.3
H2A7	Probable histone H2A.7
SPT51	Putative transcription elongation factor SPT5 homolog 1
Transcriptional activation	
MED36B	Probable mediator of RNA polymerase II transcription subunit 36b
CYP18-2	Peptidyl-prolyl cis-trans isomerase
HTR4	Histone superfamily protein
SPT51	Putative transcription elongation factor SPT5 homolog 1
Ribosome biogenesis	
CBF5	H/ACA ribonucleoprotein complex subunit 4
RL313	60S ribosomal protein L31-3 GN
Splicing	
SR45	Ribonucleoprotein
U2AFA	Isoform 3 of Arginine/serine-rich protein 45
RH51	Splicing factor U2af small subunit A
T5J8.16	DEAD-box ATP-dependent RNA helicase 51
mRNA export	
LINC1	Protein little nuclei1
SUN1	ARABIDOPSIS SAD1/UNC-84 DOMAIN PROTEIN 1
Misc	
CPFTSY	chloroplast SRP receptor homolog, alpha subunit
ASP2	ASPARTATE AMINOTRANSFERASE 2
Waxy	GBSS1, GRANULE BOUND STARCH SYNTHASE 1

Table 4.1 : IAA up-regulated proteins also down-regulated by OGs; underlined proteins present the As-1 like motif (TGA7 binding site) on their promoters.

IAA antagonism versus OG	
Signaling	
AT2G34040	Apoptosis inhibitory protein 5 (API5)
CAND1	Cullin-associated NEDD8-dissociated protein 1
CSN3 (COP13)	COP9 signalosome complex subunit 3
CSN6A	COP9 signalosome complex subunit 6a
CSN7 (FUS5)	COP9 signalosome complex subunit 7
DCAF1	DDB1- and CUL4-associated factor homolog 1
RPN8A	Probable 26S proteasome non-ATPase regulatory subunit 7
AT2G26780	ARM repeat superfamily protein
Transciption	
La1	La protein 1
NRPB3	DNA-directed RNA polymerases II, IV and V subunit 3
VIP3	At4g29830
Carbohydrate metabolism	
BGLU22	Beta-glucosidase 22
BGLU21	Beta-glucosidase 21
Miscellaneous	
AT2G40430	Uncharacterized protein
HSBP	At4g15810
PGDH1	EDA9 (embryo sac development arrest 9)
PER32	Peroxidase 32

Table 4.2 : OG up-regulated proteins also down-regulated by IAA

Interestingly, among the proteins that are up-regulated by OGs and down-regulated by auxin, we found different subunits of the COP9 signalosome and the related proteins CAND1 and DCAF1.

I have used the STRING database to build the interaction network shown in Figure 4.3 that shows the physical interactions occurring within the identified proteins.

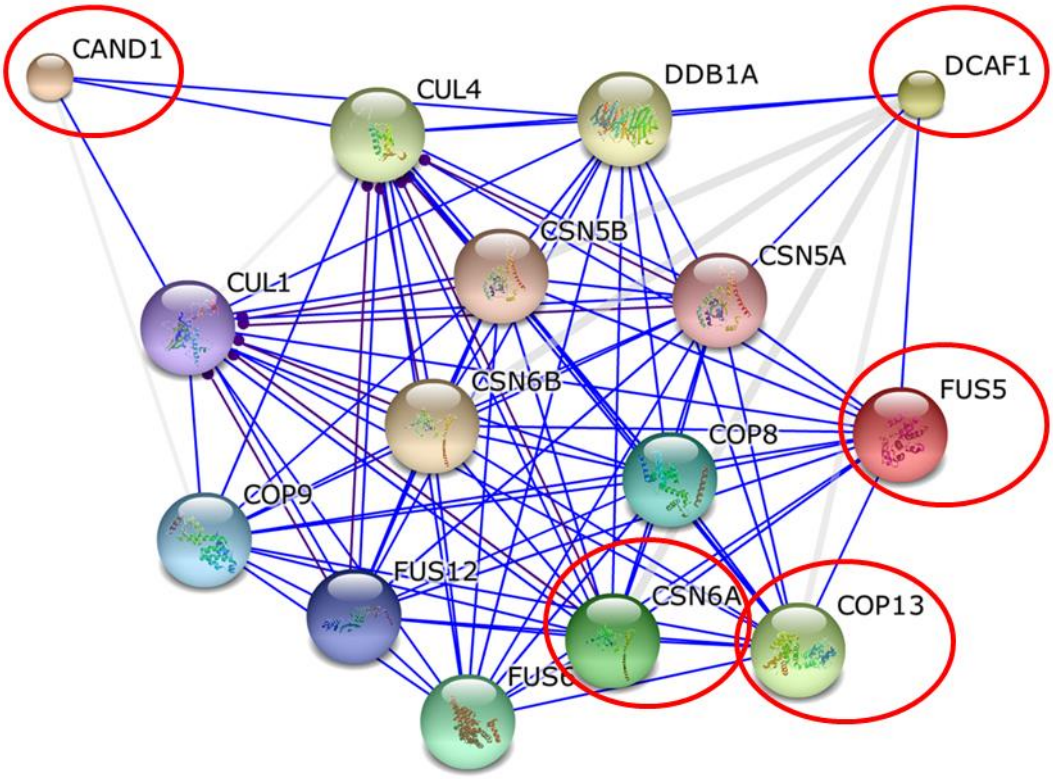

Figure 4.3. Analysis of networks using the STRING database within proteins involved in signaling that are up-regulated by OGs and down-regulated by IAA (Table 4.2). The proteins identified in this study are highlighted in red circles.

The COP9 signalosome (CSN) is a multiprotein complex that was initially identified in plants as a repressor of photomorphogenesis. The CSN complex is found throughout eukarytotes and consists of eight subunits (CSN1-8). It is now known to play major roles in several other developmental pathways, from auxin response to flower development.

CAND1 functions as a substrate adaptor exchange factor, facilitating the formation of a dynamic cellular pool of CRLs. Once assembled, the cullin subunit is neddylated. If no substrate is available, the CRL is rapidly deneddylated, returning the CRL to the CAND1 cycle. Alternatively, the presence of substrate promotes CRL activity by inhibiting CSN-mediated deneddylation. Upon substrate depletion by the 26S proteasome, the CSN deneddylates the cullin and the CRL is disassembled by CAND1, enabling new CRLs to form.

The regulation of CRL activity by NEDD8 modification of the cullin subunit is highly dynamic. NEDD8 is removed from cullins (termed deneddylation or deconjugation) by the COP9 signalosome (CSN).

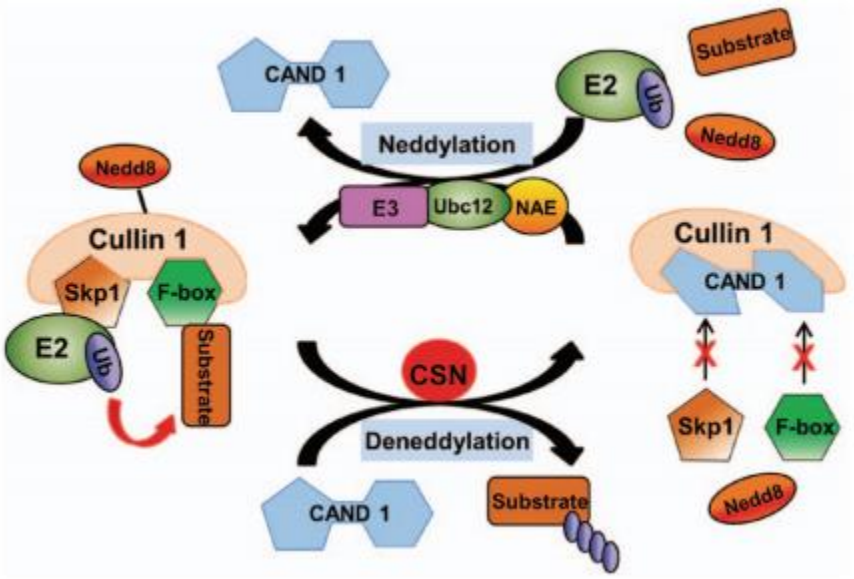

Figure 4.4. A model for the regulation of cullin-RING ligases (CRLs) by neddylation-deneddylation. Analogous to ubiquitination, neddylation covalently attaches NEDD8 to a lysine residue of a target protein (eg, cullin). As illustrated in the Skp1-Cullin1-Fbox (SCF) ubiquitin (Ub) ligase, cullin neddylation displaces cullin associated NEDD8-dissociated protein 1 (CAND1), which triggers the assembly of an active CRL complex and brings the adaptor bound substrate to a close proximity to Ub charged E2 and allows efficient transfer of the Ub from E2 to the substrate. Deneddylation counters neddylation and is done by deneddylases. The COP9 signalosome (CSN) is the deneddylase responsible for cullin deneddylation. Cullin deneddylation triggers the disassembly of the CRL-substrate complex, releases ubiquitinated substrates, and recycles NEDD8.

DCAF1 (DDB1-CUL4 ASSOCIATED FACTOR) protein has been reported to function as substrate-recognition receptors for CULLIN4-based E3 ubiquitin ligases. Yeast two-hybrid analysis demonstrated the physical interaction between DCAF1 and DDB1 from Arabidopsis. Moreover, coimmunoprecipitation assays showed that DCAF1 associates with the CSN (COP9 signalosome) in vivo.

A number of recent reports point to a role of CSN in the regulation of the activity of several E3 ubiquitin ligases.

In Arabidopsis a specific E3 ligase, SCF-TIR1, and its modification by the ubiquitin-like protein RUB1/NEDD8 (Related to Ubiquitin/Neural precursor cell-Expressed Developmentally Downregulated gene 8) have been implied as central players in the response to the plant hormone auxin. SCF-TIR1 core components are the cullin AtCUL1, the SKP1 homolog ASK1, and the RING-finger protein AtRBX1. In the presence of auxin, the AUX/IAA proteins are ubiquitylated by SCF-TIR1 and thus targeted to degradation. ARF transcription factors are then allowed to dimerize and promote the transcription of downstream genes involved in auxin response.

Loss of cullin neddylation or cullin deneddylation affect CRL function by promoting or,respectively, preventing interactions with the substrate receptor exchange factor CAND1. In plants, the Arabidopsis CULLIN1-containing E3 ligase SCF-TIR1 with the substrate recognition module composed of the F-box protein (FBP) TRANSPORT INHIBITOR RESISTANT 1(TIR1) and its adaptor subunit ARABIDOPSIS SKP1 (ASK) is highly relevant.

TIR1, functioning at the same time also as an auxin receptor, binds AUX/IAA transcriptional repressors in an auxin-dependent manner and targets AUX/IAAs for ubiquitylation and degradation by the 26S proteasome.

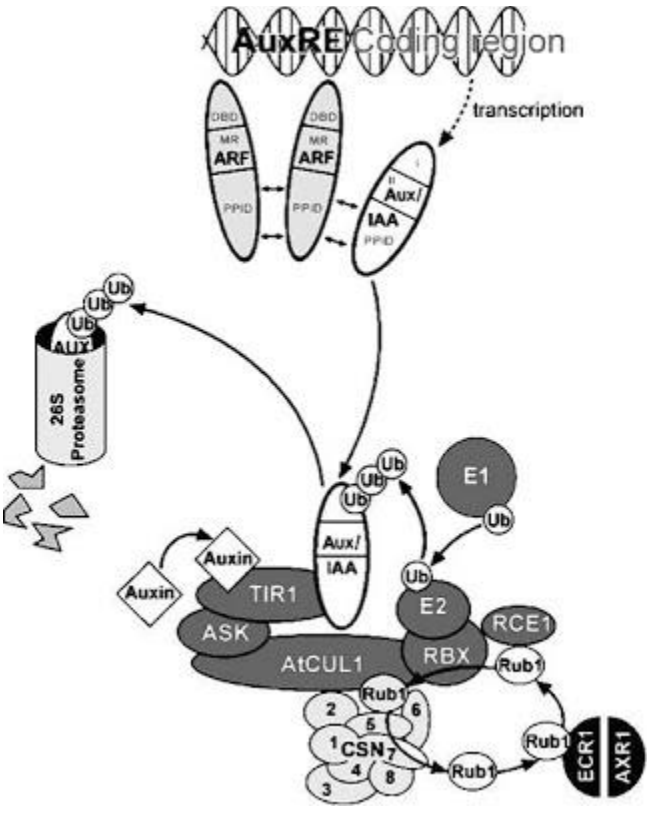

Figure 4.5. In the presence of auxin, the AUX/IAA proteins are ubiquitylated by SCF-TIR1 and thus targeted to degradation allowing the transcription of auxin responsive genes.

In this work I have found evidence that OGs up-regulate CSN subunits, CAND1 and DCAF1. However there is no evidence that this regulation may prevent the association of Cullin1 with SCF-TIR1 and therefore the degradation of AUX/IAA proteins.

Previous work has demonstrated that OGs antagonize auxin responses independently of Aux/Indole-3-Acetic Acid repressor stabilization and of posttranscriptional gene silencing (Savatin et al., 2011).

It is possible that the antagonistic effects of OGs may take place downstream in the auxin-regulated signaling cascade, perhaps through stabilization or posttranslational regulation of elements other than Aux/IAA proteins or through processes leading to the inactivation of auxin response factors.

5.Appendix

A

Differentially regulated proteins quantified in the LC/MS analysis of UNP samples

IAA up-regulated						
IAA/Mock	**OG/Mock**	**CoTr/IAA**	**CoTr/OG**	**OG/IAA**	**-Log ANOVA p value**	**Protein ID**
1.87	1.36			0.84	1.41	AT5G09590.1 MTHSC70-2 MTHSC70-2 (MITOCHONDRIAL HSP70 2);ATP binding
1.22	1.03			0.61	1.74	AT1G34000.1 OHP2 OHP2
1.66	0.92			0.71	2.14	AT3G07050.1 AT3G07050 GTP-binding family protein
1.46	0.98	0.96	1.21	0.64	1.43	AT3G09840.1 CDC48 Cell division control protein 48 homolog A;>IPIIPI00543476.1
1.61	1.11			0.52	1.39	AT3G60750.1 AT3G60750 Transketolase-like protein;>IPIIPI00992762.1
1.71	1.17	2.24	1.33	0.62	1.31	AT1G18540.1 AT1G18540 60S ribosomal protein L6-1
1.37	0.93	0.86	0.74	0.74	1.31	AT3G60750.1 AT3G60750 Transketolase-like protein;>IPIIPI00992762.1
		0.68	1.37	0.57	3.07	AT4G02570.1;CUL1 Cullin-1
1.29	0.98	0.95	1.23	0.76	1.68	AT4G13170.1 AT4G13170 60S ribosomal protein L13a-3
IAA down-regulated						
IAA/Mock	**OG/Mock**	**CoTr/IAA**	**CoTr/OG**	**OG/IAA**	**-Log ANOVA p value**	**Protein ID**
0.31	1.10	0.78	0.82	2.13	2.61	AT3G60860.1 AT3G60860 guanine nucleotide exchange family protein
0.67	2.13	1.59	0.82	2.75	1.40	AT5G55660.1 AT5G55660 unknown protein
0.35	1.32	1.19	0.62	2.90	1.42	AT1G30470.1 AT1G30470 SIT4 phosphatase-associated family protein;>IPI:IPI01019480.1
0.38	1.66			3.84	1.31	AT3G52180.1 SEX4 SEX4 (STARCH-EXCESS 4);polysaccharide binding / protein tyrosine/serine/threonine phosphatase;>IPI:IPI00530193.1
0.31	1.11			2.18	2.15	AT1G53760.1 AT1G53760 unknown protein;>IPI:IPI00992645.1
0.35	1.10			1.76	1.77	AT3G18790.1 AT3G18790 unknown protein
0.35	1.15			2.78	1.58	AT1G54220.1;AT1G54220.2 AT1G54220

						Dihydrolipoyllysine-residue acetyltransferase component 3 of pyruvate dehydrogenase complex. mitochondrial
0.37	1.24			2.17	2.26	AT5G42220.1 AT5G42220 Putative uncharacterized protein
0.39	0.97			2.09	1.42	AT3G28720.1 AT3G28720 unknown protein
0.42	0.97	1.07	0.99	1.66	1.44	AT4G39680.1;AT4G39680.2 AT4G39680 SAP domain-containing protein
0.42	1.03			2.08	1.63	AT1G35620.1 PDIL5-2 Protein disulfide-isomerase 5-2
0.44	0.75	0.82	0.85	1.72	3.41	AT3G47520.1 MDH Malate dehydrogenase. chloroplastic
0.44	1.22			2.29	2.20	AT2G14835.1;AT2G14835.2 AT2G14835 zinc finger (C3HC4-type RING finger) family protein
0.60	0.88	0.79	0.52	1.74	2.12	AT2G34420.1 LHB1B2 LHB1B2;chlorophyll binding;>IPI:IPI00527705.1
0.56	0.96			1.84	1.47	AT1G20970.1 AT1G20970 unknown protein;>IPI:IPI01019919.1
0.59	0.87			1.54	2.11	AT4G26780.1 AR192 AR192;adenyl-nucleotide exchange factor/ chaperone binding / protein binding / protein homodimerization;>IPI:IPI00520121.1
0.60	0.87			1.08	1.35	AT5G64290.1 DIT2.1 DIT2.1 (DICARBOXYLATE TRANSPORT 2.1);oxoglutarate:malate antiporter
0.60	0.95	1.02	1.24	1.56	1.80	AT5G21160.2 AT5G21160 LA RNA-binding protein;>IPI:IPI00518330.1
0.60	0.93			1.08	2.03	AT5G13280.1 AK-LYS1 Aspartokinase 1. chloroplastic
0.61	1.11	1.12	0.82	1.84	1.80	AT5G53530.1 VPS26A VPS26A
0.62	0.79			1.27	2.32	AT2G36250.1;AT2G36250.2 FTSZ2-1 Cell division protein ftsZ homolog 2-1. chloroplastic
0.63	1.15			1.63	2.30	AT3G55620.1 emb1624 Eukaryotic translation initiation factor 6-2
0.63	0.88			1.65	1.60	AT1G01910.1;AT1G01910.2;AT1G01910.4 AT1G01910 anion-transporting ATPase. putative;>IPI:IPI00891168.1
0.64	0.90			1.36	1.82	AT1G15820.1 LHCB6 Light harvesting complex photosystem II subunit 6
0.64	0.96			1.45	2.68	AT5G65020.1 ANNAT2 Annexin D2;>IPI:IPI00938637.1
0.65	1.09	1.53	0.93	1.96	1.38	AT3G02230.1 RGP1 UDP-arabinopyranose mutase 1;>IPI:IPI00520967.2
0.65	1.04	1.07	0.83	1.56	2.92	AT3G43300.1 ATMIN7 ATMIN7 (ARABIDOPSIS THALIANA HOPM INTERACTOR 7);guanyl-nucleotide exchange factor/ protein binding;>IPI:IPI00991502.1
0.66	1.22			1.60	1.41	AT3G62360.1 AT3G62360 carbohydrate binding
0.66	1.23			1.51	1.76	AT3G58730.1 AT3G58730 V-type proton ATPase subunit D
0.66	0.93			1.79	1.43	AT3G26520.1 TIP2 Aquaporin TIP1-2
0.67	0.91			1.70	1.45	AT4G01100.1 ADNT1 ADNT1 (ADENINE NUCLEOTIDE TRANSPORTER 1);ADP
0.67	1.25			2.04	1.83	AT1G04040.1 AT1G04040 acid phosphatase class B family protein

0.68	0.98	1.16	1.05	1.24	1.80	AT1G52360.2 AT1G52360 Coatomer. beta subunit;>IPI:IPI00541368.1
0.69	0.82	0.96	0.96	1.45	1.46	AT3G13300.1 VCS VCS (VARICOSE);nucleotide binding / protein homodimerization;>IPI:IPI00531059.1
0.69	1.14	1.11	0.91	1.72	3.82	AT4G24190.1 SHD Endoplasmin homolog;>IPI:IPI00531300.1
0.69	1.02	1.27	0.93	1.39	2.02	AT1G76400.1 AT1G76400 ribophorin I family protein
0.70	0.79			1.20	2.58	AT1G13320.1;AT1G13320.3 PP2AA3 Serine/threonine-protein phosphatase 2A 65 kDa regulatory subunit A gamma isoform;>IPI:IPI00656908.1
0.70	0.82			1.35	1.34	AT1G56110.1 NOP56 NOP56
0.71	0.85			1.22	2.79	AT4G26300.1 emb1027 emb1027 (embryo defective 1027);ATP binding / aminoacyl-tRNA ligase/ arginine-tRNA ligase/ nucleotide binding
0.72	1.07	0.89	0.81	1.56	1.58	AT1G73990.1 SPPA Putative protease SppA
0.72	1.04			1.48	1.65	AT1G66680.1 AR401 AR401
0.72	0.88	1.09	0.94	1.26	1.65	AT5G19760.1 AT5G19760 dicarboxylate/tricarboxylate carrier
0.73	0.99			1.47	2.13	AT2G40060.1 AT2G40060 protein binding / structural molecule
0.74	0.99	0.93	1.08	1.42	2.99	AT4G21150.1;AT4G21150.3 HAP6 HAP6 (HAPLESS 6);dolichyl-diphosphooligosaccharide-protein glycotransferase;>IPI:IPI00992247.1
0.74	0.78			1.08	3.71	AT3G52730.1 AT3G52730 ubiquinol-cytochrome C reductase UQCRX/QCR9-like family protein
0.75	1.07	0.81	0.80	1.51	1.34	AT5G23920.1 AT5G23920 unknown protein
0.78	1.08			1.69	1.63	AT3G28715.1 AT3G28715 V-type proton ATPase subunit d2;>IPI:IPI00991677.1
0.79	1.13			2.11	1.56	AT3G58730.1 AT3G58730 V-type proton ATPase subunit D
0.80	1.20	1.12	0.99	1.50	1.51	AT5G19620.1 OEP80 Outer envelope protein of 80 kDa. chloroplastic
		1.26	0.88	1.49	1.84	AT3G48870.1 HSP93-III Chaperone protein ClpC2. chloroplastic;>IPI:IPI00991611.1
		1.16	0.83	1.41	1.53	AT1G12310.1 AT1G12310 Probable calcium-binding protein CML13;>IPI:IPI00529397.1

OG up-regulated						
IAA/Mock	**OG/Mock**	**CoTr/IAA**	**CoTr/OG**	**OG/IAA**	**-Log ANOVA p value**	**Protein IDs**
0.81	4.33	1.21	1.19	0.81	1.34	AT4G10480.1 AT4G10480 Nascent polypeptide-associated complex subunit alpha-like protein 4;
1.26	2.38	7.01	1.16	6.94	1.40	AT3G12390.1 AT3G12390 Nascent polypeptide-associated complex subunit alpha-like protein 1

1.02	1.94	0.97	0.83	1.11	2.17	AT5G19690.1 STT3A STT3A (STAUROSPORIN AND TEMPERATURE SENSITIVE 3-LIKE A);oligosaccharyl transferase
0.94	1.82	1.32	1.20	1.29	1.68	AT4G10750.1 AT4G10750 HpcH/HpaI aldolase family protein
0.95	1.63	1.72	1.01	1.41	2.17	AT4G26630.1;AT4G26630.2 AT4G26630 unknown protein
0.90	1.54				3.43	AT4G08850.1 AT4G08850 Isoform 1 of Probable LRR receptor-like serine/threonine-protein kinase At4g08850;
3.47	1.73	3.57	1.58	1.67	1.79	AT1G62740.1 AT1G62740 stress-inducible protein. putative
		3.53	0.89	2.26	1.37	AT3G51550.1 FER Receptor-like protein kinase FERONIA
1.72	1.68	8.25	3.75	2.59	1.48	AT1G20440.1 COR47 Dehydrin COR47;
0.67	2.13	1.59	0.82	1.45	1.40	AT5G55660.1 AT5G55660 unknown protein
0.89	1.31			1.68	1.32	AT1G67680.1 AT1G67680 7S RNA binding
0.76	1.39			1.63	1.81	AT1G57720.1;AT1G57720.2 AT1G57720 Probable elongation factor 1-gamma 2
0.38	1.66			3.84	1.31	AT3G52180.1 SEX4 SEX4 (STARCH-EXCESS 4);polysaccharide binding / protein tyrosine/serine/threonine phosphatase;
0.78	1.44	1.52	0.91	1.83	1.57	AT4G27500.1 PPI1 Proton pump interactor
0.96	1.26	1.75	1.23	4.57	1.68	AT3G16780.1 AT3G16780 60S ribosomal protein L19-2
0.97	1.17	3.40	1.23	1.69	1.33	AT1G74720.1 QKY F25A4.30 protein;
0.87	1.12	2.84	1.08	2.10	1.37	AT5G19510.1 AT5G19510 Elongation factor 1-beta 2
0.85	1.11	2.14	1.22	1.64	2.18	AT1G16610.3 SR45 Arginine/serine-rich 45;
1.05	1.04	1.63	1.18	1.53	1.33	AT5G35530.1 AT5G35530 40S ribosomal protein S3-3
0.76	0.97	1.81	1.04	1.88	1.62	AT4G30010.1 AT4G30010 unknown protein
OG down-regulated						
IAA/Mock	**OG/Mock**	**CoTr/IAA**	**CoTr/OG**	**OG/IAA**	**-Log ANOVA p value**	**Protein IDs**
0.98	0.84	0.71	1.23	0.63	2.35	AT5G26742.2 emb1138 Isoform 1 of DEAD-box ATP-dependent RNA helicase 3. chloroplastic;
1.09	0.73	0.63	1.12	0.59	1.92	AT1G02150.1 AT1G02150 Pentatricopeptide repeat-containing protein At1g02150
1.05	0.71	0.81	1.15	0.62	2.05	AT5G30510.1 RPS1 RPS1 (RIBOSOMAL PROTEIN S1);RNA binding / structural constituent of ribosome;
1.06	0.71			0.61	1.93	AT1G79850.1 RPS17 30S ribosomal protein S17. chloroplastic
1.13	0.69	0.64	1.17	0.70	2.13	ATCG00740.1 RPOA DNA-directed RNA polymerase subunit alpha
1.13	0.69	0.64	1.17	0.70	2.13	ATCG00740.1 RPOA DNA-directed RNA polymerase subunit alpha
1.06	0.67			0.51	1.95	AT2G30520.1 RPT2 Root phototropism protein 2;
0.98	0.66			0.65	1.62	AT2G33800.1 AT2G33800 30S ribosomal protein S5. chloroplastic
0.93	0.64	0.58	1.00	1.30	1.33	AT5G54600.1 AT5G54600 50S ribosomal protein L24. chloroplastic;
0.79	0.53	0.91	1.56	0.62	2.77	AT1G79850.1 RPS17 30S ribosomal protein S17. chloroplastic

0.81	0.49			0.71	1.47	AT3G15190.1 AT3G15190 30S ribosomal protein S20. chloroplastic
		2.35	1.16	1.65	2.35	AT5G50310.1 AT5G50310 kelch repeat-containing protein;
		1.79	1.25	1.68	1.59	AT1G68890.1 AT1G68890 Isoform 1 of Protein PHYLLO. chloroplastic
		1.55	0.82	1.76	1.90	AT4G02080.1 SAR2 GTP-binding protein SAR1A;
		1.72	0.77	1.90	2.60	AT1G22280.1 PAPP2C Isoform 1 of Probabl
		0.79	1.12	0.69	2.26	AT5G13650.2 AT5G13650 elongation factor family protein;
		0.80	1.12	0.71	3.12	AT4G05400.1;AT4G05400.2 AT4G05400 unknown protein
		0.77	1.12	0.73	1.76	AT5G46580.1 AT5G46580 Pentatricopeptide repeat-containing protein At5g46580. chloroplastic
		0.94	1.12	0.73	1.92	AT5G63420.1 emb2746 emb2746 (embryo defective 2746);DNA binding / catalytic/ hydrolase
		0.83	1.06	0.74	2.02	AT3G25140.1 QUA1 Galacturonosyltransferase 8
		0.91	1.04	0.75	2.06	AT5G26742.2 emb1138 Isoform 1 of DEAD-box ATP-dependent RNA helicase 3. chloroplastic;
		0.80	1.04	0.75	1.49	AT1G02140.1 MAGO Protein mago nashi homolog
		0.65	1.13	0.53	3.03	AT1G50480.1 THFS Formate--tetrahydrofolate ligase
		0.67	0.96	0.65	2.97	AT3G62530.1 AT3G62530 Putative uncharacterized protein T12C14_230
		0.70	1.01	0.60	1.73	AT4G13930.1 SHM4 SHM4 (serine hydroxymethyltransferase 4);catalytic/ glycine hydroxymethyltransferase/ pyridoxal phosphate binding
		0.72	1.03	0.69	2.02	AT2G42520.1 AT2G42520 DEAD-box ATP-dependent RNA helicase 37
		0.74	1.22	0.66	1.53	AT3G56140.1 AT3G56140 Putative uncharacterized protein F18O21_100
		0.50	1.06	0.50	2.00	AT3G10650.1 AT3G10650 unknown protein
		0.59	1.01	0.63	1.64	AT5G58140.1;AT5G58140.2 PHOT2 Isoform 1 of Phototropin-2;
		0.87	1.04	0.74	1.76	AT5G10840.1 AT5G10840 endomembrane protein 70. putative

IAA. OG Modulated						
IAA/Mock	**OG/Mock**	**CoTr/IAA**	**CoTr/OG**	**OG/IAA**	**Log ANOVA p value**	**Protein IDs**
0.13	0.13			2.71	3.02	TREMBL:O82181 - Putative uncharacterized protein At2g35100
0.69	0.60			0.98	1.92	AT1G63680.1 MURE MURE;ATP binding / acid-amino acid ligase/ ligase
0.57	0.61	0.57	0.38	0.88	2.03	AT5G28840.1;AT5G28840.2 GME GDP-mannose 3.5-epimerase
0.51	0.63			1.34	2.12	AT2G30740.1 AT2G30740 PTI1-like tyrosine-protein kinase 2;>IPI:IPI00522951.1
0.61	0.63	0.52	0.71	0.87	1.77	AT1G37130.1 NIA2 Nitrate reductase [NADH] 2
0.63	0.64	0.81	0.91	0.81	1.32	AT5G04130.1 GYRB2 Isoform 1 of DNA gyrase subunit B. mitochondrial;>IPI:IPI00527008.2

0.62	0.66	0.80	0.72	1.09	2.11	AT2G21660.1 CCR2 Isoform 1 of Glycine-rich RNA-binding protein 7;>IPI:IPI00541933.1
0.80	0.67	0.39	0.39	1.00	1.51	AT4G09650.1 ATPD ATPD (ATP SYNTHASE DELTA-SUBUNIT GENE);hydrogen ion transporting ATP synthase. rotational mechanism / proton-transporting ATPase. rotational mechanism
0.70	0.67	0.83	0.82	0.83	1.36	AT1G12920.1 ERF1-2 Eukaryotic peptide chain release factor subunit 1-2
0.61	0.67	0.92	1.11	1.07	1.41	AT2G34040.1 AT2G34040 apoptosis inhibitory 5 (API5) family protein;>IPI:IPI00541718.1
0.53	0.69			1.63	1.89	AT1G60780.1 HAP13 HAP13 (HAPLESS 13);protein binding
0.26	0.72	0.88	0.86	1.96	1.65	AT2G20360.1 AT2G20360 NADH dehydrogenase [ubiquinone] 1 alpha subcomplex subunit 9. mitochondrial
0.80	0.72	0.35	0.27	0.94	1.48	AT2G47730.1 GSTF8 Glutathione S-transferase 6. chloroplastic
0.75	0.73	0.38	0.39	1.04	3.14	AT5G23120.1 HCF136 Photosystem II stability/assembly factor HCF136. chloroplastic
0.63	0.76	0.81	0.31	1.49	2.33	AT2G34420.1 LHB1B2 LHB1B2;chlorophyll binding;>IPI:IPI00527705.1
0.89	0.77	0.40	0.57	0.98	3.51	AT4G12800.1 PSAL Photosystem I reaction center subunit XI. chloroplastic
0.60	0.77	0.64	0.51	1.35	2.79	AT2G46520.1 AT2G46520 Exportin-2
0.66	0.77	0.54	0.35	1.10	1.78	AT2G36250.1;AT2G36250.2 FTSZ2-1 Cell division protein ftsZ homolog 2-1. chloroplastic
0.60	0.79	0.45	0.42	1.05	1.51	AT4G19710.2 AK-HSDH II Isoform 1 of Bifunctional aspartokinase/homoserine dehydrogenase 2. chloroplastic;>IPI:IPI00521909.2
		1.77	1.02		2.02	AT4G25210.1 AT4G25210 transcription regulator
0.57	0.79	0.83	0.47	1.31	2.53	AT3G47470.1 LHCA4 Chlorophyll a-b binding protein 4. chloroplastic
0.80	0.81	0.76	0.38	1.12	1.82	AT1G61520.1;AT1G61520.3 LHCA3 Photosystem I light harvesting complex gene 3;>IPI:IPI00656902.1
0.64	0.82	0.78	0.48	1.21	2.35	AT2G16950.1 TRN1 TRN1 (TRANSPORTIN 1);protein transporter;>IPI:IPI00657219.1
0.81	0.82	0.51	0.42	0.96	1.44	AT1G16350.1 AT1G16350 Probable inosine-5-monophosphate dehydrogenase
0.94	0.85	0.80	1.15	0.67	2.65	AT3G48500.2 PDE312 RNA binding;>IPI:IPI00846905.1
0.71	0.85	0.63	0.33	1.18	2.35	ATCG00130.1 ATPF ATP synthase subunit b. chloroplastic
0.75	0.89	0.85	0.61	1.13	2.43	AT1G06700.1;AT1G06700.2 AT1G06700 PTI1-like tyrosine-protein kinase 1
0.78	1.01	1.48	1.23	1.06	1.77	ATCG01130.1 ycf1;YCF1.2;YCF1.1 Putative membrane protein ycf1
1.03	1.17	1.39	1.29	1.24	1.51	AT4G15000.1 AT4G15000 60S ribosomal protein L27-3;>IPI:IPI00846627.1
		2.03	1.33		1.56	AT4G34110.1 PAB2 Polyadenylate-binding protein 2
		1.59	0.99		1.97	AT4G31700.1 RPS6 40S ribosomal protein S6-1;>IPI:IPI00846721.1
		1.38	0.84		1.62	AT2G20580.1 RPN1A 26S proteasome non-ATPase regulatory subunit 2 1A;>IPI:IPI00657061.1
		1.10	0.82		1.43	AT5G10160.1 AT5G10160 beta-hydroxyacyl-ACP dehydratase. putative
1.72	1.68	8.25	3.75	1.14	1.48	AT1G20440.1 COR47 Dehydrin COR47;>IPI:IPI00931003.1
3.47	1.73	3.57	1.58	0.81	1.79	AT1G62740.1 AT1G62740 stress-inducible protein. putative

OG antagonism vs IAA						
IAA/Mo	**OG/Mo**	**CoTr/IA**	**CoTr/O**	**OG/IA**	**Log ANOVA**	**Protein IDs**

ck	ck	A	G	A	p value	
0.59	1.03	1.81	1.12	0.59	1.97	AT2G45770.2 CPFTSY Signal recognition particle receptor protein. chloroplast (FTSY)
0.38	0.86	1.62	0.97	0.60	1.96	:AT5G19550.1 ASP2 Aspartate aminotransferase. cytoplasmic isozyme 1

IAA antagonism vs Ogs						
Auxin/Mock	**OG/Mock**	**CoTr/Auxin**	**CoTr/OG**	**OG/Auxin**	**Log ANOVA p value**	**Protein IDs**
0,76	1,90	0,89	0,72	1,40	1,40	AT4G34200.1 EDA9 (embryo sac development arrest 9);ATP binding
0,84	1,87	1,10	0,28	3,25	3,66	AT3G32980.1 Peroxidase 32

Differentially regulated proteins quantified in the LC/MS analysis of NSP samples

IAA up-regulated						
IAA/Mock	**OG/Mock**	**CoTr/IAA**	**CoTr/OG**	**OG/IAA**	**-Log ANOVA p value**	**Protein ID**
3.59	1.26	0.39	1.12	0.35	0.93	>sp|Q9FVE6|HDT1_ARATH Histone deacetylase HDT1
3.31	1.09	1.02	3.10	0.33	5.79	>sp|Q9FPJ4|RAD2B_ARATH Ras-related protein RABD2b
2.92	1.11	1.09	2.86	0.38	2.95	>sp|Q9LZG0|ADK2_ARATH Adenine kinase 2
2.86	1.27	1.28	2.88	0.45	3.64	>sp|Q9SRT9|RGP1_ARATH UDP-arabinopyrane mutase 1
2.80	1.09	1.52	3.91	0.39	0.82	>sp|Q9LHE5|TO401_ARATH Mitochondrial import receptor subunit TOM40-1
2.66	1.32	1.38	2.79	0.50	2.90	>tr|Q94KE3|Q94KE3_ARATH Pyruvate kinase
2.60	1.21	0.70	1.50	0.47	1.44	>sp|Q38882|PLDA1_ARATH Phpholipase D alpha 1
2.59	1.31	1.60	3.16	0.51	4.98	>sp|Q01474|SAR1B_ARATH GTP-binding protein SAR1B
2.59	1.46	0.08	0.15	0.57	3.16	>tr|Q9SIH1|Q9SIH1_ARATH Peptidyl-prolyl cis-trans isomerase
2.53	1.12	1.78	4.02	0.44	2.38	>sp|O04499|PMG1_ARATH 2.3-bisphphoglycerate-independent phphoglycerate mutase 1
2.48	1.08	1.17	2.69	0.44	3.09	>tr|Q9LYJ3|Q9LYJ3_ARATH ADP-ribylation factor A1B
2.20	1.46	0.61	0.92	0.66	1.21	>sp|Q9STN3|SPT51_ARATH Putative transcription elongation factor SPT5 homolog 1
2.19	1.06	1.13	2.34	0.48	1.46	>sp|O65390|APA1_ARATH Aspartic proteinase A1

2.18	1.31	0.45	0.76	0.60	3.59	>sp|Q9MAQ0|SSG1_ARATH Probable granule-bound starch synthase 1. chloroplastic/amyloplastic
2.18	1.36	0.39	0.63	0.62	2.04	>sp|Q9SH88|RRS1_ARATH Ribome biogenesis regulatory protein homolog
2.11	0.92	1.28	2.94	0.44	1.97	>sp|Q43127|GLNA2_ARATH Glutamine synthetase. chloroplastic/mitochondrial
2.09	1.08	2.19	4.24	0.52	3.62	>tr|Q9SA73|Q9SA73_ARATH At1g30580
2.07	1.32	1.27	1.99	0.64	4.26	>sp|Q96292|ACT2_ARATH Actin-2
1.98	1.22	1.42	2.29	0.62	3.74	>sp|Q9SYT0|ANXD1_ARATH Annexin D1
1.96	1.07	1.41	2.58	0.55	2.16	>sp|Q9SRH5|VDAC1_ARATH Mitochondrial outer membrane protein porin 1
1.95	1.16	1.27	2.13	0.60	2.81	>tr|Q9ZUC2|Q9ZUC2_ARATH Carbonic anhydrase
1.94	0.96	0.23	0.47	0.50	1.04	>sp|P51420|RL313_ARATH 60S ribomal protein L31-3
1.91	1.17	1.14	1.86	0.61	2.68	>sp|Q9C912|R35A3_ARATH 60S ribomal protein L35a-3
1.87	0.90	1.39	2.91	0.48	3.04	>sp|Q05431|APX1_ARATH L-ascorbate peroxidase 1. cytolic
1.87	1.06	1.18	2.07	0.57	2.31	>sp|Q05758|ILV5_ARATH Ketol-acid reductoisomerase. chloroplastic
1.79	0.97	1.37	2.52	0.54	4.87	>sp|Q42290|MPPB_ARATH Probable mitochondrial-processing peptidase subunit beta
1.79	1.02	1.59	2.78	0.57	2.41	>sp|P25696|ENO2_ARATH Bifunctional enolase 2/transcriptional activator
1.74	0.98	1.74	3.09	0.56	1.88	>sp|P20115|CISY4_ARATH Citrate synthase 4. mitochondrial
1.73	1.41	0.30	0.37	0.82	2.48	>sp|Q9FEF8|MD36B_ARATH Probable mediator of RNA polymerase II transcription subunit 36b
1.72	1.05	0.65	1.06	0.61	2.33	>sp|Q9S709|U2AFA_ARATH Splicing factor U2af small subunit A
1.70	1.42	0.48	0.57	0.84	3.17	>tr|Q8RY25|Q8RY25_ARATH At1g10390/F14N23_29
1.69	1.14	2.16	3.20	0.68	3.20	>sp|Q9LFW1|RGP2_ARATH UDP-arabinopyrane mutase 2
1.67	1.16	1.89	2.72	0.69	4.21	>sp|Q08682|RSSA1_ARATH 40S ribomal protein Sa-1
1.66	0.79	1.60	3.36	0.48	4.56	>sp|O50008|METE1_ARATH 5-methyltetrahydropteroyltriglutamate--homocysteine methyltransferase 1
1.66	1.47	0.60	0.68	0.89	3.53	>tr|F4HRT5|F4HRT5_ARATH Protein little nuclei1
1.66	1.06	2.15	3.35	0.64	3.10	>sp|P93033|FUM1_ARATH Fumarate hydratase 1. mitochondrial
1.65	1.33	0.63	0.77	0.81	1.00	>sp|Q9SEE9-3|SR45_ARATH Isoform 3 of Arginine/serine-rich protein 45
1.64	0.71	0.67	1.54	0.43	0.95	>sp|Q944G9|ALFC2_ARATH Probable fructe-bisphphate aldolase 2. chloroplastic
1.63	1.08	1.52	2.30	0.66	2.46	>sp|O82663|SDHA1_ARATH Succinate dehydrogenase [ubiquinone] flavoprotein subunit 1. mitochondrial
1.57	1.19	1.29	1.70	0.76	2.21	>sp|Q9LXG1|RS91_ARATH 40S ribomal protein S9-1
1.56	1.45	0.75	0.81	0.93	1.36	>sp|Q9MAB3|NOP5B_ARATH Probable nucleolar protein 5-2
1.55	1.43	0.70	0.76	0.92	2.12	>sp|Q9FLH0|NMCP_ARATH Putative nuclear matrix constituent protein 1-like protein
1.55	1.01	2.66	4.08	0.65	3.55	>sp|Q9FM01|UGDH4_ARATH UDP-gluce 6-dehydrogenase 4

1.55	0.76	1.19	2.43	0.49	2.01	>sp|P25858|G3PC1_ARATH Glyceraldehyde-3-phphate dehydrogenase GAPC1. cytolic
1.54	1.47	0.63	0.67	0.95	1.70	>tr|Q9FF75|Q9FF75_ARATH AT5g04990/MUG13_15
1.54	1.22	0.95	1.20	0.80	1.20	>tr|Q9ZWC4|Q9ZWC4_ARATH At1g04040/F21M11_2
1.54	0.86	1.45	2.58	0.56	3.23	>sp|P93819|MDHC1_ARATH Malate dehydrogenase. cytoplasmic 1
1.52	1.03	0.86	1.28	0.68	1.03	>sp|Q9LSA3|RL303_ARATH 60S ribomal protein L30-3
1.52	0.87	1.77	3.09	0.57	2.00	>sp|Q93VR4|ML423_ARATH MLP-like protein 423
1.52	0.48	0.11	0.35	0.32	1.01	>sp|Q9LD90|CBF5_ARATH H/ACA ribonucleoprotein complex subunit 4
1.51	0.67	1.05	2.35	0.44	2.57	>sp|Q39161|NIR_ARATH Ferredoxin--nitrite reductase. chloroplastic
1.32	0.97	0.69	0.94	0.74	1.14	>sp|Q9FJE8|H2A7_ARATH Probable histone H2A.7
3.34	0.57	0.00	0.00	0.00	2.02	Q94AH9
3.01	0.94	0.88	2.83	2.66	1.61	Q9S826
2.81	1.17	0.44	1.07	1.25	1.37	Q9LXT5
2.34	1.13	0.50	1.03	1.16	1.50	F4JHV8;Q9SY09;Q9SSF1
2.30	0.00	0.00	0.00	0.00	1.51	Q9M4T3
2.14	1.09	0.00	0.00	0.00	1.97	Q8L3X8
2.04	1.12	0.00	0.00	0.00	1.48	O81126
1.93	1.32	0.71	1.04	1.38	1.37	Q9LIH9
2.53	1.42	0.15	0.27	0.38	1.12	P59169
1.56	1.11	0.06	0.09	0.10	1.57	Q9SI96
IAA down-regulated						
IAA/Mock	**OG/Mock**	**CoTr/IAA**	**CoTr/OG**	**OG/IAA**	**-Log ANOVA p value**	**Protein ID**
0.74	0.86	1.16	1.00	1.16	1.57	>tr|Q9FND0|Q9FND0_ARATH Gb|AAD20086.1
0.73	0.78	1.34	1.26	1.06	1.08	>sp|Q9C5Z2|EIF3H_ARATH Eukaryotic translation initiation factor 3 subunit H
0.72	1.00	1.54	1.11	1.39	1.63	>sp|O23144|PPI1_ARATH Proton pump-interactor 1
0.72	0.76	1.49	1.41	1.06	1.01	>sp|P0C896|PP209_ARATH Pentatricopeptide repeat-containing protein At3g02650. mitochondrial
0.71	0.79	1.31	1.19	1.10	1.02	>tr|O04311|O04311_ARATH AT3G16450 protein
0.70	0.80	1.76	1.54	1.14	1.37	>sp|Q9SAJ6|G3PP1_ARATH Glyceraldehyde 3-phphate dehydrogenase GAPCP1. chloroplastic
0.69	0.83	1.35	1.12	1.20	1.11	>sp|Q9SGW3|PSD8A_ARATH 26S proteasome non-ATPase regulatory subunit 8 homolog A
0.69	0.80	1.26	1.09	1.15	1.15	>sp|Q9M0Y8|NSF_ARATH Vesicle-fusing ATPase
0.69	0.76	1.20	1.09	1.10	1.20	>sp|Q9LD43|ACCA_ARATH Acetyl-coenzyme A carboxylase carboxyl transferase subunit alpha. chloroplastic
0.68	0.77	1.26	1.12	1.13	1.01	>sp|Q9FIB6|PS12A_ARATH 26S proteasome non-ATPase regulatory subunit 12 homolog A

0.68	0.77	1.25	1.11	1.13	1.51	>sp|Q9LP45|PSD11_ARATH 26S proteasome non-ATPase regulatory subunit 11 homolog
0.67	0.86	1.64	1.29	1.28	1.18	>tr|Q9FME2|Q9FME2_ARATH AT5g60980/MSL3_100
0.66	0.81	1.61	1.32	1.22	2.71	>sp|Q9XEE2|ANXD2_ARATH Annexin D2
0.66	0.90	1.36	1.00	1.36	2.24	>sp|Q9LNU4|PSD3A_ARATH 26S proteasome non-ATPase regulatory subunit 3 homolog A
0.66	0.79	1.13	0.94	1.21	1.51	>tr|F4J6A1|F4J6A1_ARATH Eukaryotic translation initiation factor 3 subunit G
0.65	0.82	1.37	1.09	1.25	2.05	>sp|Q9MAK9|PS10B_ARATH 26S protease regulatory subunit S10B homolog B
0.65	0.85	1.42	1.10	1.30	1.58	>sp|Q9SEI4|PRS6B_ARATH 26S protease regulatory subunit 6B homolog
0.65	0.80	1.20	0.97	1.23	0.86	>sp|Q9LT08|PSDE_ARATH 26S proteasome non-ATPase regulatory subunit 14 homolog
0.65	0.83	0.72	0.57	1.28	3.71	>tr|Q9LSB4|Q9LSB4_ARATH DNA topoisomerase-like protein
0.65	0.85	1.27	0.97	1.31	2.49	>sp|Q93Y35|PSMD6_ARATH 26S proteasome non-ATPase regulatory subunit 6 homolog
0.64	0.77	1.61	1.34	1.21	1.07	>tr|F4JNZ8|F4JNZ8_ARATH Beta-adaptin-like protein B
0.62	0.75	1.48	1.22	1.21	2.86	>tr|Q9C5Z3|Q9C5Z3_ARATH Eukaryotic translation initiation factor 3 subunit E
0.62	0.84	1.32	0.97	1.37	2.70	>sp|Q9SSB5|PRS7A_ARATH 26S protease regulatory subunit 7 homolog A
0.61	0.80	1.34	1.03	1.30	2.53	>sp|Q9M2U2|ECR_ARATH Very-long-chain enoyl-CoA reductase
0.60	0.88	1.43	0.97	1.48	2.64	>sp|Q9SEI2|PS6AA_ARATH 26S protease regulatory subunit 6A homolog A
0.60	0.81	1.22	0.90	1.35	2.11	>sp|P56820|EIF3D_ARATH Eukaryotic translation initiation factor 3 subunit D
0.59	0.79	1.54	1.17	1.32	1.97	>sp|O04309|MB31_ARATH Myrinase-binding protein-like At3g16470
0.59	0.88	1.46	0.99	1.48	1.11	>sp|P93014|RR5_ARATH 30S ribomal protein S5. chloroplastic
0.58	0.93	1.69	1.06	1.60	1.34	>tr|Q8L7S1|Q8L7S1_ARATH At1g45200
0.57	1.07	2.15	1.13	1.89	1.84	>sp|P56808|RR19_ARATH 30S ribomal protein S19. chloroplastic
0.54	0.85	1.72	1.10	1.57	1.22	>tr|Q9FHY8|Q9FHY8_ARATH At5g41950
0.34	0.80	2.46	1.04	2.38	3.37	>tr|Q9S7M0|Q9S7M0_ARATH AT5g54270/MDK4_9
0.55	2.26	1.73	0.42	0.94	1.78	Q9C8Y9
0.68	0.95	0.93	0.67	0.64	1.67	Q9LT08
0.69	1.13	1.73	1.06	1.19	1.82	A8MRW1
0.73	1.05	1.11	0.77	0.81	1.17	IPI00525001
0.69	0.80	1.03	0.89	0.71	1.38	IPI00531300;IPI00524027

OG up-regulated						
IAA/Mock	**OG/Mock**	**CoTr/IAA**	**CoTr/OG**	**CoTr/Mock**	**Log ANOVA p**	**Protein IDs**

					value	
1.27	2.14	0.59	0.35	1.69	1.85	>sp|Q9CAQ8|RFC5_ARATH Replication factor C subunit 5
1.29	2.12	0.69	0.42	1.65	2.09	>sp|P14713|PHYB_ARATH Phytochrome B
1.40	1.56	0.88	0.79	1.12	1.12	>sp|Q9M651|RAGP2_ARATH RAN GTPase-activating protein 2
0.55	2.26	1.73	0.42	0.94	1.78	Q9C8Y9;Q9C8Y9-2
1.20	2.13	1.25	0.70	1.50	1.80	Q9C525;Q9C525-2;Q9LKR7;Q9SE50;Q9LIF9;Q3ECS3;Q8GRX1;F4HV16;Q9SE50-2
1.21	1.78	0.60	0.41	0.73	1.69	Q9ZVD0
1.33	1.75	0.00	0.00	0.00	2.06	Q9LY75;F4J100
1.38	1.71	1.60	1.29	2.21	1.38	O65719
OG down-regulated						
IAA/Mock	**OG/Mock**	**CoTr/IAA**	**CoTr/OG**	**CoTr/Mock**	**Log ANOVA p value**	**Protein IDs**
1.05	0.23	0.07	0.32	0.07	1.36	P42791
0.76	0.41	0.87	1.61	0.67	1.61	Q9LI88
0.90	0.48	1.01	1.89	0.90	1.39	P42804
0.89	0.54	0.84	1.38	0.75	1.55	Q9LS25
3.34	0.57	0.00	0.00	0.00	2.02	Q94AH9
1.27	0.58	0.41	0.89	0.52	2.08	O64644;F4IG85
1.34	0.71	0.69	1.30	0.93	1.52	F4J3M2
1.00	0.66	1.43	2.17	1.43	1.26	AT4G20360.1 RABE1b Elongation factor Tu. chloroplastic
0.89	0.58	1.37	2.09	1.21	1.51	AT5G56000.1 Hsp81.4 Heat shock protein 90-4
IAA/Mock	**OG/Mock**	**CoTr/IAA**	**CoTr/OG**	**OG/IAA**	**Log ANOVA p value**	**Protein IDs**
0.88	0.75	2.07	2.45	0.85	1.78	>tr|Q94K05|Q94K05_ARATH At3g03960
1.20	0.74	1.29	2.08	0.62	2.42	>sp|Q9SMX3|VDAC3_ARATH Mitochondrial outer membrane protein porin 3
1.00	0.73	1.35	1.86	0.73	1.33	>sp|O03042|RBL_ARATH Ribule bisphphate carboxylase large chain
0.82	0.72	3.11	3.50	0.89	3.18	>sp|P46422|GSTF2_ARATH Glutathione S-transferase F2
0.82	0.72	1.20	1.35	0.89	1.42	>sp|Q9M2Y6|Y3972_ARATH Uncharacterized protein At3g49720
1.04	0.72	1.63	2.36	0.69	2.20	>sp|Q8GUM2|HSP7I_ARATH Heat shock 70 kDa protein 9. mitochondrial
1.04	0.71	1.79	2.61	0.69	3.70	>sp|P93285|COX2_ARATH Cytochrome c oxidase subunit 2
0.78	0.70	0.71	0.79	0.90	1.51	>sp|P59232|R27AB_ARATH Ubiquitin-40S ribomal protein S27a-2
1.00	0.70	1.83	2.59	0.71	1.06	>sp|Q9ZPI5|MFP2_ARATH Peroxisomal fatty acid beta-oxidation multifunctional protein MFP2

1.04	0.69	1.86	2.81	0.66	1.35	>sp|Q9SMT7|4CLLA_ARATH 4-coumarate--CoA ligase-like 10
0.83	0.69	0.97	1.17	0.83	1.31	>sp|P56792|RK14_ARATH 50S ribomal protein L14. chloroplastic
1.20	0.69	1.29	2.27	0.57	2.51	>sp|Q9SDS7|VATC_ARATH V-type proton ATPase subunit C
0.94	0.68	1.48	2.03	0.73	1.99	>sp|P92549|ATPAM_ARATH ATP synthase subunit alpha. mitochondrial
0.86	0.68	0.69	0.88	0.78	1.25	>sp|O48549|RS61_ARATH 40S ribomal protein S6-1
1.01	0.67	1.30	1.95	0.67	1.39	>sp|Q56ZI2|PATL2_ARATH Patellin-2
0.76	0.67	2.20	2.50	0.88	4.76	>sp|Q9SH69|6PGD1_ARATH 6-phphogluconate dehydrogenase. decarboxylating 1. chloroplastic
0.76	0.66	1.60	1.84	0.87	2.56	>sp|Q9LK57|PP226_ARATH Pentatricopeptide repeat-containing protein At3g13160. mitochondrial
1.01	0.66	1.47	2.25	0.66	1.86	>sp|O23255|SAHH1_ARATH Adenylhomocysteinase 1
0.83	0.66	1.06	1.35	0.79	1.18	>sp|Q56X76|RH39_ARATH DEAD-box ATP-dependent RNA helicase 39
0.93	0.66	0.67	0.95	0.70	1.34	>sp|P83755|PSBA_ARATH Photystem Q(B) protein
0.85	0.65	1.55	2.03	0.76	1.31	>sp|Q9FGI6|NDUS1_ARATH NADH dehydrogenase [ubiquinone] iron-sulfur protein 1. mitochondrial
0.90	0.65	1.53	2.14	0.72	2.72	>sp|Q9SK66|NDUA9_ARATH NADH dehydrogenase [ubiquinone] 1 alpha subcomplex subunit 9. mitochondrial
1.08	0.63	1.36	2.33	0.58	2.66	>sp|O24456|GBLPA_ARATH Guanine nucleotide-binding protein subunit beta-like protein A
1.23	0.63	0.89	1.75	0.51	2.81	>sp|P10797|RBS2B_ARATH Ribule bisphphate carboxylase small chain 2B. chloroplastic
1.02	0.62	1.17	1.92	0.61	1.07	>sp|P42643|14331_ARATH 14-3-3-like protein GF14 chi
0.82	0.62	1.37	1.83	0.75	1.08	>sp|Q94AW8|DNAJ3_ARATH Chaperone protein dnaJ 3
0.80	0.62	0.79	1.03	0.77	1.34	>tr|F4KC80|F4KC80_ARATH Photystem I reaction center subunit N
0.87	0.61	0.80	1.14	0.70	0.86	>sp|P16180|RR17_ARATH 30S ribomal protein S17. chloroplastic
0.82	0.61	1.49	2.00	0.74	2.14	>tr|Q9ASR1|Q9ASR1_ARATH At1g56070/T6H22_13
1.10	0.61	1.07	1.93	0.55	0.97	>sp|P48347|14310_ARATH 14-3-3-like protein GF14 epsilon
0.85	0.60	0.68	0.97	0.71	1.30	>sp|O23049|RK6_ARATH 50S ribomal protein L6. chloroplastic
0.88	0.60	0.73	1.07	0.68	2.32	>sp|Q9SKX4|RK3A_ARATH 50S ribomal protein L3-1. chloroplastic
0.96	0.60	0.93	1.49	0.62	0.94	>tr|Q9M8L6|Q9M8L6_ARATH At1g80480
1.18	0.58	0.89	1.83	0.49	2.62	>sp|P10795|RBS1A_ARATH Ribule bisphphate carboxylase small chain 1A. chloroplastic
0.81	0.57	1.20	1.70	0.70	0.87	>tr|F4IWV2|F4IWV2_ARATH 2-oxoglutarate dehydrogenase. E1 component
0.91	0.57	1.27	2.03	0.62	2.10	>sp|Q96266|GSTF8_ARATH Glutathione S-transferase F8. chloroplastic
0.80	0.56	1.27	1.81	0.70	2.75	>sp|Q9FXA2|PABP8_ARATH Polyadenylate-binding protein 8
0.79	0.56	1.01	1.42	0.71	1.45	>sp|Q8LPS6|PPR3_ARATH Pentatricopeptide repeat-containing protein At1g02150

1.02	0.56	1.83	3.34	0.55	2.89	>sp|Q94A28|ACO3M_ARATH Aconitate hydratase 3. mitochondrial
0.79	0.55	1.01	1.45	0.69	1.07	>sp|P19366|ATPB_ARATH ATP synthase subunit beta. chloroplastic
0.85	0.53	1.11	1.79	0.62	1.87	>sp|P42644|14333_ARATH 14-3-3-like protein GF14 psi
0.85	0.47	1.32	2.38	0.55	1.27	>tr|Q9LXJ2|Q9LXJ2_ARATH Putative ubiquinol-cytochrome c reductase subunit 9
0.78	0.46	0.92	1.54	0.60	4.01	>sp|P31265|TCTP_ARATH Translationally-controlled tumor protein homolog
0.82	0.31	2.46	6.51	0.38	4.64	>sp|Q38900|CP19A_ARATH Peptidyl-prolyl cis-trans isomerase CYP19-1

IAA. OG regulated						
IAA/Mock	**OG/Mock**	**CoTr/IAA**	**CoTr/OG**	**CoTr/Mock**	**Log ANOVA p value**	**Protein IDs**
3.12	4.15	0.84	0.63	2.61	2.56	Q8GXC5
2.82	3.38	0.54	0.45	1.52	1.71	Q93XX8;F4IVE5
2.36	2.32	0.40	0.41	0.95	2.17	Q9LEY9
2.23	2.42	0.60	0.55	1.33	1.46	Q9LD60
2.20	2.71	0.65	0.53	1.43	2.05	O65655
2.16	2.42	0.53	0.47	1.13	2.17	Q9LZR5
2.09	1.66	0.50	0.63	1.06	2.03	Q8VZT0
2.08	2.31	1.32	1.19	2.75	1.78	Q9LHB9
1.96	2.07	0.68	0.65	1.34	3.34	F4IDK8;F4IDK9;A4GSN8
1.94	2.52	0.48	0.37	0.94	2.12	Q6NMK2
1.92	1.80	0.82	0.87	1.57	2.14	Q9FVE6;F4J378
1.84	1.61	0.81	0.93	1.49	1.42	Q9FG73
1.84	1.78	0.82	0.85	1.51	1.47	O04658
1.77	4.01	1.00	0.44	1.78	2.32	O24412;F4K0U3
1.63	1.68	0.62	0.60	1.01	1.50	P33207
6.76	2.75	0.25	0.61	1.69	1.25	AT5G52470.1 FIB1 rRNA 2-O-methyltransferase fibrillarin 1
2.64	1.70	0.00	0.00	0.00	1.53	AT2G37990.1 AT2G37990 Ribosome biogenesis regulatory protein homolog
2.29	1.59	0.00	0.00	0.00	1.28	AT3G57150.1 NAP57 H/ACA ribonucleoprotein complex subunit 4
2.15	1.82	1.17	1.38	2.52	1.52	AT5G17820.1 Peroxidase 57
1.68	1.78	0.00	0.00	0.00	2.21	AT1G01370.1;AT1G01370.2 HTR12 Histone H3-like centromeric protein HTR12
IAA/Mock	**OG/Mock**	**CoTr/IAA**	**CoTr/OG**	**OG/IAA**	**Log ANOVA p value**	

7.33	9.81	0.32	0.24	1.34	3.41	>tr|Q9SHI0|Q9SHI0_ARATH F20D23.9 protein
7.00	5.37	0.14	0.18	0.77	0.92	>tr|Q8LAK5|Q8LAK5_ARATH At4g30330
6.49	10.81	0.16	0.10	1.67	3.27	>tr|Q9M2K5|Q9M2K5_ARATH Putative uncharacterized protein F9D24.20
6.40	6.54	0.28	0.27	1.02	4.24	>tr|Q9FJW0|Q9FJW0_ARATH AT5g67630/K9I9_20
5.51	3.56	1.47	2.28	0.65	3.89	>sp|O49203|NDK3_ARATH Nucleide diphphate kinase III. chloroplastic/mitochondrial
5.40	4.84	0.20	0.22	0.90	4.79	>sp|Q93ZG9|FKB53_ARATH Peptidyl-prolyl cis-trans isomerase FKBP53
5.36	5.11	0.19	0.20	0.95	4.20	>sp|Q84TG1|RH57_ARATH DEAD-box ATP-dependent RNA helicase 57
5.29	3.91	0.18	0.25	0.74	2.70	>sp|Q9FMP4|PM14_ARATH Pre-mRNA branch site p14-like protein
4.90	3.53	0.23	0.32	0.72	7.10	>tr|Q9LXT5|Q9LXT5_ARATH Putative uncharacterized protein At3g58660
4.86	6.58	0.27	0.20	1.35	5.97	>tr|Q9LD60|Q9LD60_ARATH Spliceomal associated protein 130A
4.57	4.42	0.22	0.22	0.97	5.43	>tr|Q9FJY5|Q9FJY5_ARATH AT5g66540/K1F13_21
4.54	5.43	0.19	0.16	1.20	3.50	>tr|Q8RWQ1|Q8RWQ1_ARATH At2g44720/F16B22.21
4.53	4.41	0.22	0.22	0.97	6.36	>tr|Q9M0V4|Q9M0V4_ARATH Transducin/WD40 domain-containing protein
4.45	5.81	0.25	0.19	1.31	5.92	>tr|Q9FNE4|Q9FNE4_ARATH PWWP domain-containing protein
4.43	4.20	0.28	0.29	0.95	6.99	>tr|O82266|O82266_ARATH Putative uncharacterized protein At2g47990
4.42	4.75	0.38	0.35	1.07	5.13	>sp|Q9XIK4|U202A_ARATH UPF0202 protein At1g10490
4.32	5.22	0.18	0.15	1.21	5.74	>tr|Q9LV05|Q9LV05_ARATH Uncharacterized protein
4.31	4.12	0.17	0.18	0.96	5.43	>tr|Q9FNH2|Q9FNH2_ARATH Putative uncharacterized protein At5g06360
4.15	4.48	0.29	0.27	1.08	4.95	>sp|P43333|RU2A_ARATH U2 small nuclear ribonucleoprotein A'
3.99	5.40	0.32	0.24	1.35	5.90	>tr|Q9C923|Q9C923_ARATH Nuclear/nucleolar GTPase 2
3.87	4.07	0.34	0.32	1.05	4.89	>sp|Q6Q1P4|SMC1_ARATH Structural maintenance of chromomes protein 1
3.82	4.17	0.31	0.29	1.09	5.48	>tr|F4IDC2|F4IDC2_ARATH Protein SLOW WALKER2
3.75	2.03	0.30	0.56	0.54	3.11	>sp|Q9SUM2|RUXF_ARATH Probable small nuclear ribonucleoprotein F
3.75	3.83	0.45	0.44	1.02	6.43	>sp|Q9M060|IF62_ARATH Eukaryotic translation initiation factor 6-2
3.67	3.40	0.22	0.24	0.92	4.45	>tr|Q9LPP3|Q9LPP3_ARATH F18K10.11 protein
3.57	4.11	0.38	0.33	1.15	3.05	>tr|F4K5T4|F4K5T4_ARATH DNA-binding storekeeper protein-related transcriptional regulator
3.56	3.78	0.23	0.22	1.06	6.00	>tr|Q9LK52|Q9LK52_ARATH Genomic DNA. chromome 3. P1 clone:MJG19
3.55	3.97	0.28	0.25	1.12	5.10	>tr|Q683D4|Q683D4_ARATH Alpha-L RNA-binding motif/ribomal protein S4 family protein
3.48	3.03	0.39	0.45	0.87	4.17	>tr|Q9SYA9|Q9SYA9_ARATH AT1G61730 protein
3.48	3.11	0.32	0.36	0.89	2.99	>sp|Q9ZPV5|NOC2L_ARATH Nucleolar complex protein 2 homolog
3.47	6.70	0.50	0.26	1.93	2.15	>tr|F4JC31|F4JC31_ARATH Component of IIS longevity pathway SMK-1 domain-containing protein

3.46	4.14	0.20	0.17	1.20	3.17	>sp|Q9C587|RFC1_ARATH Replication factor C subunit 1
3.41	2.77	0.36	0.44	0.81	3.52	>tr|Q93ZH3|Q93ZH3_ARATH AT4g11790/T5C23_220
3.38	3.87	0.34	0.30	1.14	3.85	>sp|Q8GY84|RH10_ARATH DEAD-box ATP-dependent RNA helicase 10
3.38	3.50	0.34	0.33	1.04	6.18	>tr|F4JAV9|F4JAV9_ARATH Chromatin-remodeling protein 11
3.34	4.18	0.26	0.21	1.25	4.61	>sp|F4IHS2|SYD_ARATH Chromatin structure-remodeling complex protein SYD
3.27	4.78	0.19	0.13	1.46	4.05	>tr|B3H7F6|B3H7F6_ARATH Clock regulator protein time for coffee
3.26	3.32	0.37	0.36	1.02	4.78	>tr|Q9FT93|Q9FT93_ARATH KRR1 small subunit processome component
3.24	3.22	0.38	0.38	0.99	5.46	>sp|O49289|RH29_ARATH Putative DEAD-box ATP-dependent RNA helicase 29
3.22	3.80	0.38	0.32	1.18	2.46	>sp|O22212|PRP4L_ARATH U4/U6 small nuclear ribonucleoprotein PRP4-like protein
3.21	2.91	0.24	0.27	0.91	2.27	>tr|Q93VK1|Q93VK1_ARATH AT4g28450/F20O9_130
3.21	4.71	0.35	0.24	1.47	3.42	>sp|Q940Y3|ARID3_ARATH AT-rich interactive domain-containing protein 3
3.17	3.70	0.31	0.27	1.17	1.86	>tr|Q9SJT4|Q9SJT4_ARATH Expressed protein
3.13	2.88	0.30	0.32	0.92	1.32	>tr|Q9ZU66|Q9ZU66_ARATH Putative spliceome associated protein
3.08	2.36	0.50	0.66	0.77	1.90	>sp|Q9FKA5|Y5957_ARATH Uncharacterized protein At5g39570
3.06	2.93	0.34	0.36	0.96	6.27	>sp|Q9FMT4|SNF12_ARATH SWI/SNF complex component SNF12 homolog
3.05	3.20	0.38	0.36	1.05	2.68	>tr|Q9LF27|Q9LF27_ARATH Ribome biogenesis protein WDR12 homolog
3.04	5.73	0.49	0.26	1.89	4.47	>sp|O22467|MSI1_ARATH Histone-binding protein MSI1
3.01	3.10	0.31	0.30	1.03	4.24	>tr|Q9LS97|Q9LS97_ARATH AT3G18790 protein
3.01	6.32	0.22	0.10	2.10	4.26	>tr|F4IS91|F4IS91_ARATH ATP/GTP-binding protein-like protein
3.00	2.85	0.32	0.34	0.95	4.93	>tr|F4IDJ0|F4IDJ0_ARATH Nucleolar complex-associated protein domain-containing protein
2.97	3.14	0.42	0.40	1.06	4.51	>tr|F4J8K6|F4J8K6_ARATH Protein ribomal RNA processing 5
2.95	3.29	0.40	0.36	1.11	5.20	>tr|Q9M8Z5|Q9M8Z5_ARATH Nucleolar GTP-binding protein NSN1
2.93	3.69	0.29	0.23	1.26	5.13	>sp|Q84M92|ARP4_ARATH Actin-related protein 4
2.92	3.50	0.41	0.34	1.20	2.43	>tr|F4JT92|F4JT92_ARATH Nucleotide/nucleic acid binding protein
2.91	2.64	0.41	0.45	0.91	3.16	>tr|Q9M0I7|Q9M0I7_ARATH At4g28200
2.90	2.66	0.30	0.32	0.92	4.43	>sp|Q9C6I8|NOG1_ARATH Nucleolar GTP-binding protein 1
2.90	3.92	0.40	0.29	1.35	4.75	>tr|Q8RWV9|Q8RWV9_ARATH Putative uncharacterized protein At5g08450
2.90	3.12	0.45	0.42	1.08	5.06	>sp|Q9SAI5|RL71_ARATH 60S ribomal protein L7-1
2.89	3.17	0.50	0.45	1.10	3.85	>sp|Q9LIH9|RH51_ARATH DEAD-box ATP-dependent RNA helicase 51
2.88	2.77	0.31	0.32	0.96	2.18	>tr|Q9LZ65|Q9LZ65_ARATH AT5g04600/T32M21_200
2.87	3.47	0.35	0.29	1.21	5.29	>tr|F4J8G6|F4J8G6_ARATH Embryo defective 2016 protein
2.86	3.30	0.40	0.35	1.15	1.85	>sp|O22922|RU2B1_ARATH U2 small nuclear ribonucleoprotein B"
2.85	2.33	0.38	0.46	0.82	4.63	>tr|Q8L403|Q8L403_ARATH Putative uncharacterized protein

						At1g15425
2.83	2.27	0.37	0.46	0.80	3.94	>tr|Q0WRA3|Q0WRA3_ARATH ATPase E1
2.79	2.74	0.44	0.45	0.98	3.41	>tr|Q9S826|Q9S826_ARATH Putative U3 small nucleolar ribonucleoprotein
2.79	2.37	0.37	0.43	0.85	4.47	>tr|B3H5K3|B3H5K3_ARATH Uncharacterized binding protein
2.77	3.22	0.39	0.34	1.16	3.42	>tr|F4JP43|F4JP43_ARATH G2484-1 protein
2.76	2.64	0.40	0.42	0.96	4.65	>tr|Q8VYZ5|Q8VYZ5_ARATH Periodic tryptophan protein 2
2.75	2.62	0.38	0.40	0.95	5.64	>tr|F4JTD2|F4JTD2_ARATH FtsJ-like methyltransferase family protein
2.75	2.39	0.34	0.39	0.87	4.20	>tr|F4IH25|F4IH25_ARATH Ribome biogenesis protein BOP1 homolog
2.74	2.87	0.47	0.45	1.05	4.14	>tr|F4JZX8|F4JZX8_ARATH Putative crooked neck protein / cell cycle protein
2.71	3.03	0.43	0.38	1.12	3.82	>tr|Q9SUN5|Q9SUN5_ARATH Small nuclear ribonucleoprotein-associated protein
2.70	1.80	0.50	0.75	0.67	1.85	>tr|Q9SU26|Q9SU26_ARATH AT4g12600/T1P17_190
2.70	2.47	0.25	0.28	0.92	4.95	>sp|Q94BR4|PR19A_ARATH Pre-mRNA-processing factor 19 homolog 1
2.68	2.81	0.36	0.34	1.05	4.89	>sp|Q42384|PRL1_ARATH Protein pleiotropic regulatory locus 1
2.68	2.76	0.37	0.36	1.03	4.29	>tr|B5X503|B5X503_ARATH At5g11240
2.67	2.48	0.36	0.39	0.93	2.69	>tr|F4IRI1|F4IRI1_ARATH Transducin/WD40 repeat-like superfamily protein
2.66	3.14	0.29	0.24	1.18	2.50	>tr|B3H6J5|B3H6J5_ARATH Uncharacterized protein
2.65	3.81	0.26	0.18	1.44	3.57	>sp|Q6EVK6|BRM_ARATH ATP-dependent helicase BRM
2.64	3.00	0.42	0.37	1.14	4.88	>tr|Q9FGF4|Q9FGF4_ARATH DNA polymerase phi subunit
2.62	2.50	0.35	0.36	0.96	4.64	>sp|O22785|PR19B_ARATH Pre-mRNA-processing factor 19 homolog 2
2.58	2.68	0.42	0.41	1.04	5.05	>tr|F4JJM1|F4JJM1_ARATH Proline-rich spliceome-associated (PSP) family protein
2.58	2.80	0.50	0.46	1.08	3.43	>tr|Q8RXU6|Q8RXU6_ARATH Putative uncharacterized protein At4g07410
2.58	2.76	0.45	0.42	1.07	3.92	>tr|F4JR52|F4JR52_ARATH Down-regulated in metastasis (DRIM) domain-containing protein
2.58	2.98	0.49	0.42	1.16	4.90	>tr|Q9LYK7|Q9LYK7_ARATH Pescadillo homolog
2.57	1.70	0.88	1.34	0.66	1.31	>sp|P53492|ACT7_ARATH Actin-7
2.56	2.32	0.36	0.39	0.91	1.51	>tr|Q9M9V4|Q9M9V4_ARATH F6A14.6 protein
2.55	4.66	0.47	0.26	1.83	5.67	>tr|Q9M033|Q9M033_ARATH Putative uncharacterized protein T10O8_110
2.54	2.90	0.57	0.49	1.15	5.01	>sp|Q9LRZ3|PUM24_ARATH Pumilio homolog 24
2.49	2.79	0.45	0.40	1.12	5.11	>tr|Q9FMF9|Q9FMF9_ARATH Nuclear protein-like
2.49	2.81	0.39	0.35	1.13	4.91	>sp|P92948|CDC5L_ARATH Cell division cycle 5-like protein
2.48	2.41	0.46	0.47	0.97	5.03	>tr|Q9SY09|Q9SY09_ARATH At4g02840
2.46	3.89	0.50	0.32	1.58	5.03	>tr|F4IPJ1|F4IPJ1_ARATH Phphatidylinitol 3-and 4-kinase family protein with FAT domain
2.45	2.00	0.45	0.55	0.82	3.09	>tr|Q9CA42|Q9CA42_ARATH Little nuclei3 protein
2.44	2.55	0.44	0.42	1.05	3.74	>tr|F4JAY0|F4JAY0_ARATH U3snoRNP10 and NUC211 domain-

						containing protein
2.43	1.57	1.03	1.60	0.65	1.36	>sp|Q9SY33|PER7_ARATH Peroxidase 7
2.41	2.20	0.39	0.43	0.91	4.99	>tr|Q8GUP3|Q8GUP3_ARATH Putative uncharacterized protein At4g31880
2.40	3.24	0.52	0.39	1.35	5.04	>tr|F4HRR8|F4HRR8_ARATH Midasin
2.40	2.29	0.45	0.47	0.95	4.04	>sp|Q39189|RH7_ARATH DEAD-box ATP-dependent RNA helicase 7
2.39	2.62	0.44	0.41	1.09	4.51	>tr|Q9ZT71|Q9ZT71_ARATH Pre-mRNA-processing factor 6-like protein
2.39	2.39	0.45	0.45	1.00	3.39	>sp|Q94AH9|MD36A_ARATH Mediator of RNA polymerase II transcription subunit 36a
2.37	2.13	0.47	0.52	0.90	3.43	>tr|Q9C928|Q9C928_ARATH Putative uncharacterized protein At1g52930
2.37	3.04	0.49	0.38	1.28	2.95	>tr|Q9SHG6|Q9SHG6_ARATH GC-rich sequence DNA-binding factor-like protein with tuftelin interacting domain
2.36	1.84	0.49	0.63	0.78	2.34	>tr|Q9C6C2|Q9C6C2_ARATH DNA-directed RNA polymerase subunit AAC42
2.36	2.37	0.43	0.43	1.01	4.42	>tr|Q8L5Y4|Q8L5Y4_ARATH Embryo defective 2765
2.35	2.75	0.46	0.39	1.17	4.44	>tr|Q9LKU3|Q9LKU3_ARATH Putative uncharacterized protein T32B20.g
2.35	4.05	0.60	0.35	1.73	3.96	>sp|Q39117|TGT2_ARATH Trihelix transcription factor GT-2
2.33	2.84	0.43	0.35	1.22	2.28	>sp|Q56YN8|SMC3_ARATH Structural maintenance of chromomes protein 3
2.33	3.13	0.53	0.39	1.34	2.03	>sp|F4IAT2|THOC2_ARATH THO complex subunit 2
2.33	1.88	0.55	0.67	0.81	2.64	>tr|F4I366|F4I366_ARATH DNA-directed RNA polymerase
2.32	2.58	0.62	0.56	1.11	1.37	>tr|F4HY43|F4HY43_ARATH Protein embryo defective 1968
2.31	2.54	0.41	0.37	1.10	4.64	>tr|F4KBP5|F4KBP5_ARATH Chromatin remodeling 4 protein
2.28	2.07	0.38	0.42	0.91	3.80	>tr|F4K465|F4K465_ARATH Nucleoporin-related protein
2.27	3.32	0.51	0.35	1.46	3.74	>sp|Q9FMR9|RIN1_ARATH RuvB-like protein 1
2.26	2.73	0.48	0.40	1.21	3.60	>tr|A4FVN8|A4FVN8_ARATH At1g10580
2.25	2.79	0.36	0.29	1.24	4.82	>tr|A2RVJ8|A2RVJ8_ARATH At5g10010
2.23	3.13	0.12	0.09	1.41	3.51	>tr|F4KDH9|F4KDH9_ARATH FIP1 [V]-like protein
2.22	2.13	0.39	0.41	0.96	4.79	>tr|Q9CAF4|Q9CAF4_ARATH At3g10650
2.22	1.92	0.69	0.80	0.86	2.85	>sp|Q8L7E5|WIT1_ARATH WPP domain-interacting tail-anchored protein 1
2.22	2.14	0.56	0.58	0.97	2.50	>sp|O81098|RPB5A_ARATH DNA-directed RNA polymerases II and IV subunit 5A
2.21	2.10	0.42	0.44	0.95	4.89	>sp|Q949S9|SPF27_ARATH Pre-mRNA-splicing factor SPF27 homolog
2.20	2.37	0.45	0.42	1.08	5.01	>sp|O80653|SKIP_ARATH SNW/SKI-interacting protein
2.20	2.38	0.44	0.40	1.08	3.58	>tr|Q9LM92|Q9LM92_ARATH At1g20580/F2D10_6
2.19	2.57	0.52	0.44	1.17	3.71	>sp|Q6WWW4|UPL3_ARATH E3 ubiquitin-protein ligase UPL3
2.18	1.44	0.85	1.29	0.66	3.73	>sp|P0DI10|PER1_ARATH Peroxidase 1
2.16	2.22	0.65	0.64	1.03	1.51	>tr|F4K455|F4K455_ARATH Ribomal protein L7Ae/L30e/S12e/Gadd45 family protein
2.15	2.63	0.48	0.39	1.23	3.30	>sp|Q9LUG5|RPF2_ARATH Ribome production factor 2 homolog

2.15	1.79	0.31	0.37	0.83	3.58	>sp|Q9SD34|C3H44_ARATH Zinc finger CCCH domain-containing protein 44
2.14	1.90	0.37	0.41	0.89	5.01	>tr|Q4V3D1|Q4V3D1_ARATH At1g48620
2.14	2.99	0.42	0.30	1.40	5.08	>tr|Q9LFE0|Q9LFE0_ARATH Putative uncharacterized protein F5E19_120
2.11	1.65	0.38	0.49	0.78	2.34	>tr|Q9FFK6|Q9FFK6_ARATH Nuclear pore complex protein-like protein
2.11	1.59	0.40	0.53	0.75	3.52	>tr|F4I1T7|F4I1T7_ARATH Nuclear pore complex protein
2.10	2.40	0.66	0.58	1.14	3.28	>tr|Q9ZVW2|Q9ZVW2_ARATH Expressed protein
2.10	2.31	0.54	0.49	1.10	3.88	>tr|Q9SYP1|Q9SYP1_ARATH F9H16.5 protein
2.08	3.85	0.56	0.30	1.85	2.09	>sp|Q9M2Q4|U202B_ARATH UPF0202 protein At3g57940
2.08	2.33	0.73	0.66	1.12	2.43	>tr|Q9LVF2|Q9LVF2_ARATH Genomic DNA. chromome 3. P1 clone: MIL23
2.06	2.14	0.52	0.50	1.04	3.55	>tr|Q93YS7|Q93YS7_ARATH Putative WD-repeat membrane protein
2.06	2.37	0.47	0.41	1.15	2.85	>tr|O22826|O22826_ARATH At2g43770
2.05	2.08	0.51	0.50	1.01	3.74	>tr|Q9LNC5|Q9LNC5_ARATH Elongation factor like protein
2.05	1.83	0.47	0.52	0.89	3.99	>tr|F4HR73|F4HR73_ARATH Suppressor of auxin resistance1 protein
2.02	2.26	0.48	0.43	1.12	3.74	>tr|Q9SAG7|Q9SAG7_ARATH At1g80930/F23A5_23
2.01	1.82	0.67	0.74	0.91	2.56	>tr|F4HY56|F4HY56_ARATH Homeobox-1
1.99	2.19	0.56	0.51	1.10	4.40	>tr|F4KG14|F4KG14_ARATH Guanylate-binding protein
1.96	1.69	0.80	0.93	0.86	2.25	>sp|Q93V93|PER44_ARATH Peroxidase 44
1.95	3.52	0.52	0.29	1.80	3.24	>sp|Q9S775|PKL_ARATH CHD3-type chromatin-remodeling factor PICKLE
1.95	2.32	1.05	0.88	1.19	2.14	>sp|Q96511|PER69_ARATH Peroxidase 69
1.94	2.04	0.55	0.53	1.05	1.40	>tr|F4IHU8|F4IHU8_ARATH NUC173 domain-containing protein
1.94	2.59	0.79	0.59	1.34	1.70	>tr|F4I1Y3|F4I1Y3_ARATH Ubiquitin-protein ligase 1
1.94	1.63	0.42	0.50	0.84	3.26	>tr|Q9SFV2|Q9SFV2_ARATH SMAD/FHA domain-containing protein
1.93	1.57	0.36	0.45	0.81	2.00	>sp|Q9SB42|MDA1_ARATH Mediator-associated protein 1
1.93	2.08	0.52	0.49	1.08	4.32	>sp|Q9LNV5|C3H4_ARATH Zinc finger CCCH domain-containing protein 4
1.92	2.94	0.30	0.20	1.53	4.28	>sp|Q8RXF1|SF3A1_ARATH Probable splicing factor 3A subunit 1
1.88	2.86	0.39	0.26	1.52	5.85	>tr|Q9M1S4|Q9M1S4_ARATH Dentin sialophphoprotein-related protein
1.88	2.07	0.60	0.55	1.10	4.08	>tr|Q9SSD2|Q9SSD2_ARATH F18B13.15 protein
1.84	2.61	0.53	0.37	1.42	3.33	>sp|Q8RXK2|SDN3_ARATH Small RNA degrading nuclease 3
1.83	1.94	0.54	0.51	1.06	1.98	>tr|F4KCY1|F4KCY1_ARATH Fcf2 pre-rRNA processing protein
1.82	1.86	0.59	0.58	1.02	3.01	>tr|Q0WM93|Q0WM93_ARATH AAA-type ATPase family protein
1.82	1.51	0.60	0.71	0.83	3.18	>tr|F4KHD8|F4KHD8_ARATH Protein embryo defective 3012
1.80	2.04	0.47	0.41	1.14	3.85	>tr|A8MS85|A8MS85_ARATH Transcription elongation factor SPT6-like protein
1.79	1.65	0.50	0.54	0.92	3.06	>tr|F4JJC1|F4JJC1_ARATH HAT transpon superfamily
1.78	1.59	0.46	0.51	0.89	3.87	>tr|F4JS05|F4JS05_ARATH Uncharacterized protein
1.78	1.66	0.96	1.03	0.93	2.87	>sp|Q8LBI1|RL51_ARATH 60S ribomal protein L5-1
1.77	1.86	0.47	0.44	1.05	3.13	>tr|O65655|O65655_ARATH Putative uncharacterized protein

						AT4g39680
1.77	2.46	0.70	0.50	1.39	3.94	>tr|Q9M2N5|Q9M2N5_ARATH At3g42170
1.77	1.60	0.97	1.08	0.91	2.64	>sp|Q43729|PER57_ARATH Peroxidase 57
1.76	1.71	1.11	1.15	0.97	0.98	>sp|O80626|RL352_ARATH 60S ribomal protein L35-2
1.75	1.67	0.72	0.75	0.95	2.48	>tr|Q9SGT7|Q9SGT7_ARATH At1g56110/T6H22_9
1.74	1.85	0.72	0.68	1.06	1.55	>tr|Q9FM47|Q9FM47_ARATH RNA-binding (RRM/RBD/RNP motifs) family protein
1.74	1.45	1.58	1.90	0.83	1.89	>sp|Q9FJX3|VDAC2_ARATH Mitochondrial outer membrane protein porin 2
1.74	1.65	1.78	1.88	0.95	2.73	>sp|Q38946|DHE2_ARATH Glutamate dehydrogenase 2
1.70	1.92	0.36	0.31	1.13	5.30	>tr|Q9LSK7|Q9LSK7_ARATH At3g18035
1.69	1.89	1.18	1.06	1.12	2.43	>sp|Q42351|RL341_ARATH 60S ribomal protein L34-1
1.68	1.85	0.66	0.60	1.10	1.83	>sp|Q9C944|H2AV3_ARATH Probable histone H2A variant 3
1.67	1.81	0.56	0.51	1.08	2.17	>sp|Q9FVQ1|NUCL1_ARATH Nucleolin 1
1.67	1.26	1.64	2.16	0.76	1.72	>tr|O49485|O49485_ARATH D-3-phphoglycerate dehydrogenase
1.66	1.61	0.75	0.77	0.97	2.54	>sp|O04658|NOP5A_ARATH Probable nucleolar protein 5-1
1.66	1.89	0.70	0.62	1.14	2.19	>tr|Q9FM71|Q9FM71_ARATH RNA recognition motif-containing protein
1.65	1.79	0.77	0.72	1.08	2.14	>sp|Q96321|IMA1_ARATH Importin subunit alpha-1
1.64	1.55	0.77	0.82	0.94	1.74	>sp|Q8VZT0|NLAL1_ARATH Putative H/ACA ribonucleoprotein complex subunit 1-like protein 1
1.64	1.78	1.42	1.31	1.09	2.75	>sp|P28297|ACEA_ARATH Isocitrate lyase
1.64	3.25	1.22	0.62	1.99	3.47	>sp|Q96522|PER45_ARATH Peroxidase 45
1.64	3.19	0.71	0.36	1.95	2.14	>tr|Q9SYG2|Q9SYG2_ARATH 6B-interacting protein 1-like 1
1.63	1.31	0.88	1.10	0.80	1.60	>sp|P17094|RL31_ARATH 60S ribomal protein L3-1
1.61	2.71	0.80	0.47	1.69	2.96	>tr|Q9LPD9|Q9LPD9_ARATH Minichromome maintenance protein 2
1.60	1.64	1.31	1.28	1.03	3.40	>sp|Q8LC83|RS242_ARATH 40S ribomal protein S24-2
1.59	1.66	0.77	0.74	1.05	2.70	>tr|Q8GYE8|Q8GYE8_ARATH Putative uncharacterized protein At5g26180
1.59	2.20	0.51	0.37	1.39	2.25	>tr|Q9LFE2|Q9LFE2_ARATH Transducin/WD40 domain-containing protein
1.59	1.71	0.28	0.26	1.07	3.68	>tr|F4J9U9|F4J9U9_ARATH RNA binding (RRM/RBD/RNP motifs) family protein
1.57	2.17	0.73	0.53	1.39	2.85	>tr|F4ITU4|F4ITU4_ARATH WD40 repeat protein MUCILAGE-MODIFIED 1
1.57	1.58	0.67	0.67	1.01	2.39	>sp|Q9FPS4|UBP23_ARATH Ubiquitin carboxyl-terminal hydrolase 23
1.56	1.53	1.09	1.11	0.98	1.86	>sp|Q9FHG2|RL322_ARATH 60S ribomal protein L32-2
1.51	2.53	0.49	0.29	1.67	3.44	>sp|Q8VY05-3|SWI3D_ARATH Isoform 3 of SWI/SNF complex subunit SWI3D
0.71	0.69	1.00	1.03	0.71	1.97	B9DHQ0;Q56WH1
0.70	0.73	3.44	3.29	2.41	1.90	P94040
0.67	0.69	0.48	0.47	0.32	1.87	Q9XF89
0.67	0.63	1.04	1.11	0.70	1.81	P25856;F4HNZ6
0.60	0.39	1.88	2.87	1.12	1.32	Q9SRT9

0.56	0.59	1.71	1.62	0.95	1.63	Q8L7N0;Q9M888
0.52	0.41	1.46	1.86	0.76	2.63	Q96251;B9DGP8
0.49	0.65	2.78	2.10	1.38	1.73	Q9LZF6;P54609;Q9SCN8
0.46	0.29	1.53	2.44	0.70	1.89	O04450;F4IAR7
0.42	0.48	2.65	2.31	1.10	1.99	Q9FK25
0.40	0.41	1.55	1.50	0.62	2.97	Q9LV21
0.36	0.40	5.19	4.69	1.86	1.92	Q9SPK5
0.30	0.37	4.69	3.83	1.43	1.67	Q9SAJ4
0.29	0.30	4.24	4.10	1.23	2.61	O23254
0.27	0.31	3.53	3.14	0.97	1.48	P17562
0.26	0.25	3.20	3.36	0.83	1.91	Q9LV77-2;Q9LV77
0.08	0.26	7.53	2.23	3.37	2.06	>sp|Q9SHI1|IF2C_ARATH Translation initiation factor IF-2. chloroplastic
0.18	0.16	3.02	3.30	0.92	4.53	>sp|Q9LV77-2|ASNS2_ARATH Isoform 2 of Asparagine synthetase [glutamine-hydrolyzing] 2
0.18	0.34	2.47	1.33	1.86	3.70	>sp|Q9C6X2|SCAM4_ARATH Secretory carrier-associated membrane protein 4
0.20	0.08	3.06	7.43	0.41	4.96	>tr|F4I6W4|F4I6W4_ARATH Phphoglucomutase
0.21	0.20	1.39	1.40	0.99	2.01	>sp|P46310|FAD3C_ARATH Omega-3 fatty acid desaturase. chloroplastic
0.21	0.22	1.59	1.56	1.02	2.98	>sp|Q9SP35|TI172_ARATH Mitochondrial import inner membrane translocase subunit TIM17-2
0.24	0.37	1.76	1.13	1.56	5.24	>sp|C0LGN2|Y3148_ARATH Probable leucine-rich repeat receptor-like serine/threonine-protein kinase At3g14840
0.24	0.29	3.76	3.10	1.21	1.31	>sp|Q9C9K3|PFPA2_ARATH Pyrophphate--fructe 6-phphate 1-phphotransferase subunit alpha 2
0.25	0.23	3.36	3.62	0.93	5.32	>sp|F4K0E8|ISPG_ARATH 4-hydroxy-3-methylbut-2-en-1-yl diphphate synthase. chloroplastic
0.25	0.31	1.90	1.54	1.23	4.23	>sp|Q8VZG8|Y4885_ARATH Probable LRR receptor-like serine/threonine-protein kinase At4g08850
0.25	0.33	0.88	0.66	1.33	2.30	>tr|F4KG18|F4KG18_ARATH Trie phphate/phphate translocator TPT
0.25	0.15	2.42	4.19	0.58	2.75	>sp|P48421|C83A1_ARATH Cytochrome P450 83A1
0.26	0.38	2.42	1.68	1.44	1.05	>sp|Q9CAP8|LACS9_ARATH Long chain acyl-CoA synthetase 9. chloroplastic
0.27	0.38	4.18	3.02	1.39	4.19	>sp|Q9SPK5|FTHS_ARATH Formate--tetrahydrofolate ligase
0.27	0.32	1.06	0.92	1.15	3.80	>sp|P46312|FAD6C_ARATH Omega-6 fatty acid desaturase. chloroplastic
0.28	0.54	3.70	1.95	1.89	1.24	>tr|O81629|O81629_ARATH AT4g10840/F25I24_50
0.29	0.26	2.63	2.91	0.91	5.09	>sp|Q9FK25|OMT1_ARATH Flavone 3'-O-methyltransferase 1
0.29	0.29	4.12	4.08	1.01	6.03	>sp|Q8W4M5|PFPB1_ARATH Pyrophphate--fructe 6-phphate 1-phphotransferase subunit beta 1
0.29	0.61	3.97	1.88	2.11	3.57	>tr|F4JLY4|F4JLY4_ARATH Cytochrome P450. family 706. subfamily A. polypeptide 1
0.29	0.29	3.03	2.99	1.01	5.27	>sp|O49299|PGMC1_ARATH Probable phphoglucomutase. cytoplasmic 1

0.29	0.29	0.50	0.50	1.00	1.58	>sp|O48963|PHOT1_ARATH Phototropin-1
0.29	0.28	1.56	1.63	0.96	4.30	>tr|F4JHE9|F4JHE9_ARATH K(+) efflux antiporter 2
0.29	0.38	2.36	1.81	1.31	2.88	>sp|O80983|FTSH4_ARATH ATP-dependent zinc metalloprotease FTSH 4. mitochondrial
0.30	0.28	2.55	2.73	0.94	4.60	>sp|Q9LD57|PGKH1_ARATH Phphoglycerate kinase 1. chloroplastic
0.31	0.34	1.99	1.78	1.12	3.92	>tr|O23247|O23247_ARATH Arginyl-tRNA synthetase
0.32	0.18	0.78	1.37	0.57	1.18	>sp|Q9SIE1|PAT_ARATH Bifunctional aspartate aminotransferase and glutamate/aspartate-prephenate aminotransferase
0.32	0.19	1.91	3.16	0.60	4.82	>sp|Q8RWV0|TKTC1_ARATH Transketolase-1. chloroplastic
0.32	0.45	1.10	0.77	1.43	3.28	>tr|Q9C8G5|Q9C8G5_ARATH Early-responsive to dehydration stress protein (ERD4)
0.32	0.28	3.41	3.97	0.86	4.95	>sp|Q9SJL8|METK3_ARATH S-adenylmethionine synthase 3
0.32	0.58	2.53	1.40	1.80	3.40	>sp|Q9FWA4|GAUT9_ARATH Probable galacturonyltransferase 9
0.33	0.32	1.79	1.82	0.98	2.61	>sp|Q9SA34|IMDH2_ARATH Inine-5'-monophphate dehydrogenase 2
0.33	0.48	3.07	2.09	1.47	3.23	>sp|Q38970|ACC1_ARATH Acetyl-CoA carboxylase 1
0.34	0.35	3.07	2.95	1.04	1.87	>tr|Q9M888|Q9M888_ARATH Putative chaperonin
0.34	0.40	3.65	3.12	1.17	3.90	>sp|Q9FWA3|6GPD3_ARATH 6-phphogluconate dehydrogenase. decarboxylating 3
0.34	0.34	3.26	3.27	1.00	5.79	>sp|P16127|CHLI1_ARATH Magnesium-chelatase subunit ChlI-1. chloroplastic
0.34	0.23	0.85	1.26	0.67	5.02	>tr|O80503|O80503_ARATH Expressed protein
0.35	0.25	1.48	2.07	0.72	4.21	>sp|Q9FR44|PEAM1_ARATH Phphoethanolamine N-methyltransferase 1
0.35	0.29	1.44	1.71	0.84	3.11	>tr|Q949M9|Q949M9_ARATH ATPase ASNA1 homolog
0.35	0.28	1.31	1.64	0.80	2.24	>sp|P56786|YCF2_ARATH Protein Ycf2
0.35	0.34	1.62	1.67	0.97	2.60	>sp|Q39102|FTSH1_ARATH ATP-dependent zinc metalloprotease FTSH 1. chloroplastic
0.35	0.47	1.69	1.25	1.34	4.01	>tr|Q93VP9|Q93VP9_ARATH Putative uncharacterized protein At4g27585
0.35	0.34	1.23	1.27	0.97	4.20	>sp|Q9SAJ3|FTSHC_ARATH ATP-dependent zinc metalloprotease FTSH 12. chloroplastic
0.35	0.34	0.24	0.25	0.96	1.39	>sp|O04209|CLC2_ARATH Clathrin light chain 2
0.36	0.37	2.07	2.01	1.03	2.78	>sp|Q9ZUG4|MTNA_ARATH Methylthioribe-1-phphate isomerase
0.36	0.36	1.68	1.70	0.99	3.04	>tr|F4J4K6|F4J4K6_ARATH Tubulin binding cofactor C domain-containing protein
0.36	0.42	2.83	2.44	1.16	3.42	>tr|F4IAG5|F4IAG5_ARATH ATP-dependent Clp protease proteolytic subunit
0.36	0.44	1.44	1.18	1.22	4.84	>sp|Q8L940|PDX13_ARATH Pyridoxal biynthesis protein PDX1.3
0.37	0.38	3.62	3.48	1.04	5.92	>sp|P46645|AAT2_ARATH Aspartate aminotransferase. cytoplasmic isozyme 1
0.37	0.47	1.82	1.42	1.28	3.07	>tr|Q9C8P0|Q9C8P0_ARATH At1g34430/F7P12_2
0.38	0.40	1.47	1.37	1.07	3.80	>sp|P20649|PMA1_ARATH ATPase 1. plasma membrane-type
0.38	0.48	1.45	1.15	1.26	2.88	>sp|Q9XGM1|VATD_ARATH V-type proton ATPase subunit D
0.38	0.38	1.52	1.52	1.00	3.30	>sp|P93042|RHD3_ARATH Protein ROOT HAIR DEFECTIVE 3

0.38	0.48	1.71	1.37	1.25	3.92	>sp|Q941L0|CESA3_ARATH Cellule synthase A catalytic subunit 3 [UDP-forming]
0.38	0.37	1.42	1.47	0.96	3.58	>tr|Q9FXD4|Q9FXD4_ARATH Signal recognition particle subunit SRP72
0.38	0.37	2.09	2.19	0.95	3.14	>sp|Q9S7E4|FDH_ARATH Formate dehydrogenase. mitochondrial
0.39	0.60	1.79	1.16	1.55	3.68	>sp|Q9XIE2|AB36G_ARATH ABC transporter G family member 36
0.39	0.33	2.83	3.35	0.84	1.35	>tr|B9DH97|B9DH97_ARATH AT2G33120 protein
0.39	0.31	1.22	1.54	0.79	1.63	>sp|P48349|14336_ARATH 14-3-3-like protein GF14 lambda
0.39	0.48	2.44	1.99	1.23	2.48	>tr|F4IAP5|F4IAP5_ARATH Kete-bisphphate aldolase class-II family protein
0.39	0.35	1.67	1.85	0.90	1.51	>tr|Q9FYF8|Q9FYF8_ARATH At1g67350
0.40	0.38	0.98	1.03	0.95	2.40	>tr|Q9M2P9|Q9M2P9_ARATH Putative uncharacterized protein At3g57990
0.40	0.57	1.56	1.09	1.42	1.26	>sp|Q9ZPY7|XPO2_ARATH Exportin-2
0.40	0.31	3.33	4.40	0.76	4.73	>sp|P17562|METK2_ARATH S-adenylmethionine synthase 2
0.41	0.45	1.39	1.25	1.11	3.76	>sp|Q9SKR2|SYT1_ARATH Synaptotagmin-1
0.41	0.33	2.00	2.50	0.80	3.82	>sp|P50318|PGKH2_ARATH Phphoglycerate kinase 2. chloroplastic
0.41	0.53	1.75	1.34	1.30	3.20	>sp|Q9LVA0|BAG7_ARATH BAG family molecular chaperone regulator 7
0.41	0.49	2.00	1.66	1.20	1.82	>sp|O48946|CESA1_ARATH Cellule synthase A catalytic subunit 1 [UDP-forming]
0.41	0.34	0.59	0.73	0.81	3.39	>sp|P56759|ATPF_ARATH ATP synthase subunit b. chloroplastic
0.42	0.51	1.50	1.23	1.23	2.64	>sp|Q9FNX5|DRP1E_ARATH Dynamin-related protein 1E
0.42	0.40	1.29	1.35	0.95	3.82	>sp|P92935|TLC2_ARATH ADP.ATP carrier protein 2. chloroplastic
0.42	0.51	1.30	1.06	1.23	3.48	>sp|Q9STX5|ENPL_ARATH Endoplasmin homolog
0.42	0.38	0.68	0.75	0.91	3.35	>tr|A8MPR5|A8MPR5_ARATH AAA-type ATPase family protein
0.42	0.55	2.17	1.67	1.30	3.73	>tr|F4HS68|F4HS68_ARATH Tetratricopeptide repeat-containing protein
0.42	0.48	1.27	1.11	1.14	2.52	>sp|Q9M5P2|SCAM3_ARATH Secretory carrier-associated membrane protein 3
0.42	0.28	1.41	2.15	0.66	1.58	>tr|F4J5T2|F4J5T2_ARATH Dihydrolipoyllysine-residue acetyltransferase component 1 of pyruvate dehydrogenase complex
0.42	0.45	1.77	1.66	1.07	5.95	>sp|Q38884|EIF3I_ARATH Eukaryotic translation initiation factor 3 subunit I
0.42	0.49	1.41	1.23	1.15	3.35	>sp|P19456|PMA2_ARATH ATPase 2. plasma membrane-type
0.43	0.38	3.07	3.45	0.89	3.26	>sp|Q9LUT2|METK4_ARATH S-adenylmethionine synthase 4
0.43	0.38	2.89	3.31	0.87	4.85	>sp|O23254|GLYC4_ARATH Serine hydroxymethyltransferase 4
0.43	0.32	1.89	2.55	0.74	4.52	>sp|Q42547|CATA3_ARATH Catalase-3
0.43	0.49	2.24	1.96	1.14	1.63	>tr|Q9ASV5|Q9ASV5_ARATH AT4g39690/T19P19_80
0.43	0.47	1.85	1.69	1.09	2.15	>tr|Q9LV21|Q9LV21_ARATH T-complex protein 1 subunit delta
0.43	0.37	3.16	3.72	0.85	5.25	>sp|Q9LIK9|APS1_ARATH ATP sulfurylase 1. chloroplastic
0.43	0.41	3.06	3.23	0.95	3.92	>sp|P23686|METK1_ARATH S-adenylmethionine synthase 1
0.43	0.44	1.36	1.33	1.02	3.81	>tr|Q9ZPW5|Q9ZPW5_ARATH AAA-type ATPase-like protein
0.44	0.49	1.49	1.32	1.13	1.51	>tr|Q940S0|Q940S0_ARATH At1g14670/T5E21.14
0.44	0.60	2.28	1.68	1.35	2.09	>tr|F4HVV6|F4HVV6_ARATH CCR4-NOT transcription complex

						subunit 1 domain protein
0.44	0.42	3.16	3.36	0.94	3.95	>sp|Q9SYP2|PFPA1_ARATH Pyrophphate--fructe 6-phphate 1-phphotransferase subunit alpha 1
0.44	0.62	1.42	1.01	1.41	1.44	>sp|Q9S7Z3|PCS1_ARATH Glutathione gamma-glutamylcysteinyltransferase 1
0.45	0.47	1.31	1.25	1.05	2.96	>tr|Q8LPR8|Q8LPR8_ARATH AT5g22640/MDJ22_6
0.45	0.45	1.15	1.16	0.99	3.13	>tr|Q9FN50|Q9FN50_ARATH AT5g23040/MYJ24_3
0.45	0.46	1.68	1.67	1.01	2.77	>sp|P29513|TBB5_ARATH Tubulin beta-5 chain
0.45	0.51	2.18	1.93	1.13	2.24	>sp|Q9LK25|PHB4_ARATH Prohibitin-4. mitochondrial
0.46	0.42	1.18	1.28	0.92	2.53	>sp|P29517|TBB9_ARATH Tubulin beta-9 chain
0.46	0.79	2.21	1.29	1.72	1.41	>sp|Q9T029|RS254_ARATH 40S ribomal protein S25-4
0.46	0.44	1.88	1.97	0.95	1.04	>sp|Q9SA52|CP41B_ARATH Chloroplast stem-loop binding protein of 41 kDa b. chloroplastic
0.46	0.45	1.26	1.29	0.98	2.16	>sp|P56785|YCF1_ARATH Putative membrane protein ycf1
0.46	0.49	1.98	1.89	1.05	3.91	>sp|P54609|CD48A_ARATH Cell division control protein 48 homolog A
0.47	0.65	1.11	0.80	1.40	2.73	>tr|Q9FMM3|Q9FMM3_ARATH GYF domain-containing protein
0.47	0.36	1.15	1.50	0.77	1.35	>sp|Q9LY66|RK1_ARATH 50S ribomal protein L1. chloroplastic
0.47	0.42	1.04	1.16	0.90	1.33	>sp|P56795|RK22_ARATH 50S ribomal protein L22. chloroplastic
0.47	0.64	1.82	1.34	1.36	1.68	>sp|Q9SE83|DRP2A_ARATH Dynamin-2A
0.47	0.64	2.35	1.73	1.36	1.02	>sp|O49460|PHB1_ARATH Prohibitin-1. mitochondrial
0.47	0.37	1.46	1.88	0.78	4.86	>sp|Q8RWN9|ODP22_ARATH Dihydrolipoyllysine-residue acetyltransferase component 2 of pyruvate dehydrogenase complex. mitochondrial
0.47	0.56	1.53	1.27	1.20	3.07	>tr|Q9LEX1|Q9LEX1_ARATH At3g61050
0.47	0.42	0.93	1.06	0.88	2.62	>sp|Q9C5J8|OEP80_ARATH Outer envelope protein 80. chloroplastic
0.47	0.62	1.82	1.40	1.30	2.86	>sp|P29514|TBB6_ARATH Tubulin beta-6 chain
0.47	0.66	1.53	1.10	1.39	2.46	>sp|Q570B4|KCS10_ARATH 3-ketoacyl-CoA synthase 10
0.48	0.57	2.07	1.73	1.20	1.56	>sp|O49313|NDADB_ARATH NADH dehydrogenase [ubiquinone] 1 alpha subcomplex subunit 13-B
0.48	0.77	2.09	1.30	1.61	3.30	>sp|Q8RVQ5|SEC10_ARATH Exocyst complex component SEC10
0.48	0.52	2.42	2.23	1.09	2.20	>sp|O04450|TCPE_ARATH T-complex protein 1 subunit epsilon
0.48	0.41	2.39	2.80	0.85	4.19	>sp|Q9FFR3|6PGD2_ARATH 6-phphogluconate dehydrogenase. decarboxylating 2. chloroplastic
0.48	0.45	1.26	1.35	0.93	1.81	>tr|Q93W02|Q93W02_ARATH AT5g24690/MXC17_8
0.49	0.39	1.36	1.68	0.81	2.88	>sp|O80860|FTSH2_ARATH ATP-dependent zinc metalloprotease FTSH 2. chloroplastic
0.49	0.37	1.30	1.71	0.76	1.24	>sp|O48528-2|OP163_ARATH Isoform 2 of Outer envelope pore protein 16-3. chloroplastic/mitochondrial
0.49	0.42	1.55	1.81	0.85	1.98	>sp|P17745|EFTU_ARATH Elongation factor Tu. chloroplastic
0.50	0.48	1.14	1.18	0.97	2.36	>tr|Q93Y08|Q93Y08_ARATH ABC transporter-like
0.50	0.49	1.35	1.37	0.98	1.29	>sp|O80448|PDX11_ARATH Pyridoxal biynthesis protein PDX1.1
0.50	0.32	1.14	1.78	0.64	1.88	>sp|Q01908|ATPG1_ARATH ATP synthase gamma chain 1. chloroplastic
0.50	0.54	1.59	1.46	1.08	2.47	>sp|P31167|ADT1_ARATH ADP.ATP carrier protein 1. mitochondrial

0.50	0.53	2.12	2.01	1.05	1.18	>sp|Q93VP3|IF5A2_ARATH Eukaryotic translation initiation factor 5A-2
0.50	0.53	1.66	1.57	1.06	2.33	>sp|O04331|PHB3_ARATH Prohibitin-3. mitochondrial
0.50	0.79	5.81	3.72	1.56	2.70	>sp|O80852|GSTF9_ARATH Glutathione S-transferase F9
0.51	0.50	1.53	1.57	0.98	2.21	>sp|O81845|PUMP1_ARATH Mitochondrial uncoupling protein 1
0.51	0.29	0.92	1.63	0.56	1.78	>sp|O80796|VIPP1_ARATH Membrane-associated protein VIPP1. chloroplastic
0.51	0.70	1.17	0.84	1.38	0.87	>sp|O04202|EIF3F_ARATH Eukaryotic translation initiation factor 3 subunit F
0.51	0.39	0.91	1.19	0.77	2.91	>tr|Q9C9I7|Q9C9I7_ARATH Putative uncharacterized protein At1g71500
0.51	0.42	1.46	1.77	0.82	3.05	>sp|O22218|ACA4_ARATH Calcium-transporting ATPase 4. plasma membrane-type
0.51	0.55	1.90	1.76	1.08	3.37	>tr|F4JHS4|F4JHS4_ARATH Adenine nucleotide transporter 1
0.51	0.53	1.76	1.70	1.03	3.61	>sp|P24636|TBB4_ARATH Tubulin beta-4 chain
0.51	0.53	1.32	1.29	1.02	2.05	>tr|F4JYQ8|F4JYQ8_ARATH Protein embryo defective 2737
0.51	0.48	1.14	1.23	0.93	1.93	>tr|Q93VT6|Q93VT6_ARATH Putative uncharacterized protein At5g08540
0.51	0.51	1.16	1.18	0.98	1.77	>sp|Q9SRU2|BIG_ARATH Auxin transport protein BIG
0.52	0.44	1.50	1.74	0.86	1.73	>sp|P52410|KASC1_ARATH 3-oxoacyl-[acyl-carrier-protein] synthase I. chloroplastic
0.52	0.62	1.32	1.09	1.21	3.30	>tr|Q8GUN1|Q8GUN1_ARATH AT4G31340 protein
0.52	0.53	1.80	1.74	1.03	3.14	>sp|F4J8D3|TPLAT_ARATH Protein TPLATE
0.52	0.50	1.86	1.92	0.97	2.83	>tr|Q8W498|Q8W498_ARATH ARM repeat superfamily protein
0.52	0.52	1.67	1.65	1.01	1.06	>tr|Q9ZNT0|Q9ZNT0_ARATH F10A12.27/F10A12.27
0.52	0.54	1.36	1.31	1.04	2.21	>tr|Q0WT48|Q0WT48_ARATH J domain protein DjC21
0.52	0.61	1.58	1.34	1.18	3.50	>sp|Q38950|2AAB_ARATH Serine/threonine-protein phphatase 2A 65 kDa regulatory subunit A beta isoform
0.52	0.55	1.33	1.26	1.05	2.91	>sp|Q9LTT8|VCS_ARATH Enhancer of mRNA-decapping protein 4
0.52	0.57	1.67	1.52	1.10	1.01	>tr|Q9ZQ87|Q9ZQ87_ARATH Expressed protein
0.52	0.49	0.99	1.05	0.94	0.83	>sp|O22265|SR43C_ARATH Signal recognition particle 43 kDa protein. chloroplastic
0.52	0.52	0.97	0.99	0.99	2.94	>tr|Q9STF2|Q9STF2_ARATH Protein plastid transcriptionally active 16
0.53	0.56	1.94	1.83	1.06	1.78	>sp|Q9SFU0|SC24A_ARATH Protein transport protein Sec24-like At3g07100
0.53	0.53	0.98	0.97	1.01	1.28	>tr|Q9SYW8|Q9SYW8_ARATH Lhca2 protein
0.53	0.54	1.51	1.48	1.02	1.58	>sp|B9DGT7|TBA2_ARATH Tubulin alpha-2 chain
0.53	0.50	2.93	3.09	0.95	4.25	>tr|Q9SAJ4|Q9SAJ4_ARATH Phphoglycerate kinase
0.53	0.45	1.54	1.80	0.86	2.75	>tr|Q9SQI8|Q9SQI8_ARATH AT3g25860/MPE11_1
0.53	0.74	1.71	1.22	1.40	1.53	>sp|Q9M7Z1|ODB2_ARATH Lipoamide acyltransferase component of branched-chain alpha-keto acid dehydrogenase complex. mitochondrial
0.53	0.50	2.03	2.15	0.94	2.68	>tr|Q93VS8|Q93VS8_ARATH Protein EMBRYO DEFECTIVE 2734
0.53	0.42	2.34	2.99	0.78	3.60	>tr|F4I116|F4I116_ARATH ATP binding/leucine-tRNA ligases/aminoacyl-tRNA ligases

0.53	0.50	2.00	2.15	0.93	3.35	>sp|P46643|AAT1_ARATH Aspartate aminotransferase. mitochondrial
0.53	0.62	2.27	1.95	1.16	1.61	>sp|Q9LXS6|CISY2_ARATH Citrate synthase 2. peroxisomal
0.53	0.42	1.01	1.29	0.78	2.06	>sp|O82533|FTZ21_ARATH Cell division protein FtsZ homolog 2-1. chloroplastic
0.54	0.46	1.66	1.92	0.87	1.95	>sp|Q9LIB2|PHS1_ARATH Alpha-glucan phphorylase 1
0.54	0.42	1.51	1.94	0.78	2.37	>sp|P21218|PORB_ARATH Protochlorophyllide reductase B. chloroplastic
0.54	0.40	1.46	1.96	0.74	4.07	>tr|O80576|O80576_ARATH At2g44060
0.54	0.61	1.33	1.18	1.12	1.81	>sp|P92994|TCMO_ARATH Trans-cinnamate 4-monooxygenase
0.54	0.60	1.49	1.35	1.10	0.87	>tr|Q8GY46|Q8GY46_ARATH At5g13560
0.54	0.48	1.17	1.33	0.88	0.83	>sp|O80891|CSLB4_ARATH Cellule synthase-like protein B4
0.54	0.43	0.93	1.18	0.79	1.12	>sp|Q76E23|IF4G_ARATH Eukaryotic translation initiation factor 4G
0.55	0.53	2.16	2.22	0.97	2.41	>tr|Q940P8|Q940P8_ARATH AT5g20890/F22D1_60
0.55	0.38	1.84	2.63	0.70	4.26	>sp|Q96251|ATPO_ARATH ATP synthase subunit O. mitochondrial
0.55	0.59	1.00	0.92	1.09	2.10	>tr|Q94CJ5|Q94CJ5_ARATH At5g12470
0.55	0.40	1.55	2.11	0.74	3.74	>sp|Q9SI75|EFGC_ARATH Elongation factor G. chloroplastic
0.55	0.55	1.66	1.65	1.01	3.36	>tr|F4IIM1|F4IIM1_ARATH Cellule synthase-interactive protein 1
0.55	0.44	1.72	2.12	0.81	2.99	>sp|P25856|G3PA1_ARATH Glyceraldehyde-3-phphate dehydrogenase GAPA1. chloroplastic
0.55	0.44	0.77	0.97	0.80	3.11	>tr|Q9FFJ2|Q9FFJ2_ARATH Putative uncharacterized protein At5g17170
0.55	0.46	1.10	1.32	0.83	3.47	>sp|P56805|RR15_ARATH 30S ribomal protein S15. chloroplastic
0.55	0.41	1.39	1.86	0.75	0.90	>sp|P42732|RR13_ARATH 30S ribomal protein S13. chloroplastic
0.55	0.68	1.60	1.31	1.23	2.04	>sp|Q9LQ55|DRP2B_ARATH Dynamin-2B
0.55	0.56	1.11	1.08	1.02	2.49	>tr|Q9FF91|Q9FF91_ARATH Uncharacterized protein
0.55	0.74	1.61	1.20	1.34	3.34	>sp|Q9LD55|EIF3A_ARATH Eukaryotic translation initiation factor 3 subunit A
0.56	0.45	1.56	1.92	0.81	2.04	>sp|Q9FLQ4|ODO2A_ARATH Dihydrolipoyllysine-residue succinyltransferase component of 2-oxoglutarate dehydrogenase complex 1. mitochondrial
0.56	0.59	0.98	0.93	1.06	1.98	>sp|O81283|TC159_ARATH Translocase of chloroplast 159. chloroplastic
0.56	0.46	1.07	1.30	0.82	1.84	>sp|Q42472|DCE2_ARATH Glutamate decarboxylase 2
0.56	0.42	0.91	1.21	0.75	2.42	>tr|Q94AZ5|Q94AZ5_ARATH At2g45060/T14P1.13
0.56	0.46	1.22	1.49	0.82	2.68	>sp|Q9LY74|BQMT_ARATH 2-methyl-6-phytyl-1.4-hydroquinone methyltransferase. chloroplastic
0.56	0.60	1.25	1.15	1.08	2.18	>sp|P56778|PSBC_ARATH Photystem II CP43 chlorophyll apoprotein
0.56	0.53	0.88	0.93	0.94	2.79	>tr|Q9SY97|Q9SY97_ARATH PSI type III chlorophyll a/b-binding protein
0.56	0.52	0.77	0.82	0.94	0.99	>sp|Q9ZUU4|ROC1_ARATH Ribonucleoprotein At2g37220. chloroplastic
0.56	0.64	1.52	1.32	1.15	1.79	>sp|Q93XM7|MCAT_ARATH Mitochondrial carnitine/acylcarnitine carrier-like protein
0.56	0.45	1.37	1.72	0.80	2.89	>sp|B9DHQ0|TBA5_ARATH Tubulin alpha-5 chain

0.56	0.69	1.54	1.25	1.23	1.52	>tr|F4K4D5|F4K4D5_ARATH Eukaryotic translation initiation factor 3 subunit B
0.56	0.42	1.85	2.49	0.75	3.43	>sp|P93303|YMF19_ARATH ATP synthase protein YMF19
0.56	0.44	1.45	1.84	0.79	2.36	>sp|Q9LMI0|TPS7_ARATH Probable alpha.alpha-trehale-phphate synthase [UDP-forming] 7
0.56	0.70	1.58	1.27	1.25	2.71	>sp|Q9C5U3|PRS8A_ARATH 26S protease regulatory subunit 8 homolog A
0.56	0.35	2.80	4.59	0.61	4.18	>sp|P42760|GSTF6_ARATH Glutathione S-transferase F6
0.57	0.66	1.34	1.16	1.16	2.86	>sp|Q9SUR3|RTNLA_ARATH Reticulon-like protein B1
0.57	0.56	1.26	1.27	0.99	2.29	>sp|Q9SHE8|PSAF_ARATH Photystem I reaction center subunit III. chloroplastic
0.57	0.64	1.40	1.24	1.13	2.87	>sp|Q9LMM0|GPAT4_ARATH Glycerol-3-phphate 2-O-acyltransferase 4
0.57	0.41	1.21	1.68	0.72	2.69	>sp|P56757|ATPA_ARATH ATP synthase subunit alpha. chloroplastic
0.57	0.60	2.53	2.39	1.06	3.22	>sp|Q9LXL5|SUS4_ARATH Sucre synthase 4
0.57	0.52	1.32	1.45	0.91	1.65	>tr|F4K409|F4K409_ARATH Putative TypA-like translation elongation factor SVR3
0.57	0.61	0.87	0.82	1.06	1.71	>sp|P92959|RK24_ARATH 50S ribomal protein L24. chloroplastic
0.57	0.47	1.09	1.32	0.83	1.86	>sp|Q8LPR9|TI110_ARATH Protein TIC110. chloroplastic
0.57	0.58	1.29	1.28	1.00	3.90	>tr|F4IFG2|F4IFG2_ARATH Dynamin-related protein 3B
0.58	0.51	1.38	1.55	0.89	1.22	>sp|Q9ZNT7|PHB2_ARATH Prohibitin-2. mitochondrial
0.58	0.62	1.42	1.34	1.06	3.21	>sp|P42697|DRP1A_ARATH Dynamin-related protein 1A
0.58	0.45	1.20	1.53	0.78	3.22	>sp|Q8GWE0|PP314_ARATH Pentatricopeptide repeat-containing protein At4g16390. chloroplastic
0.58	0.73	1.87	1.49	1.25	1.35	>sp|P29976|AROF_ARATH Phpho-2-dehydro-3-deoxyheptonate aldolase 1. chloroplastic
0.58	0.59	1.37	1.36	1.01	1.30	>tr|F4KIH8|F4KIH8_ARATH WD40 domain-containing protein
0.58	0.52	1.47	1.64	0.89	2.68	>tr|F4JFN3|F4JFN3_ARATH HEAT SHOCK PROTEIN 89.1
0.58	0.68	2.15	1.83	1.17	2.94	>sp|Q9SYM5|RHM1_ARATH Probable rhamne biynthetic enzyme 1
0.59	0.57	1.55	1.59	0.97	1.19	>sp|Q9SIL6|PHB6_ARATH Prohibitin-6. mitochondrial
0.59	0.54	0.81	0.89	0.91	3.12	>sp|P37107|SR54C_ARATH Signal recognition particle 54 kDa protein. chloroplastic
0.59	0.39	1.03	1.56	0.66	2.29	>sp|P09468|ATPE_ARATH ATP synthase epsilon chain. chloroplastic
0.59	0.60	1.37	1.34	1.03	0.88	>tr|Q9C9M1|Q9C9M1_ARATH Pheromone receptor. putative (AR401)
0.59	0.56	0.97	1.02	0.96	1.60	>sp|Q9M591|CRD1_ARATH Magnesium-protoporphyrin IX monomethyl ester [oxidative] cyclase. chloroplastic
0.59	0.58	1.23	1.25	0.99	2.79	>sp|Q9XF88|CB4B_ARATH Chlorophyll a-b binding protein CP29.2. chloroplastic
0.59	0.59	1.55	1.55	1.00	2.37	>sp|Q38820|TI232_ARATH Mitochondrial import inner membrane translocase subunit TIM23-2
0.59	0.54	1.21	1.33	0.91	1.66	>sp|P55737|HS902_ARATH Heat shock protein 90-2
0.59	0.43	0.90	1.24	0.73	1.94	>sp|O82660|P2SAF_ARATH Photystem II stability/assembly factor HCF136. chloroplastic
0.59	0.66	1.48	1.32	1.12	2.29	>tr|F4JY76|F4JY76_ARATH Eukaryotic translation initiation factor 3 subunit L

0.59	0.50	1.07	1.28	0.83	1.54	>sp|Q944K2|T48_ARATH Dolichyl-diphphooligaccharide--protein glycyltransferase 48 kDa subunit
0.60	0.68	1.58	1.38	1.15	1.90	>sp|Q94A40|COPA1_ARATH Coatomer subunit alpha-1
0.60	0.52	1.08	1.25	0.86	1.36	>sp|Q9FNB0|CHLH_ARATH Magnesium-chelatase subunit ChlH. chloroplastic
0.60	0.59	0.86	0.87	0.98	3.44	>tr|Q9XF87|Q9XF87_ARATH At3g27700
0.60	0.68	1.34	1.18	1.13	0.99	>sp|O49160|EIF3C_ARATH Eukaryotic translation initiation factor 3 subunit C
0.60	0.60	1.36	1.36	1.00	1.83	>tr|F4IYK3|F4IYK3_ARATH Armadillo/beta-catenin-like repeat-containing protein
0.61	0.71	1.25	1.06	1.18	2.16	>sp|Q9SIV2|PSD2A_ARATH 26S proteasome non-ATPase regulatory subunit 2 homolog A
0.61	0.61	0.92	0.91	1.01	2.67	>sp|P04778|CB1C_ARATH Chlorophyll a-b binding protein 1. chloroplastic
0.61	0.69	1.21	1.06	1.14	2.15	>sp|Q93ZT6|IF4G1_ARATH Eukaryotic translation initiation factor isoform 4G-1
0.61	0.45	1.97	2.66	0.74	1.78	>sp|Q9C4Z6|GPLPB_ARATH Guanine nucleotide-binding protein subunit beta-like protein B
0.61	0.45	2.13	2.91	0.73	1.69	>sp|Q96250|ATPG3_ARATH ATP synthase subunit gamma. mitochondrial
0.61	0.56	0.88	0.95	0.92	2.89	>sp|P10896|RCA_ARATH Ribule bisphphate carboxylase/oxygenase activase. chloroplastic
0.61	0.50	0.84	1.03	0.81	2.01	>sp|Q9XF89|CB5_ARATH Chlorophyll a-b binding protein CP26. chloroplastic
0.61	0.72	1.53	1.29	1.18	1.83	>sp|Q0WNJ6|CLAH1_ARATH Clathrin heavy chain 1
0.61	0.62	2.83	2.82	1.01	1.78	>sp|Q42601|CARB_ARATH Carbamoyl-phphate synthase large chain. chloroplastic
0.61	0.57	1.05	1.13	0.93	2.32	>tr|Q9SIF2|Q9SIF2_ARATH At2g04030/F3C11.14
0.61	0.53	1.15	1.35	0.86	2.77	>sp|Q9SXJ7|CLPC2_ARATH Chaperone protein ClpC2. chloroplastic
0.61	0.64	1.37	1.32	1.04	1.64	>tr|F4K470|F4K470_ARATH Putative galactinol--sucre galactyltransferase 6
0.62	0.59	1.02	1.06	0.95	1.25	>sp|P25864|RK9_ARATH 50S ribomal protein L9. chloroplastic
0.62	0.51	1.40	1.70	0.82	2.54	>sp|Q8L7S8|RH3_ARATH DEAD-box ATP-dependent RNA helicase 3. chloroplastic
0.62	0.58	1.01	1.09	0.93	2.25	>sp|P56798|RR3_ARATH 30S ribomal protein S3. chloroplastic
0.62	0.61	1.31	1.32	0.99	2.16	>sp|Q9S7W1|CB4C_ARATH Chlorophyll a-b binding protein CP29.3. chloroplastic
0.62	0.57	0.95	1.03	0.92	1.46	>sp|Q01667|CAB6_ARATH Chlorophyll a-b binding protein 6. chloroplastic
0.62	0.63	1.38	1.35	1.02	1.58	>sp|Q8W4H8|GDL19_ARATH Inactive GDSL esterase/lipase-like protein 23
0.62	0.54	1.05	1.22	0.86	1.13	>sp|O22173|PABP4_ARATH Polyadenylate-binding protein 4
0.62	0.57	1.90	2.08	0.91	1.57	>sp|Q9SJ12|ATP7_ARATH Probable ATP synthase 24 kDa subunit. mitochondrial
0.62	0.66	1.01	0.95	1.06	2.09	>tr|Q9LMQ2|Q9LMQ2_ARATH Chlorophyll A-B binding protein

0.63	0.59	1.31	1.40	0.94	1.13	>sp|O04487|EF1G1_ARATH Probable elongation factor 1-gamma 1
0.63	0.49	1.49	1.91	0.78	2.01	>sp|P25857|G3PB_ARATH Glyceraldehyde-3-phphate dehydrogenase GAPB. chloroplastic
0.63	0.69	1.59	1.45	1.10	1.81	>sp|Q0WLB5|CLAH2_ARATH Clathrin heavy chain 2
0.63	0.49	1.06	1.36	0.78	2.86	>sp|Q9FI56|CLPC1_ARATH Chaperone protein ClpC1. chloroplastic
0.63	0.52	1.22	1.48	0.83	1.94	>sp|Q9SCX3|EF1B2_ARATH Elongation factor 1-beta 2
0.63	0.69	1.11	1.01	1.10	1.24	>sp|Q9SZD4|PRS4A_ARATH 26S proteasome regulatory subunit 4 homolog A
0.63	0.71	1.23	1.09	1.12	2.07	>tr|F4HS99|F4HS99_ARATH Tetratricopeptide repeat-containing protein
0.63	0.57	1.51	1.67	0.90	1.10	>sp|P40941|ADT2_ARATH ADP.ATP carrier protein 2. mitochondrial
0.63	0.60	1.47	1.57	0.94	1.51	>sp|Q9FMU6|MPCP3_ARATH Mitochondrial phphate carrier protein 3. mitochondrial
0.63	0.69	1.57	1.44	1.09	1.22	>tr|F4I894|F4I894_ARATH Protein ILITYHIA
0.63	0.48	1.93	2.58	0.75	3.28	>sp|Q9LV03|GLUT1_ARATH Glutamate synthase 1 [NADH]. chloroplastic
0.64	0.69	1.30	1.20	1.08	0.87	>sp|P56765|ACCD_ARATH Acetyl-coenzyme A carboxylase carboxyl transferase subunit beta. chloroplastic
0.64	0.65	1.35	1.33	1.02	0.84	>sp|P48578|PP2A3_ARATH Serine/threonine-protein phphatase PP2A-3 catalytic subunit
0.64	0.68	1.49	1.41	1.06	1.54	>tr|F4KIB2|F4KIB2_ARATH Endomembrane family protein 70
0.64	0.58	1.21	1.35	0.90	1.64	>sp|Q9FVT2|EF1G2_ARATH Probable elongation factor 1-gamma 2
0.64	0.55	1.24	1.46	0.85	2.09	>sp|Q9LS25|PP420_ARATH Pentatricopeptide repeat-containing protein At5g46580. chloroplastic
0.65	0.70	0.73	0.67	1.09	3.85	>sp|O82628|VAGT1_ARATH V-type proton ATPase subunit G1
0.65	0.63	1.06	1.09	0.98	1.68	>sp|Q9SJE1|CHLD_ARATH Magnesium-chelatase subunit ChlD. chloroplastic
0.65	0.64	1.81	1.84	0.98	2.80	>sp|Q9LZ72|KCS21_ARATH 3-ketoacyl-CoA synthase 21
0.65	0.69	1.44	1.35	1.07	2.28	>sp|P29515|TBB7_ARATH Tubulin beta-7 chain
0.65	0.69	1.30	1.24	1.05	1.78	>tr|Q9FJD4|Q9FJD4_ARATH Armadillo/beta-catenin-like repeat-containing protein
0.66	0.47	1.62	2.25	0.72	1.42	>sp|Q9FY99|G6PD2_ARATH Gluce-6-phphate 1-dehydrogenase 2. chloroplastic
0.66	0.59	1.34	1.50	0.89	2.44	>sp|Q9LX65|VATH_ARATH V-type proton ATPase subunit H
0.66	0.52	1.55	1.99	0.78	1.60	>sp|Q9FLX7|NDUA5_ARATH Probable NADH dehydrogenase [ubiquinone] 1 alpha subcomplex subunit 5. mitochondrial
0.66	0.51	2.42	3.14	0.77	4.80	>sp|Q9ZT91|EFTM_ARATH Elongation factor Tu. mitochondrial
0.67	0.66	1.46	1.47	0.99	0.82	>tr|Q8L6Z4|Q8L6Z4_ARATH At3g49080
0.67	0.69	1.43	1.38	1.03	1.63	>tr|O82462|O82462_ARATH Glutamyl-tRNA synthetase
0.67	0.71	1.56	1.47	1.06	0.86	>tr|Q93VB0|Q93VB0_ARATH Nucleic acid-binding. OB-fold-like protein
0.67	0.67	1.61	1.61	1.00	2.49	>sp|P49040|SUSY1_ARATH Sucre synthase 1
0.67	0.50	1.71	2.27	0.75	0.83	>sp|P28769|TCPA_ARATH T-complex protein 1 subunit alpha
0.67	0.67	1.45	1.45	1.00	1.88	>sp|Q39085|DIM_ARATH Delta(24)-sterol reductase
0.67	0.39	1.89	3.27	0.58	1.26	>sp|Q9LRR9|GLO1_ARATH Peroxisomal (S)-2-hydroxy-acid oxidase

						GLO1
0.67	0.74	1.65	1.50	1.10	1.63	>sp|Q8LF21|DRP1C_ARATH Dynamin-related protein 1C
0.68	0.65	1.17	1.22	0.96	1.38	>sp|Q07473|CB4A_ARATH Chlorophyll a-b binding protein CP29.1. chloroplastic
0.68	0.71	1.35	1.29	1.05	1.27	>sp|Q9C5M0|DTC_ARATH Mitochondrial dicarboxylate/tricarboxylate transporter DTC
0.68	0.67	1.63	1.65	0.99	1.05	>sp|Q9CAV0|RS3A1_ARATH 40S ribomal protein S3a-1
0.68	0.56	1.11	1.35	0.82	0.88	>sp|Q8L7Z3|DRE2_ARATH Anamorsin homolog
0.68	0.73	1.40	1.31	1.07	1.37	>sp|Q56YW9|TBB2_ARATH Tubulin beta-2 chain
0.68	0.73	1.40	1.30	1.08	1.20	>tr|F4JLM5|F4JLM5_ARATH Isoleucyl-tRNA synthetase
0.68	0.54	1.21	1.53	0.79	1.70	>sp|Q9SN86|MDHP_ARATH Malate dehydrogenase. chloroplastic
0.68	0.61	0.72	0.81	0.89	3.67	>sp|Q39258|VATE1_ARATH V-type proton ATPase subunit E1
0.68	0.53	0.95	1.23	0.77	1.23	>sp|O23680|TOC33_ARATH Translocase of chloroplast 33. chloroplastic
0.68	0.72	1.96	1.85	1.06	0.93	>sp|O49543|NFS1_ARATH Cysteine desulfurase 1. mitochondrial
0.68	0.68	1.48	1.50	0.99	1.63	>tr|F4IB98|F4IB98_ARATH Jacalin-like lectin domain-containing protein
0.68	0.57	0.99	1.19	0.84	2.23	>sp|Q9FN48|CAS_ARATH Calcium sensing receptor. chloroplastic
0.69	0.62	1.62	1.81	0.90	2.26	>tr|Q9CAD1|Q9CAD1_ARATH At1g63660
0.70	0.54	1.40	1.80	0.78	2.37	>tr|Q9S791|Q9S791_ARATH AT1G70770 protein
0.70	0.57	1.99	2.43	0.82	2.51	>sp|P25819|CATA2_ARATH Catalase-2
0.70	0.58	0.99	1.20	0.82	1.77	>sp|O80565|OEP37_ARATH Outer envelope pore protein 37. chloroplastic
0.71	0.60	2.19	2.58	0.85	1.97	>sp|Q70E96|AL3F1_ARATH Aldehyde dehydrogenase family 3 member F1
0.71	0.71	1.46	1.45	1.00	1.26	>tr|F4ICX0|F4ICX0_ARATH Coatomer subunit beta'-2
0.71	0.61	1.07	1.24	0.86	2.26	>sp|P36210|RK121_ARATH 50S ribomal protein L12-1. chloroplastic
0.71	0.53	1.68	2.24	0.75	1.62	>sp|P21240|CPNB1_ARATH Chaperonin 60 subunit beta 1. chloroplastic
0.71	0.47	0.79	1.20	0.66	1.83	>tr|F4K874|F4K874_ARATH Carbonic anhydrase
0.71	0.50	1.69	2.40	0.71	2.90	>sp|P92947|MDARP_ARATH Monodehydroascorbate reductase. chloroplastic
0.72	0.53	2.18	2.97	0.73	2.31	>sp|Q56WD9|THIK2_ARATH 3-ketoacyl-CoA thiolase 2. peroxisomal
0.72	0.54	1.73	2.28	0.76	1.88	>sp|O64517|MCA4_ARATH Metacaspase-4
0.72	0.72	1.37	1.36	1.01	1.20	>sp|O81062|SIP_ARATH Signal peptide peptidase
0.72	0.68	2.05	2.17	0.94	1.36	>sp|Q9ZSK4|ADF3_ARATH Actin-depolymerizing factor 3
0.72	0.49	1.29	1.91	0.67	1.66	>sp|Q9CA67|CHLP_ARATH Geranylgeranyl diphphate reductase. chloroplastic
0.72	0.54	1.44	1.93	0.75	1.22	>tr|Q9SF16|Q9SF16_ARATH AT3g11830/F26K24_12
0.72	0.72	1.87	1.87	1.00	2.21	>sp|Q9SIB9|ACO2M_ARATH Aconitate hydratase 2. mitochondrial
0.73	0.67	0.83	0.90	0.91	1.02	>sp|P27521|CA4_ARATH Chlorophyll a-b binding protein 4. chloroplastic
0.74	0.62	1.28	1.52	0.84	2.70	>sp|Q95748|NDUS3_ARATH NADH dehydrogenase [ubiquinone] iron-sulfur protein 3
0.74	0.74	1.67	1.65	1.01	1.07	>tr|F4I5V8|F4I5V8_ARATH ATP-citrate lyase A-1

0.75	0.52	0.78	1.11	0.70	1.77	>sp|P50546|RPOB_ARATH DNA-directed RNA polymerase subunit beta
0.75	0.50	0.90	1.35	0.66	1.35	>sp|Q9FY50|RK10_ARATH 50S ribomal protein L10. chloroplastic
0.75	0.45	1.40	2.33	0.60	1.57	>sp|Q41931|ACCO2_ARATH 1-aminocyclopropane-1-carboxylate oxidase 2

OG antagonism vs IAA						
IAA/Mock	**OG/Mock**	**CoTr/IAA**	**CoTr/OG**	**CoTr/Mock**	**Log ANOVA p value**	**Protein IDs**
2.59	1.46	0.08	0.15	0.57	3.16	>tr|Q9SIH1|Q9SIH1_ARATH Peptidyl-prolyl cis-trans isomerase OS
1.52	0.48	0.11	0.35	0.32	1.01	>sp|Q9LD90|CBF5_ARATH H/ACA ribonucleoprotein complex subunit 4 OS
1.94	0.96	0.23	0.47	0.50	1.04	>sp|P51420|RL313_ARATH 60S ribosomal protein L31-3 OS
1.73	1.41	0.30	0.37	0.82	2.48	>sp|Q9FEF8|MD36B_ARATH Probable mediator of RNA polymerase II transcription subunit 36b OS
2.18	1.31	0.45	0.76	0.60	3.59	>sp|Q9MAQ0|SSG1_ARATH Probable granule-bound starch synthase 1. chloroplastic/amyloplastic OS
1.66	1.47	0.60	0.68	0.89	3.53	>tr|F4HRT5|F4HRT5_ARATH Protein little nuclei1 OS
2.20	1.46	0.61	0.92	0.66	1.21	>sp|Q9STN3|SPT51_ARATH Putative transcription elongation factor SPT5 homolog 1 OS
1.65	1.33	0.63	0.77	0.81	1.00	>sp|Q9SEE9-3|SR45_ARATH Isoform 3 of Arginine/serine-rich protein 45 OS
1.54	1.47	0.63	0.67	0.95	1.70	>tr|Q9FF75|Q9FF75_ARATH AT5g04990/MUG13_15 OS
1.72	1.05	0.65	1.06	0.61	2.33	>sp|Q9S709|U2AFA_ARATH Splicing factor U2af small subunit A OS
1.64	0.71	0.67	1.54	0.43	0.95	>sp|Q944G9|ALFC2_ARATH Probable fructose-bisphosphate aldolase 2. chloroplastic OS
1.32	0.97	0.69	0.94	0.74	1.14	>sp|Q9FJE8|H2A7_ARATH Probable histone H2A.7 OS
2.60	1.21	0.70	1.50	0.47	1.44	>sp|Q38882|PLDA1_ARATH Phospholipase D alpha 1 OS
2.81	1.17	0.44	1.07	1.25	1.37	Q9LXT5
2.34	1.13	0.50	1.03	1.16	1.50	F4JHV8;Q9SY09;Q9SSF1
1.93	1.32	0.71	1.04	1.38	1.37	Q9LIH9
1.56	1.11	0.06	0.09	0.10	1.57	AT2G28720 Histone H2B.3;
2.53	1.42	0.15	0.27	0.38	1.12	AT4G40040;AT4G40030;AT5G10980 Histone H3.3

IAA antagonism vs Ogs						
Auxin/Mock	**OG/Mock**	**CoTr/Auxin**	**CoTr/OG**	**CoTr/Mock**	**Log ANOVA p value**	**Protein IDs**
0.55	2.26	1.73	0.42	0.94	1.78	Q9C8Y9;Q9C8Y9-2
1.77	4.01	1.00	0.44	1.78	2.32	O24412;F4K0U3
1.20	2.13	1.25	0.70	1.50	1.80	Q9C525;Q9C525-2
Auxin/Mock	**OG/Mock**	**CoTr/Auxin**	**CoTr/OG**	**OG/Auxin**	**Log ANOVA p value**	**Protein IDs**
1.37	2.24	0.55	0.34	1.63	1.42	>tr|F4IH36|F4IH36_ARATH Uncharacterized protein
1.12	2.11	0.94	0.50	1.89	1.31	>sp|Q8W206|CSN6A_ARATH COP9 signalome complex subunit 6a
1.44	1.81	0.65	0.52	1.25	1.54	>sp|Q9M086|DCAF1_ARATH DDB1- and CUL4-associated factor homolog 1
1.14	1.58	0.75	0.54	1.38	2.50	>sp|Q94JU3|CSN7_ARATH COP9 signalome complex subunit 7
1.39	1.72	0.74	0.59	1.24	1.95	>sp|Q39211|NRPB3_ARATH DNA-directed RNA polymerases II. IV and V subunit 3
1.39	1.57	0.67	0.59	1.13	1.54	>tr|Q8GW48|Q8GW48_ARATH At4g15810
1.15	1.55	0.85	0.64	1.34	1.44	>tr|Q9SZQ5|Q9SZQ5_ARATH At4g29830
1.29	1.83	0.91	0.64	1.42	2.10	>sp|Q8W575|CSN3_ARATH COP9 signalome complex subunit 3
0.92	1.71	1.25	0.68	1.85	0.93	>tr|O22957|O22957_ARATH Apoptis inhibitory protein 5 (API5)
1.06	1.75	1.15	0.69	1.65	2.57	>tr|Q93ZV7|Q93ZV7_ARATH La protein 1
1.36	1.78	0.94	0.72	1.30	2.55	>tr|F4IVJ8|F4IVJ8_ARATH ARM repeat superfamily protein
1.22	1.59	0.95	0.72	1.31	2.23	>sp|Q8L5Y6|CAND1_ARATH Cullin-associated NEDD8-dissociated protein 1

B

Biological process overrepresentation of differentially-regulated nuclear proteins

IAA up-regulated processes	Term	P-Value	Fold Enrichment	Proteins
	response to cadmium ion	3.86E-12	11.42	Q05431, P54609, P25858, P25696, Q9LDZ0, P20115, Q05758, O50008, Q9LFW1, Q38882,

				Q9SA73, O04499, P93819, Q94KE3, Q9SYT0, Q944G9
	response to osmotic stress	8.14E-08	7.60	P93033, Q08682, Q05431, P25858, P25696, Q9LDZ0, O50008, Q9LFW1, Q43127, O65390, P93819, Q9SYT0, Q9SRT9
	ribosome biogenesis	7.37E-06	8.68	Q08682, Q9LD90, Q9MAB3, Q9C912, Q9S826, P51420, Q9FEF8, Q94AH9, Q9SH88
	generation of precursor metabolites and energy	4.45E-05	5.77	P93033, O04499, P93819, Q94KE3, P25858, Q944G9, O82663, P25696, P20115, Q39161
	nucleosome organization	2.01E-04	16.91	P59169, Q9FJE8, Q9SI96
	RNA processing	0.002285	4.28	Q8L3X8, Q9LD90, Q9S826, Q9LXT5, O81126, Q9FEF8, Q9S709, Q94AH9
IAA down-regulated processes	ubiquitin-dependent protein catabolic process	1.06E-05	8.21	Q93Y35, Q9LNU4, Q9LP45, Q9LT08, Q9SSB5, Q9SEI2, Q9SGW3, Q9FIB6, Q9SEI4
	response to salt stress	1.04E-05	6.90	Q9C8Y9, A8MRW1, Q9STX5, Q9LT08, P29512, Q9LSB4, Q9C5Z3, O04309, Q9SRT9
	translational initiation	0.033057	10.32	P56820, Q9C5Z2, Q9M060
	macromolecular complex assembly	0.003764	5.66	P29512, Q9C5Z3, Q9SGW3, Q9M060, O82533
	embryonic development ending in seed dormancy	0.014057	4.10	Q9C5J8, Q9LNU4, O23247, Q9SGW3, Q9FIB6, Q9M060
	photosynthesis, light harvesting	0.006728	23.86	Q9S7M0, Q9LMQ2, Q39141
	response to cadmium ion	0.037089	3.89	Q9STX5, Q9LP45, P29512, P93014
	glycolysis	0.037253	9.66	Q9SN86, Q5M729, Q9SAJ6

	Term	P-Value	Fold Enrichment	Proteins
OG up-regulated process	response to osmotic stress	1.95E-05	11.16	Q9C8Y9, Q93ZY3, Q9C525, P31168, Q9FJA6, Q9LHG9, Q9M651
OG down-regulated process	translation	0.004145	2.62	Q9ASV6, P92959, P16180, P59232, Q9SKX4, Q9LI88, P42791, O48549, Q93VC7, P56792, P93014, O23049
	response to cadmium ion	2.30E-07	9.06	P42643, Q94A28, O24456, Q9SMT7, Q9SPK5, P46422, P93014, Q8GUM2,

				O23254, Q9FXA2, P31265
	response to abiotic stimulus	2.68E-04	3.15	Q96266, P59232, P46422, Q9SH69, P42804, P93014, Q9SK66, Q8GUM2, P93025, Q9ASR1, Q682S0, P10797, O64644, P10795
	response to abiotic stimulus	2.68E-04	3.15	Q96266, P59232, P46422, Q9SH69, P42804, P93014, Q9SK66, Q8GUM2, P93025, Q9ASR1, Q682S0, P10797, O64644, P10795
	photorespiration	0.01021	19.23	Q9FGI6, P10797, P10795
	oxidative phosphorylation	3.17E-04	14.96	Q9SDS7, P92549, P19366, Q9FGI6, Q9LXJ2
	embryonic development ending in seed dormancy	0.046126	3.62	Q8L7S8, Q9FGI6, O23049, O23676, O23255
	Term	P-Value	Fold Enrichment	Proteins
IAA and OG up-regulated processes	RNA processing	7.01E-25	10.50	Q9SSD2, Q9M0I7, Q9LD90, Q9SUN5, O80653, Q9ZT71, Q93YS7, O22212, Q9FMF9, Q9LYK7, Q9LK52, Q94BR4, Q9FVQ1, P43333, Q9FMP4, Q93XX8, O22922, Q9FEF8, Q9M033, Q8RXF1, O22785, Q9LKU3, Q9LF27, Q9S826, Q9FJY5, Q9LEY9, O82266, Q9SUM2, Q9FG73, Q9LXT5, Q8VZT0, Q9LFE2, Q94AH9, Q9LVF2
	mRNA processing	1.78E-11	13.96	O22785, Q9SSD2, Q9SUN5, O80653, Q9ZT71, O22212, Q9FMF9, Q94BR4, Q9LK52, P43333, Q9FMP4, Q9SUM2, O22922, Q8RXF1
	chromosome organization	5.86E-09	7.83	Q8VY05, Q9LZR5, Q9FMT4, Q9C944, Q9LSK7, Q4V3D1, Q9SD34, Q9FVE6, Q84M92, Q6EVK6, Q9S775, Q8RVQ9, Q56YN8, O22467, A8MS85
	chromatin assembly or disassembly	6.23E-05	10.13	Q9S775, Q8RVQ9, Q9C944, O22467, Q9LSK7, A8MS85, Q4V3D1
	root system development	9.78E-05	6.18	Q42384, Q9FG73, Q9S775, Q9FVQ1, Q9FMT4, Q9LFE0, P53492, Q9LPD9, Q8LBI1
	cell proliferation	1.08E-04	19.79	Q9FG73, Q9S775, Q9LYK7, O22467, Q8LBI1
	hydrogen peroxide catabolic process	4.03E-04	9.50	Q93V93, Q43729, Q96511, Q9SY33, Q96522, Q9LHB9
	defense response signaling pathway, resistance gene-independent	0.002824	36.71	Q42384, P92948, Q949S9
	megagametogenesis	0.003607	12.82	O22212, O82266, O49485, Q93XX8
	defense response to bacterium	0.011545	4.39	O22785, Q42384, Q94BR4, P92948, Q9C944, Q949S9
	embryonic development ending in seed dormancy	0.019876	2.89	Q42384, Q9ZU66, P17094, Q9SYP1, Q9LFE2, Q9LNC5, O22467, Q9M060

	DNA metabolic process	0.044416	2.69	O22785, Q9FGF4, Q6WWW4, Q94BR4, Q9C587, O22467, Q9LPD9

	Term	P-Value	Fold Enrichment	Proteins
IAA and OG down-regulated processes	generation of precursor metabolites and energy	7.00E-22	6.00	P56778, Q9LX65, Q9S7W1, P09468, P04778, Q8W4M5, P25856, Q39102, Q9LMQ2, P56759, Q9FLQ4, P25857, Q39141, P56757, Q9SAJ4, Q9SIB9, P27521, Q96251, P93303, Q9LXS6, Q9XGM1, Q9SY97, Q9SYW8, Q9C9K3, Q07473, Q9XF88, Q39258, Q9XF89, Q9XF87, P19366, P50318, Q01667, Q9SN86, Q9SUI4, Q96250, Q2V3P9, Q01908, Q9SYP2, Q8RWN9, Q9FLX7, Q95748, Q9LD57
	response to cadmium ion	5.96E-20	6.42	Q9ZSK4, Q9SZD4, O49299, Q8W4M5, P25857, Q9FNX5, Q9SIB9, Q38884, P23686, Q9SF16, Q9S7E4, P29515, Q8RWV0, P29517, Q93VP3, Q9STX5, P54609, Q9S7Z3, Q9FFR3, O22173, P50318, P42760, Q9LV03, Q9LV21, O80576, Q03250, Q9M888, P49040, Q9SPK5, P48349, Q9FVT2, O82660, Q42547, Q9LIK9, P92947, Q38950, O23254, P46643, Q9LD57
	proton transport	1.11E-12	11.44	Q9LX65, P09468, Q39258, P56759, Q9SJ12, P19366, P56757, P19456, Q96251, Q96250, P20649, O82628, P93303, Q2V3P9, Q01908, Q9XGM1
	response to cold	2.21E-09	5.08	Q9LUT2, Q9STX5, Q9SA52, Q39258, Q96266, P21240, P25856, P25857, Q9LZ72, P46310, Q570B4, Q9SN86, Q9ZUU4, P10896, Q03250, P49040, P29514, P25819, Q42547, P92947, Q9SKR2, Q9LD57
	glucose metabolic process	2.23E-07	6.50	Q9FY99, Q9FFR3, O49299, P25856, Q8W4M5, P25857, P50318, Q9SAJ4, Q9SN86, Q9SYP2, Q9FWA3, Q8RWN9, Q9C9K3, Q9LD57
	intracellular transport	3.63E-07	3.39	Q8LPR9, Q8W498, Q9SFU0, Q9C5M0, O23680, Q9FI56, O22715, Q9SKR2, Q93XM7, P93042, O04209, Q9FJD4, Q0WNJ6, Q9FXD4, Q9SXJ7, O22265, Q9SE83, Q03250, Q9ZPY7, O81283, Q0WLB5, O81845, P37107, Q38820, Q94A40
	cofactor metabolic process	4.49E-06	3.67	Q9SQI8, Q9FFR3, Q9FY99, Q8L940, Q9FLQ4, Q9M591, O49543, Q9M7Z1, Q9FNB0, Q9SIB9, Q9SN86, Q9LY74, P21218, P16127, Q9LXS6, Q9SPK5, Q9SJE1, Q9CA67, Q9FWA3
	S-adenosylmethionine biosynthetic process	2.47E-05	53.84	Q9LUT2, P23686, P17562, Q9SJL8
	carboxylic acid biosynthetic process	7.37E-05	2.77	Q9LUT2, P52410, O81852, Q93VR3, P56765, P17562, Q42601, Q9LZ72, P46310, Q56WD9, Q570B4, P46312, Q9LV03, Q38970, P23686, Q9LMM0, Q9SJL8, Q9LV77, P29976, Q9LX13, Q9CAP8
	cellular protein complex assembly	1.01E-04	4.78	Q9FJD4, Q9SZD4, Q9ZPY7, P29514, Q8W498, P37107, P29513, P24636, P29515, P29517, O82533

	carbohydrate biosynthetic process	2.76E-04	3.18	P48421, Q9LMI0, Q941L0, O48946, P25856, Q9LXL5, P25857, Q944K2, P50318, P49040, O80891, Q9SYM5, P94040, Q9FWA4, Q9SRT9
	translational initiation	4.28E-04	5.82	Q93VP3, Q93ZT6, Q9ZUG4, O49160, P42731, Q9SHI1, O04202, Q9LD55
	protein import	6.89E-04	5.38	Q8LPR9, Q9FJD4, O22265, Q9FI56, Q9ZPY7, Q8W498, P37107, Q9SXJ7
	defense response to bacterium	0.002249	3.22	Q9SCX3, P10896, Q93VP3, Q9SA52, Q39258, Q9S7Z3, Q96266, O80852, P48349, P42760, Q9XIE2
	cellular amino acid derivative biosynthetic process	0.003294	3.05	Q9FR44, Q9LUT2, P92994, Q9FK25, Q03250, P23686, Q9S7Z3, P17562, Q9SJL8, Q9SYM5, Q41931
	coenzyme metabolic process	0.003417	3.04	Q9SQI8, Q9FFR3, Q9FY99, Q9LXS6, Q9SPK5, Q9FLQ4, Q9M7Z1, Q9FWA3, Q9SIB9, Q9LY74, Q9SN86
	protein folding	0.007085	2.57	P55737, Q9LV21, Q9STX5, Q9M888, P21240, O04450, Q940P8, Q9SF16, Q8L7N0, Q9SIF2, P28769, Q0WT48
	glycoside metabolic process	0.019716	3.85	Q9LMI0, P48421, P49040, Q9S7Z3, Q9LXL5, Q9XIE2
	embryonic development ending in seed dormancy	0.021318	2.03	Q93VS8, Q9C5J8, Q8L7S8, Q8LPR8, Q39258, A8MPR5, Q9SAJ3, P42697, Q9C8P0, O80576, Q38970, Q9SIE1, O23247, Q9SIF2
	reductive pentose-phosphate cycle	0.026804	11.54	P25856, P25857, P50318
	response to sucrose stimulus	0.028533	5.98	Q9FFR3, Q9SYP2, P25856, P25857
	translation	0.0311	1.44	Q9CAV0, P42731, Q9SHI1, P42732, Q9ZT91, Q9SI75, Q9LY66, Q9LPV8, Q38884, Q9SCX3, P36210, Q9T029, Q93ZT6, P92959, O23247, P56795, P56805, P56798, Q93VP3, P25864, Q76E23, O82462, Q9ZUG4, Q8L6Z4, O04202, P51419, O04487, Q9FY50, P17745, O49160, Q9FVT2, O48549, Q9LD55
	vesicle-mediated transport	0.043867	2.04	Q9ZNT0, O04209, Q9SE83, Q0WNJ6, Q8RVQ5, Q0WLB5, O22715, Q9FNX5, Q9SFU0, Q94A40, P93042

	Term	PValue	Fold Enrichment	Proteins
IAA + OG up-regulated processes	response to salt stress	1.39E-04	10.84	Q9C525, Q9ZP06, Q8H1Y0, Q9SRZ6, Q9LF98, Q9SIP7
	translation	0.001112	4.33	P49688, Q9FZ76, Q9LUQ6, P51430, P61847, O22860, Q9SIP7
	defense response to bacterium	0.00216	14.49	Q9ZP06, Q42139, O22832, Q96291
IAA + OG down-regulated processes	photosynthesis	4.59E-10	27.69	P56761, P56777, P56767, P56771, Q9LMQ2, P83755, Q9SUI7, Q9S831, P10795
	response to abiotic stimulus	1.37E-04	4.50	O49377, P29510, Q8L940, Q9LMQ2, P42763, Q84JU6, P92947, Q9ZU25, P10795
	oxidation reduction	0.003794	3.63	P56761, P56777, P56767, P56771, P83755, P92947, Q9ZU25, P10795
	oxidation reduction	0,003794	3,63	P56761, P56777, P56767, P56771, P83755, P92947, Q9ZU25, P10795

6 References

Adie B, Chico JM, Rubio-Somoza I, Solano R (2007) Modulation of plant defenses by ethylene. Journal of Plant Growth Regulation 26: 160-177

Agrios GN (1997) Plant pathology. Academic Press, San Diego, CA, USA

Akira S, Uematsu S, Takeuchi O (2006) Pathogen recognition and innate immunity. Cell 124: 783-801

Allan AC, Fluhr R (1997) Two distinct sources of elicited reactive oxygen species in tobacco epidermal cells. Plant Cell 9: 1559-1572

Altamura MM, Zaghi D, Salvi G, De Lorenzo G, Bellincampi D (1998) Oligogalacturonides stimulate pericycle cell wall thickening and cell divisions leading to stoma formation in tobacco leaf explants. Planta 204: 429-436

Apel K, Hirt H (2004) REACTIVE OXYGEN SPECIES: Metabolism, Oxidative Stress, and Signal Transduction. Annu Rev Plant Biol 55: 373-399

Asai T, Tena G, Plotnikova J, Willmann MR, Chiu WL, Gomez-Gomez L, Boller T, Ausubel FM, Sheen J (2002) MAP kinase signalling cascade in Arabidopsis innate immunity. Nature 415: 977-983

Asiegbu FO, Daniel G, Johansson M (1994) Defense-related reactions of seedling roots of Norway spruce to infection by *Heterobasidion annosum* (Fr.) Bref. Physiol Mol Plant Pathol 45: 1-19

Ausubel FM (2005) Are innate immune signaling pathways in plants and animals conserved? Nat Immunol 6: 973-979

Aziz A, Heyraud A, Lambert B (2004) Oligogalacturonide signal transduction, induction of defense-related responses and protection of grapevine against Botrytis cinerea. Planta 218: 767-774

Balbi V, Devoto A (2008) Jasmonate signalling network in Arabidopsis thaliana: crucial regulatory nodes and new physiological scenarios. New Phytol 177: 301-318

Beckers GJ, Spoel SH (2006) Fine-Tuning Plant Defence Signalling: Salicylate versus Jasmonate. Plant Biol (Stuttg) 8: 1-10

Bellincampi D, Salvi G, De Lorenzo G, Cervone F, Marfà V, Eberhard S, Darvill A, Albersheim P (1993) Oligogalacturonides inhibit the formation of roots on tobacco explants. Plant J 4: 207-213

Benedetti M, Pontiggia D, Raggi S, Cheng Z, Scaloni F, Ferrari S, Ausubel FM, Cervone F, De Lorenzo G (2015) Plant immunity triggered by engineered in vivo release of oligogalacturonides, damage-associated molecular patterns. Proc Natl Acad Sci U S A

Benschop JJ, Mohammed S, O'Flaherty M, Heck AJ, Slijper M, Menke FL (2007) Quantitative phosphoproteomics of early elicitor signaling in Arabidopsis. Mol Cell Proteomics 6: 1198-1214

Bilgin DD, Zavala JA, Zhu J, Clough SJ, Ort DR, DeLucia EH (2010) Biotic stress globally downregulates photosynthesis genes. Plant Cell and Environment 33: 1597-1613

Binet MN, Bourque S, Lebrun-Garcia A, Chiltz A, Pugin A (1998) Comparison of the effects of cryptogein and oligogalacturonides on tobacco cells and evidence of different form of desensitization induced by these elicitors. Plant Sci 137: 33-41

Bishop PD, Makus DJ, Pearce G, Ryan CA (1981) Proteinase inhibitor-inducing factor activity in tomato leaves resides in oligosaccharides enzymically released from cell walls. Proc Natl Acad Sci U S A 78: 3536-3540

Blume B, Nurnberger T, Nass N, Scheel D (2000) Receptor-mediated increase in cytoplasmic free calcium required for activation of pathogen defense in parsley [In Process Citation]. Plant Cell 12: 1425-1440

Boersema PJ, Raijmakers R, Lemeer S, Mohammed S, Heck AJ (2009) Multiplex peptide stable isotope dimethyl labeling for quantitative proteomics. Nat Protoc 4: 484-494

Boller T (1995) Chemoperception of microbial signals in plant cells. Annu Rev Plant Physiol Plant Mol Biol 46: 189-214

Boller T, Felix G (2009) A renaissance of elicitors: perception of microbe-associated molecular patterns and danger signals by pattern-recognition receptors. Annu Rev Plant Biol 60: 379-406

Bolwell GP, Blee KA, Butt VS, Davies DR, Gardner SL, Gerrish C, Minibayeva F, Rowntree EG, Wojtaszek P (1999) Recent advances in understanding the origin of the apoplastic oxidative burst in plant cells. Free Radic Res 31 Suppl: S137-S145

Bolwell GP, Buti VS, Davies DR, Zimmerlin A (1995) The origin of the oxidative burst in plants. Free Radic Res 23: 517-532

Bondarenko PV, Chelius D, Shaler TA (2002) Identification and Relative Quantitation of Protein Mixtures by Enzymatic Digestion Followed by Capillary Reversed-Phase Liquid Chromatography-Tandem Mass Spectrometry. Anal Chem

Boudsocq M, Willmann MR, McCormack M, Lee H, Shan L, He P, Bush J, Cheng SH, Sheen J (2010) Differential innate immune signalling via Ca^{2+} sensor protein kinases. Nature 464: 418-422

Bradford MM (1976) A rapid and sensitive method for the quantitation of microgram quantities of protein utilizing the principle of protein-dye binding. Anal Biochem 72: 248-254

Branca C, De Lorenzo G, Cervone F (1988) Competitive inhibition of the auxin-induced elongation by α-D-oligogalacturonides in pea stem segments. Physiol Plant 72: 499-504

Broekaert WF, Delaure SL, De Bolle MF, Cammue BP (2006) The role of ethylene in host-pathogen interactions. Annu Rev Phytopathol 44: 393-416

Broekaert WF, Pneumas WJ (1988) Pectic polysaccharides elicit chitinase accumulation in tobacco. Physiol Plant 74: 740-744

Brunner F, et al. (2002) Pep-13, a plant defenseinducing pathogen-associated pattern from Phytophthora transglutaminases . EMBO J 21: 6681-6688

Calikowski T, Meier I (2007) Isolation of nuclear proteins. Methods in Molecular Biology

Chen Z, Agnew JL, Cohen JD, He P, Shan L, Sheen J, Kunkel BN (2007) Pseudomonas syringae type III effector AvrRpt2 alters Arabidopsis thaliana auxin physiology. Proc Natl Acad Sci U S A 104: 20131-20136

Chinchilla D, Zipfel C, Robatzek S, Kemmerling B, Nurnberger T, Jones JD, Felix G, Boller T (2007) A flagellin-induced complex of the receptor FLS2 and BAK1 initiates plant defence. Nature 448: 497-500

Chisholm ST, Coaker G, Day B, Staskawicz BJ (2006) Host-microbe interactions: shaping the evolution of the plant immune response. Cell 124: 803-814

Clough SJ, Bent AF (1998) Floral dip: a simplified method for Agrobacterium-mediated transformation of Arabidopsis thaliana. Plant J 16: 735-43

Cote F, Hahn MG (1994) Oligosaccharins: structures and signal transduction. Plant Mol Biol 26: 1379-1411

Cote F, Ham KS, Hahn MG, Bergmann CW (1998) Oligosaccharide elicitors in host-pathogen interactions. Generation, perception, and signal transduction. Subcell Biochem 29: 385-432

Cox J, Hein M, Luber C, Paron I, Nagaraj N, Mann M (2014) MaxLFQ allows accurate proteome-wide label-free quantification by delayed normalization and maximal peptide ratio extraction. Molecular and Cellular Proteomics

Cui J, Bahrami AK, Pringle EG, Hernandez-Guzman G, Bender CL, Pierce NE, Ausubel FM (2005) Pseudomonas syringae manipulates systemic plant defenses against pathogens and herbivores. Proc Natl Acad Sci U S A 102: 1791-1796

Dangl JL, Jones JD (2001) Plant pathogens and integrated defence responses to infection. Nature 411: 826-833

Davis KR, Darvill AG, Albersheim P, Dell A (1986) Host-pathogen interactions. XXIX. Oligogalacturonides released from sodium polypectate by endopolygalacturonic acid lyase are elicitors of phytoalexins in soybean. Plant Physiol 80: 568-577

Davis KR, Hahlbrock K (1987) Induction of defense responses in cultured parsley cells by plant cell wall fragments. Plant Physiol 85: 1286-1290

De Lorenzo G, D'Ovidio R, Cervone F (2001) The role of polygacturonase-inhibiting proteins (PGIPs) in defense against pathogenic fungi. Annu Rev Phytopathol 39: 313-335

De Lorenzo G, Ferrari S (2002) Polygalacturonase-inhibiting proteins in defense against phytopathogenic fungi. Curr Opin Plant Biol 5: 295-299

Denoux C, Galletti R, Mammarella N, Gopalan S, Werck D, De Lorenzo G, Ferrari S, Ausubel FM, Dewdney J (2008) Activation of defense response pathways by OGs and Flg22 elicitors in Arabidopsis seedlings. Mol Plant 1: 423-445

Desiderio A, Aracri B, Leckie F, Mattei B, Salvi G, Tigelaar H, Van Roekel JS, Baulcombe DC, Melchers LS, De Lorenzo G and others (1997) Polygalacturonase-inhibiting proteins (PGIPs) with different specificities are expressed in *Phaseolus vulgaris*. Mol Plant-Microbe Interact 10: 852-60

Després C, Chubak C, Rochon A, Clark R, Bethune T, Desveaux D, Fobert PR (2003) The Arabidopsis NPR1 disease resistance protein is a novel cofactor that confers redox regulation of DNA binding activity to the basic domain/leucine zipper transcription factor TGA1. Plant Cell

Dharmasiri N, Dharmasiri S, Estelle M (2005) The F-box protein TIR1 is an auxin receptor. Nature 435: 441-445

Dittrich H, Kutchan TM (1991) Molecular cloning, expression, and induction of berberine bridge enzyme, an enzyme essential to the formation of benzophenanthridine alkaloids in the response of plants to pathogenic attack. Proc Natl Acad Sci U S A 88: 9969-9973

Dodds PN, Rathjen JP (2010) Plant immunity: towards an integrated view of plant-pathogen interactions. Nat Rev Genet 11: 539-548

Dumas B, Sailland A, Cheviet JP, Freyssinet G, Pallett K (1993) Identification of barley oxalate oxidase as a germin-like protein. C R Acad Sci III 316: 793-798

Eberhard S, Doubrava N, Marfà V, Mohnen D, Southwick A, Darvill A, Albersheim P (1989) Pectic cell wall fragments regulate tobacco thin-cell-layer explant morphogenesis. Plant Cell 1: 747-755

Eulgem T, Somssich IE (2007) Networks of WRKY transcription factors in defense signaling. Curr Opin Plant Biol 10: 366-371

Felix G, Boller T (2003) Molecular sensing of bacteria in plants. The highly conserved RNAbinding motif RNP-1 of bacterial cold shock proteins is recognized as an elicitor signal in tobacco. J Biol Chem 278: 6201-6208

Felix G, Duran JD, Volko S, Boller T (1999) Plants have a sensitive perception system for the most conserved domain of bacterial flagellin. Plant J 18: 265-276

Fellbrich G, Romanski A, Varet A, Blume B, Brunner F, Engelhardt S, Felix G, Kemmerling B, Krzymowska M, Nurnberger T (2002) NPP1, a Phytopthora-associated trigger of plant defense in parsley and Arabidopsis. Plant J 32: 375-390

Ferrari S, Galletti R, Denoux C, De Lorenzo G, Ausubel FM, Dewdney J (2007) Resistance to *Botrytis cinerea* induced in Arabidopsis by elicitors is independent of salicylic acid, ethylene, or jasmonate signaling but requires PHYTOALEXIN DEFICIENT3. Plant Physiol 144: 367-379

Ferrari S, Galletti R, Vairo D, Cervone F, De Lorenzo G (2006) Antisense expression of the *Arabidopsis thaliana AtPGIP1* gene reduces polygalacturonase-inhibiting protein accumulation and enhances susceptibility to *Botrytis cinerea*. Mol Plant Microbe Interact 19: 931-936

Ferrari S, Savatin DV, Sicilia F, Gramegna G, Cervone F, De Lorenzo G (2013) Oligogalacturonides: plant damage-associated molecular patterns and regulators of growth and development. Front Plant Sci 4: 49. doi: 10.3389/fpls.2013.00049

Folta K, Kaufman LS (2007) Isolation of Arabidopsis nuclei and measurement of gene transcription rates using nuclear run-on assays. Nature Methods

Frahry G, Schopfer P (1998) Hydrogen peroxide production by roots and its stimulation by exogenous NADH. Physiol Plant 103: 395-404

Galletti R, De Lorenzo G, Ferrari S (2009) Host-derived signals activate plant innate immunity. Plant Signal Behav 4: 33-34

Galletti R, Denoux C, Gambetta S, Dewdney J, Ausubel FM, De Lorenzo G, Ferrari S (2008) The AtrbohD-mediated oxidative burst elicited by oligogalacturonides in Arabidopsis is dispensable for the activation of defense responses effective against *Botrytis cinerea*. Plant Physiol 148: 1695-1706

Galletti R, Ferrari S, De Lorenzo G (2011) Arabidopsis MPK3 and MPK6 play different roles in basal and oligogalacturonide- or flagellin-induced resistance against *Botrytis cinerea*. Plant Physiol 157: 804-814

Geldner N, Friml J, Stierhof YD, Jurgens G, Palmer K (2001) Auxin transport inhibitors block PIN1 cycling and vesicle trafficking. Nature

Gilchrist A, Au CE, Hiding J, Bell AW, Fernandez-Rodriguez J, Lesimple S, Nagaya H, Roy L, Gosline SJ, Hallet M and others (2006) Quantitative Proteomics Analysis of the Secretory Pathway. Cell

Glazebrook J (2005) Contrasting mechanisms of defense against biotrophic and necrotrophic pathogens. Annu Rev Phytopathol 43: 205-227

Gobom J, Nordhoff E, Mirgorodskaya E, Ekman R, Roepstorff P (1999) Sample purification and prepartion technique based on nano-scale reversed-phase columns for the sensitive analysis of complex peptide mixtures by matrix-assisted laser desorption/ionization mass spectrometry. J Mass Spectrom 34: 105-116

Gomez-Gomez L (2004) Plant perception systems for pathogen recognition and defence. Mol Immunol 41: 1055-1062

Gomez-Gomez L, Boller T (2002) Flagellin perception: a paradigm for innate immunity. Trends Plant Sci 7: 251-256

Gomez-Gomez L, Felix G, Boller T (1999) A single locus determines sensitivity to bacterial flagellin in *Arabidopsis thaliana*. Plant J 18: 277-284

Gonzalez-Camacho F, Medina FJ (2007) Extraction of nuclear proteins from root meristematic cells. Methods in Molecular Biology

Grant M, Lamb C (2006) Systemic immunity. Curr Opin Plant Biol 9: 414-420

Hahn MG (1981) Fragments of plant and fungal cell wall polysaccharides elicit the accumulation of phytoalexins in plants. Ph.D. Thesis, University of Colorado, Boulder, CO

Hardtke CS, Ckurshumova W, Vidaurre DP, Singh SA, Hagen G, Guilfoyle TJ, Berleth T (2004) Overlapping and non-redundant functions of the Arabidopsis auxin response factors MONOPTEROS and NONPHOTOTROPIC HYPOCOTYL 4. Development

Hsieh WP, Hsieh HL, Wu SH (2012) Arabidopsis bZIP16 Transcription Factor Integrates Light and Hormone Signaling Pathways to Regulate Early Seedling Development. Plant Cell

Huang dW, Sherman BT, Lempicki RA (2009) Systematic and integrative analysis of large gene lists using DAVID bioinformatics resources. Nat Protoc

Huffaker A, Pearce G, Ryan CA (2006) An endogenous peptide signal in Arabidopsis activates components of the innate immune response. Proc Natl Acad Sci U S A 103:

Jakoby M, Weisshaar B, Droge-Laser W, Vicente-Carbajosa J, Tiedemann J, Kroy T, Parcy F (2002) bZIP transcription factors in Arabidopsis. Trends Plant Sci

Jefferson RA, Kavanagh TA, Bevan MW (1987) GUS fusions: β-glucuronidase as a sensitive and versatile gene fusion marker in higher plants. EMBO J 6: 3901-3907

Jones JD, Dangl JL (2006) The plant immune system. Nature 444: 323-329

Jung C, Lyou SH, Yeu S, Kim MA, Rhee S, Kim M, Lee JS, Do Choi Y, Cheong JJ (2007) Microarray-based screening of jasmonate-responsive genes in Arabidopsis thaliana. Plant Cell Rep 26: 1053-1063

Kazan K (2013) Auxin and the integration of environmental signals into plant root development. Ann Bot 112: 1655-1665

Kunze G, Zipfel C, Robatzek S, Niehaus K, Boller T, Felix G (2004) The N Terminus of bacterial elongation factor Tu elicits innate immunity in Arabidopsis plants. Plant Cell 16: 3496-3507

Lamb C, Dixon RA (1997) The oxidative burst in plant disease resistance. Annu Rev Plant Physiol Plant Mol Biol 48: 251-275

Landschulz WH, Johnson PF, McKnight SL (1988) The leucine zipper: a hypotetical structure common to new DNA binding proteins. Science 240: 1795-1764

Laurie-Berry N, Joardar V, Street IH, Kunkel BN (2006) The Arabidopsis thaliana JASMONATE INSENSITIVE 1 gene is required for suppression of salicylic acid-dependent defenses during infection by Pseudomonas syringae. Mol Plant Microbe Interact 19: 789-800

Lecourieux D, Mazars C, Pauly N, Ranjeva R, Pugin A (2002) Analysis and effects of cytosolic free calcium increases in response to elicitors in Nicotiana plumbaginifolia cells. Plant Cell 14: 2627-2641

Lee S, Choi H, Suh S, Doo IS, Oh KY, Choi EJ, Schroeder Taylor AT, Low PS, Lee Y (1999) Oligogalacturonic acid and chitosan reduce stomatal aperture by inducing the evolution of reactive oxygen species from guard cells of tomato and Commelina communis. Plant Physiol 121: 147-152

Legendre L, Rueter S, Heinstein PF, Low PS (1993) Characterization of the oligogalacturonide-induced oxidative burst in cultured soybean (*Glycine max*) cells. Plant Physiol 102: 233-240

Leyser O (2006) Dynamic integration of auxin transport and signalling. Curr Biol 16: R424-R433

Lorenzo O, Piqueras R, Sanchez-Serrano JJ, Solano R (2003) ETHYLENE RESPONSE FACTOR1 integrates signals from ethylene and jasmonate pathways in plant defense. Plant Cell 15: 165-178

Lorenzo O, Solano R (2005) Molecular players regulating the jasmonate signalling network. Curr Opin Plant Biol 8: 532-540

Lotze MT, Zeh HJ, Rubartelli A, Sparvero LJ, Amoscato AA, Washburn NR, Devera ME, Liang X, Tor M, Billiar T (2007) The grateful dead: damage-associated molecular pattern molecules and reduction/oxidation regulate immunity. Immunol Rev 220: 60-81

Low PS, Merida JR (1996) The oxidative burst in plant defense: Function and signal transduction. Physiol Plant 96: 533-542

Matzinger P (2002) The danger model: a renewed sense of self. Science 296: 301-305

McGrath KC, Dombrecht B, Manners JM, Schenk PM, Edgar CI, Maclean DJ, Scheible WR, Udvardi MK, Kazan K (2005) Repressor- and activator-type ethylene response factors functioning in jasmonate signaling and disease resistance identified via a genome-wide screen of Arabidopsis transcription factor gene expression. Plant Physiol 139: 949-959

Medzhitov R, Janeway CA, Jr. (1997) Innate immunity: the virtues of a nonclonal system of recognition. Cell 91: 295-298

Melotto M, Underwood W, Koczan J, Nomura K, He SY (2006) Plant stomata function in innate immunity against bacterial invasion. Cell 126: 969-980

Moerschbacher BM, Mierau M, Graeßner B, Noll U, Mor AJ (1999) Small oligomers of galacturonic acid are endogenous suppressors of disease resistance reactions in wheat leaves. J Exp Bot 50: 605-612

Mohnen D, Eberhard S, Marfà V, Doubrava N, Toubart P, Gollin DJ, Gruber TA, Nuri W, Albersheim P, Darvill A (1990) The control of root, vegetative shoot and flower morphogenesis in tobacco thin cell-layer explants (TCLs). Development 108: 191-201

Mur LA, Kenton P, Atzorn R, Miersch O, Wasternack C (2006) The outcomes of concentration-specific interactions between salicylate and jasmonate signaling include synergy, antagonism, and oxidative stress leading to cell death. Plant Physiol 140: 249-262

Navarro L, Zipfel C, Rowland O, Keller I, Robatzek S, Boller T, Jones JD (2004) The transcriptional innate immune response to flg22. Interplay and overlap with Avr gene-dependent defense responses and bacterial pathogenesis. Plant Physiol 135: 1113-1128

Navarro L, Dunoyer P, Jay F, Arnold B, Dharmasiri N, Estelle M, Voinnet O, Jones JD (2006) A plant miRNA contributes to antibacterial resistance by repressing auxin signaling. Science 312: 436-439

Neill S, Bright J, Desikan R, Hancock J, Harrison J, Wilson I (2008) Nitric oxide evolution and perception. J Exp Bot 59: 25-35

Nishimura T, Wada T, Yamamoto KT, Okada K (2005) The Arabidopsis STV1 Protein, Responsible for Translation Reinitiation, Is Required for Auxin-Mediated Gynoecium Patterning. Plant Cell

Nuhse TS, Bottrill AR, Jones AM, Peck SC (2007) Quantitative phosphoproteomic analysis of plasma membrane proteins reveals regulatory mechanisms of plant innate immune responses. Plant J 51: 931-940

Nuhse TS, Peck SC, Hirt H, Boller T (2000) Microbial elicitors induce activation and dual phosphorylation of the Arabidopsis thaliana MAPK 6. J Biol Chem 275: 7521-7526

Nurnberger T, Brunner F, Kemmerling B, Piater L (2004) Innate immunity in plants and animals: striking similarities and obvious differences. Immunol Rev 198: 249-266

Nurnberger T, Kemmerling B (2006) Receptor protein kinases--pattern recognition receptors in plant immunity. Trends Plant Sci 11: 519-522

Nurnberger T, Lipka V (2005) Non-host resistance in plants: new insights into an old phenomenon. Mol Plant Pathol 6: 335-345

Nurnberger T, Nennstiel D, Jabs T, Sacks WR, Hahlbrock K, Scheel D (1994) High affinity binding of a fungal oligopeptide elicitor to parsley plasma membranes triggers multiple defense responses. Cell 78: 449-460

O'Donnell PJ, Schmelz EA, Moussatche P, Lund ST, Jones JB, Klee HJ (2003) Susceptible to intolerance--a range of hormonal actions in a susceptible Arabidopsis pathogen response. Plant J 33: 245-257

Park SW, Kaimoyo E, Kumar D, Mosher S, Klessig DF (2007) Methyl salicylate is a critical mobile signal for plant systemic acquired resistance. Science 318: 113-116

Parry G, Estelle M (2006) Auxin receptors: a new role for F-box proteins. Curr Opin Cell Biol 18: 152-156

Peck SC, Nuhse TS, Hess D, Iglesias A, Meins F, Boller T (2001) Directed proteomics identifies a plant-specific protein rapidly phosphorylated in response to bacterial and fungal elicitors. Plant Cell 13: 1467-1475

Pedley KF, Martin GB (2005) Role of mitogen-activated protein kinases in plant immunity. Curr Opin Plant Biol 8: 541-547

Penninckx IAMA, Thomma BPHJ, Buchala A, Métraux JP, Broekaert WF (1998) Concomitant activation of jasmonate and ethylene response pathways is required for induction of a plant defensin gene in Arabidopsis. Plant Cell 10: 2103-2113

Pfaffl MW (2001) A new mathematical model for relative quantification in real-time RT-PCR. Nucleic Acids Res 29: e45

Ramonell KM, Zhang B, Erwing RM, Chen Y, Xu D, Stacey G, Somerville S (2002) Microarray analysis of chitin elicitation in *Arabidopsis thaliana*. Mol Plant Pathol 3: 301-311

Rasul S, Dubreuil-Maurizi C, Lamotte O, Koen E, Poinssot B, Alcaraz G, Wendehenne D, Jeandroz S (2012) Nitric oxide production mediates oligogalacturonide-triggered immunity and resistance to *Botrytis cinerea* in *Arabidopsis thaliana*. Plant Cell Environ 35: 1483-1499

Reymond P, Kunz B, Paul-Pletzer K, Grimm R, Eckerskorn C, Farmer EE (1996) Cloning of a cDNA encoding a plasma membrane-associated, uronide binding phosphoprotein with physical properties similar to viral movement proteins. Plant Cell 8: 2265-2276

Riechmann JL, Heard J, Martin G, Reuber L, Jiang C, Keddie J, Adam L, Sherman BK, Yu G (2000) Arabidopsis transcription factors: genome-wide comparative analysis among eukaryotes. Science

Robatzek S, Chinchilla D, Boller T (2006) Ligand-induced endocytosis of the pattern recognition receptor FLS2 in Arabidopsis. Genes Dev 20: 537-542

Robert-Seilaniantz A, Navarro L, Bari R, Jones JD (2007) Pathological hormone imbalances. Curr Opin Plant Biol 10: 372-379

Rout-Mayer M-A, Mathieu Y, Cazale AC, Guern J, Lauriere C (1997) Extracellular alkalinization and oxidative burst induced by fungal pectin lyase in tobacco cells are not due to the perception of oligolalacturonide fragments. Plant Physiol Biochem 35: 330

Ruxton GD (2006) The unequal variance t-test is an underused alternative to Student's t-test and the Mann-Whitney U test. Behavioral Ecology

Savatin DV, Ferrari S, Sicilia F, De Lorenzo G (2011) Oligogalacturonide-auxin antagonism does not require posttranscriptional gene silencing or stabilization of auxin response repressors in Arabidopsis. Plant Physiol 157: 1163-1174

Schenk PM, Kazan K, Wilson I, Anderson JP, Richmond T, Somerville SC, Manners JM (2000) Coordinated plant defense responses in arabidopsis revealed by microarray analysis. Proc Natl Acad Sci U S A 97: 11655-11660

Spanu P, Grosskopf DG, Felix G, Boller T (1994) The apparent turnover of 1-aminocyclopropane-1-carboxylate synthase in tomato cells is regulated by protein phosphorylation and dephosphorylation. Plant Physiol 106: 529-535

Spoel SH, Johnson JS, Dong X (2007) Regulation of tradeoffs between plant defenses against pathogens with different lifestyles. Proc Natl Acad Sci U S A 104: 18842-18847

Staswick PE, Serban B, Rowe M, Tiryaki I, Maldonado MT, Maldonado MC, Suza W (2005) Characterization of an Arabidopsis enzyme family that conjugates amino acids to indole-3-acetic acid. Plant Cell 17: 616-627

Stennis MJ, Chandra S, Ryan CA, Low PS (1998) Systemin potentiates the oxidative burst in cultured tomato cells. Plant Physiol 117: 1031-1036

Sticher L, Mauch-Mani B, Métraux JP (1997) Systemic acquired resistance. Annu Rev Phytopathol 35: 235-270

Sun W, Dunning FM, Pfund C, Weingarten R, Bent AF (2006) Within-species flagellin polymorphism in Xanthomonas campestris pv campestris and its impact on elicitation of Arabidopsis FLAGELLIN SENSING2-dependent defenses. Plant Cell 18: 764-779

Tanz KA, Castleden I, Hooper CM, Vacher M, Small I, Millar HA (2012) SUBA3: a database for integrating experimentation and prediction to define the SUBcellular location of proteins in Arabidopsis. Nucl Acids Res

Tena G, Asai T, Chiu WL, Sheen J (2001) Plant mitogen-activated protein kinase signaling cascades. Curr Opin Plant Biol 4: 392-400

Thilmony R, Underwood W, He SY (2006) Genome-wide transcriptional analysis of the *Arabidopsis thaliana* interaction with the plant pathogen *Pseudomonas syringae* pv. *tomato* DC3000 and the human pathogen *Escherichia coli* O157:H7. Plant J 46: 34-53

Thomma BP, Penninckx IA, Broekaert WF, Cammue BP (2001) The complexity of disease signaling in Arabidopsis. Curr Opin Immunol 13: 63-68

Ting L, Cowley MJ, Lay H, Guilhaus M, Cavicchioli R (2009) Normalization and Statistical Analysis of Quantitative Proteomics Data Generated by Metabolic Labeling. Mol Cell Prot

Torres MA, Dangl JL (2005) Functions of the respiratory burst oxidase in biotic interactions, abiotic stress and development. Curr Opin Plant Biol 8: 397-403

Torres MA, Jones JD, Dangl JL (2006) Reactive oxygen species signaling in response to pathogens. Plant Physiol 141: 373-378

Tran Thanh Van K, Toubart P, Cousson A, Darvill AG, Gollin DJ, Chelf P, Albersheim P (1985) Manipulation of the morphogenetic pathways of tobacco explants by oligosaccharins. Nature 314: 615-617

Ulmasov T, Murfett J, Hagen G, Guilfoyle TJ (1997) Aux/IAA proteins repress expression of reporter genes containing natural and highly active synthetic auxin response elements. Plant Cell 9: 1963-1971

Vos IA, Pieterse CMJ, Van Wees SCM (2013) Costs and benefits of hormone-regulated plant defences. Plant Pathol

Wang D, Pajerowska-Mukhtar K, Culler AH, Dong X (2007) Salicylic acid inhibits pathogen growth in plants through repression of the auxin signaling pathway. Curr Biol 17: 1784-1790

Wang XH, Li QT, Chen HW, Zhang WK, Zhang JS (2014) Trihelix transcription factor GT-4 mediates salt tolerance via interaction with TEM2 in Arabidopsis. BMC Plant Biol

Wendehenne D, Lamotte O, Frachisse JM, Barbier-Brygoo H, Pugin A (2002) Nitrate efflux is an essential component of the cryptogein signaling pathway leading to defense responses and hypersensitive cell death in tobacco. Plant Cell 14: 1937-1951

Widmann C, Gibson S, Jarpe MB, Johnson GL (1999) Mitogen-activated protein kinase: conservation of a three-kinase module from yeast to human. Physiol Rev 79: 143-180

Woodward AW, Bartel B (2005) Auxin: regulation, action, and interaction. Ann Bot 95: 707-735

Xiang CB, Miao ZH, Lam E (1996) Coordinated activation of *as-1*-type elements and a tobacco glutathione S-transferase gene by auxins, salicylic acid, methyl- jasmonate and hydrogen peroxide. Plant Mol Biol 32: 415-426

Xu X, Chen C, Fan B, Chen Z (2006) Physical and functional interactions between pathogen-induced Arabidopsis WRKY18, WRKY40, and WRKY60 transcription factors. Plant Cell 18: 1310-1326

Yamada T (1993) The role of auxin in plant-disease development. Annu Rev Phytopathol 31: 253-273

Yoshioka K, Nakashita H, Klessig DF, Yamaguchi I (2001) Probenazole induces systemic acquired resistance in Arabidopsis with a novel type of action. Plant J 25: 149-157

Zhang Z, Li Q, Li Z, Staswick PE, Wang M, Zhu Y, He Z (2007) Dual regulation role of GH3.5 in salicylic acid and auxin signaling during Arabidopsis-Pseudomonas syringae interaction. Plant Physiol 145: 450-464

Zhou N, Tootle TL, Glazebrook J (1999) Arabidopsis PAD3, a gene required for camalexin biosynthesis, encodes a putative cytochrome P450 monooxygenase. Plant Cell 11: 2419-28

Zipfel C, Kunze G, Chinchilla D, Caniard A, Jones JDG, Boller T, Felix G (2006) Perception of the bacterial PAMP EF-Tu by the receptor EFR restricts *Agrobacterium*-mediated transformation. Cell 125: 749-760

Zipfel C, Robatzek S, Navarro L, Oakeley EJ, Jones JD, Felix G, Boller T (2004) Bacterial disease resistance in Arabidopsis through flagellin perception. Nature 428: 764-767